USDA

United States Department of Agriculture

Forest Health Monitoring: National Status, Trends, and Analysis 2015

Editors Kevin M. Potter Barbara L. Conkling

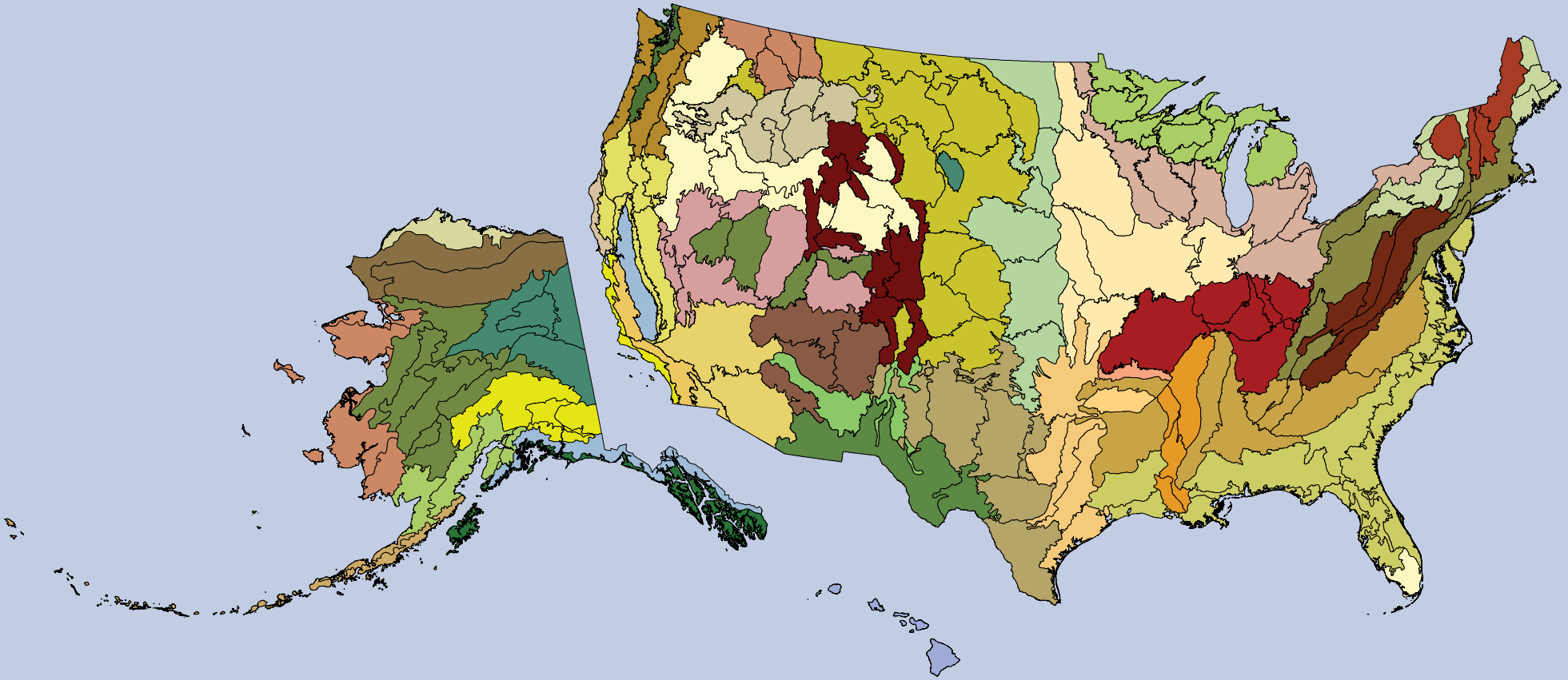

Forest Service
Research & Development
Southern Research Station
General Technical Report SRS-213

Front cover map: Ecoregion provinces and ecoregion sections for the conterminous United States (Cleland and others 2007) and for Alaska (Nowacki and Brock 1995).

Back cover map: Forest cover (green) backdrop derived from Moderate Resolution Imaging Spectroradiometer (MODIS) satellite imagery by the U.S. Forest Service Remote Sensing Applications Center.

July 2016

Southern Research Station
200 W.T. Weaver Blvd.
Asheville, NC 28804

www.srs.fs.usda.gov

Forest Health Monitoring:

National Status, Trends, and Analysis 2015

Editors

Kevin M. Potter, Research Associate Professor, North Carolina State University, Department of Forestry and Environmental Resources, Raleigh, NC 27695

Barbara L. Conkling, Research Assistant Professor, North Carolina State University, Department of Forestry and Environmental Resources, Raleigh, NC 27695

ABSTRACT

The annual national report of the Forest Health Monitoring (FHM) Program of the Forest Service, U.S. Department of Agriculture, presents forest health status and trends from a national or multi-State regional perspective using a variety of sources, introduces new techniques for analyzing forest health data, and summarizes results of recently completed Evaluation Monitoring projects funded through the FHM national program. In this 15th edition in a series of annual reports, survey data are used to identify geographic patterns of insect and disease activity. Satellite data are employed to detect geographic patterns of forest fire occurrence. Recent drought and moisture surplus conditions are compared across the conterminous United States. Data collected by the Forest Inventory and Analysis Program are employed to detect regional differences in tree mortality. National Land Cover Database land cover maps are used to summarize temporal trends in forest fragmentation for the conterminous United States from 2001 to 2011. Eleven recently completed Evaluation Monitoring projects are summarized, addressing forest health concerns at smaller scales.

Keywords—Change detection, drought, fire, forest health, forest insects and disease, fragmentation, tree mortality.

CONTENTS

SECTION 3.

CHAPTER 7.

CHAPTER 8.

CHAPTER 9.

CHAPTER 10.

LIST OF FIGURES

LIST OF TABLES

EXECUTIVE SUMMARY

Healthy ecosystems are those that are stable and sustainable, able to maintain their organization and autonomy over time while remaining resilient to stress (Costanza 1992). Healthy forests are vital to our future (Edmonds and others 2011), and consistent, large-scale, and long-term monitoring of key indicators of forest health status, change, and trends is necessary to identify forest resources deteriorating across large regions (Riitters and Tkacz 2004). The Forest Health Monitoring (FHM) Program of the Forest Service, U.S. Department of Agriculture, with cooperating researchers within and outside the Forest Service and with State partners, quantifies status and trends in the health of U.S. forests (chapter 1). The analyses and results outlined in sections 1 and 2 of this FHM annual national report offer a snapshot of the current condition of U.S. forests from a national or multi-State regional perspective, incorporating baseline investigations of forest ecosystem health, examinations of change over time in forest health metrics, and assessments of developing threats to forest stability and sustainability. For datasets collected on an annual basis, analyses are presented from 2014 data. For datasets collected over several years, analyses are presented at a longer temporal scale. Finally, section 3 of this report presents summaries of results from recently completed Evaluation Monitoring (EM) projects that have been funded through the FHM national program to determine the extent, severity and/or causes of specific forest health problems (FHM 2015).

Monitoring the occurrence of forest pest and pathogen outbreaks is important at regional scales because of the significant impact insects and disease can have on forest health across landscapes (chapter 2). National Insect and Disease Survey data collected in 2014 by the Forest Health Protection Program of the Forest Service and by its partners in State agencies identified 88 different mortality-causing agents and complexes on 1.75 million ha in the conterminous United States, and 67 defoliating agents and complexes on approximately 1.73 million ha. Geographic hot spots of forest mortality were associated with bark beetle infestations (mostly mountain pine beetle, spruce beetle, fir engraver, and western pine beetle) in the West. Hot spots of defoliation were associated with western spruce budworm in the West, and with gypsy moth, fall cankerworm, winter moth, forest tent caterpillar, baldcypress leafroller, jack pine budworm, large aspen tortrix, and spruce budworm in the East. Mortality was recorded on a very small proportion of the surveyed area in Alaska. The most important defoliation agents in Alaska were aspen leafminer and birch leafroller.

Forest fire occurrence outside the historic range of frequency and intensity can result in extensive economic and ecological impacts. The detection of regional patterns of fire occurrence density can allow for the identification of areas at greatest risk of significant impact and for the selection of locations for more intensive analysis (chapter 3). In 2014, more satellite-detected forest fire occurrences were recorded

for the conterminous States than for all but one year (2012) since the beginning of data collection in 2001. Ecoregions in northern California and southwestern Oregon, in north-central Washington, in central Oklahoma, and across several Southeastern States experienced the most fires per 100 km^2 of forested area. Geographic hot spots of high fire occurrence density were detected in these same areas. Ecoregions in the Pacific Northwest, Southwest, Great Lakes States, Northeast, and Mid-Atlantic and Southern States experienced greater fire occurrence density than normal compared to the 12-year mean and accounting for variability over time. Alaska experienced low fire occurrence densities in 2014, except in one south-central ecoregion. The Big Island of Hawai'i experienced very high fire occurrence density as a result of a months-long volcanic eruption.

Most U.S. forests experience droughts, with varying degrees of intensity and duration between and within forest ecosystems. Arguably, the duration of a drought event is more critical than its intensity. A standardized drought and moisture surplus indexing approach was applied to monthly climate data from 2014 to map drought conditions across the conterminous United States at a fine scale (chapter 4). Much of the country experienced moisture surplus conditions. Drought conditions existed from central California east through central Texas, with severe drought conditions in parts of New Mexico and Arizona. Areas with the highest moisture surpluses included the Great Lakes States, the Central Plains, and parts of the Southeast. Analyses of longer term (3-year and 5-year) conditions underscore the duration of recent severe drought conditions across the Southwest.

Mortality is a natural process in all forested ecosystems, but high levels of mortality at large scales may indicate that the health of forests is declining. Phase 2 data collected by the Forest Inventory and Analysis (FIA) Program of the Forest Service offer tree mortality information on a relatively spatially intense basis of approximately 1 plot per 6,000 acres (chapter 5). An analysis of FIA plots from 37 States found that the highest ratios of annual mortality to gross growth occurred in ecoregion sections located in western South Dakota and Nebraska, and in southern and eastern Kansas. In Plains ecoregions with the highest mortality relative to growth, tree growth is quite low because of naturally dry conditions, and most of the species experiencing the greatest mortality are commonly found in riparian areas. Two exceptions were the ecoregion that encompasses the Black Hills of South Dakota and the neighboring ecoregion in Nebraska, where ponderosa pine constituted the vast majority of trees that died, most likely the result of mountain pine beetle. Drought may also have contributed to mortality, as was likely the situation in the regions of Kansas with high mortality relative to growth.

The goal of national monitoring of forest fragmentation is to provide a consistent characterization of the status and trends of forest spatial patterns in a way that can potentially

address a large number of specific concerns about a variety of ecological goods and services (chapter 6). National Land Cover Database (NLCD) forest maps from 2001, 2006, and 2011 were used to update the status and trends of forest fragmentation. The results indicate that from 2001 to 2011 there was a widespread shift of the extant forest to a more fragmented condition, including places with relatively small changes in total forest cover. Decreases in total forest cover underestimated forest fragmentation for several criteria used to define fragmentation. Although forest tends to be the dominant land cover type where forest occurs, fragmentation is pervasive and increasing over time, even in regions exhibiting relatively small changes in total forest cover area. In addition to regional differences in the change of total forest cover, there is important regional variation in the area and rate of change of relatively unfragmented forest.

Finally, 11 recently completed Evaluation Monitoring projects address a wide variety of forest health concerns at a scale smaller than the national or multi-State regional analyses included in the first sections of the report. These EM projects (funded by the FHM Program):

- Quantified the distribution and intensification of bur oak blight in Iowa and elsewhere in the Midwest (chapter 7);
- Determined the extent of the nonnative invasive *Ailanthus* tree using helicopter mapping within Appalachian Ohio oak forests (chapter 8);
- Assessed the current health status of American beech and the distribution of beech bark disease in Wisconsin (chapter 9);
- Investigated rapid white oak mortality within the Ozark Plateau and the adjacent forest-prairie transition ecoregion in Missouri (chapter 10);
- Evaluated the influence of mountain pine beetle outbreaks on carbon productivity and storage in central Rocky Mountain lodgepole pine forests (chapter 11);
- Quantified changes in stand structure, fuel loading and predicted fire behavior during the first 5 years following high levels of bark-beetle-caused mortality in the Black Hills National Forest (chapter 12);
- Evaluated how whitebark pine responds to wildland fire in the Greater Yellowstone Ecoregion in order to develop short- and long-term whitebark pine management strategies (chapter 13);
- Quantified the impact of bark beetle infestation on fuel loads and fire behavior in old-stage ponderosa pine forests in the Southwest (chapter 14);
- Monitored mountain pine beetle life cycle timing and phloem temperatures at multiple elevations and latitudes in California (chapter 15);

- Used monitoring plots in northern California to evaluate how management and site disturbance affect the incidence and impacts of black stain root disease in Douglas-fir plantations (chapter 16);

- Developed an automated land cover mapping algorithm to assess changes in land cover in the South Coast bioregion of California (chapter 17).

The FHM Program, in cooperation with forest health specialists and researchers inside and outside the Forest Service, continues to investigate a broad range of issues relating to forest health using a wide variety of data and techniques. This report presents some of the latest results from ongoing national-scale detection monitoring and smaller-scale environmental monitoring efforts by FHM and its cooperators. For more information about efforts to determine the status, changes, and trends in indicators of the condition of U.S. forests, please visit the FHM Web site at www.fs.fed.us/foresthealth/fhm.

LITERATURE CITED

Costanza, R. 1992. Toward an operational definition of ecosystem health. In: Costanza, R.; Norton, B.G.; Haskell, B.D., eds. Ecosystem health: new goals for environmental management. Washington, DC: Island Press: 239–256.

Edmonds, R.L.; Agee, J.K.; Gara, R.I. 2011. Forest health and protection. Long Grove, IL: Waveland Press, Inc. 667 p.

Forest Health Monitoring (FHM). 2015. Program description. Forest Health Monitoring fact sheet series. http://www.fhm.fs.fed.us/fact/. [Date accessed: August 20, 2015].

Riitters, K.H.; Tkacz, B. 2004. The U.S. Forest Health Monitoring Program. In: Wiersma, G.B., ed. Environmental monitoring. Boca Raton, FL: CRC Press: 669–683.

CHAPTER 1.
Introduction

Kevin M. Potter

Forests cover a vast area of the United States, 304 million ha or approximately one-third of the Nation's land area (Smith and others 2009). These forests possess the capacity to provide a broad range of goods and services to current and future generations, to safeguard biological diversity, and to contribute to the resilience of ecosystems, societies, and economies (USDA Forest Service 2011). Their ecological roles include supplying large and consistent quantities of clean water, preventing soil erosion, and providing habitat for a broad diversity of plant and animal species. Their socioeconomic benefits include wood products, nontimber goods, recreational opportunities, and pleasing natural beauty. Both the ecological integrity and the continued capacity of these forests to provide ecological and economic goods and services are of concern, however, in the face of a long list of threats, including insect and disease infestation, fragmentation, catastrophic fire, invasive species, and the effects of climate change.

Natural and anthropogenic stresses vary among biophysical regions and local environments; they also change over time and interact with each other. These and other factors make it challenging to establish baselines of forest health and to detect important departures from normal forest ecosystem functioning (Riitters and Tkacz 2004). Monitoring the health of forests is a critically important task, however, reflected within the Criteria and Indicators for the Conservation and Sustainable Management of Temperate and Boreal Forests (Montréal Process Working Group 1995), which the Forest Service, U.S. Department of Agriculture (USDA), uses as a forest sustainability assessment framework (USDA Forest Service 2004, 2011). The primary objective of such monitoring is to identify ecological resources whose condition is deteriorating in subtle ways over large regions in response to cumulative stresses, a goal that requires consistent, large-scale, and long-term monitoring of key indicators of forest health status, change, and trends (Riitters and Tkacz 2004). This is best accomplished through the participation of multiple Federal, State, academic, and private partners.

Although the concept of a healthy forest has universal appeal, forest ecologists and managers have struggled with how exactly to define forest health (Teale and Castello 2011), and there is no universally accepted definition. Most definitions of forest health can be categorized as representing an ecological or a utilitarian perspective (Kolb and others 1994). From an ecological perspective, the current understanding of ecosystem dynamics suggests that healthy ecosystems are those that are able to maintain their organization and autonomy over time while remaining resilient to stress (Costanza 1992), and that evaluations of forest health should emphasize factors that affect the inherent processes and resilience of forests (Edmonds and others 2011, Kolb and others 1994, Raffa and others 2009). On the other hand, the utilitarian perspective holds that a forest is healthy if management objectives are met, and that a forest is unhealthy if not (Kolb and others 1994). Although this definition may be appropriate when a single, unambiguous

management objective exists, such as the production of wood fiber or the maintenance of wilderness attributes, it is too narrow when multiple management objectives are required (Edmonds and others 2011, Teale and Castello 2011). Teale and Castello (2011) incorporate both ecological and utilitarian perspectives into their two-component definition of forest health: First, a healthy forest must be sustainable with respect to its size structure, including a correspondence between baseline and observed mortality; second, a healthy forest must meet the landowner's objectives, provided that these objectives do not conflict with sustainability.

This national report, the 15th in an annual series sponsored by the Forest Health Monitoring (FHM) Program of the Forest Service, U.S. Department of Agriculture, attempts to quantify the status of, changes to, and trends in a wide variety of broadly defined indicators of forest health. The indicators described in this report encompass forest insect and disease activity, wildland fire occurrence, drought, tree mortality, and fragmentation, among others. The previous reports in this series are Ambrose and Conkling (2007, 2009), Conkling (2011), Conkling and others (2005), Coulston and others (2005a, 2005b, 2005c), and Potter and Conkling (2012a, 2012b; 2013a, 2013b; 2014; 2015a, 2015b).

This report has three specific objectives. The first is to present information about forest health from a national perspective, or from a multi-State regional perspective when appropriate, using data collected by the Forest Health Protection (FHP) and Forest Inventory and Analysis (FIA) programs of the Forest Service, as well as from other sources available at a wide extent. The chapters that present analyses at a national-scale, or multi-State regional scale, are divided between section 1 and section 2 of the report. Section 1 presents results from the analyses of forest health data that are available on an annual basis. Such repeated analyses of regularly collected indicator measurements allow for the detection of trends over time and help establish a baseline for future comparisons (Riitters and Tkacz 2004). Section 2 presents longer-term forest health trends, in addition to describing new techniques for analyzing forest health data at national or regional scales (the second objective of the report). While in-depth interpretation and analysis of specific geographic or ecological regions are beyond the scope of these parts of the report, the chapters in sections 1 and 2 present information that can be used to identify areas that may require investigation at a finer scale.

The second objective of the report, as noted above, is to present new techniques for analyzing forest health data as well as new applications of established techniques, presented in selected chapters of section 2. The example in this report is chapter 6, which assesses long-term trends in fragmentation using national land cover data.

The third objective of the report is to present results of recently completed Evaluation Monitoring (EM) projects funded through the FHM national program. These project summaries, presented in section 3, determine

the extent, severity, and/or cause of forest health problems (FHM 2014), generally at a finer scale than that addressed by the analyses in sections 1 and 2. Each of the 11 chapters in section 3 contains an overview of an EM project, key results, and contacts for more information.

When appropriate throughout this report, authors use the USDA Forest Service revised ecoregions (Cleland and others 2007, Nowacki and Brock 1995) as a common ecologically-based spatial framework for their forest health assessments (fig. 1.1). Specifically, when the spatial scale of the data and the expectation of an identifiable pattern in the data are appropriate, authors use ecoregion sections or provinces as assessment units for their analyses. Bailey's hierarchical system bases the two broadest ecoregion scales, domains and divisions, on large ecological climate zones, while each division is broken into provinces based on vegetation macro features (Bailey 1995). Provinces are further divided into sections, which may be thousands of square kilometers in extent and are expected to encompass regions similar in their geology, climate, soils, potential natural vegetation, and potential natural communities (Cleland and others 1997).

THE FOREST HEALTH MONITORING PROGRAM

The national FHM Program is designed to determine the status, changes, and trends in indicators of forest condition on an annual basis and covers all forested lands through a partnership encompassing the Forest Service, State foresters, and other State and Federal agencies and academic groups (FHM 2014). The FHM Program utilizes data from a wide variety of data sources, both inside and outside the Forest Service, and develops analytical approaches for addressing forest health issues that affect the sustainability of forest ecosystems. The FHM Program has five major components (fig. 1.2):

- Detection Monitoring—nationally standardized aerial and ground surveys to evaluate status and change in condition of forest ecosystems (sections 1 and 2 of this report).
- Evaluation Monitoring—projects to determine the extent, severity, and causes of undesirable changes in forest health identified through Detection Monitoring (section 3 of this report).
- Intensive Site Monitoring—projects to enhance an understanding of cause-effect relationships by linking Detection Monitoring to ecosystem process studies and to assess specific issues, such as calcium depletion and carbon sequestration, at multiple spatial scales (section 3 of this report).
- Research on Monitoring Techniques—work to develop or improve indicators, monitoring systems, and analytical techniques, such as urban and riparian forest health monitoring, early detection of invasive species, multivariate analyses of forest health indicators, and spatial scan statistics (section 2 of this report).

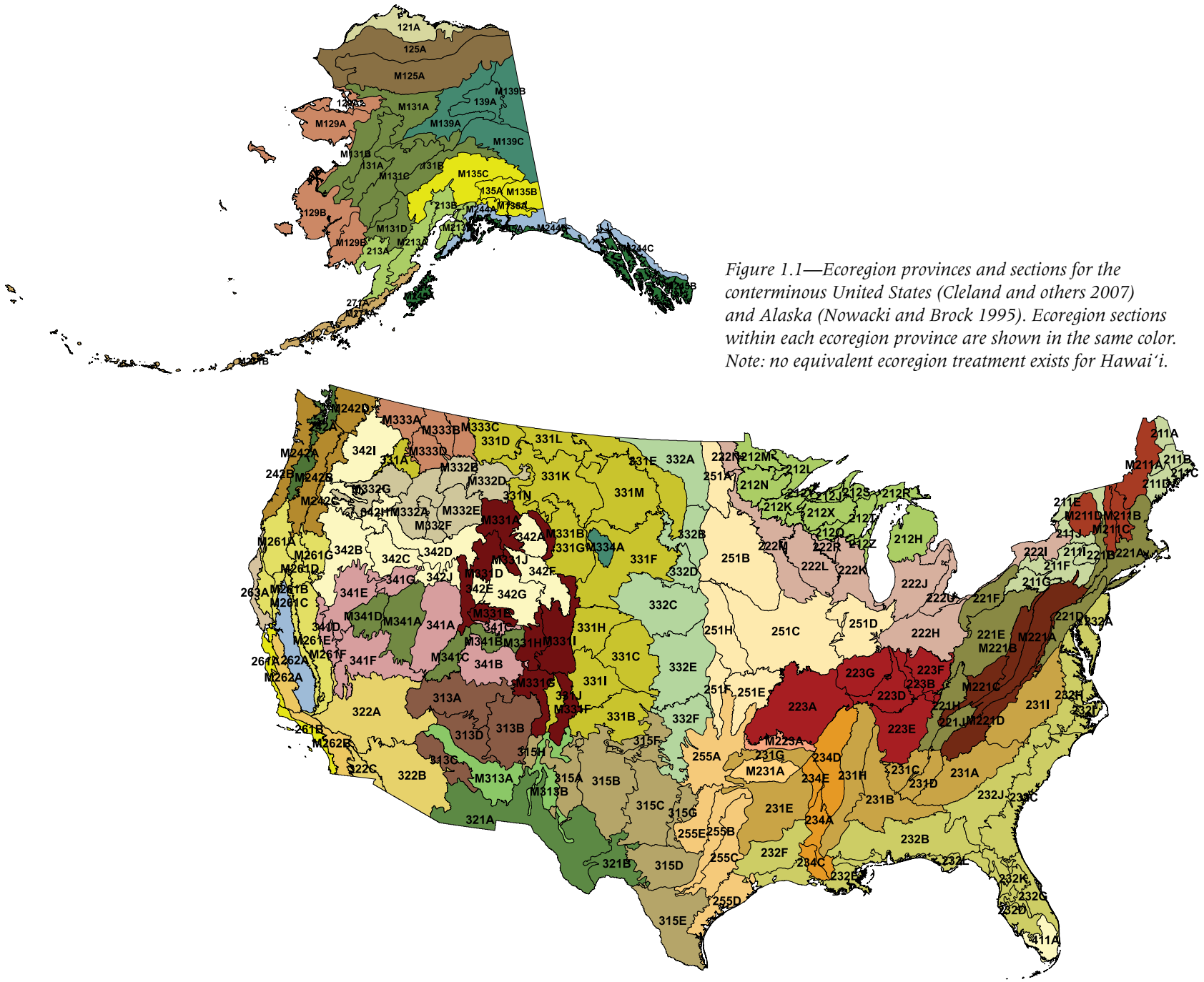

Figure 1.1—Ecoregion provinces and sections for the conterminous United States (Cleland and others 2007) and Alaska (Nowacki and Brock 1995). Ecoregion sections within each ecoregion province are shown in the same color. Note: no equivalent ecoregion treatment exists for Hawai'i.

Alaska Ecoregion Provinces

- Alaska Mixed Forest (213)
- Alaska Range Taiga (135)
- Aleutian Meadow (271)
- Arctic Tundra (121)
- Bering Sea Tundra (129)
- Brooks Range Tundra (125)
- Pacific Coastal Icefields (244)
- Pacific Gulf Coast Forest (245)
- Upper Yukon Taiga (139)
- Yukon Intermontaine Taiga (131)

Conterminous States Ecoregion Provinces

- Adirondack-New England Mixed Forest—Coniferous Forest—Alpine Meadow (M211)
- American Semi-Desert and Desert (322)
- Arizona-New Mexico Mountains Semi-Desert—Open Woodland—Coniferous Forest—Alpine Meadow (M313)
- Black Hills Coniferous Forest (M334)
- California Coastal Chaparral Forest and Shrub (261)
- California Coastal Range Open Woodland—Shrub—Coniferous Forest—Meadow (M262)
- California Coastal Steppe—Mixed Forest—Redwood Forest (263)
- California Dry Steppe (262)
- Cascade Mixed Forest—Coniferous Forest—Alpine Meadow (M242)
- Central Appalachian Broadleaf Forest—Coniferous Forest—Meadow (M221)
- Central Interior Broadleaf Forest (223)
- Chihuahuan Semi-Desert (321)
- Colorado Plateau Semi-Desert (313)
- Eastern Broadleaf Forest (221)
- Everglades (411)
- Great Plains—Palouse Dry Steppe (331)
- Great Plains Steppe (332)
- Intermountain Semi-Desert and Desert (341)
- Intermountain Semi-Desert (342)
- Laurentian Mixed Forest (212)
- Lower Mississippi Riverine Forest (234)
- Middle Rocky Mountain Steppe—Coniferous Forest—Alpine Meadow (M332)
- Midwest Broadleaf Forest (222)
- Nevada-Utah Mountains Semi-Desert—Coniferous Forest—Alpine Meadow (M341)
- Northeastern Mixed Forest (211)
- Northern Rocky Mountain Forest—Steppe—Coniferous Forest—Alpine Meadow (M333)
- Ouachita Mixed Forest—Meadow (M231)
- Outer Coastal Plain Mixed Forest (232)
- Ozark Broadleaf Forest (M223)
- Pacific Lowland Mixed Forest (242)
- Prairie Parkland (Subtropical) (255)
- Prairie Parkland (Temperate) (251)
- Sierran Steppe—Mixed Forest—Coniferous Forest—Alpine Meadow (M261)
- Southeastern Mixed Forest (231)
- Southern Rocky Mountain Steppe—Open Woodland—Coniferous Forest—Alpine Meadow (M331)
- Southwest Plateau and Plains Dry Steppe and Shrub (315)

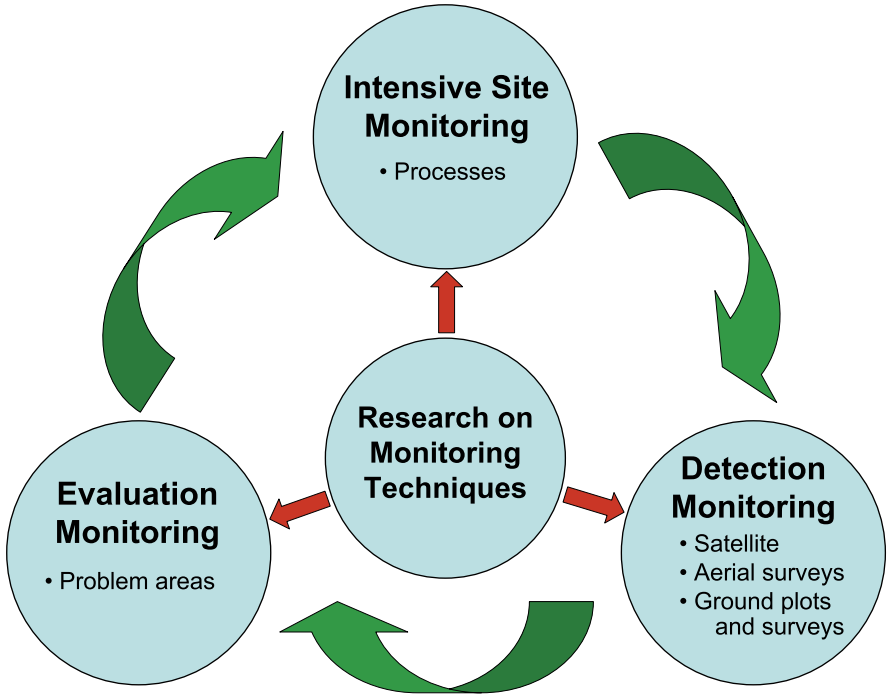

Figure 1.2—The design of the Forest Health Monitoring (FHM) Program of the Forest Service, U.S. Department of Agriculture (FHM 2003). A fifth component, Analysis and Reporting of Results, draws from the four FHM components shown here and provides information to help support land management policies and decisions.

- Analysis and Reporting—synthesis of information from various data sources within and external to the Forest Service to produce issue-driven reports on status and change in forest health at national, regional, and State levels (sections 1, 2, and 3 of this report).

The FHM Program, in addition to national reporting, generates regional and State reports, often in cooperation with FHM partners, both within the Forest Service and in State forestry and agricultural departments. For example, the FHM regions cooperate with their respective State partners to produce the annual Forest Health Highlights report series, available on the FHM Web site at www.fs.fed.us/foresthealth/fhm. Other examples include Steinman (2004) and Harris and others (2011).

The FHM Program and its partners also produce reports and journal articles on monitoring techniques and analytical methods, including forest health data (Smith and Conkling 2004); soils as an indicator of forest health (O'Neill and others 2005); urban forest health monitoring (Bigsby and others 2014; Cumming and others 2006, 2007; Lake and others 2006); remote sensing of forest disturbances (Chastain and others 2015); health conditions in National forests (Morin and others 2006); crown conditions (Morin and others 2015; Randolph 2010a, 2010b, 2013; Randolph and Moser 2009; Schomaker and others 2007); vegetation diversity and structure (Schulz and Gray 2013, Schulz and others 2009); forest lichen indicators (Jovan and others 2012, Root and others 2014); downed woody materials in forests (Woodall and others 2012, 2013); ozone monitoring (Rose and Coulston 2009); patterns of nonnative invasive plant occurrence (Oswalt and others 2015); assessments of alien-invasive forest insect and disease risk (Koch and others 2011, 2014; Krist and others 2014, Yemshanov and others 2014); spatial patterns of land cover (Riitters 2011, Riitters and others 2012, Riitters and Wickham 2012); broad-scale assessments of forest biodiversity (Potter and Koch 2014; Potter and Woodall 2012, 2014); predictions of climate change effects on forest tree species (Potter and Hargrove 2013); and the overall forest health indicator program (Woodall and others 2010).

For more information about the FHM Program, visit the FHM Web site at www.fs.fed.us/foresthealth/fhm. Among other things, this Web site includes links to all past national forest health reports (www.fs.fed.us/foresthealth/fhm/pubs), information about funded Evaluation Monitoring projects (www.fs.fed.us/foresthealth/fhm/em), and annual State forest health highlight reports (www.fs.fed.us/foresthealth/fhm/fhh/fhmusamap.shtml).

DATA SOURCES

Forest Service data sources in this edition of the FHM national report include FIA annualized phase 2 and phase 3 survey data (Bechtold and Patterson 2005, Woodall and others 2010, Woudenberg and others 2010); FHP national Insect and Disease Survey forest mortality and defoliation data for 2014 (FHP 2014); Moderate Resolution Imaging Spectroradiometer (MODIS) Active Fire Detections for the United States database for 2014 (USDA Forest Service 2015); and forest cover data developed from MODIS satellite imagery by the U.S. Forest Service Remote Sensing Applications Center. Other sources of data include Parameter-elevation Regression on Independent Slopes (PRISM) climate mapping system data (PRISM Climate Group 2015) and 2001, 2006, and 2011 National Land Cover Database land cover maps (U.S. Geological Survey 2014a, 2014b, 2014c).

As a major source of data for several FHM analyses, the FIA Program merits detailed description. The FIA Program collects forest

inventory information across all forest land ownerships in the United States and maintains a network of more than 125,000 permanent forested ground plots across the conterminous United States and southeastern Alaska, with a sampling intensity of approximately one plot per 2 428 ha. FIA phase 2 encompasses the annualized inventory measured on plots at regular intervals, with each plot surveyed every 5 to 7 years in most Eastern States, but with plots in the Rocky Mountain and Pacific Northwest regions surveyed once every 10 years (Reams and others 2005). The standard 0.067-ha plot (fig. 1.3) consists of four 7.315-m radius subplots (approximately 168.6 m^2 or 1/24th acre), on which field crews measure trees at least 12.7 cm in diameter. Within each of these subplots is nested a 2.073-m radius microplot (approximately 13.48 m^2 or 1/300th acre), on which crews measure trees smaller than 12.7 cm in diameter. A core-optional variant of the standard design includes four "macroplots," each with a radius of 17.953 m (or approximately 0.1012 ha) that originates at the center of each subplot (Woudenberg and others 2010).

FIA phase 3 plots represent a subset of these phase 2 plots, with one phase 3 plot for every 16 standard FIA phase 2 plots. In addition to traditional forest inventory measurements, data for a variety of important ecological indicators are collected from phase 3 plots, including tree crown condition, lichen communities, down woody material, soil condition, and vegetation structure and diversity, whereas data on ozone bioindicator plants are collected on a separate grid of plots (Woodall and others 2010, 2011). Most of these additional forest health indicators

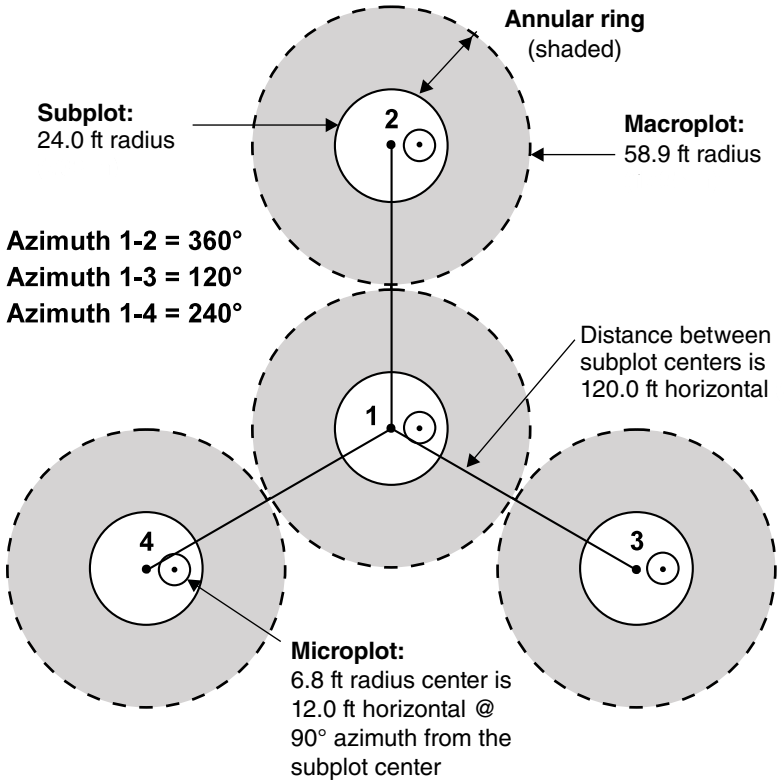

Figure 1.3—The Forest Inventory and Analysis mapped plot design. Subplot 1 is the center of the cluster with subplots 2, 3, and 4 located 120 feet away at azimuths of 360°, 120°, and 240°, respectively (Woudenberg and others 2010).

were measured as part of the FHM Detection Monitoring ground plot system prior to 2000[1] (Palmer and others 1991).

FHM REPORT PRODUCTION

This FHM national report, the 15th in a series of such annual documents, is produced by forest health monitoring researchers at the Eastern Forest Environmental Threat Assessment Center (EFETAC) in collaboration with North Carolina State University cooperators. A unit of the Southern Research Station of the Forest Service, EFETAC was established under the Healthy Forests Restoration Act of 2003 to generate the knowledge and tools needed to anticipate and respond to environmental threats. For more information about the research team and about threats to U.S. forests, please visit www.forestthreats.org/about.

LITERATURE CITED

Ambrose, M.J; Conkling, B.L., eds. 2007. Forest Health Monitoring 2005 national technical report. Gen. Tech. Rep. SRS-104. Asheville, NC: U.S. Department of Agriculture, Forest Service, Southern Research Station. 76 p.

Ambrose, M.J; Conkling, B.L., eds. 2009. Forest Health Monitoring 2006 national technical report. Gen. Tech. Rep. SRS-117. Asheville, NC: U.S. Department of Agriculture, Forest Service, Southern Research Station. 118 p.

[1] U.S. Department of Agriculture Forest Service. 1998. Forest Health Monitoring 1998 field methods guide. Research Triangle Park, NC: U.S. Department of Agriculture Forest Service, Forest Health Monitoring Program, 473 p. On file with: Forest Health Monitoring Program, 3041 Cornwallis Rd., Research Triangle Park, NC 27709.

Bailey, R.G. 1995. Descriptions of the ecoregions of the United States. 2d ed. Misc. Publ. No. 1391. Washington, DC: U.S. Department of Agriculture, Forest Service. 108 p. [Map scale 1:7,500,000].

Bechtold, W.A.; Patterson, P.L., eds. 2005. The enhanced Forest Inventory and Analysis program—national sampling design and estimation procedures. Gen. Tech. Rep. SRS-80. Asheville, NC: U.S. Department of Agriculture, Forest Service, Southern Research Station. 85 p.

Bigsby, K.M; Ambrose, M.J.; Tobin, P.C.; Sills, E.O. 2014. The cost of gypsy moth sex in the city. Urban Forestry & Urban Greening. 13(3): 459–468.

Chastain, R.A.; Fisk, H.; Ellenwood, J.R. [and others]. 2015. Near-real time delivery of MODIS-based information on forest disturbances. In: Lippitt, C.D.; Stow, D.A.; Coulter, L.L., eds. Time sensitive remote sensing. New York, NY: Springer: 147–164.

Cleland, D.T.; Avers, P.E.; McNab, W.H. [and others]. 1997. National hierarchical framework of ecological units. In: Boyce, M. S.; Haney, A., eds. Ecosystem management applications for sustainable forest and wildlife resources. New Haven, CT: Yale University Press: 181–200.

Cleland, D.T.; Freeouf, J. A.; Keys, J.E.; [and others]. 2007. Ecological subregions: sections and subsections for the conterminous United States. In: Sloan, A.M., tech. ed. Washington, DC: U.S. Department of Agriculture, Forest Service. Gen. Tech. Rep. WO-76D. Map, presentation scale 1:3,500,000; colored. Also on CD-ROM as a GIS coverage in ArcINFO format.

Conkling, B.L., ed. 2011. Forest Health Monitoring 2007 national technical report. Gen. Tech. Rep. SRS-147. Asheville, North Carolina: U.S. Department of Agriculture, Forest Service, Southern Research Station. 159 p.

Conkling, B.L.; J.W. Coulston; M.J. Ambrose, eds. 2005. Forest Health Monitoring 2001 national technical report. Gen. Tech. Rep. SRS-81. Asheville, NC: U.S. Department of Agriculture, Forest Service, Southern Research Station. 204 p.

Costanza, R. 1992. Toward an operational definition of ecosystem health. In: Costanza, R.; Norton, B.G.; Haskell, B.D., eds. Ecosystem health: new goals for environmental management. Washington, DC: Island Press: 239–256.

Coulston, J.W.; Riitters, K.H.; Conkling, B.L., eds. 2005a. Forest Health Monitoring 2002 national technical report. Gen. Tech. Rep. SRS-84. Asheville, North Carolina: U.S. Department of Agriculture, Forest Service, Southern Research Station. 97 p.

Coulston, J.W.; Ambrose, M.J.; Riitters, K.H. [and others], eds. 2005b. Forest Health Monitoring 2003 national technical report. Gen. Tech. Rep. SRS-85. Asheville, North Carolina: U.S. Department of Agriculture Forest Service, Southern Research Station. 97 p.

Coulston, J.W.; Ambrose, M.J.; Riitters, K.H.; Conkling, B.L., eds. 2005c. Forest Health Monitoring 2004 national technical report. Gen. Tech. Rep. SRS-90. Asheville, North Carolina: U.S. Department of Agriculture, Forest Service, Southern Research Station. 81 p.

Cumming, A.B.; Nowak, D.J.; Twardus, D.B. [and others]. 2007. Urban forests of Wisconsin: pilot monitoring project 2002. NA-FR-05-07. Newtown Square, PA: U.S. Department of Agriculture, Forest Service, Northeastern Area State and Private Forestry. 33 p. Available online: Low resolution: http://www.na.fs.fed.us/pubs/fhm/pilot/pilot_study_wisconsin_02_lr.pdf. High resolution: http://www.na.fs.fed.us/pubs/fhm/pilot/pilot_study_wisconsin2_02_hr.pdf. [Date accessed: October 19, 2007].

Cumming, A.B.; Twardus, D.B.; Smith, W.D. 2006. National Forest Health Monitoring Program, Maryland and Massachusetts street tree monitoring pilot projects. NA-FR-01-06. Newtown Square, PA: U.S. Department of Agriculture, Forest Service Northeastern Area, State and Private Forestry. 23 p.

Edmonds, R.L.; Agee, J.K.; Gara, R.I. 2011. Forest health and protection. Long Grove, IL: Waveland Press, Inc. 667 p.

Forest Health Monitoring (FHM). 2003. Forest Health Monitoring: a national strategic plan. http://fhm.fs.fed.us/annc/strategic_plan03.pdf. 7 p. [Date accessed: June 28, 2013].

Forest Health Monitoring (FHM). 2014. Program description. Forest Health Monitoring Fact Sheet Series. http://www.fhm.fs.fed.us/fact/. [Date accessed: July 29, 2014].

Forest Health Protection (FHP). 2014. Insect and Disease Detection Survey Database (IDS) [database on the Internet]. Fort Collins, CO: U.S. Department of Agriculture, Forest Service, Forest Health Technology Enterprise Team. Available: http://foresthealth.fs.usda.gov/ids. [Date accessed: July 20, 2015].

Harris, J.L., comp.; Region 2 Forest Health Protection staff. 2011. Forest health conditions, 2009–2010: Rocky Mountain Region (R2). R2-11-RO-31. Golden, CO: U.S. Department of Agriculture, Forest Service, Renewable Resources, Forest Health Protection, Rocky Mountain Region. 108 p.

Jovan, S.; Riddell, J.; Padgett, P.E.; Nash, T.H, III. 2012. Eutrophic lichens respond to multiple forms of N: implications for critical levels and critical loads research. Ecological Applications. 22(7): 1910–1922.

Koch, F.H.; Yemshanov, D.; Colunga-Garcia, M. [and others]. 2011. Potential establishment of alien-invasive forest insect species in the United States: where and how many? Biological Invasions. 13: 969–985.

Koch, F.H.; Yemshanov, D.; Haack, R.A.; Magarey, R.D. 2014. Using a network model to assess risk of forest pest spread via recreational travel. PLoS ONE 9(7): e102105.

Kolb, T.E.; Wagner, M.R.; Covington, W.W. 1994. Concepts of forest health: utilitarian and ecosystem perspectives. Journal of Forestry. 92: 10–15.

Krist, F.J., Jr.; Ellenwood, J.R.; Woods, M.E. [and others]. 2014. 2012–2027 national insect and disease forest risk assessment. FHTET-14-01. U.S. Department of Agriculture, Forest Service, Forest Health Technology Enterprise Team. 199 p. http://www.fs.fed.us/foresthealth/technology/pdfs/2012_RiskMap_Report_web.pdf. [Date accessed: July 24, 2014].

Lake, M.; Marshall, P.; Mielke, M. [and others]. 2006. National Forest Health Monitoring Program monitoring urban forests in Indiana: pilot study 2002, part 1. Analysis of field methods and data collection. Gen. Tech Rep. NA FR-06-06. Newtown Square, PA: U.S. Department of Agriculture, Forest Service, Northeastern Area. Available at: http://www.fhm.fs.fed.us/pubs/ufhm/indianaforests02/indianaforests02.html. [Date accessed: November 6, 2007].

Montréal Process Working Group. 1995. Criteria and indicators for the conservation and sustainable management of temperate and boreal forests. http://www.montrealprocess.org/. [Date accessed: March 4, 2015].

Morin, R.S.; Liebhold, A.M.; Gottschalk, K.W. [and others]. 2006. Analysis of Forest Health Monitoring surveys on the Allegheny National Forest (1998–2001). Gen. Tech. Rep. NE-339. Newtown Square, PA: U.S. Department of Agriculture, Forest Service, Northeastern Research Station. 102 p. http://www.fs.fed.us/ne/newtown_square/publications. [Date accessed: November 6, 2007].

Morin, R.S.; Randolph, K.C.; Steinman, J. 2015. Mortality rates associated with crown health for eastern forest tree species. Environmental Monitoring and Assessment. 187(3): 87.

Nowacki, G.; Brock, T. 1995. Ecoregions and subregions of Alaska [EcoMap]. Version 2.0. Juneau, AK: U.S. Department of Agriculture, Forest Service, Alaska Region. [Map, presentation scale 1:5,000,000; colored].

O'Neill, K.P.; Amacher, M.C.; Perry, C.H. 2005. Soils as an indicator of forest health: a guide to the collection, analysis, and interpretation of soil indicator data in the Forest Inventory and Analysis Program. Gen. Tech. Rep. NC-258. St. Paul, MN: U.S. Department of Agriculture, Forest Service, North Central Research Station. 53 p.

Oswalt, C.M.; Fei, S.; Guo, G. [and others]. 2015. A subcontinental view of forest plant invasions. NeoBiota. 24: 49–54.

Palmer, C.J.; Riitters, K.H.; Strickland, T. [and others]. 1991. Monitoring and research strategy for forests—Environmental Monitoring and Assessment Program (EMAP). EPA/600/4-91/012. Washington, DC: U.S. Environmental Protection Agency. 189 p.

Potter, K.M.; Conkling, B.L., eds. 2012a. Forest Health Monitoring 2008 national technical report. Gen. Tech. Rep. SRS-158. Asheville, NC: U.S. Department of Agriculture, Forest Service, Southern Research Station. 179 p.

Potter, K.M.; Conkling, B.L., eds. 2012b. Forest Health Monitoring 2009 national technical report. Gen. Tech. Rep. SRS-167. Asheville, NC: U.S. Department of Agriculture, Forest Service, Southern Research Station. 252 p.

Potter, K.M.; Conkling, B.L., eds. 2013a. Forest Health Monitoring: national status, trends, and analysis 2010. Gen. Tech. Rep. SRS-176. Asheville, NC: U.S. Department of Agriculture, Forest Service, Southern Research Station. 162 p.

Potter, K.M.; Conkling, B.L., eds. 2013b. Forest Health Monitoring: national status, trends, and analysis 2011. Gen. Tech. Rep. SRS-185. Asheville, NC: U.S. Department of Agriculture, Forest Service, Southern Research Station. 149 p.

Potter, K.M.; Conkling, B.L., eds. 2014. Forest Health Monitoring: national status, trends, and analysis 2012. Gen. Tech. Rep. SRS-198. Asheville, NC: U.S. Department of Agriculture, Forest Service, Southern Research Station. 192 p.

Potter, K.M.; Conkling, B.L., eds. 2015a. Forest Health Monitoring: national status, trends, and analysis 2013. Gen. Tech. Rep. SRS-207. Asheville, NC: U.S. Department of Agriculture, Forest Service, Southern Research Station. 199 p.

Potter, K.M.; Conkling, B.L., eds. 2015b. Forest Health Monitoring: national status, trends, and analysis 2014. Gen. Tech. Rep. SRS-209. Asheville, NC: U.S. Department of Agriculture, Forest Service, Southern Research Station. 190 p.

Potter, K.M; Hargrove, W.W. 2013. Quantitative metrics for assessing predicted climate change pressure on North American tree species. Mathematical and Computational Forestry and Natural Resources Sciences. 5(2): 151–169.

Potter, K.M.; Koch, F.H. 2014. Phylogenetic community structure of forests across the conterminous United States: regional ecological patterns and forest health implications. Forest Science. 60(5): 851–861.

Potter, K.M.; Woodall, C.W. 2012. Trends over time in tree and seedling phylogenetic diversity indicate regional differences in forest biodiversity change. Ecological Applications. 22(2): 517–531.

Potter, K.M.; Woodall, C.W. 2014. Does biodiversity make a difference? Relationships between species richness, evolutionary diversity, and aboveground live tree biomass across U.S. forests. Forest Ecology and Management. 321: 117–129.

PRISM Climate Group. 2015. 2.5-arcmin (4 km) gridded monthly climate data. http://www.prism.oregonstate.edu. [Date accessed: June 23, 2015].

Raffa, K.F.; Aukema, B.; Bentz, B.J. [and others]. 2009. A literal use of "forest health" safeguards against misuse and misapplication. Journal of Forestry. 107: 276–277.

Randolph, K.C. 2010a. Equations relating compacted and uncompacted live crown ratio for common tree species in the South. Southern Journal of Applied Forestry. 34(3): 118–123.

Randolph, K.C. 2010b. Comparison of the arithmetic and geometric means in estimating crown diameter and crown cross-sectional area. Southern Journal of Applied Forestry. 34(4): 186–189.

Randolph, K.C. 2013. Development history and bibliography of the U.S. Forest Service crown-condition indicator for forest health monitoring. Environmental Monitoring and Assessment. 185(6): 4977–4993.

Randolph, K.C.; Moser, W.K. 2009. Tree crown condition in Missouri, 2000–2003. Gen. Tech. Rep. SRS–113. Asheville, NC: U.S. Department of Agriculture, Forest Service, Southern Research Station. 11 p.

Reams, G.A.; Smith, W. D.; Hansen, M.H. [and others]. 2005. The Forest Inventory and Analysis sampling frame. In: Bechtold, W.A.; Patterson, P.L., ed. The enhanced Forest Inventory and Analysis Program—national sampling design and estimation procedures. Asheville, NC: U.S. Department of Agriculture, Forest Service, Southern Research Station: 11–26.

Riitters, K.H. 2011. Spatial patterns of land cover in the United States: a technical document supporting the Forest Service 2010 RPA assessment. Gen. Tech. Rep. SRS-136. Asheville, NC: U.S. Department of Agriculture, Forest Service, Southern Research Station. 64 p.

Riitters, K.H.; Coulston, J.W.; Wickham, J.D. 2012. Fragmentation of forest communities in the Eastern United States. Forest Ecology and Management. 263: 85–93.

Riitters, K.H.; Tkacz, B. 2004. The U.S. Forest Health Monitoring Program. In: Wiersma, G.B., ed. Environmental monitoring. Boca Raton, FL: CRC Press: 669–683.

Riitters, K.H.; Wickham, J.D. 2012. Decline of forest interior conditions in the conterminous United States. Scientific Reports. 2: 653. 4 p. DOI: 10.1038.srep00653. [Published online: September 13, 2012].

Root, H.T.; McCune, B.; Jovan, S. 2014. Lichen communities and species indicate climate thresholds in southeast and south-central Alaska, USA. The Bryologist. 117(3): 241–252.

Rose, A.K.; Coulston, J.W. 2009. Ozone injury across the Southern United States, 2002–06. Gen. Tech. Rep. SRS-118. Asheville, NC: U.S. Department of Agriculture, Forest Service, Southern Research Station. 25 p.

Schomaker, M.E.; Zarnoch, S.J.; Bechtold, W.A. [and others]. 2007. Crown-condition classification: a guide to data collection and analysis. Gen. Tech. Rep SRS-102. Asheville, NC: U.S. Department of Agriculture, Forest Service, Southern Research Station. 78 p.

Schulz, B.K.; Bechtold, W.A.; Zarnoch, S.J. 2009. Sampling and estimation procedures for the vegetation diversity and structure indicator. Gen. Tech. Rep. PNW-GTR-781. Portland, OR: U.S. Department of Agriculture, Forest Service, Pacific Northwest Research Station. 53 p.

Schulz, B.K.; Gray, A.N. 2013. The new flora of Northeastern USA: quantifying introduced plant species occupancy in forest ecosystems. Environmental Monitoring and Assessment. 185: 3931–3957.

Smith, W.B.; Miles, P.D.; Perry, C.H.; Pugh, S.A. 2009. Forest resources of the United States, 2007. Gen. Tech. Rep. WO-78. St. Paul, MN: U.S. Department of Agriculture, Forest Service, Washington Office. 336 p.

Smith, W.D.; Conkling, B.L. 2004. Analyzing forest health data. Gen. Tech. Rep. SRS-077. Asheville, NC: U.S. Department of Agriculture, Forest Service, Southern Research Station. 33 p. http://www.srs.fs.usda.gov/pubs/gtr/gtr_srs077.pdf. [Date accessed: November 6, 2007].

Steinman, J. 2004. Forest Health Monitoring in the Northeastern United States: disturbances and conditions during 1993-2002. NA-Technical Paper 01-04. Newtown Square, PA: U.S. Department of Agriculture, Forest Service, Northeastern Area State and Private Forestry. 46 p. http://fhm.fs.fed.us/pubs/tp/dist_cond/dc.shtml. [Date accessed: December 8, 2009].

Teale, S.A.; Castello, J.D. 2011. The past as key to the future: A new perspective on forest health. In: Castello, J.D.; Teale, S.A., eds. Forest health: an integrated perspective. New York: Cambridge University Press: 3–16.

U.S. Department of Agriculture (USDA) Forest Service. 2004. National report on sustainable forests—2003. FS-766. Washington, DC: U.S. Department of Agriculture, Forest Service. 139 p.

U.S. Department of Agriculture (USDA) Forest Service. 2011. National report on sustainable forests—2010. Report FS-979. Washington, DC: U.S. Department of Agriculture, Forest Service. 134 p.

U.S. Department of Agriculture (USDA) Forest Service. 2015. MODIS active fire mapping program: fire detection GIS data. http://activefiremaps.fs.fed.us/gisdata.php. [Date accessed: February 13, 2015].

U.S. Geological Survey. 2014a. NLCD 2001 Land Cover (2011 edition). Sioux Falls, SD: U.S. Geological Survey.

U.S. Geological Survey. 2014b. NLCD 2006 Land Cover (2011 edition). Sioux Falls, SD: U.S. Geological Survey.

U.S. Geological Survey. 2014c. NLCD 2011 Land Cover (2011 edition). Sioux Falls, SD: U.S. Geological Survey.

Woodall, C.W.; Conkling, B.L.; Amacher, M.C. [and others]. 2010. The Forest Inventory and Analysis database version 4.0: database description and users manual for phase 3. Gen. Tech. Rep. NRS-61. Newtown Square, PA: U.S. Department of Agriculture, Forest Service, Northern Research Station. 180 p.

Woodall, C.W.; Amacher, M.C.; Bechtold, W.A. [and others]. 2011. Status and future of the forest health indicators program of the USA. Environmental Monitoring and Assessment. 177:419–436.

Woodall, C.W.; Walters, B.F.; Westfall, J.A. 2012. Tracking downed dead wood in forests over time: development of a piece matching algorithm for line intercept sampling. Forest Ecology and Management. 277: 196–204.

Woodall, C.W.; Walters, B.F.; Oswalt, S.N. [and others]. 2013. Biomass and carbon attributes of downed woody materials in forests of the United States. Forest Ecology and Management. 305: 48–59.

Woudenberg, S.W.; Conkling, B.L.; O'Connell, B.M. [and others]. 2010. The Forest Inventory and Analysis database: database description and users manual version 4.0 for phase 2. Gen. Tech. Rep. RMRS-GTR-245. Fort Collins, CO: U.S. Department of Agriculture, Forest Service, Rocky Mountain Research Station. 336 p.

Yemshanov, D.; Koch, F.H.; Lu, B. [and others]. 2014. There is no silver bullet: the value of diversification in planning invasive species surveillance. Ecological Economics. 104: 61–72.

SECTION 1.

Analyses of Short-Term Forest Health Data

CHAPTER 2.

Large-Scale Patterns of Insect and Disease Activity in the Conterminous United States and Alaska from the National Insect and Disease Survey, 2014

Kevin M. Potter
Jeanine L. Paschke

INTRODUCTION

Insects and diseases cause changes in forest structure and function, species succession, and biodiversity, which may be considered negative or positive depending on management objectives (Edmonds and others 2011). An important task for forest managers, pathologists, and entomologists is recognizing and distinguishing between natural and excessive mortality, a task that relates to ecologically based or commodity-based management objectives (Teale and Castello 2011). The impacts of insects and diseases on forests vary from natural thinning to extraordinary levels of tree mortality, but insects and diseases are not necessarily enemies of the forest because they kill trees (Teale and Castello 2011). If disturbances, including insects and diseases, are viewed in their full ecological context, then some amount can be considered "healthy" to sustain the structure of the forest (Manion 2003, Zhang and others 2011) by causing tree mortality that culls weak competitors and releases resources that are needed to support the growth of surviving trees (Teale and Castello 2011).

Analyzing patterns of forest insect infestations, disease occurrences, forest declines, and related biotic stress factors is necessary to monitor the health of forested ecosystems and their potential impacts on forest structure, composition, biodiversity, and species distributions (Castello and others 1995). Introduced nonnative insects and diseases, in particular, can extensively damage the diversity, ecology, and economy of affected areas (Brockerhoff and others 2006, Mack and others 2000). Few forests remain unaffected by invasive species, and their devastating impacts in forests are undeniable, including, in some cases, wholesale changes to the structure and function of an ecosystem (Parry and Teale 2011).

Examining insect pest occurrences and related stress factors from a landscape-scale perspective is useful, given the regional extent of many infestations and the large-scale complexity of interactions between host distribution, stress factors, and the development of insect pest outbreaks (Holdenrieder and others 2004, Liebhold and others 2013). One such landscape-scale approach is detecting geographic patterns of disturbance, which allows for the identification of areas at greater risk of significant ecological and economic impacts and for the selection of locations for more intensive monitoring and analysis.

METHODS

Data

Forest Health Protection (FHP) national Insect and Disease Survey (IDS) data (FHP 2014) consist of information from low-altitude aerial survey and ground survey efforts by FHP and partners in State agencies. These data can be used to identify forest landscape-scale patterns associated with geographic hot spots of forest insect and disease activity in the conterminous 48 States and to summarize insect and disease activity by ecoregion in Alaska (Potter 2012, 2013; Potter and Koch 2012; Potter and Paschke 2013, 2014, 2015a, 2015b). In 2014,

IDS surveys covered about 159.27 million ha of the forested area in the conterminous United States (approximately 62.5 percent of the total), and about 7.74 million ha of Alaska's forested area (approximately 15.1 percent of the total) (fig. 2.1).

These surveys identify areas of mortality and defoliation caused by insect and disease activity, although some important forest insects [such as emerald ash borer (*Agrilus planipennis*) and hemlock woolly adelgid (*Adelges tsugae*)], diseases (such as laurel wilt, Dutch elm disease, white pine blister rust, and thousand cankers disease), and mortality complexes (such as oak decline) are not easily detected or thoroughly quantified through aerial detection surveys. Such pests may attack hosts that are widely dispersed throughout forests with high tree species diversity or may cause mortality or defoliation that is otherwise difficult to detect. A pathogen or insect might be considered a mortality-causing agent in one location and a defoliation-causing agent in another, depending on the level of damage to the forest in a given area and the convergence of other stress factors such as drought. In some cases, the identified agents of mortality or defoliation are actually complexes of multiple agents summarized under an impact label related to a specific host tree species (e.g., "subalpine fir mortality complex" or "aspen defoliation"). Additionally, differences in data collection, attribute recognition, and coding procedures among States and regions can complicate data analysis and interpretation of the results.

The 2014 mortality and defoliation polygons were used to identify the select mortality and defoliation agents and complexes causing damage on more than 5000 ha of forest in the conterminous United States in that year, and to identify and list the most widely detected mortality and defoliation agents for Alaska. Because of the insect and disease aerial sketch-mapping process (i.e., digitization of polygons by a human interpreter aboard the aircraft), all quantities are approximate "footprint" areas for each agent or complex, delineating areas of visible damage within which the agent or complex is present. Unaffected trees may exist within the footprint, and the amount of damage within the footprint is not reflected in the estimates of forest area affected. The sum of agents and complexes is not equal to the total affected area as a result of reporting multiple agents per polygon in some situations.

Analyses

We used the Spatial Association of Scalable Hexagons (SASH) analytical approach to identify surveyed forest areas with the greatest exposure to the detected mortality-causing and defoliation-causing agents and complexes. This method identifies locations where ecological phenomena occur at greater or lower occurrences than expected by random chance and is based on a sampling frame optimized for spatial neighborhood analysis, adjustable to the appropriate spatial resolution, and applicable to multiple data types (Potter and others 2016). Specifically, it consists of dividing an analysis area into scalable equal-area hexagonal cells

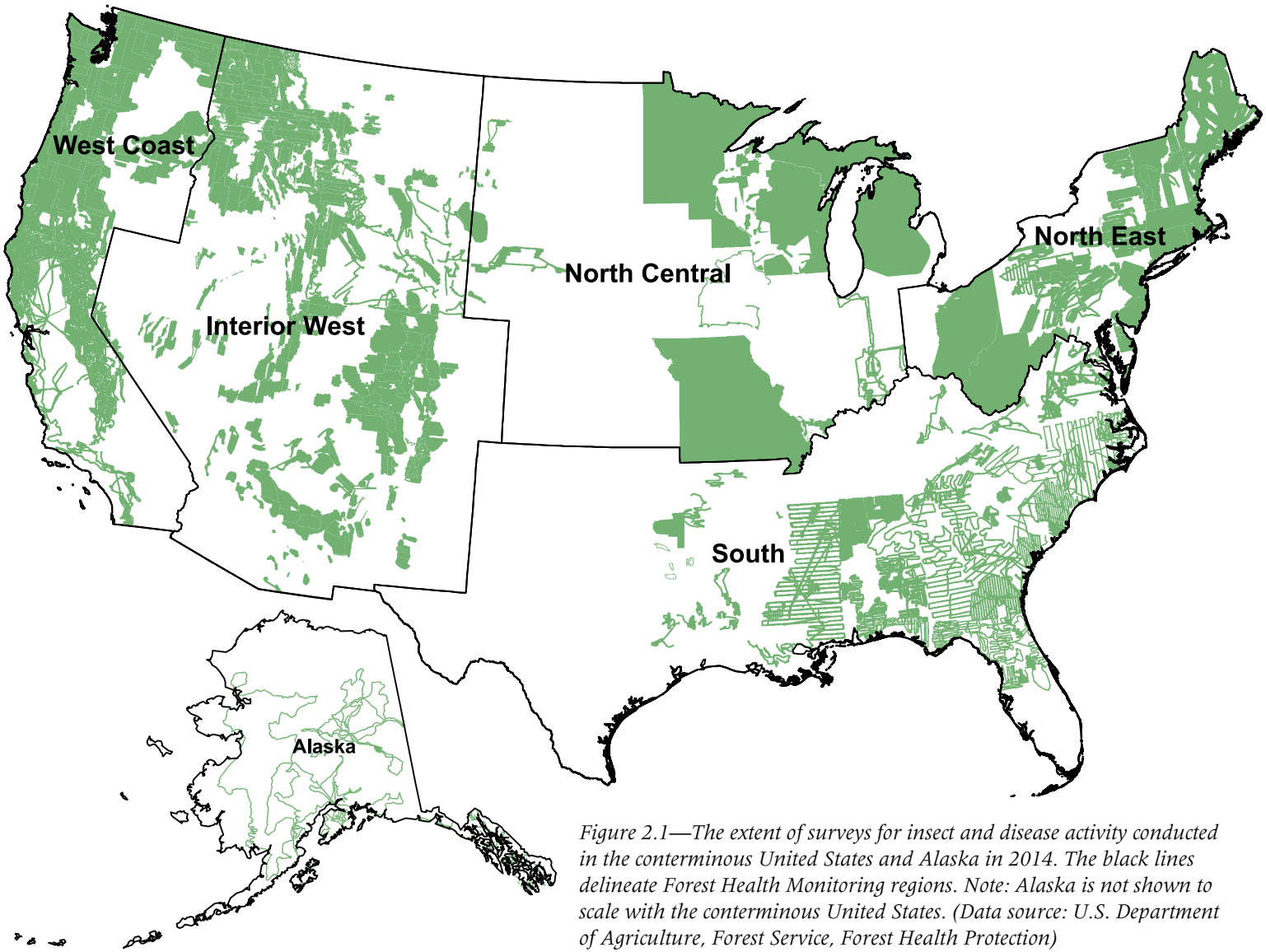

Figure 2.1—The extent of surveys for insect and disease activity conducted in the conterminous United States and Alaska in 2014. The black lines delineate Forest Health Monitoring regions. Note: Alaska is not shown to scale with the conterminous United States. (Data source: U.S. Department of Agriculture, Forest Service, Forest Health Protection)

within which data are aggregated, followed by identifying statistically significant geographic clusters of hexagonal cells within which mean values are greater or less than those expected by chance. To identify these clusters, we employ a Getis-Ord (G_i^*) hot spot analysis (Getis and Ord 1992) in ArcMap® 10.1 (ESRI 2012).

The units of analysis were 9,810 hexagonal cells, each approximately 834 km^2 in area, generated in a lattice across the conterminous United States using intensification of the Environmental Monitoring and Assessment Program (EMAP) North American hexagon coordinates (White and others 1992). These coordinates are the foundation of a sampling frame in which a hexagonal lattice was projected onto the conterminous United States by centering a large base hexagon over the region (Reams and others 2005, White and others 1992). This base hexagon can be subdivided into many smaller hexagons, depending on sampling needs, and serves as the basis of the plot sampling frame for the Forest Inventory and Analysis (FIA) Program (Reams and others 2005). Importantly, the hexagons maintain equal areas across the study region regardless of the degree of intensification of the EMAP hexagon coordinates. In addition, the hexagons are compact and uniform in their distance to the centroids of neighboring hexagons, meaning that a hexagonal lattice has a higher degree of isotropy (uniformity in all directions) than does a square grid (Shima and others 2010). These are convenient and highly useful attributes for spatial neighborhood analyses. These scalable hexagons also are independent of geopolitical and ecological boundaries, avoiding the possibility of different sample units (such as counties, States, or watersheds) encompassing vastly different areas (Potter and others 2016). We selected hexagons 834 km^2 in area because this is a manageable size for making monitoring and management decisions in analyses that are national in extent (Potter and others 2016).

The variable used in the hot spot analysis was the percentage of surveyed forest area in each hexagon exposed to either mortality-causing or defoliation-causing agents. This required first separately dissolving the mortality and defoliation polygon boundaries to generate an overall footprint of each general type of disturbance, then masking the dissolved polygons using a forest cover map (1-km^2 resolution) derived from Moderate Resolution Imaging Spectroradiometer (MODIS) satellite imagery by the U.S. Forest Service Remote Sensing Applications Center (USDA Forest Service 2008). The same process was undertaken with the polygons of the surveyed area. Finally, the percentage of surveyed forest within each hexagon exposed to mortality or defoliation agents was calculated by dividing the total forest-masked damage area by the forest-masked surveyed area.

The Getis-Ord G_i^* statistic was used to identify clusters of hexagonal cells in which the percentage of surveyed forest exposed to mortality or defoliation agents was higher than expected by chance. This statistic allows for the

decomposition of a global measure of spatial association into its contributing factors, by location, and is therefore particularly suitable for detecting nonstationarities in a dataset, such as when spatial clustering is concentrated in one subregion of the data (Anselin 1992).

The Getis-Ord G_i^* statistic for each hexagon summed the differences between the mean values in a local sample, determined by a moving window consisting of the hexagon and its 18 first- and second-order neighbors (the 6 adjacent hexagons and the 12 additional hexagons contiguous to those 6) and the global mean of all the forested hexagonal cells in the conterminous 48 States. It is then standardized as a *z*-score with a mean of 0 and a standard deviation of 1, with values > 1.96 representing significant ($p < 0.025$) local clustering of high values and values < -1.96 representing significant clustering of low values ($p < 0.025$), since 95 percent of the observations under a normal distribution should be within approximately 2 (exactly 1.96) standard deviations of the mean (Laffan 2006). In other words, a G_i^* value of 1.96 indicates that the local mean of the percentage of forest exposed to mortality-causing or defoliation-causing agents for a hexagon and its 18 neighbors is approximately 2 standard deviations greater than the mean expected in the absence of spatial clustering, while a G_i^* value of -1.96 indicates that the local mortality or defoliation mean for a hexagon and its 18 neighbors is approximately 2 standard deviations less than the mean expected in the absence of spatial clustering. Values between -1.96 and 1.96 have no statistically significant concentration of high or low values. In other words, when a hexagon has a G_i^* value between -1.96 and 1.96, mortality or defoliation damage within it and its 18 neighbors is not statistically different from a normal expectation.

It is worth noting that the -1.96 and 1.96 threshold values are not exact because the correlation of spatial data violates the assumption of independence required for statistical significance (Laffan 2006). The Getis-Ord approach does not require that the input data be normally distributed because the local G_i^* values are computed under a randomization assumption, with G_i^* equating to a standardized *z*-score that asymptotically tends to a normal distribution (Anselin 1992). The *z*-scores are reliable, even with skewed data, as long as the distance band used to define the local sample around the target observation is large enough to include several neighbors for each feature (ESRI 2012).

The low density of survey data from Alaska in 2014 (fig. 2.1) precluded the use of Getis-Ord hot spot analyses for this State. Instead, Alaska mortality and defoliation data were summarized by ecoregion section (Nowacki and Brock 1995), calculated as the percent of the forest within the surveyed areas affected by agents of mortality or defoliation. (As with the mortality and defoliation data, the flown area polygons were first dissolved to create an overall footprint.) For reference purposes, ecoregion sections (Cleland and others 2007) were also displayed on the geographic hot spot maps of the conterminous 48 United States.

RESULTS AND DISCUSSION

Conterminous United States Mortality

The national IDS survey data identified 88 different mortality-causing agents and complexes on approximately 1.75 million ha across the conterminous United States in 2014, slightly less than the combined land area of Connecticut and Delaware. (Three of these mortality-cause categories were "rollups" of multiple agents.) By way of comparison, forests are estimated to cover approximately 252 million ha of the conterminous 48 States (Smith and others 2009).

Mountain pine beetle (*Dendroctonus ponderosae*) was the most widespread mortality agent in 2014, detected on 707 649 ha (table 2.1), reversing a downward trend in the area affected by this insect in recent years; this area declined from 3.47 million ha in 2009 (Potter 2013) to 653 700 ha in 2013 (Potter and Paschke 2015b). The total footprint, or nonoverlapping sum of areas, of detected mountain pine beetle mortality from 2000 through 2014 exceeds 9.84 million ha, with the large majority occurring in the Forest Health Monitoring (FHM) Program Interior West region (as defined by the FHM Program) (table 2.2). This footprint is slightly larger than the State of Indiana.

Five other mortality agents and complexes were detected on more than 100 000 ha in 2014: spruce beetle (*Dendroctonus rufipennis*), fir engraver (*Scolytus ventralis*), western pine beetle (*Dendroctonus brevicomis*), five-needle pine decline, and subalpine fir (*Abies lasiocarpa*)

Table 2.1—Mortality agents and complexes affecting more than 5000 ha in the conterminous United States during 2014

Agents/complexes causing mortality, 2014	Area
	ha
Mountain pine beetle[a]	707 649
Spruce beetle	291 086
Fir engraver	285 896
Western pine beetle	133 968
Five-needle pine decline[a]	133 143
Subalpine fir mortality complex[a]	113 538
Douglas-fir beetle	77 814
Ips engraver beetles	66 083
Pinyon ips	44 948
Emerald ash borer	41 571
Mortality (unclassified)	24 904
Eastern larch beetle	18 335
California flatheaded borer	18 263
Jeffrey pine beetle	17 964
Beech bark disease	12 646
Sudden oak death	11 606
Balsam woolly adelgid	9 900
Multi-damage (insect/disease)	9 821
California fivespined ips	8 133
Unknown	7 985
Pine engraver	7 033
Flatheaded fir borer	5 992
Western balsam bark beetle[b]	5 376
Other mortality agents (65)	43 167
Total, all mortality agents	**1 753 763**

Note: All values are "footprint" areas for each agent or complex. The sum of the individual agents is not equal to the total for all agents due to the reporting of multiple agents per polygon.

[a] Rollup of multiple agent codes from the Insect and Disease Survey database.

[b] Also included in the subalpine fir mortality rollup.

Table 2.2—Footprint area affected by mountain pine beetle *(Dendroctonus ponderosae)*, by Forest Health Monitoring region, from 2000 through 2014

FHM region	Area
	ha
Interior West	7 615 518
West Coast	164 877
North Central	2 063 866
Total, all regions	**9 844 261**

mortality complex. Mortality from the western bark beetle group was detected on approximately 1.60 million ha in 2014, representing a large majority of the total area on which mortality was recorded across the conterminous States. This group encompasses 28 different agents in the IDS data (table 2.3).

The Interior West region had approximately 1.02 million ha on which mortality-causing agents and complexes were detected in 2014, an area that exceeded that of all other FHM regions combined (table 2.4). About 41 percent of this was associated with mountain pine beetle; also constituting a considerable area were spruce beetle (27 percent), subalpine fir mortality complex (11 percent), fir engraver (7 percent), and ips engraver beetles (*Ips* spp.) (6 percent). A total of 28 mortality agents and complexes were detected in the region.

The Getis-Ord analysis detected several major hot spots of intense mortality exposure in the Interior West region (fig. 2.2). As in 2012 and 2013, the most intense was a hot spot of very

Table 2.3—Beetle taxa included in the "western bark beetle" group

Western bark beetle mortality agents	Taxonomic classification
Bark beetles (non-specific)	Family Curculionidae, subfamily Scolytinae
California fivespined ips	*Ips paraconfusus*
Cedar and cypress bark beetles	*Phloeosinus* spp.
Douglas-fir beetle	*Dendroctonus pseudotsugae*
Douglas-fir engraver	*Scolytus unispinosus*
Douglas-fir pole beetle	*Pseudohylesinus nebulosus*
Fir engraver	*Scolytus ventralis*
Five-needle pine decline	—
Flatheaded borer	Family Buprestidae
Ips engraver beetles	*Ips* spp.
Jeffrey pine beetle	*Dendroctonus jeffreyi*
Lodgepole pine beetle	*Dendroctonus murrayanae*
Mountain pine beetle	*Dendroctonus ponderosae*
Pine engraver	*Ips pini*
Pinyon ips	*Ips confuses*
Pinyon pine mortality	—
Red turpentine beetle	*Dendroctonus valens*
Roundheaded pine beetle	*Dendroctonus adjunctus*
Silver fir beetle	*Pseudohylesinus sericeus*
Southern pine beetle	*Dendroctonus frontalis*
Spruce beetle	*Dendroctonus rufipennis*
Tip beetles	*Pityogenes* spp.
True fir bark beetles	*Scolytus* spp.
True fir *(Abies)* pest complex	—
Twig beetles	*Pityophthorus* spp.
Western balsam bark beetle	*Dryocoetes confuses*
Western cedar bark beetle	*Phloeosinus punctatus*
Western pine beetle	*Dendroctonus brevicomis*

— = not applicable.

Table 2.4—The top five mortality agents or complexes for each Forest Health Monitoring region and for Alaska in 2014

2014 mortality agents and complexes	Area
	ha
Interior West	
Mountain pine beetle[a]	418 815
Spruce beetle	276 030
Subalpine fir mortality complex[a]	112 084
Fir engraver	73 786
Ips engraver beetles	56 542
Other mortality agents and complexes (23)	151 213
Total, all mortality agents and complexes	**1 018 930**
North Central	
Emerald ash borer	38 790
Eastern larch beetle	18 335
Mortality	15 824
Beech bark disease	11 676
Mountain pine beetle[a]	6 121
Other mortality agents (12)	7 976
Total, all mortality agents and complexes	**98 723**
North East	
Mortality	8 974
Balsam woolly adelgid	6 851
Fir needle cast[b]	4 825
True fir bark beetles[b]	4 825
Emerald ash borer	2 761
Other mortality agents (39)	10 886
Total, all mortality agents and complexes	**28 173**

2014 mortality agents and complexes	Area
	ha
South	
Unknown	5 282
Hemlock woolly adelgid	1 469
Southern pine beetle	382
Other root or butt disease (known)	380
Ips engraver beetles	247
Other mortality agents (8)	48
Total, all mortality agents and complexes	**7 806**
West Coast	
Mountain pine beetle[a]	282 712
Fir engraver	212 110
Western pine beetle	120 236
Douglas-fir beetle	22 112
California flatheaded borer	18 263
Other mortality agents (25)	106 909
Total, all mortality agents and complexes	**600 131**
Alaska	
Yellow-cedar decline	8 055
Spruce beetle	5 987
Northern spruce engraver	2 970
Western balsam bark beetle	75
Defoliators	39
Total, all mortality agents and complexes	**17 109**

Note: The total area affected by other agents is listed at the end of each section. All values are "footprint" areas for each agent or complex. The sum of the individual agents is not equal to the total for all agents because of the reporting of multiple agents per polygon.

[a] Rollup of multiple agent codes from the Insect and Disease Survey database.

[b] Fir needle cast and true fir bark beetles co-occurred along with balsam woolly adelgid.

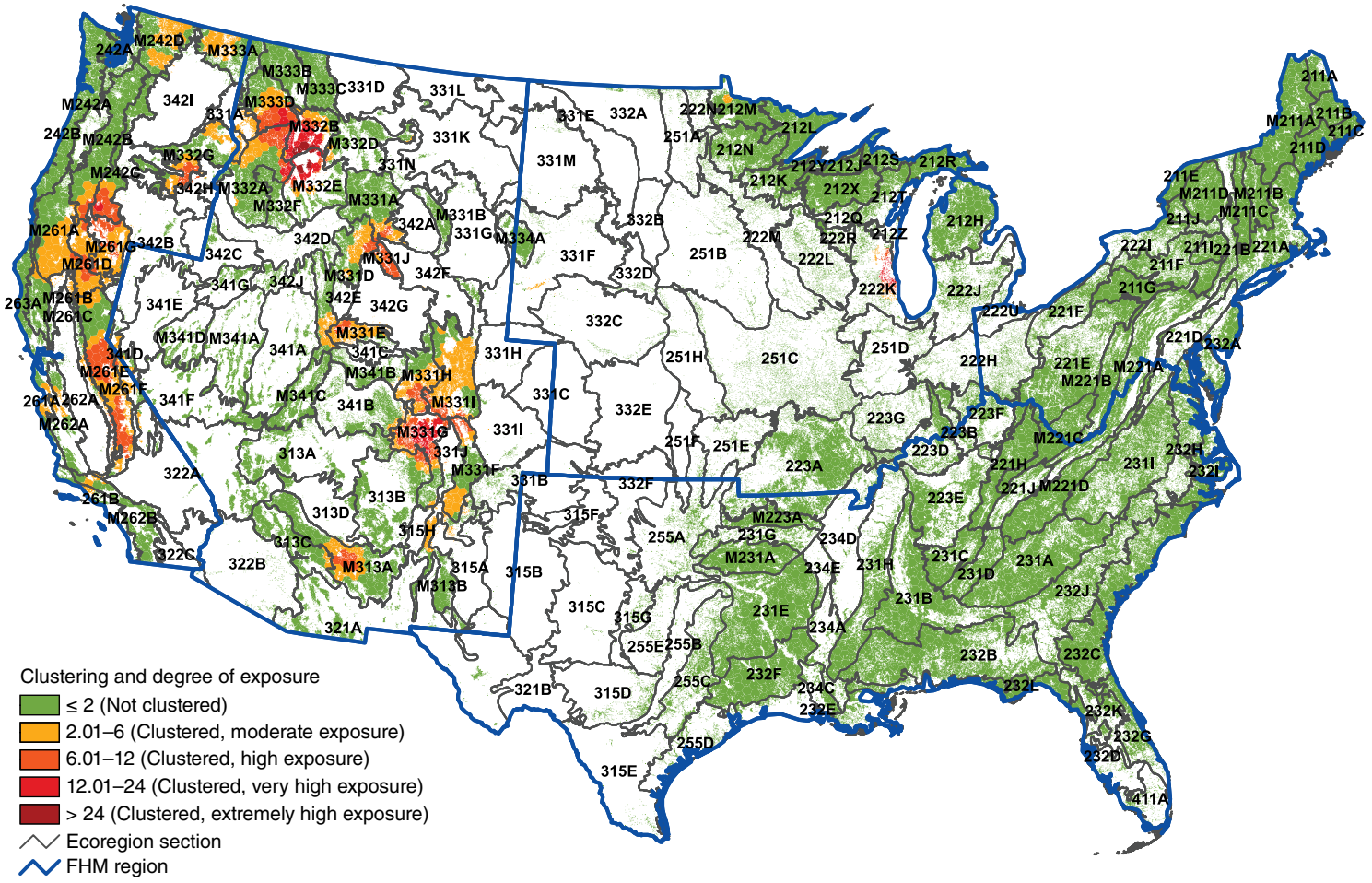

Figure 2.2—Hot spots of exposure to mortality-causing insects and diseases in 2014. Values are Getis-Ord G_i^* scores, with values >2 representing significant clustering of high percentages of forest area exposed to mortality agents. (No areas of significant clustering of low percentages of exposure, <-2, were detected.) The gray lines delineate ecoregion sections (Cleland and others 2007), and the blue lines delineate Forest Health Monitoring regions. Background forest cover is derived from Moderate Resolution Imaging Spectroradiometer (MODIS) imagery by the U.S. Forest Service Remote Sensing Applications Center. (Data source: U.S. Department of Agriculture, Forest Service, Forest Health Protection)

high and extremely high mortality exposure centered on the border between eastern Idaho and western Montana, especially in ecoregions M332B–Northern Rockies and Bitterroot Valley, M332E–Beaverhead Mountains, M332D–Belt Mountains, and M332A–Idaho Batholith. Mortality in this area was attributed almost entirely to mountain pine beetle in lodgepole pine (*Pinus contorta*), ponderosa pine (*Pinus ponderosa*), and whitebark pine (*Pinus albicaulis*) forests, along with some fir engraver in grand fir (*Abies grandis*) stands and Douglas-fir beetle (*Dendroctonus pseudotsugae*) in Douglas-fir (*Pseudotsuga menziesii*) stands.

A hot spot of very high mortality exposure was also detected in southwestern Colorado, centered on M331G–South-Central Highlands and extending into M331H–North-Central Highlands and Rocky Mountains, M331I–Northern Parks and Ranges, and M331F–Southern Parks and Rocky Mountain Range (fig. 2.2). A large majority of the mortality here was caused by spruce beetle in Engelmann spruce (*Picea engelmannii*) stands, although mortality was also associated with subalpine fir mortality complex in subalpine fir forests, with fir engraver in white fir (*Abies concolor*) forests, and with mountain pine beetle in ponderosa pine forests. Meanwhile, a hot spot of high mortality exposure associated with five-needle pine decline in whitebark and limber pine (*Pinus flexilis*) stands, spruce beetle in Engelmann spruce stands, and mountain pine beetle in whitebark pine stands was detected in M331J–Wind River Mountains, M331A–Yellowstone Highlands, and M331D–Overthrust Mountains.

In M331E–Uinta Mountains of northeastern Utah, a high-intensity hot spot, was mainly associated with spruce beetle-caused mortality in Engelmann spruce and with subalpine fir mortality complex in subalpine fir (fig. 2.2). Finally, farther south in east-central Arizona and west-central New Mexico, fir engraver in white fir and ips engraver beetle in ponderosa pine caused a hot spot of high mortality exposure in M313A–White Mountains-San Francisco Peaks-Mogollon Rim.

The FHM West Coast region had the second largest area on which mortality agents and complexes were detected, about 600 100 ha (table 2.4). Of the 30 agents and complexes detected, mountain pine beetle was the leading cause of mortality and was identified on about 282 700 ha, approximately 47 percent of the entire area. Other bark beetles, including fir engraver, western pine beetle, and Douglas-fir beetle, were also widespread causes of mortality in the region, as was the California flatheaded borer (*Phaenops californica*).

Bark beetles, primarily mountain pine beetle in lodgepole and ponderosa pine stands, were the primary agent associated with a hot spot of very high mortality exposure in southern Oregon, centered on M242C–Eastern Cascades and extending into M261G–Modoc Plateau, M242B–Western Cascades, and M261D–Southern Cascades (fig. 2.2). To the south, a hot spot of high mortality in M261D–Southern Cascades in northern California was associated with fir engraver in white fir and California red fir (*Abies magnifica*) and with western pine beetle

in ponderosa pine. To the northeast in eastern Oregon, a hot spot of high mountain pine beetle mortality in lodgepole pine was detected in M332G–Blue Mountains. Mountain pine beetle and spruce beetle also caused hot spots of moderate mortality exposure in northern Washington, in M242D–Northern Cascades and M333A–Okanogan Highland.

Two hot spots of high mortality exposure were detected in M261E–Sierra Nevada, in California (fig. 2.2). The more northerly of these was associated with mortality caused by western pine beetle in ponderosa pine; mountain pine beetle in sugar pine (*Pinus lambertiana*), whitebark pine, and lodgepole pine; fir engraver in white fir and California red fir; and Jeffrey pine beetle (*Dendroctonus jeffreyi*) in Jeffrey pine (*Pinus jeffreyi*). The more southerly Sierra Nevada mortality hot spot was caused by California flatheaded borer in Jeffrey pine, western pine beetle in ponderosa pine, fir engraver in California red fir, pinyon ips (*Ips confusus*) in single-leaf pinyon (*Pinus monophylla*), and mountain pine beetle in lodgepole and sugar pine.

Meanwhile, sudden oak death mortality in tanoak (*Lithocarpus densiflorus*) forests and multiple insect and disease damage in grey pine (*Pinus sabaniana*) stands caused a hot spot of moderate mortality near the central California coast, in 261A–Central California Coast and M262A–Central California Coast Ranges. Farther south, pinyon ips in single-leaf pinyon and California fivespined ips (*Ips paraconfusus*) in Jeffrey pine resulted in a moderate mortality hot spot in M262B–Southern California Mountain and Valley.

In the North Central FHM region, mortality was recorded on nearly 99 000 ha, with emerald ash borer the most widely identified causal agent, found on almost 39 000 ha (table 2.4). Two more of the 17 agents and complexes detected in the region affected areas exceeding 10 000 ha: eastern larch beetle (*Dendroctonus simplex*) and beech bark disease complex. Mortality with unclassified causes also was detected on nearly 16 000 ha. Emerald ash borer was the cause of the single mortality hot spot in the region, in 222K–Southwestern Great Lakes Morainal, in southeastern Wisconsin (fig. 2.2).

In the North East FHM region, the FHP survey recorded mortality-causing agents and complexes on approximately 28 000 ha (table 2.4). Of the classified mortality agents and complexes, balsam woolly adelgid (*Adelges piceae*) was the most widely detected, followed by fir needle cast/true fir bark beetles, and emerald ash borer. Mortality with an unclassified cause was identified on nearly 9 000 ha. In the South, mortality was detected on about 7 800 ha, mostly with an unknown cause. Hemlock woolly adelgid was the most commonly identified agent (table 2.4). No geographic hot spots of mortality were detected in the North East and South FHM regions.

Conterminous United States Defoliation

In 2014, the national IDS survey identified 67 defoliation agents and complexes affecting approximately 1.73 million ha across the

conterminous United States, an area slightly smaller than the combined land area of Connecticut and Delaware. The two most widespread defoliation causes were "rollups" of multiple agents: eastern and western spruce budworms (*Choristoneura occidentalis* and *C. fumiferana*), affecting nearly 954 000 ha, and tent caterpillars (*Malacosoma* spp.), detected on approximately 233 000 ha (table 2.5). Two other insects—gypsy moth (*Lymantria dispar*) and baldcypress leafroller (*Archips goyerana*)—each also affected more than 100 000 ha, and fall cankerworm (*Alsophila pometaria*) was detected on nearly 99 000 ha (table 2.5).

The Interior West FHM region had the largest area on which defoliating agents and complexes were detected in 2014, approximately 904 000 ha (table 2.6). Approximately 89 percent of this (about 804 000 ha) was attributed to western spruce budworm (*Choristoneura occidentalis*) (table 2.6). Unknown defoliators and aspen defoliation were the next most widely detected defoliation agents of the 21 that were identified.

All four defoliation hot spots in the region (fig. 2.3) were associated with western spruce budworm, along with other agents or complexes. The largest of these, caused by western spruce budworm in fir forests, was a hot spot of very high defoliation exposure that centered on M333B–Flathead Valley and M333C–Northern Rockies and extended into M332B–Northern Rockies and Bitterroot Valley and M332D–Belt Mountains. Similarly, western spruce budworm activity in Douglas-fir forests generated a hot

Table 2.5—Defoliation agents and complexes affecting more than 5000 ha in the conterminous United States in 2014

Agents/complexes causing defoliation, 2014	Area
	ha
Spruce budworm (eastern and western)[a]	953 918
Tent caterpillars[a]	233 259
Gypsy moth	158 965
Baldcypress leafroller	111 337
Fall cankerworm	98 680
Defoliators (unclassified)	81 149
Unknown defoliator	41 619
Jack pine budworm	41 271
Aspen defoliation	28 879
Large aspen tortrix	22 576
Oak leafroller	21 490
Winter moth	19 714
Douglas-fir tussock moth	12 633
Larch casebearer	10 352
Other defoliator (known)	8 974
Lophodermium needle cast of pines	8 353
Western blackheaded budworm	8 129
Larch needle cast	7 670
Leafroller/seed moth	7 278
Loopers	6 608
Pinyon needle scale	6 137
Other defoliation agents (46)	27 208
Total, all defoliation agents	**1 728 098**

Note: All values are "footprint" areas for each agent or complex. The sum of the individual agents is not equal to the total for all agents due to the reporting of multiple agents per polygon.

[a] Rollup of multiple agent codes from the Insect and Disease Survey database.

Table 2.6—The top five defoliation agents or complexes for each Forest Health Monitoring region and for Alaska in 2014

2014 defoliation agents and complexes	Area
	ha
Interior West	
Western spruce budworm[a]	804 123
Unknown defoliator	39 986
Aspen defoliation	28 879
Other defoliator (known)	8 974
Larch needle cast	7 099
Other defoliation agents and complexes (16)	22 658
Total, all defoliation agents and complexes	**903 617**
North Central	
Spruce budworm[a]	111 361
Defoliators (unclassified)	80 612
Forest tent caterpillar[b]	63 059
Jack pine budworm	41 271
Large aspen tortrix	22 576
Other defoliation agents and complexes (13)	36 168
Total, all defoliation agents and complexes	**355 046**
North East	
Gypsy moth	142 076
Fall cankerworm	75 587
Oak leafroller	21 490
Winter moth	19 714
Loopers	6 608
Other defoliation agents and complexes (22)	7 846
Total, all defoliation agents and complexes	**198 689**

2014 defoliation agents and complexes	Area
	ha
South	
Forest tent caterpillar[b]	163 675
Baldcypress leafroller	111 337
Fall cankerworm	23 093
Jumping oak gall wasp	359
Unknown	56
Other defoliation agents and complexes (7)	23
Total, all defoliation agents and complexes	**193 577**
West Coast	
Western spruce budworm[a]	38 413
Douglas-fir tussock moth	11 434
Western blackheaded budworm	8 129
Western tent caterpillar[b]	5 623
Lodgepole needleminer	3 667
Other defoliation agents and complexes (14)	10 107
Total, all defoliation agents and complexes	**77 170**
Alaska	
Defoliators (unclassified)	120 016
Aspen leafminer	50 048
Birch leafroller	48 987
Unknown	23 835
Willow leaf blotchminer	8 029
Other defoliation agents and complexes (7)	6 795
Total, all defoliation agents and complexes	**252 833**

Note: The total area affected by other agents is listed at the end of each section. All values are "footprint" areas for each agent or complex. The sum of the individual agents is not equal to the total for all agents due to the reporting of multiple agents per polygon.

[a] Included in spruce budworm rollup.

[b] Included in tent caterpillar rollup.

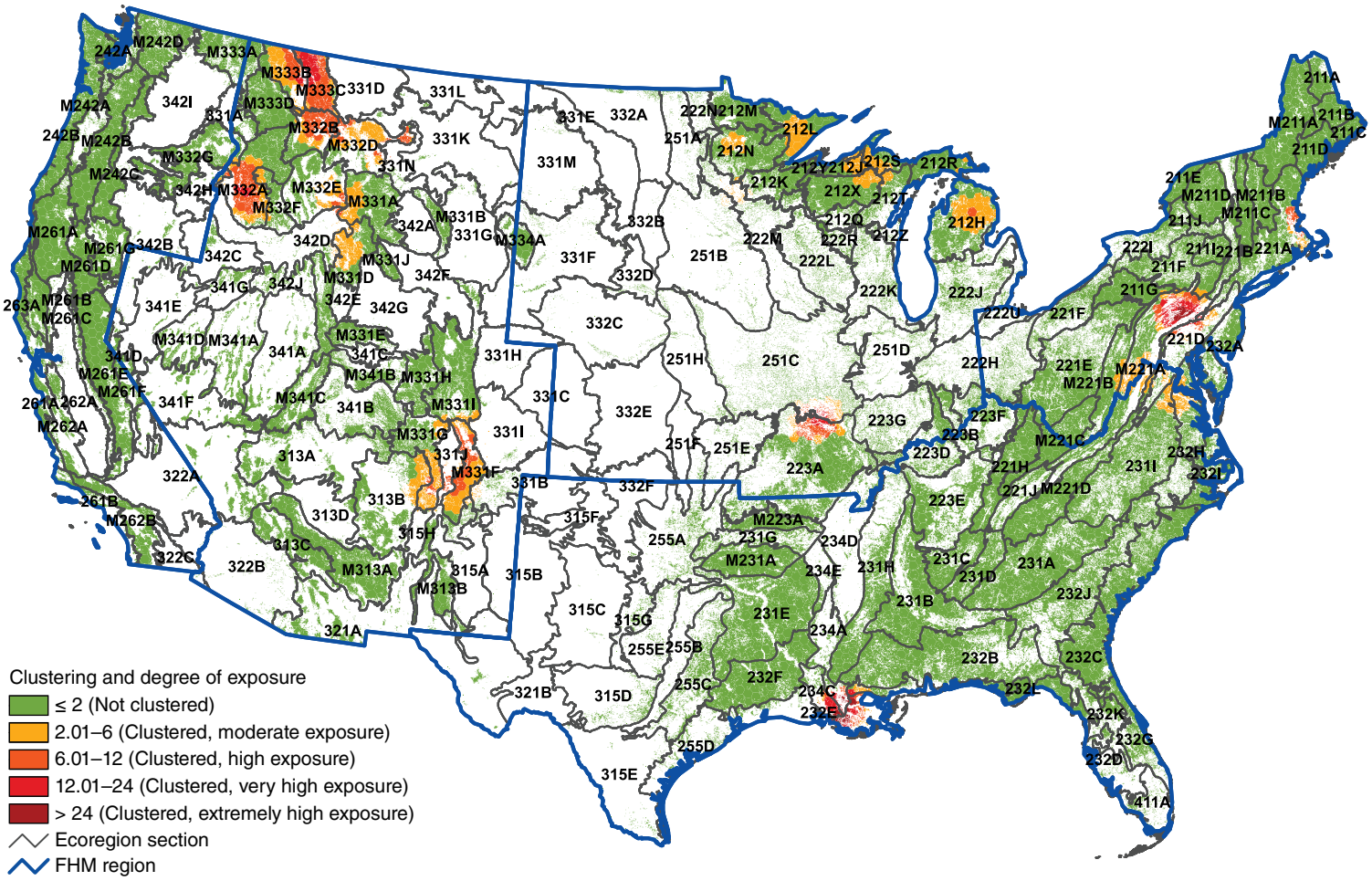

Figure 2.3—Hot spots of exposure to defoliation-causing insects and diseases in 2014. Values are Getis-Ord G_i scores, with values > 2 representing significant clustering of high percentages of forest area exposed to defoliation agents. (No areas of significant clustering of low percentages of exposure, < -2, were detected). The gray lines delineate ecoregion sections (Cleland and others 2007), and the blue lines delineate Forest Health Monitoring regions. Background forest cover is derived from Moderate Resolution Imaging Spectroradiometer (MODIS) imagery by the U.S. Forest Service Remote Sensing Applications Center. (Data source: U.S. Department of Agriculture, Forest Service, Forest Health Protection)*

spot of very high defoliation exposure in central Idaho (M332A–Idaho Batholith). Western spruce budworm defoliation of fir and Douglas-fir resulted in a hot spot in M332E–Beaverhead Mountains and M331A–Yellowstone Highlands at the intersection of Montana, Idaho, and Wyoming. Finally, a hot spot in southern Colorado and northern New Mexico (M331F–Southern Parks and Rocky Mountain Range and M331G–South-Central Highlands) was associated with western spruce budworm defoliation of Douglas-fir and with aspen defoliation.

Western spruce budworm, meanwhile, accounted for about 50 percent of the approximately 77 200 ha of defoliation recorded in the FHM West Coast region (table 2.6). The other most commonly detected defoliators of the 19 recorded in the region were Douglas-fir tussock moth, western blackheaded budworm (*Acleris gloverana*), and western tent caterpillar (*Malacosoma californicum*). No geographic hot spots of defoliation were identified in the region.

Eighteen different defoliation agents and complexes resulted in the detection of about 355 000 ha of defoliation in the North Central FHM region. Eastern and western spruce budworm together represented the most commonly detected defoliation agent in the region, detected on more than 111 000 ha. After the spruce budworms, unclassified defoliators, forest tent caterpillar (*Malacosoma disstria*), jack pine budworm (*Choristoneura pinus*), and large aspen tortrix (*Choristoneura conflictana*) were the most commonly recorded defoliators, affecting approximately 80 600 ha, 63 000 ha, 41 300 ha, and 22 600 ha, respectively (table 2.6).

Our hot spot analysis detected four main geographic clusters of defoliation exposure in the North Central FHM region (fig. 2.3). One in 212H–Northern Lower Peninsula of Michigan was associated with jack pine budworm in jack pine (*Pinus banksiana*), gypsy moth and large aspen tortrix in quaking aspen (*Populus tremuloides*), and spruce budworm in spruce. Meanwhile, spruce budworm in white spruce (*Picea glauca*) and balsam fir (*Abies balsamea*) forests caused a hot spot of moderate defoliation exposure on the Upper Peninsula of Michigan, at the intersection of four ecoregions: 212J–Southern Superior Highlands, 212S–Northern Upper Peninsula, 212T–Northern Green Bay Lobe, and 212X–Northern Highlands. A hot spot in 212L–Northern Superior Uplands of northeastern Minnesota was the result of spruce budworm defoliation in balsam fir stands. A short distance to the west, a hot spot of moderate defoliation exposure in north-central Minnesota (212N–Northern Minnesota Drift and Lake Plains) was associated with forest tent caterpillar activity in hardwood forests. Finally, low-severity unclassified defoliators in oak forests of east-central Missouri resulted in a hot spot in 223A–Ozark Highlands.

Twenty-seven defoliation agents and complexes were identified on about 199 000 ha in the North East FHM region, with gypsy moth the most widely detected on nearly 72 percent of this area (more than 142 000 ha). Fall cankerworm was recorded on nearly 75 600 ha, oak leafroller on 21 500 ha, and winter moth on 19 700 ha (table 2.6). A gypsy moth outbreak in eastern Pennsylvania caused a hot spot of

extremely high defoliation exposure in M221A–Northern Ridge and Valley (fig. 2.3). Gypsy moth, fall cankerworm, and loopers together resulted in a hot spot of moderate defoliation in the same ecoregion, but farther south in eastern West Virginia. Finally, a hot spot of high defoliation exposure was caused by winter moth in 221A–Lower New England.

In the South FHM region, 12 defoliators were identified on approximately 193 600 ha, with forest tent caterpillar the most widely detected on nearly 163 700 ha, followed by baldcypress leafroller and fall cankerworm. In southern Louisiana, these two insects caused a hot spot of extremely high defoliation exposure in ecoregions 232E–Louisiana Coastal Prairies and Marshes and 234C–Atchafalaya and Red River Alluvial Plains (fig. 2.3). Meanwhile, fall cankerworm caused a hot spot of moderate defoliation exposure spanning two ecoregions in northern Virginia and southern Maryland (in the North East FHM region), 232H–Middle Atlantic Coastal Plains and Flatwoods and 231I–Central Appalachian Piedmont.

Alaska

In Alaska, approximately 7.74 million ha of forested area was surveyed, 15.1 percent of the total forested land in the State (approximately 51.36 million ha). Mortality was recorded on approximately 17 100 ha in 2014, associated with five agents and complexes (table 2.4). This is a very small proportion (> 1 percent) of the forested area surveyed. Yellow-cedar (*Chamaecyparis nootkatensis*) decline was the most widely detected mortality agent, found on about 8 100 ha in the Alaska panhandle, whereas spruce beetle was identified on almost 6 000 ha, mostly in southern parts of the State, and northern spruce engraver (*Ips perturbatus*) was detected on just under 3 000 ha mostly in the central and northern forested areas of Alaska. The percentage of surveyed forest exposed to mortality agents in 2014 did not exceed 1 percent in any of Alaska's ecoregions (fig. 2.4).

Meanwhile, defoliators were detected on a much larger area of Alaska during 2014, with 12 defoliating agents recorded on approximately 252 800 ha (table 2.6). Of this area, about 120 000 ha consisted of unclassified defoliators. Aspen leafminer (*Phyllocnistis populiella*) and birch leafroller (*Epinotia solandriana*) were both detected on about 50 000 ha, with aspen leafminer mostly in the central parts of the State and birch leafroller in the southwestern and central areas.

The Alaska ecoregions with the highest proportion of surveyed forest area affected by defoliators in 2014 were located in the west-central and south-central parts of the State (fig. 2.5). M131B–Nulato Hills had the highest proportion of surveyed area affected by defoliators (13.6 percent), followed by M213A–Northern Aleutian Range with 8 percent. Activity by general defoliators, mostly in willow (*Salix* spp.) stands, was the situation in the first of these, while activity by birch leafroller in birch (*Beluta* spp.) stands and general defoliators in red alder (*Alnus rubra*) forests caused the recorded defoliation in the latter ecoregion. Areas of moderately high defoliation (1–5 percent) extended across the middle of the State and along the southwestern coast.

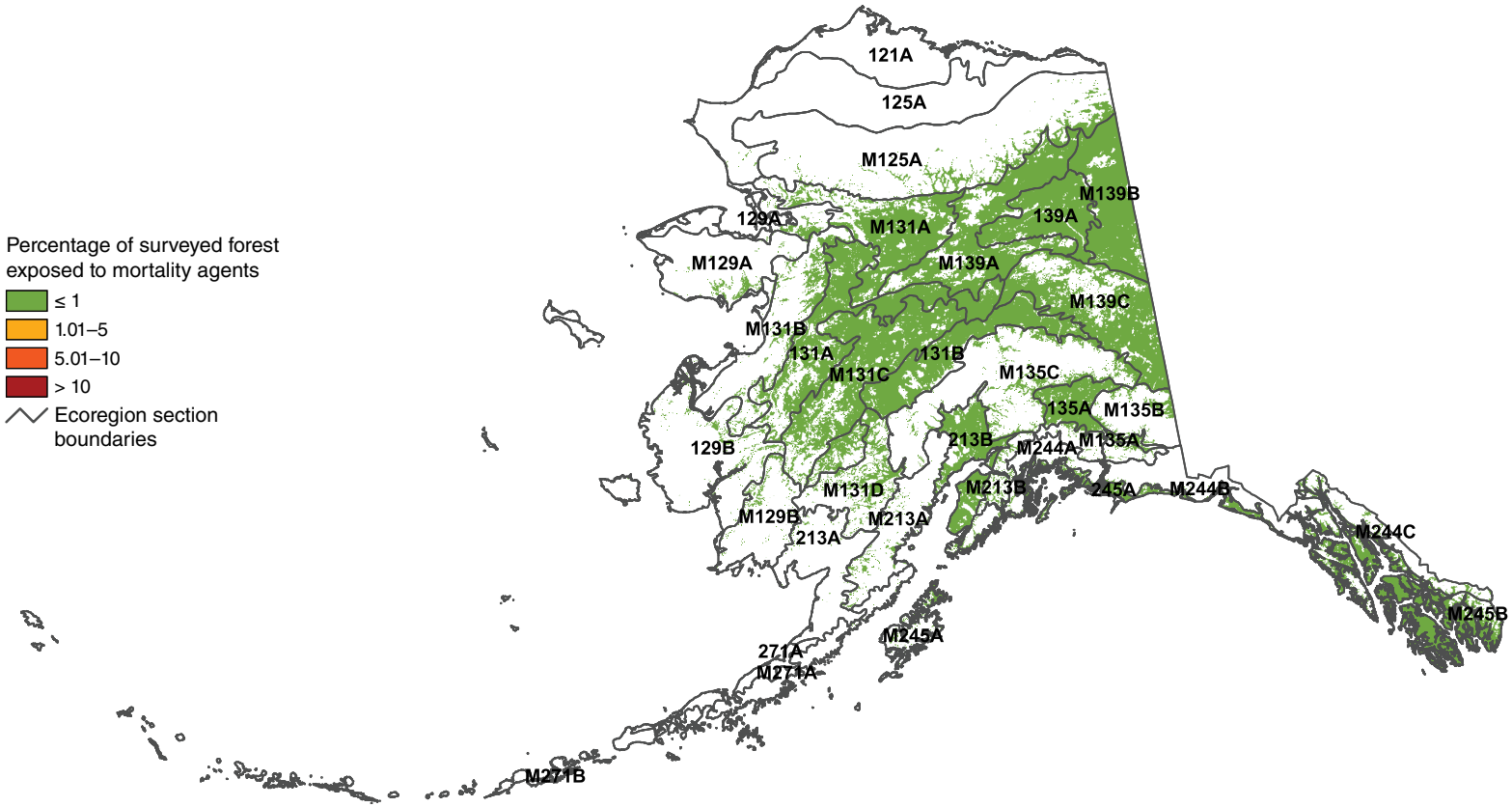

Figure 2.4—Percentage of surveyed forest in Alaska ecoregion sections exposed to mortality-causing insects and diseases in 2014. The gray lines delineate ecoregion sections (Nowacki and Brock 1995). Background forest cover is derived from Moderate Resolution Imaging Spectroradiometer (MODIS) imagery by the U.S. Forest Service Remote Sensing Applications Center. (Data source: U.S. Department of Agriculture, Forest Service, Forest Health Protection)

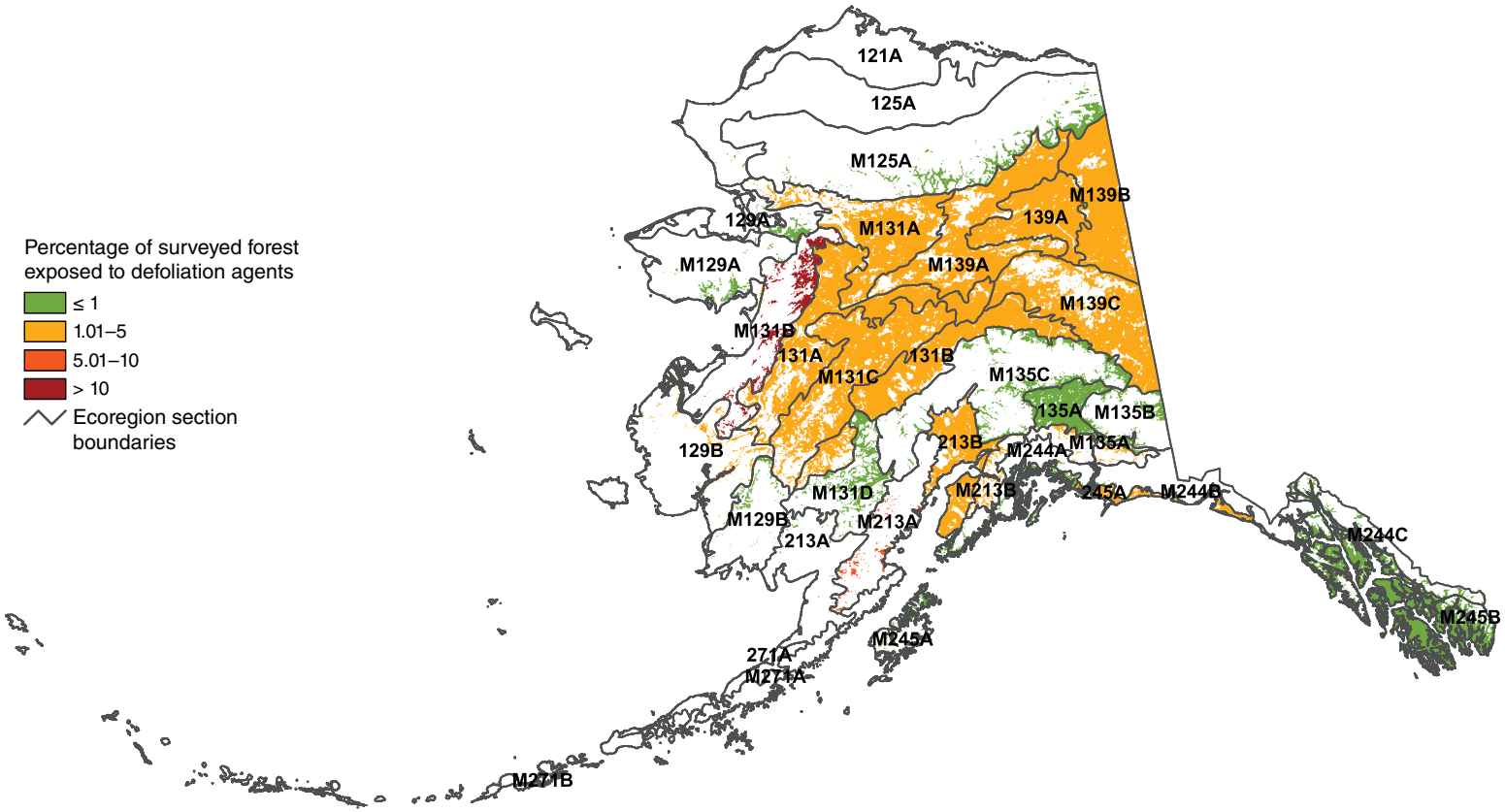

Figure 2.5—Percentage of surveyed forest in Alaska ecoregion sections exposed to defoliation-causing insects and diseases in 2014. The gray lines delineate ecoregion sections (Nowacki and Brock 1995). Background forest cover is derived from Moderate Resolution Imaging Spectroradiometer (MODIS) imagery by the U.S. Forest Service Remote Sensing Applications Center. (Data source: U.S. Department of Agriculture, Forest Service, Forest Health Protection)

CONCLUSION

Continued monitoring of insect and disease outbreaks across the United States will be necessary for determining appropriate follow-up investigation and management activities. Because of the limitations of survey efforts to detect certain important forest insects and diseases, the pests and pathogens discussed in this chapter do not include all the biotic forest health threats that should be considered when making management decisions and budget allocations. However, large-scale assessments of mortality and defoliation exposure, including geographical hot spot detection analyses, offer a useful approach for identifying geographic areas where the concentration of monitoring and management activities might be most effective.

LITERATURE CITED

Anselin, L. 1992. Spatial data analysis with GIS: an introduction to application in the social sciences. Tech. Rep. 92-10. Santa Barbara, CA: National Center for Geographic Information and Analysis. 53 p.

Brockerhoff, E.G.; Liebhold, A.M.; Jactel, H. 2006. The ecology of forest insect invasions and advances in their management. Canadian Journal of Forest Research. 36(2): 263–268.

Castello, J.D.; Leopold, D.J.; Smallidge, P.J. 1995. Pathogens, patterns, and processes in forest ecosystems. BioScience. 45(1): 16–24.

Cleland, D.T.; Freeouf, J. A.; Keys, J.E.; [and others]. 2007. Ecological subregions: sections and subsections for the conterminous United States. In: Sloan, A.M., tech. ed. Washington, DC: U.S. Department of Agriculture, Forest Service. Gen. Tech. Rep. WO-76D. [Map, presentation scale 1:3,500,000; colored]. Also on CD-ROM as a GIS coverage in ArcINFO format.

Edmonds, R.L.; Agee, J.K.; Gara, R.I. 2011. Forest health and protection. Long Grove, IL: Waveland Press, Inc. 667 p.

ESRI. 2012. ArcMap® 10.1. Redlands, CA: Environmental Systems Research Institute, Inc.

Forest Health Protection (FHP). 2014. Insect and Disease Detection Survey Database (IDS) [database on the Internet]. Fort Collins, CO: U.S. Department of Agriculture, Forest Service, Forest Health Technology Enterprise Team. http://foresthealth.fs.usda.gov/ids. [Date accessed: July 20, 2015].

Getis, A.; Ord, J. K. 1992. The analysis of spatial association by use of distance statistics. Geographical Analysis. 24(3): 189–206.

Holdenrieder, O.; Pautasso, M.; Weisberg, P.J.; Lonsdale, D. 2004. Tree diseases and landscape processes: the challenge of landscape pathology. Trends in Ecology & Evolution. 19(8): 446–452.

Laffan, S.W. 2006. Assessing regional scale weed distributions, with an Australian example using *Nassella trichotoma*. Weed Research. 46(3): 194–206.

Liebhold, A.M.; McCullough, D.G.; Blackburn, L.M. [and others]. 2013. A highly aggregated geographical distribution of forest pest invasions in the USA. Diversity and Distributions. 19: 1208–1216.

Mack, R.N.; Simberloff, D.; Lonsdale, W.M. [and others]. 2000. Biotic invasions: causes, epidemiology, global consequences, and control. Ecological Applications. 10(3): 689–710.

Manion, P.D. 2003. Evolution of concepts in forest pathology. Phytopathology. 93: 1052–1055.

Nowacki, G.; Brock, T. 1995. Ecoregions and subregions of Alaska [EcoMap]. Version 2.0. Juneau, AK: U.S. Department of Agriculture, Forest Service, Alaska Region. [Map, presentation scale 1:5,000,000; colored].

Parry, D.; Teale, S.A. 2011. Alien invasions: the effects of introduced species on forest structure and function. In: Castello, J.D.; Teale, S.A., eds. Forest health: an integrated perspective. New York: Cambridge University Press. 115–162.

Potter, K.M. 2012. Large-scale patterns of insect and disease activity in the conterminous United States and Alaska from the national Insect and Disease Detection Survey database, 2007 and 2008. In: Potter, K.M.; Conkling, B.L., eds. Forest Health Monitoring 2009 national technical report. Gen. Tech. Rep. SRS-167. Asheville, NC: U.S. Department of Agriculture, Forest Service, Southern Research Station: 63–78.

Potter, K.M. 2013. Large-scale patterns of insect and disease activity in the conterminous United States and Alaska from the national Insect and Disease Detection Survey, 2009. In: Potter, K.M.; Conkling, B.L., eds. Forest Health Monitoring: national status, trends, and analysis 2010. Gen. Tech. Rep. SRS-176. Asheville, NC: U.S. Department of Agriculture, Forest Service, Southern Research Station: 15–29.

Potter, K.M.; Koch, F.H. 2012. Large-scale patterns of insect and disease activity in the conterminous United States and Alaska, 2006. In: Potter, K.M.; Conkling, B.L., eds. Forest Health Monitoring 2008 national technical report. Gen. Tech. Rep. SRS-158. Asheville, NC: U.S. Department of Agriculture, Forest Service, Southern Research Station: 63–72.

Potter, K.M.; Koch, F.H.; Oswalt, C.M.; Iannone, B.V. 2016. Data, data everywhere: detecting spatial patterns in fine-scale ecological information collected across a continent. Landscape Ecology. 31(1): 67–84.

Potter, K.M.; Paschke, J.L. 2013. Large-scale patterns of insect and disease activity in the conterminous United States and Alaska from the national Insect and Disease Detection Survey database, 2010. In: Potter, K.M.; Conkling, B.L., eds. Forest Health Monitoring: national status, trends, and analysis 2011. Gen. Tech. Rep. SRS-185. Asheville, NC: U.S. Department of Agriculture, Forest Service, Southern Research Station: 15–28.

Potter, K.M.; Paschke, J.L. 2014. Large-scale patterns of insect and disease activity in the conterminous United States and Alaska from the national Insect and Disease Survey database, 2011. In: Potter, K.M.; Conkling, B.L., eds. Forest Health Monitoring: national status, trends, and analysis 2012. Gen. Tech. Rep. SRS-198. Asheville, NC: U.S. Department of Agriculture, Forest Service, Southern Research Station: 19–34.

Potter, K.M.; Paschke, J.L. 2015a. Large-scale patterns of insect and disease activity in the conterminous United States and Alaska from the national Insect and Disease Survey database, 2012. In: Potter, K.M.; Conkling, B.L., eds. Forest Health Monitoring: national status, trends, and analysis 2013. Gen. Tech. Rep. SRS-207. Asheville, NC: U.S. Department of Agriculture, Forest Service, Southern Research Station: 19–36.

Potter, K.M.; Paschke, J.L. 2015b. Large-scale patterns of insect and disease activity in the conterminous United States and Alaska from the national Insect and Disease Survey database, 2013. In: Potter, K.M.; Conkling, B.L., eds. Forest Health Monitoring: national status, trends, and analysis 2014. Gen. Tech. Rep. SRS-209. Asheville, NC: U.S. Department of Agriculture, Forest Service, Southern Research Station: 19–38.

Reams, G.A.; Smith, W.D.; Hansen, M.H. [and others]. 2005. The Forest Inventory and Analysis sampling frame. In: Bechtold, W.A.; Patterson, P.L., eds. The enhanced Forest Inventory and Analysis Program—national sampling design and estimation procedures. Asheville, NC: U.S. Department of Agriculture, Forest Service, Southern Research Station: 11–26.

Shima T.; Sugimoto S.; Okutomi, M. 2010. Comparison of image alignment on hexagonal and square lattices. 2010 IEEE International Conference on Image Processing: 141–144. DOI:10.1109/icip.2010.5654351.

Smith, W.B.; Miles, P.D.; Perry, C.H.; Pugh, S.A. 2009. Forest resources of the United States, 2007. Gen. Tech. Rep. WO-78. Washington, DC: U.S. Department of Agriculture Forest Service. 336 p.

Teale, S.A.; Castello, J.D. 2011. Regulators and terminators: the importance of biotic factors to a healthy forest. In: Castello, J.D.; Teale, S.A., eds. Forest health: an integrated perspective. New York: Cambridge University Press: 81–114.

U.S. Department of Agriculture (USDA) Forest Service. 2008. National forest type data development. http://svinetfc4.fs.fed.us/rastergateway/forest_type/. [Date accessed: May 13, 2008].

White, D.; Kimerling, A.J.; Overton, W.S. 1992. Cartographic and geometric components of a global sampling design for environmental monitoring. Cartography and Geographic Information Systems. 19(1): 5–22.

Zhang, L.; Rubin, B.D.; Manion, P.D. 2011. Mortality: the essence of a healthy forest. In: Castello, J.D.; Teale, S.A., eds. Forest health: an integrated perspective. New York: Cambridge University Press: 17–49.

CHAPTER 3.

Large-Scale Patterns of Forest Fire Occurrence in the Conterminous United States, Alaska, and Hawai'i, 2014

Kevin M. Potter

INTRODUCTION

Free-burning wildland fire has been a frequent ecological phenomenon on the American landscape, and its expression has changed as new peoples and land uses have become predominant (Pyne 2010). As a pervasive disturbance agent operating at many spatial and temporal scales, wildland fire is a key abiotic factor affecting forest health both positively and negatively. In some ecosystems, wildland fires have been essential for regulating processes that maintain forest health (Lundquist and others 2011). Wildland fire, for example, is an important ecological mechanism that shapes the distributions of species, maintains the structure and function of fire-prone communities, and acts as a significant evolutionary force (Bond and Keeley 2005).

At the same time, wildland fires have created forest health problems in some ecosystems (Edmonds and others 2011). Specifically, fire outside the historic range of frequency and intensity can impose extensive ecological and socioeconomic impacts. Current fire regimes on more than half of the forested area in the conterminous United States have been moderately or significantly altered from historical regimes, potentially altering key ecosystem components such as species composition, structural stage, stand age, canopy closure, and fuel loadings (Schmidt and others 2002). Understanding existing fire regimes is essential to properly assessing the impact of fire on forest health because changes to historical fire regimes can alter forest developmental patterns, including the establishment, growth, and mortality of trees (Lundquist and others 2011).

As a result of intense suppression efforts during most of the 20th century, the forest area burned annually decreased from approximately 16 million to 20 million ha (40–50 million acres) in the early 1930s to about 2 million ha (5 million acres) in the 1970s (Vinton 2004). In some regions, plant communities have experienced or are undergoing rapid compositional and structural changes as a result of fire suppression (Nowacki and Abrams 2008). At the same time, fires in some regions and ecosystems have become larger, more intense, and more damaging because of the accumulation of fuels as a result of prolonged fire suppression (Pyne 2010). Such large wildland fires also can have long lasting social and economic consequences, which include the loss of human life and property, smoke-related human health impacts, and the economic cost and dangers of fighting the fires themselves (Gill and others 2013, Richardson and others 2012).

Fire regimes have been dramatically altered, in particular, by fire suppression (Barbour and others 1999) and by the introduction of nonnative invasive plants, which can change fuel properties and in turn both affect fire behavior and alter fire regime characteristics such as frequency, intensity, type, and seasonality (Brooks and others 2004). Additionally, changes in fire intensity

and recurrence could result in decreased forest resilience and persistence (Lundquist and others 2011), and fire regimes altered by global climate change could cause large-scale shifts in vegetation spatial patterns (McKenzie and others 1996).

This chapter presents analyses of fire occurrence data, collected nationally each day by satellite, that map and quantify where fire occurrences have been concentrated spatially across the conterminous United States, Alaska, and Hawai'i in 2014. It also, within a geographic context, compares 2014 fire occurrences to all the recent years for which such data are available. Quantifying and monitoring such medium-scale patterns of fire occurrence across the United States can help improve the understanding of the ecological and economic impacts of fire as well as the appropriate management and prescribed use of fire. Specifically, large-scale assessments of fire occurrence can help identify areas where specific management activities may be needed, or where research into the ecological and socioeconomic impacts of fires may be required.

METHODS

Data

Annual monitoring and reporting of active wildland fire events using the Moderate Resolution Imaging Spectroradiometer (MODIS) Active Fire Detections for the United States database (USDA Forest Service 2015) allows analysts to spatially display and summarize fire occurrences across broad geographic regions (Coulston and others 2005; Potter 2012a, 2012b, 2013a, 2013b, 2014, 2015a, 2015b). A fire occurrence is defined as one daily satellite detection of wildland fire in a 1-km^2 pixel, with multiple fire occurrences possible on a pixel across multiple days resulting from a single wildland fire lasting multiple days. The data are derived using the MODIS Rapid Response System (Justice and others 2002, 2011) to extract fire location and intensity information from the thermal infrared bands of imagery collected daily by two satellites at a resolution of 1 km^2, with the center of a pixel recorded as a fire occurrence (USDA Forest Service 2015). The Terra and Aqua satellites' MODIS sensors identify the presence of a fire at the time of image collection, with Terra observations collected in the morning and Aqua observations collected in the afternoon. The resulting fire occurrence data represent only whether a fire was active because the MODIS data bands do not differentiate between a hot fire in a relatively small area (0.01 km^2, for example) and a cooler fire over a larger area (1 km^2, for example). The MODIS Active Fire database does well at capturing large fires during cloud-free conditions but may underrepresent rapidly burning, small, and low-intensity fires, as well as fires in areas with frequent cloud cover (Hawbaker and others 2008). For large-scale assessments, the dataset represents a good alternative to the use of information on ignition points, which may

be preferable but can be difficult to obtain or may not exist (Tonini and others 2009). For more information about the performance of this product, see Justice and others (2011).

It is important to underscore that estimates of burned area and calculations of MODIS-detected fire occurrences are two different metrics for quantifying fire activity within a given year. Most importantly, the MODIS data contain both spatial and temporal components because persistent fire will be detected repeatedly over several days on a given 1-km^2 pixel. In other words, a location can be counted as having a fire occurrence multiple times, once for each day a fire is detected at the location. Analyses of the MODIS-detected fire occurrences, therefore, measure the total number of daily 1-km^2 pixels with fire during a year, as opposed to quantifying only the area on which fire occurred at some point during the course of the year.

Analyses

These MODIS products for 2014 were processed in ArcMap® (ESRI 2012) to determine number of fire occurrences per 100 km^2 (10 000 ha) of forested area for each ecoregion section in the conterminous 48 States (Cleland and others 2007) and Alaska (Nowacki and Brock 1995) and for each of the major islands of Hawai'i. This forest fire occurrence density measure was calculated after screening out wildland fires on nonforested pixels using a forest cover layer derived from MODIS imagery by the U.S. Forest Service Remote Sensing Applications Center (RSAC) (USDA Forest Service 2008). The total numbers of forest fire occurrences were also determined separately for the conterminous States, Alaska, and Hawai'i.

The fire occurrence density value for each ecoregion in 2014 was then compared with the mean fire density values for the first 13 full years of MODIS Active Fire data collection (2001–13). Specifically, the difference of the 2014 value and the previous 13-year mean for an ecoregion was divided by the standard deviation across the previous 13-year period, assuming normal distribution of fire density over time in the ecoregion. The result for each ecoregion was a standardized *z*-score, which is a dimensionless quantity describing the degree to which the fire occurrence density in the ecoregion in 2014 was higher, lower, or the same relative to all the previous years for which data have been collected, accounting for the variability in the previous years. The *z*-score is the number of standard deviations between the observation and the mean of the previous observations. Approximately 68 percent of observations would be expected within one standard deviation of the mean, and 95 percent within two standard deviations. Near-normal conditions are classified as those within a single standard deviation of the mean, although such a threshold is somewhat arbitrary. Conditions between about one and two standard deviations of the mean are moderately different from mean conditions, but are not significantly different statistically. Those outside about two standard deviations would be

considered statistically greater than or less than the long-term mean (at $p < 0.025$ at each tail of the distribution).

Additionally, we used the Spatial Association of Scalable Hexagons (SASH) analytical approach to identify forested areas in the conterminous 48 States with higher-than-expected fire occurrence density in 2014. This method identifies locations where ecological phenomena occur at greater or lower occurrences than expected by random chance and is based on a sampling frame optimized for spatial neighborhood analysis, adjustable to the appropriate spatial resolution, and applicable to multiple data types (Potter and others 2016). Specifically, it consists of dividing an analysis area into scalable equal-area hexagonal cells within which data are aggregated, followed by identifying statistically significant geographic clusters of hexagonal cells within which mean values are greater or less than those expected by chance. To identify these clusters, we employed a Getis-Ord (G_i^*) hot spot analysis (Getis and Ord 1992) in ArcMap® 10.1 (ESRI 2012).

The spatial units of analysis were 9,810 hexagonal cells, each approximately 834 km^2 in area, generated in a lattice across the conterminous United States using intensification of the Environmental Monitoring and Assessment Program (EMAP) North American hexagon coordinates (White and others 1992). These coordinates are the foundation of a sampling frame in which a hexagonal lattice was projected onto the conterminous United States by centering a large base hexagon over the region (Reams and others 2005, White and others 1992). This base hexagon can be subdivided into many smaller hexagons, depending on sampling needs, and serves as the basis of the plot sampling frame for the FIA program (Reams and others 2005). Importantly, the hexagons maintain equal areas across the study region regardless of the degree of intensification of the EMAP hexagon coordinates. In addition, the hexagons are compact and uniform in their distance to the centroids of neighboring hexagons, meaning that a hexagonal lattice has a higher degree of isotropy (uniformity in all directions) than does a square grid (Shima and others 2010). These are convenient and highly useful attributes for spatial neighborhood analyses. These scalable hexagons also are independent of geopolitical and ecological boundaries, avoiding the possibility of different sample units (such as counties, States, or watersheds) encompassing vastly different areas (Potter and others 2016). We selected hexagons 834 km^2 in area because this is a manageable size for making monitoring and management decisions in nationwide analyses (Potter and others 2016).

Fire occurrence density values for each hexagon were quantified as the number of forest fire occurrences per 100 km^2 of forested area within the hexagon. The Getis-Ord G_i^* statistic was used to identify clusters of hexagonal cells with fire occurrence density values higher than expected by chance. This statistic allows for the

decomposition of a global measure of spatial association into its contributing factors, by location, and is therefore particularly suitable for detecting outlier assemblages of similar conditions (i.e., nonstationarities) in a dataset, such as when spatial clustering is concentrated in one subregion of the data (Anselin 1992).

Briefly, G_i^* sums the differences between the mean values in a local sample, determined in this case by a moving window of each hexagon and its 18 first- and second-order neighbors (the 6 adjacent hexagons and the 12 additional hexagons contiguous to those 6) and the global mean of all the forested hexagonal cells in the conterminous 48 States. G_i^* is standardized as a z-score with a mean of 0 and a standard deviation of 1, with values >1.96 representing significant local clustering of higher fire occurrence densities ($p < 0.025$) and values <-1.96 representing significant clustering of lower fire occurrence densities ($p < 0.025$) because 95 percent of the observations under a normal distribution should be within approximately 2 standard deviations of the mean (Laffan 2006). Values between -1.96 and 1.96 have no statistically significant concentration of high or low values; a hexagon and its 18 neighbors, in other words, have a range of both high and low numbers of fire occurrences per 100 km^2 of forested area. It is worth noting that the threshold values are not exact because the correlation of spatial data violates the assumption of independence required for statistical significance (Laffan 2006). The Getis-Ord approach does not require that the input data be normally distributed, because the local G_i^* values are computed under a randomization assumption, with G_i^* equating to a standardized z-score that asymptotically tends to a normal distribution (Anselin 1992). The z-scores are reliable, even with skewed data, as long as the distance band is large enough to include several neighbors for each feature (ESRI 2012).

RESULTS AND DISCUSSION

The MODIS Active Fire database recorded 106,242 wildland forest fire occurrences across the conterminous United States in 2014, the second largest annual number of fire occurrences since the first full year of data collection in 2001 (fig. 3.1). This number was approximately 8 percent greater than in 2013 (98,682 forest fire occurrences), and about 72 percent more than the annual mean of 61,784 forest fire occurrences across the previous 13 full years of data collection. In contrast, the MODIS database captured only 904 forest fire occurrences in Alaska in 2014, 89 percent fewer than the preceding year (8,110) and about 7.5 percent of the previous 13-year annual mean of 12,108. For the first year since the beginning of MODIS data collection, Hawai‘i had more forest fire occurrences than Alaska, with 1,797. This was 706 percent more than the previous annual average of 223 forest fire occurrences, and 132 percent greater than 2013 (773).

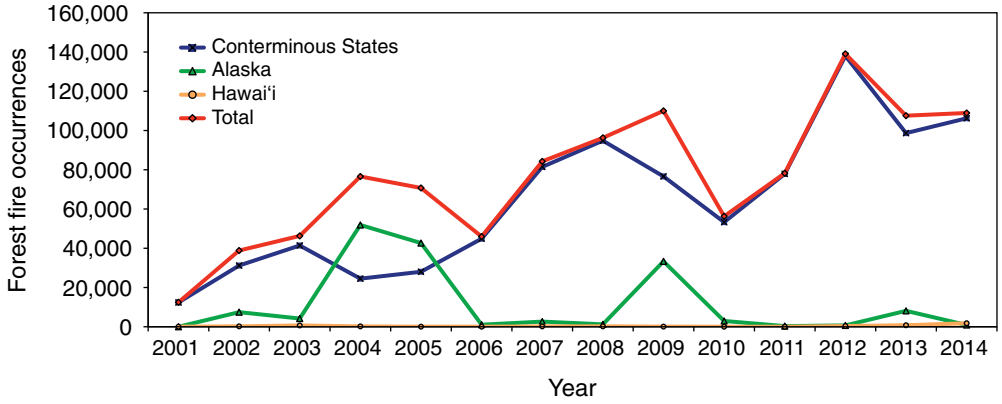

Figure 3.1—Forest fire occurrences detected by Moderate Resolution Imaging Spectroradiometer (MODIS) from 2001 to 2014 for the conterminous United States, Alaska and Hawai'i, and for the entire Nation combined. (Data source: U.S. Department of Agriculture, Forest Service, Remote Sensing Applications Center, in conjunction with the NASA MODIS Rapid Response group)

The increase in the total number of fire occurrences across the conterminous United States is generally consistent with the official wildland fire statistics (National Interagency Coordination Center 2015). In 2014, 63,612 wildfires were reported nationally, compared to 47,579 the previous year. The area burned nationally in 2014 (1 455 092 ha) was 53 percent of the 10-year average, with 9 fires exceeding 16 187 ha (11 fewer than in 2013) (National Interagency Coordination Center 2015). The total area burned nationally represented a 17 percent decrease from 2013 (1 748 058 ha) (National Interagency Coordination Center 2014). As noted in Methods section, such estimates of burned area are different metrics for quantifying fire activity than calculations of MODIS-detected fire occurrences, though the two may be correlated.

In 2014, the highest forest fire occurrence densities occurred in northern California, in southern Oregon, in northern Washington, and across parts of the Southeast (fig. 3.2), reflecting the severe to exceptional drought conditions that continued from previous years and extended from the Pacific Coast to the western slope of the Rocky Mountains, and also existed across the southern plains (National Interagency Coordination Center 2015). The forested ecoregion with the highest wildland forest fire occurrence density in 2014 (27.7 fire occurrences per 100 km^2 of forest)

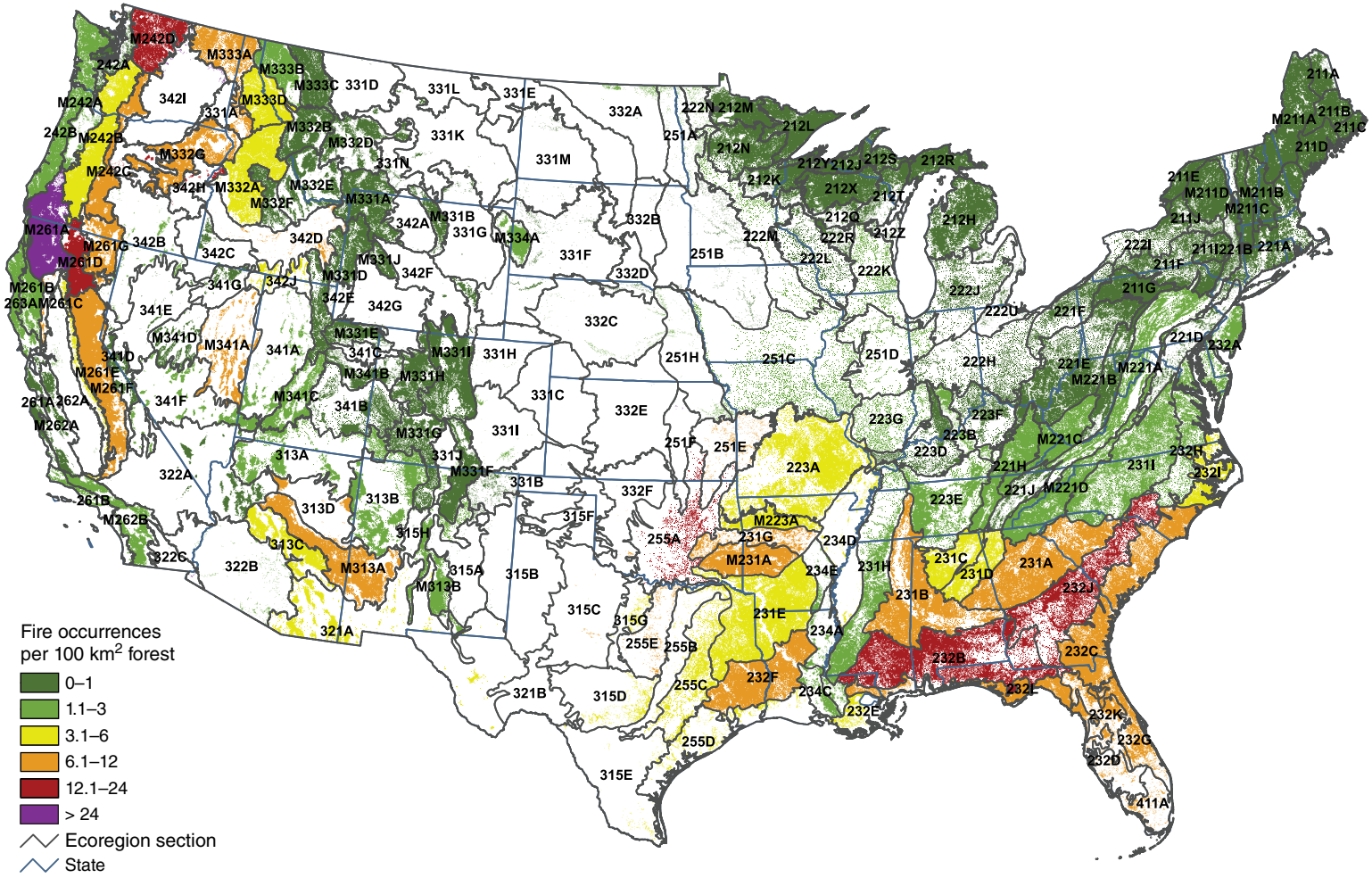

Figure 3.2—The number of forest fire occurrences, per 100 km^2 (10 000 ha) of forested area, by ecoregion section within the conterminous 48 States, for 2014. The gray lines delineate ecoregion sections (Cleland and others 2007). Forest cover is derived from Moderate Resolution Imaging Spectroradiometer (MODIS) imagery by the U.S. Forest Service Remote Sensing Applications Center. (Source of fire data: U.S. Department of Agriculture, Forest Service, Remote Sensing Applications Center, in conjunction with the NASA MODIS Rapid Response group)

was section M261A–Klamath Mountains (fig. 3.2) in northern California and southern Oregon. Immediately to the east is M261D–Southern Cascades, with a high fire density of 14.5 per 100 km^2 of forest. In these areas, the lightning-ignited Happy Camp fire complex burned 542.5 km^2, and the July complex burned 202.5 km^2. Fire occurrence density was 20.7 in M242D–Northern Cascades, location of the Carlton complex fire, the largest fire in the history of Washington State, burning 1,036.4 km^2. Meanwhile, two ecoregions that stretch in an arc from southern Mississippi to North Carolina experienced high fire occurrence densities: 15.9 fires per 100 km^2 of forest in 232J–Southern Atlantic Coastal Plains and Flatwoods, and 14.8 fires in 232B–Gulf Coastal Plains and Flatwoods. In central Oklahoma, 255A–Cross Timbers and Prairie had 15.7 fires per 100 km^2 of forest.

Additionally, several ecoregions that contain relatively small amounts of forest (and therefore do not stand out as easily on fig. 3.2) also had high fire occurrence densities in 2014, including 342I–Columbia Basin in central Washington (41.3 fire occurrences per 100 km^2 of forest), 251F–Flint Hills in eastern Kansas (26.4 fire occurrences), and 342H–Blue Mountain Foothills in eastern Oregon (12.1 fire occurrences).

Several ecoregions of the Southeastern United States experienced relatively high fire occurrence densities in 2014 (fig. 3.2). These encompassed all of the ecoregions of peninsular Florida: 232D–Florida Coastal Lowlands-Gulf, 11.9 fire occurrences per 100 km^2 of forest; 232G–Florida Coastal Lowlands-Atlantic, 11.6 fire occurrences; 232K–Florida Coastal Plains Central Highlands, 10.7 fire occurrences; 411A–Everglades, 10.1 fire occurrences; 232L–Gulf Coast Lowlands, 8.2 fire occurrences. Other Southeastern ecoregions with relatively high fire occurrence included the following:

- 232C–Atlantic Coastal Flatwoods (northeastern Florida, eastern Georgia, eastern South Carolina, and southeastern North Carolina), 9.4 fire occurrences;
- 232F–Coastal Plains and Flatwoods-Western Gulf (west-central Louisiana and east-central Texas), 8.0 fire occurrences;
- 231B–Coastal Plains-Middle (central Alabama, northeastern Mississippi, and southwestern Tennessee), 7.8 fire occurrences;
- 231A–Southern Appalachian Piedmont (east-central Alabama, northern Georgia, and northern South Carolina), 7.4 fire occurrences;
- 231G–Arkansas Valley (west-central Arkansas and east-central Oklahoma), 7.6 fire occurrences; and
- M231A–Ouchita Mountains (west-central Arkansas and southeastern Oklahoma), 7.5 fire occurrences.

In the Pacific Coast States, ecoregions stretching from the Washington border with Canada (M333A–Okanogan Highland, 7.8 fire

occurrences per 100 km^2 of forest) to the Sierra Nevada range of central California (M261E–Sierra Nevada) experienced moderate fire occurrence densities. Farther east, M341A–East Great Basin and Mountains in eastern Nevada (7.2 fire occurrences) and 313D–Painted Desert and M313A–White Mountains-San Francisco Peaks-Mogollon Rim in eastern Arizona (9.1 and 6.1 fire occurrences, respectively) had similarly moderate fire occurrence densities. Fire occurrence densities, meanwhile, were generally low in the Northeastern, Mid-Atlantic, Midwestern, and central Rocky Mountain States (fig. 3.2).

Alaska had warm, dry, and windy conditions in the spring and summer months of 2014, which led to fuels becoming rapidly snow free across the southern two-thirds of the State (National Interagency Coordination Center 2015). Still, Alaska saw a relatively small number of fires, and all but one ecoregion in the State had low fire occurrence densities (fig. 3.3). The exception was 213B–Cook Inlet Lowlands, with 3.5 fire occurrences per 100 km^2 of forest, stemming from the human-ignited Funny River fire on the Kenai Peninsula, which burned 79 260 ha in late May and early June and cost $11.4 million to control (National Interagency Coordination Center 2015).

The first half of 2014 was abnormally dry in Hawai‘i (National Interagency Coordination Center 2015), but most forest fire occurrences were associated with the months-long eruption of Pu‘u ‘Ō‘ō, a vent on the flank of the Kilauea volcano, which sent a slow moving flow of lava through dense forest near the eastern edge of the Big Island (Miner 2014). As a result, fire occurrence density on the Big Island was 44.1 per 100 km^2 of forest (fig. 3.4). Densities on the other islands were all less than one fire per 100 km^2 of forest.

Comparison to Longer Term Trends

Contrasting short-term (1-year) wildland forest fire occurrence densities with longer term trends is possible by comparing these results for each ecoregion section to the first 13 full years of MODIS Active Fire data collection (2001–2013). In general, most ecoregions within the Northeastern, Midwestern, Mid-Atlantic, and Appalachian regions experienced less than 1 fire per 100 km^2 of forest during the multiyear period, with means higher in the Northern Rocky Mountain, California, Southwestern, and Southeastern regions (fig. 3.5A). The forested ecoregion that experienced the most fires on average was M332A–Idaho Batholith in central Idaho (mean annual fire occurrence density of 13.9). Other ecoregions with mean fire occurrence densities of 6.1–12.0 were located in coastal and central California, in central Arizona and New Mexico, and in north-central Texas. Ecoregions with the greatest variation in fire occurrence densities from 2001 to 2013 were also located in central Idaho and near the California coast, with more moderate variation in northern and central California, southwestern

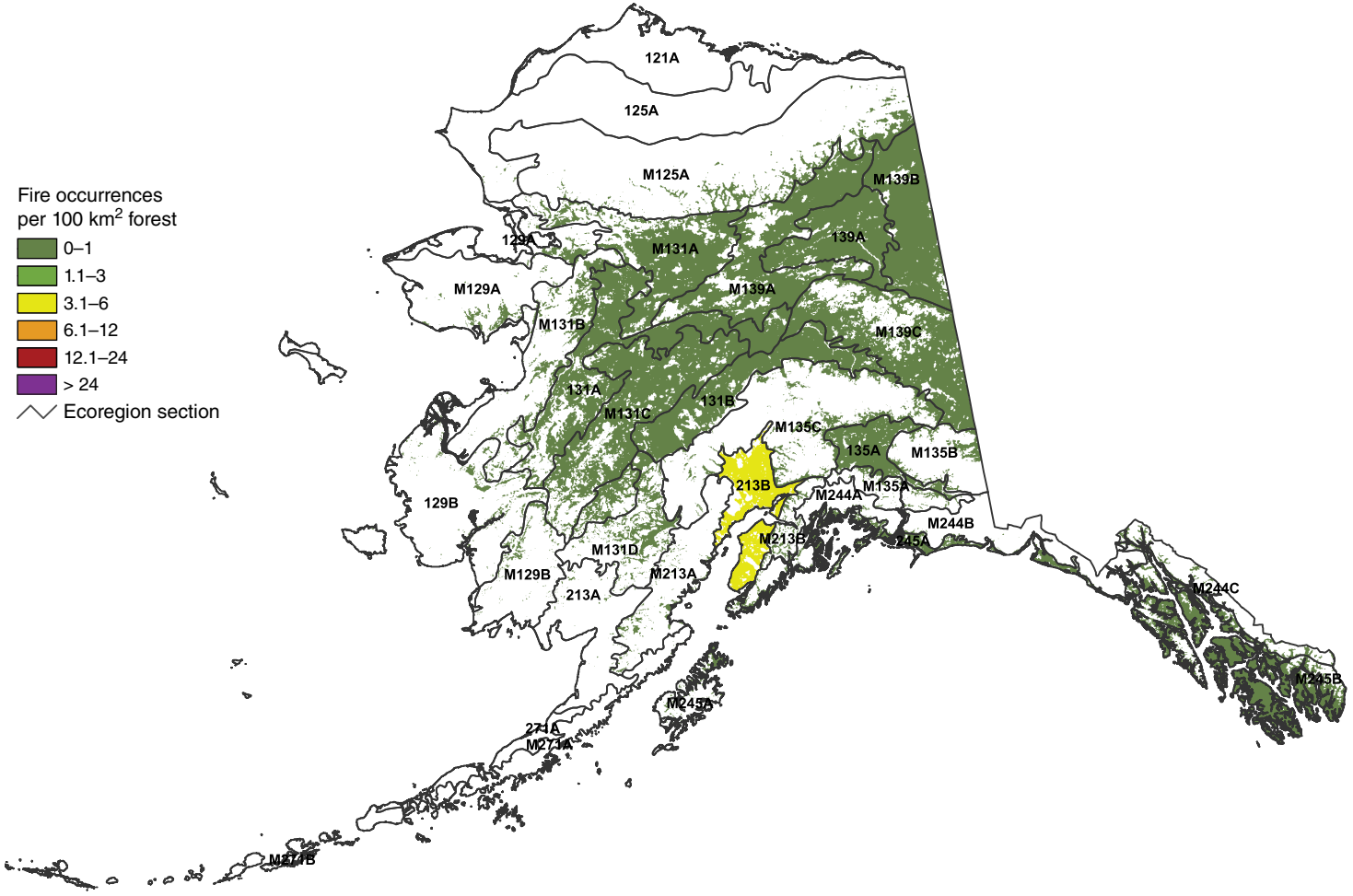

Figure 3.3—The number of forest fire occurrences, per 100 km^2 (10 000 ha) of forested area, by ecoregion section within Alaska, for 2014. The gray lines delineate ecoregion sections (Nowacki and Brock 1995). Forest cover is derived from Moderate Resolution Imaging Spectroradiometer (MODIS) imagery by the U.S. Forest Service Remote Sensing Applications Center. (Source of fire data: U.S. Department of Agriculture, Forest Service, Remote Sensing Applications Center, in conjunction with the NASA MODIS Rapid Response group)

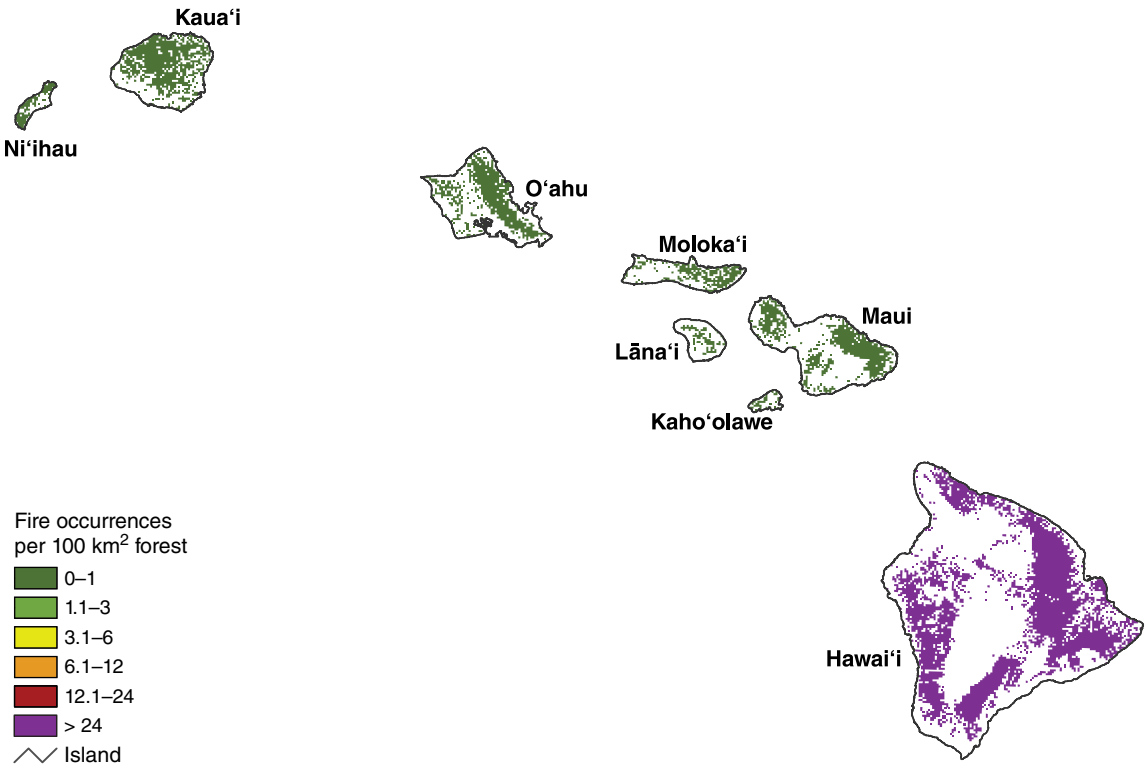

Figure 3.4—The number of forest fire occurrences, per 100 km^2 (10 000 ha) of forested area, by island in Hawai‘i, for 2014. Forest cover is derived from MODIS imagery by the U.S. Forest Service Remote Sensing Applications Center. (Source of fire data: U.S. Department of Agriculture, Forest Service, Remote Sensing Applications Center, in conjunction with the NASA MODIS Rapid Response group)

Oregon, north-central Washington, western Montana, western Utah, northeastern Nevada, central and southeastern Arizona, southwestern New Mexico, and eastern North Carolina (fig. 3.5B). Less variation occurred throughout the Southeast, coastal and eastern Oregon and Washington, the Rocky Mountain States, and northern Minnesota. The lowest levels of variation were apparent throughout most of the Midwest and Northeast.

In 2014, ecoregions in the Pacific Northwest, in the Great Basin, in the Southwest, and across much of the Eastern United States experienced greater fire occurrence densities than normal, compared to the previous 13-year mean and accounting for variability over time, as determined by the calculation of standardized fire occurrence *z*-scores (fig. 3.5C). These included ecoregions in the Midwest, Mid-Atlantic, and New England States, which had high *z*-scores despite a relatively low density of fire occurrences in 2014 (fig. 3.2) because these were slightly higher than normal in areas that typically have very little variation over time in fire occurrence density. On the other hand, several of the western and southeastern ecoregions with high *z*-scores also had very high fire occurrence densities in 2014 (fig. 3.2), including M261A–Klamath Mountains in northwestern California and southwestern Oregon, M242D–Northern Cascades in north-central Washington, 232B–Gulf Coastal Plains and Flatwoods in southern Mississippi and Alabama and northwestern Florida, and 232J–Southern Atlantic Coastal Plains and Flatwoods in central Georgia, central South Carolina, and south-central North Carolina (fig. 3.2). No ecoregions had lower fire occurrence densities in 2014 compared to the longer term.

In Alaska, meanwhile, the highest mean annual fire occurrence density between 2001 and 2013 occurred in the east-central and central parts of the State (fig. 3.6A) in the 139A–Yukon Flats ecoregion, with moderate mean fire occurrence density in neighboring areas. As expected, many of those same areas experienced the greatest degree of variability over the 13-year period (fig. 3.6B). In 2014, only one ecoregion was outside the range of near-normal fire occurrence density, compared to the mean of the previous 13 years and accounting for variability (fig. 3.6C). This was 213B–Cook Inlet Lowlands, an area with typically very low mean fire occurrence density (fig. 3.6A) and variability (fig. 3.6B) that was the location of the Funny River fire, the third largest wildfire nationally in 2014.

In Hawai‘i, both the mean annual fire occurrence density (fig. 3.7A) and variability (fig. 3.7B) were highest on the Big Island during the 2001–2013 period. The annual mean was less than 1 fire per 100 km^2 of forest for all islands except the Big Island (8.1) and Kaho‘olawe (1.9). The annual fire occurrence standard deviation exceeded 1 for only the Big Island (11.9), Kaho‘olawe (5.4), and Lāna‘i (1.3). In 2014, the Big Island was well outside the range of near-normal fire occurrence density, controlling for variability over the previous 13 years (fig. 3.7C), with many more fires than expected.

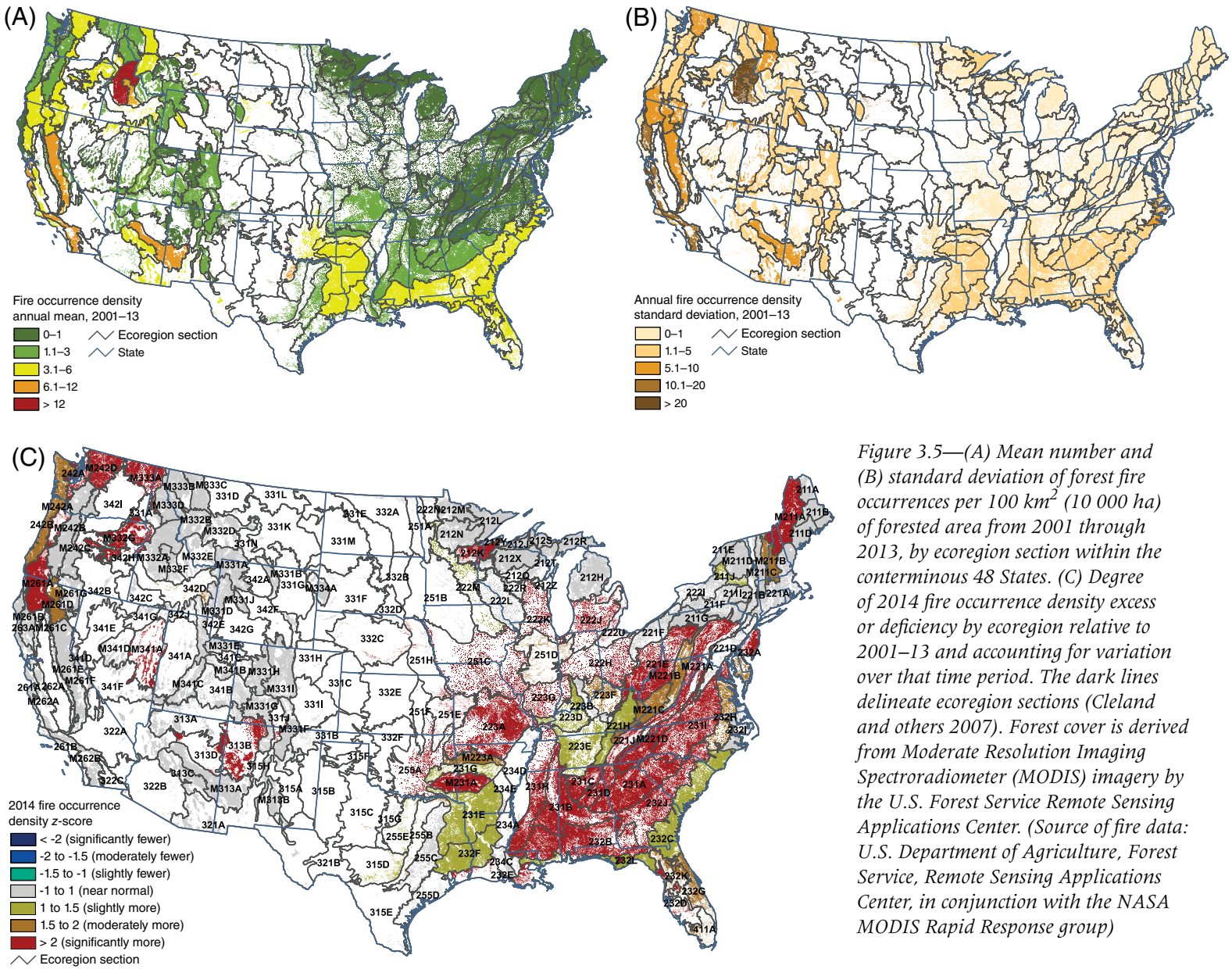

Figure 3.5—(A) Mean number and (B) standard deviation of forest fire occurrences per 100 km^2 (10 000 ha) of forested area from 2001 through 2013, by ecoregion section within the conterminous 48 States. (C) Degree of 2014 fire occurrence density excess or deficiency by ecoregion relative to 2001–13 and accounting for variation over that time period. The dark lines delineate ecoregion sections (Cleland and others 2007). Forest cover is derived from Moderate Resolution Imaging Spectroradiometer (MODIS) imagery by the U.S. Forest Service Remote Sensing Applications Center. (Source of fire data: U.S. Department of Agriculture, Forest Service, Remote Sensing Applications Center, in conjunction with the NASA MODIS Rapid Response group)

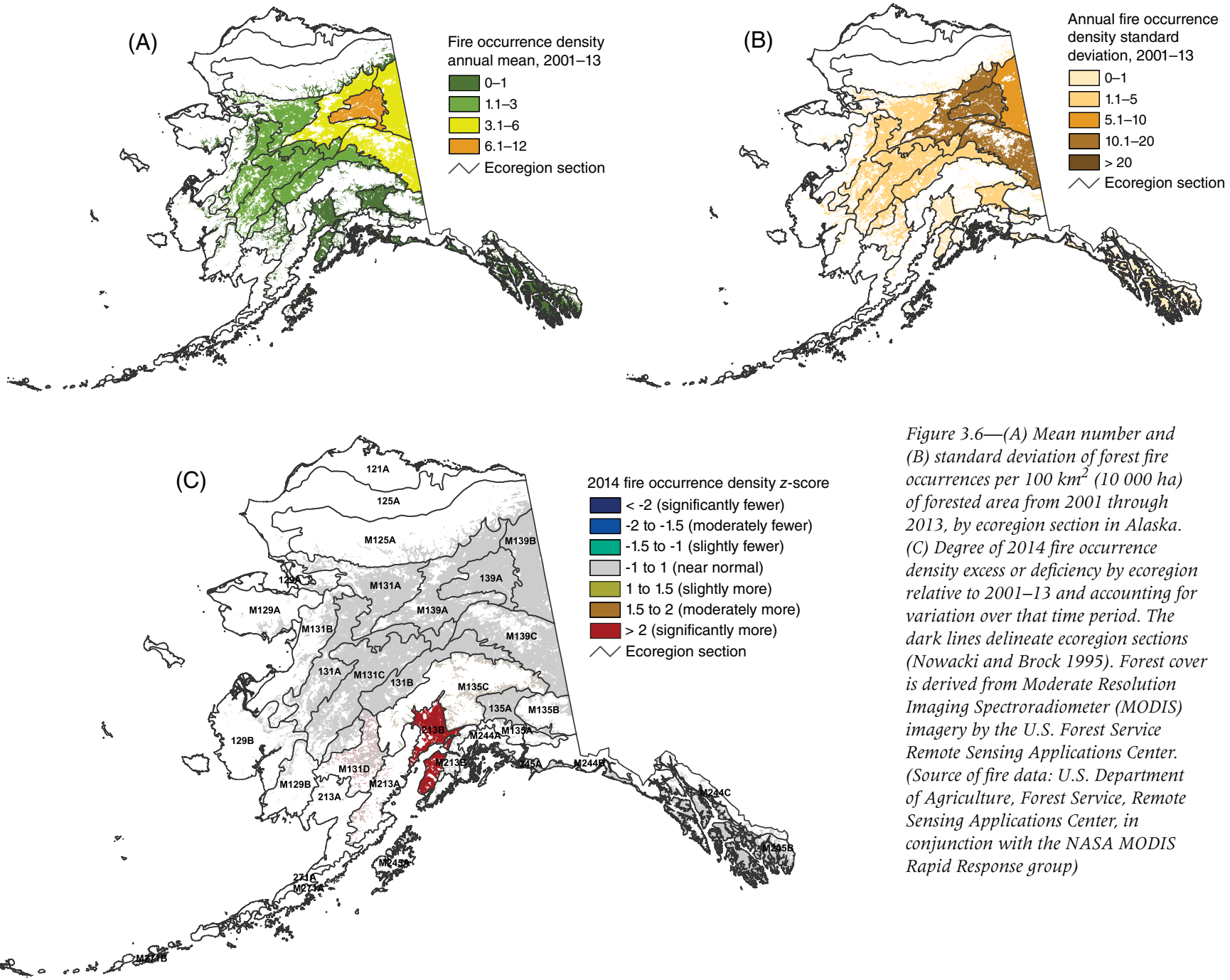

Figure 3.6—(A) Mean number and (B) standard deviation of forest fire occurrences per 100 km^2 (10 000 ha) of forested area from 2001 through 2013, by ecoregion section in Alaska. (C) Degree of 2014 fire occurrence density excess or deficiency by ecoregion relative to 2001–13 and accounting for variation over that time period. The dark lines delineate ecoregion sections (Nowacki and Brock 1995). Forest cover is derived from Moderate Resolution Imaging Spectroradiometer (MODIS) imagery by the U.S. Forest Service Remote Sensing Applications Center. (Source of fire data: U.S. Department of Agriculture, Forest Service, Remote Sensing Applications Center, in conjunction with the NASA MODIS Rapid Response group)

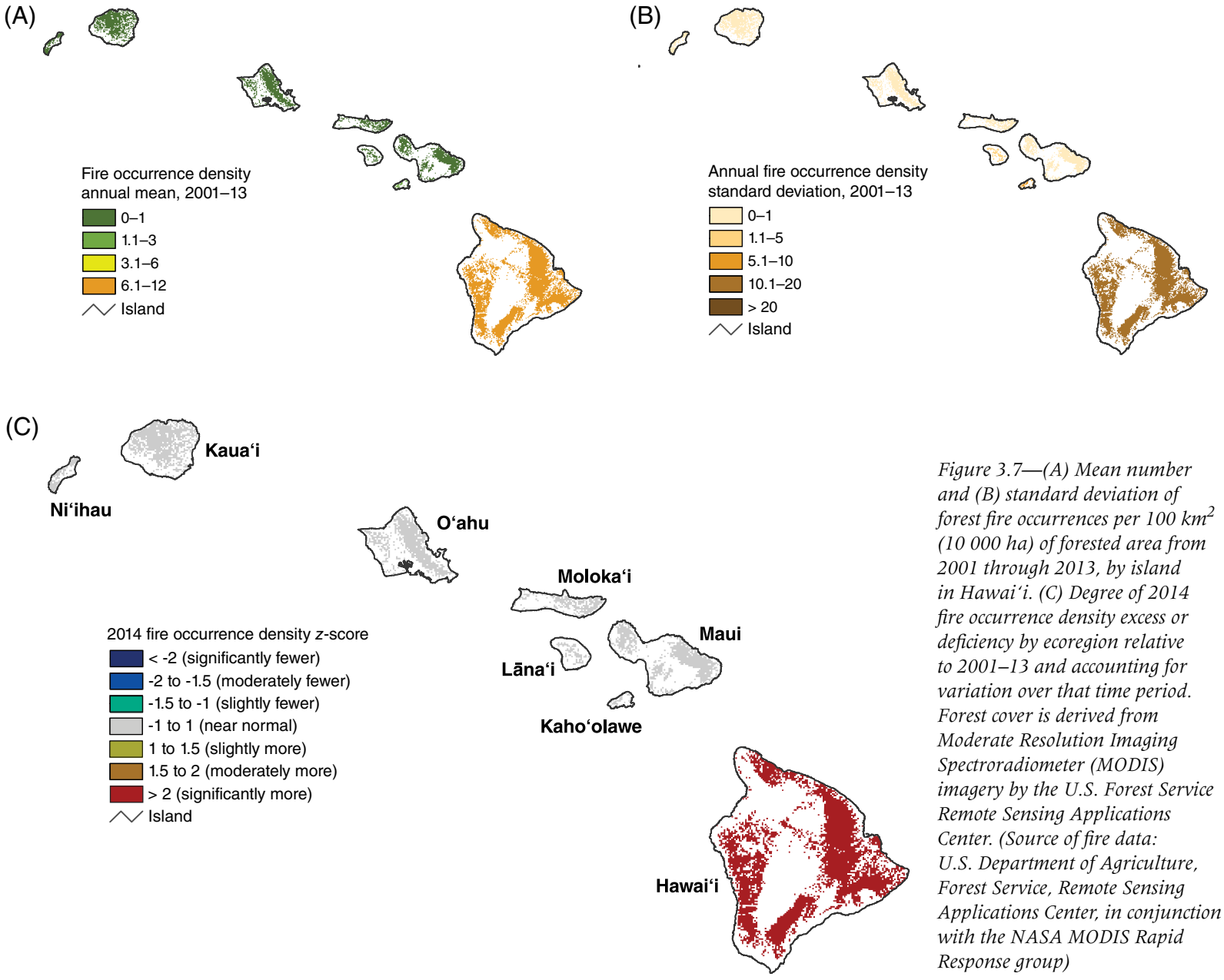

Figure 3.7—(A) Mean number and (B) standard deviation of forest fire occurrences per 100 km^2 (10 000 ha) of forested area from 2001 through 2013, by island in Hawai‘i. (C) Degree of 2014 fire occurrence density excess or deficiency by ecoregion relative to 2001–13 and accounting for variation over that time period. Forest cover is derived from Moderate Resolution Imaging Spectroradiometer (MODIS) imagery by the U.S. Forest Service Remote Sensing Applications Center. (Source of fire data: U.S. Department of Agriculture, Forest Service, Remote Sensing Applications Center, in conjunction with the NASA MODIS Rapid Response group)

Geographical Hot Spots of Fire Occurrence Density

Although summarizing fire occurrence data at the ecoregion scale allows for the quantification of fire occurrence density across the country, a geographical hot spot analysis can offer insights into where, statistically, fire occurrences are more concentrated than expected by chance. In 2014, the two geographical hot spots with the highest fire occurrence densities were located in northwestern California/southwestern Oregon and in north-central Washington (fig. 3.8). The larger of these was detected in M261A–Klamath Mountains, the area with the highest wildland forest fire occurrence density in 2014. This hot spot extended, at lower levels of fire occurrence density, into M261D–Southern Cascades and M221G–Modoc Plateau. The other hot spot of very high fire occurrence density was in M242D–Northern Cascades, extending with lower fire occurrence density into the neighboring M333A–Okanogan Highland.

Several hot spots of moderate to high fire density were scattered elsewhere across the Western United States (fig. 3.8), including in the following regions:

- Central Oregon (M332G–Blue Mountains, M242C–Eastern Cascades, and M242B–Western Cascades),
- West-central Idaho and northeastern Oregon (M332A–Idaho Batholith and M332G–Blue Mountains),
- East-central Nevada (M341A–East Great Basin and Mountains),
- East-central Arizona (M313A–White Mountains-San Francisco Peaks-Mogollon Rim and 313C–Tonto Transition),
- Southern California (261B–Southern California Coast and M262B–Southern California Mountain and Valley), and
- Central California (M261E–Sierra Nevada and M261F–Sierra Nevada Foothills).

The geographic clustering analysis detected a large hot spot in the Southeast, extending across four States and having its high fire density core in ecoregion 232B–Gulf Coast Plains and Flatwoods in southwestern Georgia and north-central Florida (fig. 3.8). Within the East, other hot spots of high fire occurrence density were located in southern Florida (232D–Florida Coastal Lowlands-Gulf and 411A–Everglades), southern Louisiana (234C–Atchafalaya and Red River Alluvial Plains), and southeastern Kansas and northeastern Oklahoma (255A–Cross Timbers and Prairie). The Southeastern United States was the region with the greatest area burned in 2014 (National Interagency Coordination Center 2015), but these were mostly small, short-duration fires occurring in the spring or autumn.

CONCLUSION

The results of these geographic analyses are intended to offer insights into where fire occurrences have been concentrated spatially in a given year and compared to previous years, but are not intended to quantify the severity of a given fire season. Given the limits of MODIS active fire detection using 1-km^2 resolution

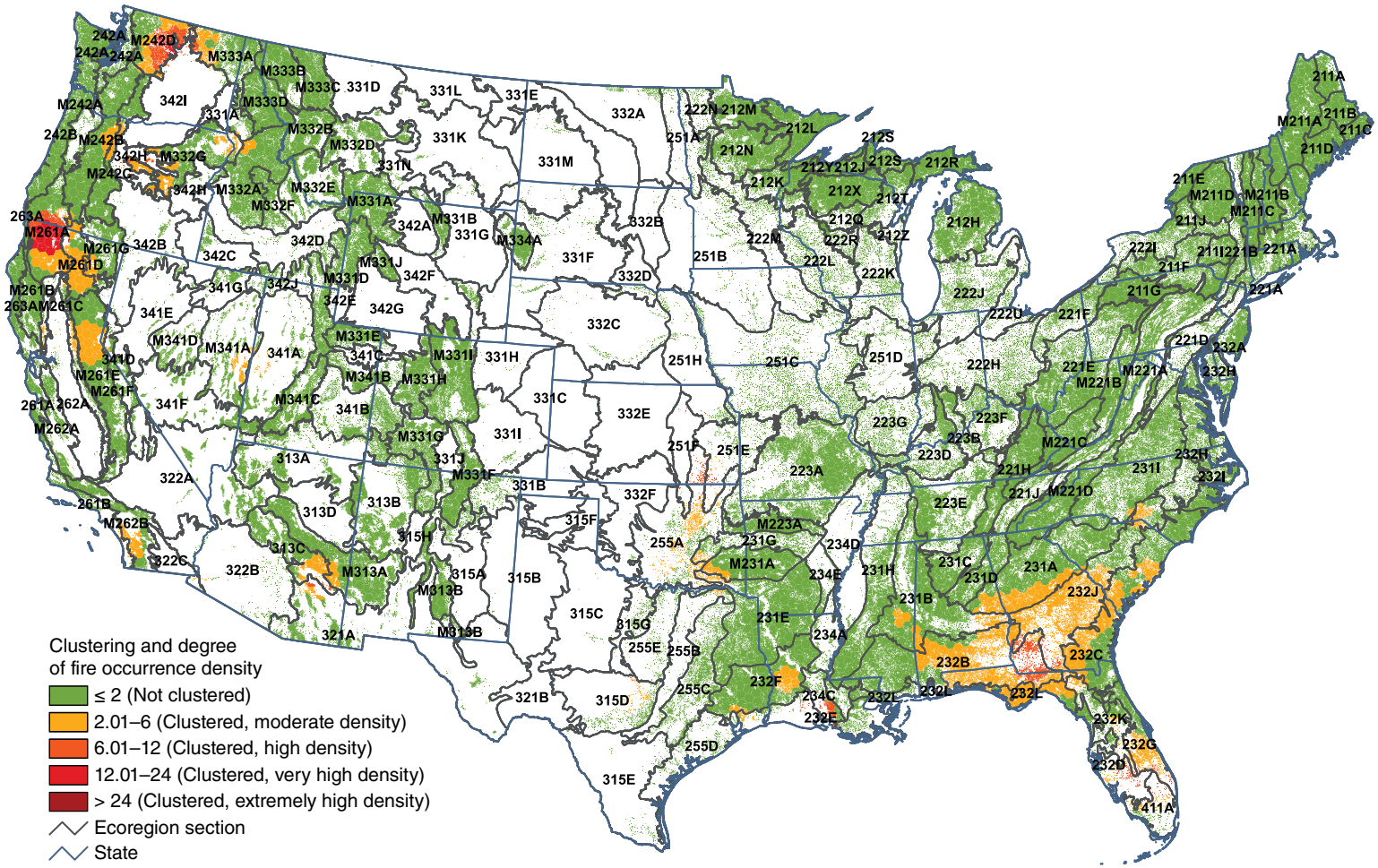

Figure 3.8— Hot spots of fire occurrence across the conterminous United States for 2014. Values are Getis-Ord G_i scores, with values > 2 representing significant clustering of high fire occurrence densities. (No areas of significant clustering of low fire occurrence densities, < -2, were detected). The gray lines delineate ecoregion sections (Cleland and others 2007). Background forest cover is derived from Moderate Resolution Imaging Spectroradiometer (MODIS) imagery by the U.S. Forest Service Remote Sensing Applications Center. (Source of fire data: U.S. Department of Agriculture, Forest Service, Remote Sensing Applications Center, in conjunction with the NASA MODIS Rapid Response group)*

data, these products also may underrepresent the number of fire occurrences in some ecosystems where small and low-intensity fires are common. These products can also have commission errors. However, these high temporal fidelity products currently offer the best means for daily monitoring of wildfire impacts. Ecological and forest health impacts relating to fire and other abiotic disturbances are scale-dependent properties, which in turn are affected by management objectives (Lundquist and others 2011). Information about the concentration of fire occurrences may help pinpoint areas of concern for aiding management activities and for investigations into the ecological and socioeconomic impacts of wildland forest fire potentially outside the range of historic frequency.

LITERATURE CITED

Anselin, L. 1992. Spatial data analysis with GIS: an introduction to application in the social sciences. Tech. Rep. 92-10. Santa Barbara, CA: National Center for Geographic Information and Analysis. 53 p.

Barbour, M.G.; Burk, J.H.; Pitts, W.D. [and others]. 1999. Terrestrial plant ecology. Menlo Park, CA: Addison Wesley Longman, Inc. 649 p.

Bond, W.J.; Keeley, J.E. 2005. Fire as a global "herbivore": the ecology and evolution of flammable ecosystems. Trends in Ecology & Evolution. 20(7): 387–394.

Brooks, M.L.; D'Antonio, C.M.; Richardson, D.M. [and others]. 2004. Effects of invasive alien plants on fire regimes. BioScience. 54(7): 677–688.

Cleland, D.T.; Freeouf, J.A.; Keys, J.E.; [and others]. 2007. Ecological subregions: sections and subsections for the conterminous United States. In: Sloan, A.M., tech. ed. Washington, DC: U.S. Department of Agriculture, Forest Service. Gen. Tech. Rep. WO-76D. [Map, presentation scale 1:3,500,000; colored]. Also on CD-ROM as a GIS coverage in ArcINFO format.

Coulston, J.W.; Ambrose, M.J.; Riitters, K.H.; Conkling, B.L. 2005. Forest Health Monitoring 2004 national technical report. Gen. Tech. Rep. SRS-90. Asheville, NC: U.S. Department of Agriculture, Forest Service, Southern Research Station. 81 p.

Edmonds, R.L.; Agee, J.K.; Gara, R.I. 2011. Forest health and protection. Long Grove, IL: Waveland Press, Inc. 667 p.

ESRI. 2012. ArcMap® 10.1. Redlands, CA: Environmental Systems Research Institute.

Getis, A.; Ord, J.K. 1992. The analysis of spatial association by use of distance statistics. Geographical Analysis. 24(3): 189–206.

Gill, A.M.; Stephens, S.L.; Cary, G.J. 2013. The worldwide "wildfire" problem. Ecological Applications. 23(2): 438–454.

Hawbaker, T.J.; Radeloff, V.C.; Syphard, A.D. [and others]. 2008. Detection rates of the MODIS active fire product. Remote Sensing of Environment. 112: 2656–2664.

Justice, C.O.; Giglio, L.; Korontzi, S. [and others]. 2002. The MODIS fire products. Remote Sensing of Environment. 83(1–2): 244–262.

Justice, C.O.; Giglio, L.; Roy, D. [and others]. 2011. MODIS-derived global fire products. In: Ramachandran, B.; Justice, C.O.; Abrams, M.J., eds. Land remote sensing and global environmental change: NASA's earth observing system and the science of ASTER and MODIS. New York: Springer: 661–679.

Laffan, S.W. 2006. Assessing regional scale weed distributions, with an Australian example using *Nassella trichotoma*. Weed Research. 46(3): 194–206.

Lundquist, J.E.; Camp, A.E.; Tyrrell, M.L. [and others]. 2011. Earth, wind and fire: abiotic factors and the impacts of global environmental change on forest health. In: Castello, J.D.; Teale, S.A., eds. Forest health: an integrated perspective. New York: Cambridge University Press: 195–243.

McKenzie, D.; Peterson, D.L.; Alvarado, E. 1996. Predicting the effect of fire on large-scale vegetation patterns in North America. Research Paper PNW-RP-489. U.S. Department of Agriculture, Forest Service, Pacific Northwest Research Station. 38 p.

Miner, M. 2014. Kilauea Volcano lava flow approaching homes in Hawai'i Island's Puna district. Hawaii Magazine. http://www.hawaiimagazine.com/blogs/hawaii_today/2014/9/12/kilauea_volcano_lava_flow_Puna_Big_Island. [Date accessed: August 11, 2015].

National Interagency Coordination Center. 2014. Wildland fire summary and statistics annual report: 2013. http://www.predictiveservices.nifc.gov/intelligence/2013_Statssumm/intro_summary13.pdf. [Date accessed: May 28, 2014].

National Interagency Coordination Center. 2015. Wildland fire summary and statistics annual report: 2015. http://www.predictiveservices.nifc.gov/intelligence/2014_Statssumm/intro_summary14.pdf. [Date accessed: May 11, 2015].

Nowacki, G.J.; Abrams, M.D. 2008. The demise of fire and "mesophication" of forests in the Eastern United States. BioScience. 58(2): 123–138.

Nowacki, G.; Brock, T. 1995. Ecoregions and subregions of Alaska [EcoMap]. Version 2.0. Juneau, AK: U.S. Department of Agriculture, Forest Service, Alaska Region. [Map, presentation scale 1:5,000,000; colored].

Potter, K.M. 2012a. Large-scale patterns of forest fire occurrence in the conterminous United States and Alaska, 2005–07. In: Potter, K.M.; Conkling, B.L., eds. Forest Health Monitoring 2008 national technical report. Gen. Tech. Rep. SRS-158. Asheville, NC: U.S. Department of Agriculture, Forest Service, Southern Research Station: 73–83.

Potter, K.M. 2012b. Large-scale patterns of forest fire occurrence in the conterminous United States and Alaska, 2001-08. In: Potter, K.M.; Conkling, B.L., eds. Forest health monitoring 2009 national rechnical report. Gen. Tech. Rep. SRS-167. Asheville, NC: U.S. Department of Agriculture, Forest Service, Southern Research Station: 151-161.

Potter, K.M. 2013a. Large-scale patterns of forest fire occurrence in the conterminous United States and Alaska, 2009. In: Potter, K.M.; Conkling, B.L., eds. Forest Health Monitoring: national status, trends and analysis 2010. Gen. Tech. Rep. SRS-176. Asheville, NC: U.S. Department of Agriculture, Forest Service, Southern Research Station: 31–39.

Potter, K.M. 2013b. Large-scale patterns of forest fire occurrence in the conterminous United States and Alaska, 2010. In: Potter, K.M.; Conkling, B.L., eds. Forest Health Monitoring: national status, trends and analysis 2011. Gen. Tech. Rep. SRS-185. Asheville, NC: U.S. Department of Agriculture, Forest Service, Southern Research Station: 29–40.

Potter, K.M. 2014. Large-scale patterns of forest fire occurrence in the conterminous United States and Alaska, 2011. In: Potter, K.M.; Conkling, B.L., eds. Forest Health Monitoring: national status, trends and analysis 2012. Gen. Tech. Rep. SRS-198. Asheville, NC: U.S. Department of Agriculture, Forest Service, Southern Research Station: 35–48.

Potter, K.M. 2015a. Large-scale patterns of forest fire occurrence in the conterminous United States and Alaska, 2012. In: Potter, K. M.; Conkling, B. L., ed. Forest Health Monitoring: national status, trends, and analysis 2013. Gen. Tech. Rep. SRS-207. Asheville, North Carolina: U.S. Department of Agriculture, Forest Service, Southern Research Station: 37–53.

Potter, K.M. 2015b. Large-scale patterns of forest fire occurrence in the conterminous United States and Alaska, 2013. In: Potter, K. M.; Conkling, B. L., ed. Forest Health Monitoring: national status, trends, and analysis 2014. Gen. Tech. Rep. SRS-209. Asheville, North Carolina: U.S. Department of Agriculture, Forest Service, Southern Research Station: 39–55.

Potter, K.M.; Koch, F.H.; Oswalt, C.M.; Iannone, B.V. 2016. Data, data everywhere: Detecting spatial patterns in fine-scale ecological information collected across a continent. Landscape Ecology. 31(1): 67–84.

Pyne, S.J. 2010. America's fires: a historical context for policy and practice. Durham, NC: Forest History Society. 91 p.

Reams, G.A.; Smith, W.D.; Hansen, M.H. [and others]. 2005. The Forest Inventory and Analysis sampling frame. In: Bechtold, W.A.; Patterson, P.L., eds. The enhanced Forest Inventory and Analysis program—national sampling design and estimation procedures. Asheville, NC: U.S. Department of Agriculture, Forest Service, Southern Research Station: 11–26.

Richardson, L.A.; Champ, P.A.; Loomis, J.B. 2012. The hidden cost of wildfires: economic valuation of health effects of wildfire smoke exposure in southern California. Journal of Forest Economics. 18(1): 14–35.

Schmidt, K.M.; Menakis, J.P.; Hardy, C.C. [and others]. 2002. Development of coarse-scale spatial data for wildland fire and fuel management. Gen. Tech. Rep. RMRS-GTR-87. Fort Collins, CO: U.S. Department of Agriculture, Forest Service, Rocky Mountain Research Station. 41 p.

Shima T.; Sugimoto S.; Okutomi, M. 2010. Comparison of image alignment on hexagonal and square lattices. 2010 IEEE International Conference on Image Processing: 141–144. DOI:10.1109/icip.2010.5654351.

Tonini, M.; Tuia, D.; Ratle, F. 2009. Detection of clusters using space-time scan statistics. International Journal of Wildland Fire. 18(7): 830–836.

U.S. Department of Agriculture (USDA) Forest Service. 2008. National forest type data development. http://svinetfc4.fs.fed.us/rastergateway/forest_type/. [Date accessed: May 13, 2008].

U.S. Department of Agriculture (USDA) Forest Service. 2015. MODIS active fire mapping program: fire detection GIS data. http://activefiremaps.fs.fed.us/gisdata.php. [Date accessed: February 13, 2015].

Vinton, J.V., ed. 2004. Wildfires: issues and consequences. Hauppauge, NY: Nova Science Publishers, Inc. 127 p.

White, D.; Kimerling, A.J.; Overton, W.S. 1992. Cartographic and geometric components of a global sampling design for environmental monitoring. Cartography and Geographic Information Systems. 19(1): 5–22.

CHAPTER 4.

1-Year (2014), 3-Year (2012—2014), and 5-Year (2010—2014) Maps of Drought and Moisture Surplus for the Conterminous United States

Frank H. Koch
John W. Coulston

INTRODUCTION

Droughts occur in most forest ecosystems of the United States, but their frequency and intensity vary widely (Hanson and Weltzin 2000). Annual seasonal droughts are typical in Western U.S. forests. In contrast, Eastern U.S. forests usually exhibit one of two predominant drought patterns: random (i.e., occurring at any time of year) occasional droughts, as typically seen in the Appalachian Mountains and the Northeast, or frequent late-summer droughts, as observed in the Southeastern Coastal Plain and the eastern side of the Great Plains (Hanson and Weltzin 2000).

In forests, diminished moisture availability during droughts, especially since they are regularly accompanied by high temperatures, can lead to substantial tree stress (Anderegg and others 2013, Peters and others 2015, Williams and others 2013). Initially, trees, like other plants, respond to this stress by decreasing fundamental growth processes such as cell division and enlargement. Photosynthesis, which is less sensitive than these fundamental processes, decreases slowly at low levels of drought stress but decreases more sharply as drought stress becomes moderate to severe (Kareiva and others 1993, Mattson and Haack 1987). In addition to these direct effects, drought stress often makes forests susceptible to attack by tree-damaging insects and diseases (Clinton and others 1993, Mattson and Haack 1987, Raffa and others 2008). Furthermore, drought increases wildland fire risk by inhibiting organic matter decomposition and lowering the moisture content of downed woody debris and other potential fire fuels (Clark 1989, Keetch and Byram 1968, Schoennagel and others 2004, Trouet and others 2010).

Forests are generally resistant to short-term droughts (Archaux and Wolters 2006), although individual tree species differ in their levels of resistance. Regardless, because of this resistance, the duration of a drought event may be more important than its intensity (Archaux and Wolters 2006). For instance, multiple consecutive years of drought (2–5 years) in a forested area are much more likely to cause high tree mortality than one very dry year (Guarín and Taylor 2005, Millar and others 2007). Therefore, a comprehensive evaluation of drought impact in forests should include analysis of moisture conditions over multiyear time windows.

In the 2010 FHM national report, we presented a methodology for mapping drought conditions across the conterminous United States (Koch and others 2013b). Our goal was to generate drought-related spatial data sets that are finer in scale than similar products available from sources such as the National Climatic Data Center (2015b) or the U.S. Drought Monitor Program (Svoboda and others 2002). The principal inputs are gridded climate data (i.e., monthly raster maps of precipitation and temperature over a 100-year period) created with the Parameter-elevation Regression on Independent Slopes (PRISM) climate mapping system (Daly and others 2002). The methodology employs a standardized indexing

approach that facilitates comparison of a given location's moisture status during different time windows, regardless of their length. The index is easier to calculate than the commonly used Palmer Drought Severity Index, or PDSI (Palmer 1965), and sidesteps some criticisms of the PDSI (summarized by Alley 1984) regarding its underlying assumptions and limited comparability across space and time. In this chapter, we applied the methodology to the most currently available climate data (i.e., the monthly PRISM data through 2014), thereby providing a sixth time step in an ongoing annual record of drought status in the conterminous United States from 2009 forward (Koch and Coulston 2015; Koch and others 2013a, 2013b, 2014, 2015).

For the first time in this series, we also mapped the degree of moisture surplus during multiple time windows. Recently, much refereed literature (e.g., Adams and others 2009, Allen and others 2010, Martínez-Vilalta and others 2012, Peng and others 2011, Williams and others 2013) has focused on reports of widespread, regional-scale forest decline and mortality due to persistent drought conditions, especially in conjunction with periods of extremely high temperatures (i.e., heat waves). However, surplus moisture availability can also be detrimental to forests. Abnormally high moisture can be a short-term stressor (e.g., an extreme rainfall event with subsequent flooding) or a long-term stressor (e.g., persistent wetness driven by a macroscale climatic pattern such as the El Niño-Southern Oscillation), either of which may contribute to tree dieback and mortality (Rozas and García-González 2012, Rozas and Sampedro 2013). Such impacts have been observed in both tropical and temperate forests (Laurance and others 2009, Rozas and García-González 2012). Although surplus-induced impacts in forests are probably not as common as drought-induced impacts, it seems sensible to develop a single index that depicts both moisture surplus and deficit conditions, thereby providing a fuller accounting of potential forest health issues.

METHODS

We acquired grids for monthly precipitation and monthly mean temperature for the conterminous United States from the PRISM Climate Group Web site (PRISM Climate Group 2015). At the time of these analyses, gridded data sets were available for all years from 1895 to 2014. However, the grids for November and December 2014 were only provisional versions (i.e., finalized grids had not yet been released for these months). For analytical purposes, we treated these provisional grids as if they were the final versions. The spatial resolution of the grids was approximately 4 km (cell area = 16 km^2). For future applications and to ensure better compatibility with other spatial data sets, all output grids were resampled to a spatial resolution of approximately 2 km (cell area = 4 km^2) using a nearest neighbor approach. The nearest neighbor approach is a computationally simple resampling method that avoids the smoothing of data values observed with methods such as bilinear interpolation or cubic convolution.

Potential Evapotranspiration Maps

As in our previous drought mapping efforts (Koch and Coulston 2015; Koch and others 2012a, 2012b, 2013a, 2013b, 2014, 2015), we adopted an approach in which a moisture index value is calculated for each location of interest (i.e., each grid cell in a map of the conterminous United States) during a given time period. Moisture indices are intended to reflect the amount of available water in a location (e.g., to support plant growth). In our case, the index is calculated based on how much precipitation falls on a location during the period of interest as well as the level of potential evapotranspiration during this period. Potential evapotranspiration measures the loss of soil moisture through plant uptake and transpiration (Akin 1991). It does not measure actual moisture loss but rather the loss that would occur if there was no possible shortage of moisture for plants to transpire (Akin 1991, Thornthwaite 1948). By including potential evapotranspiration along with precipitation, the index accounts for this expected moisture loss and thus presents a more complete picture of a location's water supply than precipitation alone.

To complement the available PRISM monthly precipitation grids, we computed corresponding monthly potential evapotranspiration (*PET*) grids using Thornthwaite's formula (Akin 1991, Thornthwaite 1948):

$$PET_m = 1.6 L_{lm} \left(10 \frac{T_m}{I}\right)^a \qquad (1)$$

where

PET_m = the potential evapotranspiration for a given month m in cm

L_{lm} = a correction factor for the mean possible duration of sunlight during month m for all locations (i.e., grid cells) at a particular latitude l [see table V in Thornthwaite (1948) for a list of L correction factors by month and latitude]

T_m = the mean temperature for month m in degrees C

I = an annual heat index, calculated as

$$I = \sum_{m=1}^{12} \left(\frac{T_m}{5}\right)^{1.514}$$

where

T_m = the mean temperature for each month m of the year

a = an exponent calculated as $a = 6.75 \times 10^{-7} I^3 - 7.71 \times 10^{-5} I^2 + 1.792 \times 10^{-2} I + 0.49239$ [see appendix I in Thornthwaite (1948) regarding calculation of I and the empirical derivation of a]

Although only a simple approximation, a key advantage of Thornthwaite's formula is that it has modest input data requirements (i.e., mean temperature values) compared to more sophisticated methods of estimating *PET* such as the Penman-Monteith equation (Monteith 1965), which requires less readily available data on factors such as humidity, radiation, and wind speed. To implement equation 1 spatially, we

created a grid of latitude values for determining the L adjustment for any given grid cell (and any given month) in the conterminous United States. We extracted the T_m values for the grid cells from the corresponding PRISM mean monthly temperature grids.

Moisture Index Maps

To estimate baseline conditions, we used the precipitation (P) and PET grids to generate moisture index grids for the past 100 years (i.e., 1915–2014) for the conterminous United States. We used a moisture index described by Willmott and Feddema (1992), which has been applied in a variety of contexts, including global vegetation modeling (Potter and Klooster 1999) and climate change analysis (Grundstein 2009). Willmott and Feddema (1992) devised the index as a refinement of one described earlier by Thornthwaite (1948) and Thornthwaite and Mather (1955). Their revised index, MI', has the following form:

$$MI' = \begin{cases} P/PET - 1 & , \quad P < PET \\ 1 - PET/P & , \quad P \geq PET \\ 0 & , \quad P = PET = 0 \end{cases} \qquad (2)$$

where

P = precipitation

PET = potential evapotranspiration

(P and PET must be in equivalent measurement units, e.g., mm)

This set of equations yields a symmetric, dimensionless index scaled between -1 and 1. MI' can be calculated for any time period, but is commonly calculated on an annual basis using summed P and PET values (Willmott and Feddema 1992). An alternative to this summation approach is to calculate MI' from monthly precipitation and potential evapotranspiration values and then, for a given time window of interest, calculate its moisture index as the mean of the MI' values for all months in the time window. This "mean-of-months" approach limits the ability of short-term peaks in either precipitation or potential evapotranspiration to negate corresponding short-term deficits, as would happen under a summation approach.

For each year in our study period (i.e., 1915–2014), we used the mean-of-months approach to calculate moisture index grids for three different time windows: 1 year (MI_1'), 3 years (MI_3'), and 5 years (MI_5'). Briefly, the MI_1' grids are the mean (i.e., the mean value for each grid cell) of the 12 monthly MI' grids for each year in the study period, the MI_3' grids are the mean of the 36 monthly grids from January 2 years prior through December of the target year, and the MI_5' grids are the mean of the 60 consecutive monthly MI' grids from January 4 years prior to December of the target year. Thus, the MI_1' grid for the year 2014 is the mean of the monthly MI' grids from January to December 2014, whereas the MI_3' grid is the mean of the grids from January 2012 to December 2014 and the MI_5' grid is the mean of the grids from January 2010 to December 2014.

Annual and Multiyear Drought Maps

To determine degree of departure from typical moisture conditions, we first created a normal grid, $MI_{i\,norm}'$, for each of our three time windows, representing the mean (i.e., the mean value for each grid cell) of the 100 corresponding moisture index grids (i.e., the MI_1', MI_3', or MI_5' grids, depending on the window; see fig. 4.1). We also created a standard deviation grid, $MI_{i\,SD}'$, for each time window, calculated from the window's 100 individual moisture index grids as well as its $MI_{i\,norm}'$ grid. We subsequently calculated moisture difference *z*-scores, MDZ_{ij}, for each time window using these derived data sets:

$$MDZ_{ij} = \frac{MI_i' - MI_{i\,norm}'}{MI_{i\,SD}'} \qquad (3)$$

where

i = the analytical time window (i.e., 1, 3, or 5 years) and

j = a particular target year in our 100-year study period (i.e., 1915–2014).

MDZ scores serve as a single numerical index that may be classified in terms of degree of moisture deficit or moisture surplus (table 4.1). The classification scheme includes categories (e.g., severe drought, extreme drought) like those associated with the PDSI. The scheme has also been adopted for other drought indices such as the Standardized Precipitation Index, or SPI (McKee and others 1993). Moreover, the breakpoints between *MDZ* categories resemble those used for the SPI, such that we expect the *MDZ* categories to have theoretical frequencies of occurrence that are similar to their SPI counterparts (e.g., approximately 2.3 percent of the time for extreme drought; see McKee and others 1993, Steinemann 2003). More importantly, because of the standardization in equation 3, the breakpoints between categories remain the same regardless of the size of the time window of interest. For comparative analysis, we generated and classified *MDZ* maps of the conterminous United States, based on all three time windows, for the target year 2014.

RESULTS AND DISCUSSION

The 100-year (1915–2014) mean annual moisture index, or $MI_{1\,norm}'$, grid (fig. 4.1) provides an overview of climatic regimes in the conterminous United States. (The 100-year $MI_{3\,norm}'$ and $MI_{5\,norm}'$ grids were very similar to the mean $MI_{1\,norm}'$ grid, and so are not shown here.) Wet climates ($MI' > 0$) are common in the Eastern United States, particularly the Northeast. A noteworthy anomaly is southern Florida, especially ecoregion sections 232G–Florida Coastal Lowlands-Atlantic, 232D–Florida Coastal Lowlands-Gulf, and 411A–Everglades. This region appears to be dry relative to other parts of the East. Although southern Florida usually receives a high level of precipitation over the course of a year, this is countered by a high level of potential evapotranspiration, which results in negative MI' values. This is categorically different from the pattern observed in the driest parts of the Western United States, especially the Southwest (e.g., sections 322A–Mojave Desert,

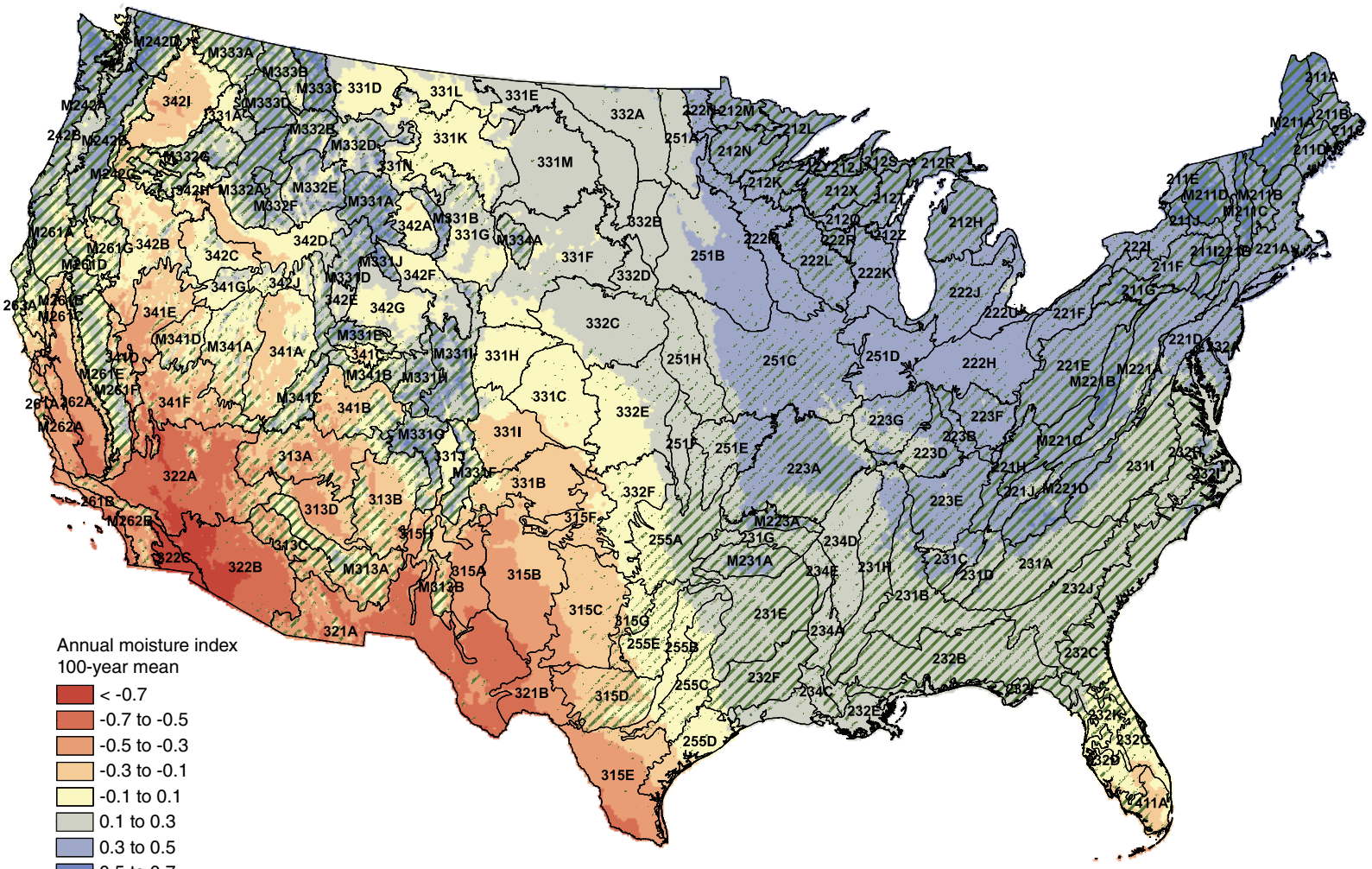

Figure 4.1—The 100-year (1915–2014) mean annual moisture index, or $MI_{1\,norm}$*, for the conterminous United States. Ecoregion section (Cleland and others 2007) boundaries and labels are included for reference. Forest cover data (overlaid green hatching) derived from Moderate Resolution Imaging Spectroradiometer (MODIS) imagery by the U.S. Department of Agriculture, Forest Service, Remote Sensing Applications Center. (Data source: PRISM Climate Group, Oregon State University)*

Table 4.1—Moisture difference *z*-score *(MDZ)* value ranges for nine wetness and drought categories, along with each category's approximate theoretical frequency of occurrence

MDZ score	Category	Frequency
		percent
< -2	Extreme drought	2.3
-2 to -1.5	Severe drought	4.4
-1.5 to -1	Moderate drought	9.2
-1 to -0.5	Mild drought	15.0
-0.5 to 0.5	Near normal conditions	38.2
0.5 to 1	Mild moisture surplus	15.0
1 to 1.5	Moderate moisture surplus	9.2
1.5 to 2	Severe moisture surplus	4.4
> 2	Extreme moisture surplus	2.3

322B–Sonoran Desert, and 322C–Colorado Desert), where potential evapotranspiration is very high, but precipitation levels are very low. In fact, dry climates ($MI' < 0$) are typical across much of the Western United States because of generally lower precipitation than the East. Nevertheless, mountainous areas in the central and northern Rocky Mountains as well as the Pacific Northwest are relatively wet, such as ecoregion sections (Cleland and others 2007) M242A–Oregon and Washington Coast Ranges, M242B–Western Cascades, M331G–South-Central Highlands, and M333C–Northern Rockies. This may be driven in part by large amounts of winter snowfall in these regions.

Figure 4.2 shows the annual (i.e., 1-year) *MDZ* map for 2014 for the conterminous United States. Much of the country saw near-normal to surplus moisture conditions during the year, but a large portion of the Southwestern United States, in a swath reaching from California to Texas, experienced moderate to extreme drought (*MDZ* < -1) conditions in 2014. Most conspicuously, a large contiguous area of extreme drought (*MDZ* < -2) covered most of northern Arizona and northwestern New Mexico. This contiguous area fell across the forested portions of several ecoregion sections: 313A–Grand Canyon, 313B–Navaho Canyonlands, 313C–Tonto Transition, 313D–Painted Desert, M313A–White Mountains-San Francisco Peaks-Mogollon Rim, 322A–Mojave Desert, and 341B–Northern Canyonlands. It also extended into the sparsely forested section 315H–Central Rio Grande Intermontane. A smaller hot spot of extreme drought occurred just to the west of this large contiguous area, primarily within sections 322A and 341F–Southeastern Great Basin. There was also a hot spot of severe to extreme drought (*MDZ* < -1.5) in central Texas, mostly in sections 255E–Texas Cross Plains and Prairie, 315D–Edwards Plateau, and 315G–Eastern Rolling Plains; only section 315D contains much forest.

Most of California experienced at least mild drought conditions (*MDZ* < -0.5) during 2014, although conditions were generally worse in the southern part of the State. For example,

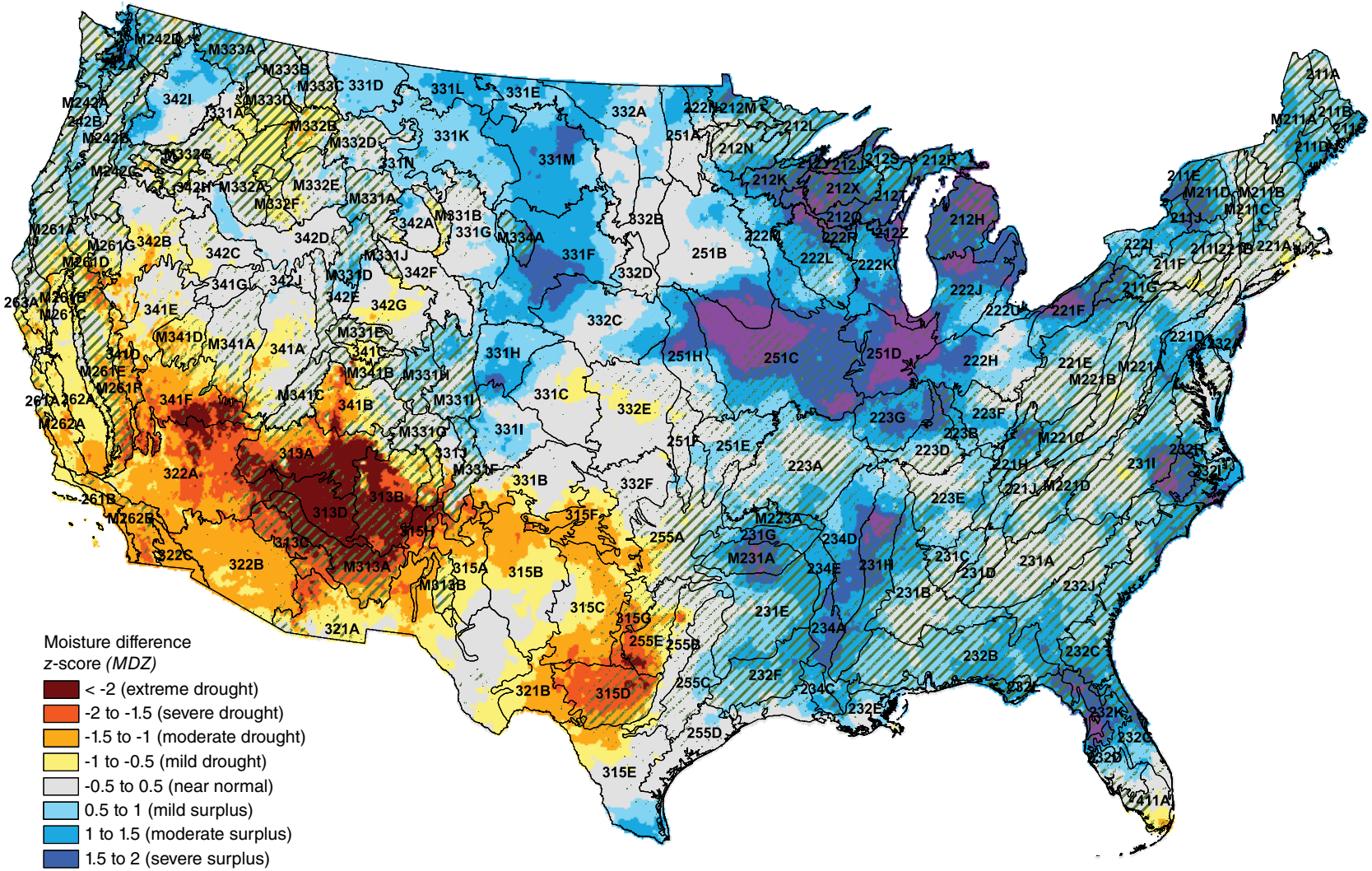

Figure 4.2—The 2014 annual (i.e., 1-year) moisture difference z*-score, or* MDZ*, for the conterminous United States. Ecoregion section (Cleland and others 2007) boundaries and labels are included for reference. Forest cover data (overlaid green hatching) derived from Moderate Resolution Imaging Spectroradiometer (MODIS) imagery by the U.S. Department of Agriculture, Forest Service, Remote Sensing Applications Center. (Data source: PRISM Climate Group, Oregon State University)*

the southern portion of section M261E–Sierra Nevada, as well as the southwestern spur of the aforementioned section 341F, contained small hot spots of severe to extreme drought conditions. In contrast, some areas within California's northernmost ecoregion sections (e.g., 263A–Northern California Coast and M261A–Klamath Mountains) actually had mild moisture surpluses during 2014. This represents a departure from the intense drought conditions that occurred almost uniformly throughout the State during the previous year, as shown in the 1-year *MDZ* map for 2013 (fig. 4.3). Indeed, 2013 was California's driest calendar year since 1895 (National Climatic Data Center 2014), as emphasized by the long list of ecoregion sections with sizeable areas of extreme drought during the year, including the aforementioned sections M261A and M261E, as well as 261A–Central California Coast, M261B–Northern California Coast Ranges, M261F–Sierra Nevada Foothills, M262B–Southern California Mountain and Valley, 263A–Northern California Coast, and 341D–Mono.

Broad-scale differences between the 2014 (fig. 4.2) and 2013 (fig. 4.3) *MDZ* maps are explained by a couple of factors. First, unusually high temperatures affected the entire Southwest in 2014 (National Climatic Data Center 2015c). Arizona, California, and Nevada had their warmest years on record; Utah had its fourth warmest year; and New Mexico had its sixth warmest year (National Climatic Data Center 2015a). For much of the region, these high temperatures increased evapotranspiration to levels that far exceeded available precipitation (National Climatic Data Center 2015c). In northern California, however, this was partially mitigated by a series of storms near the end of 2014 that pushed precipitation above normal levels. Unfortunately, these storms did not have a commensurate mitigating effect in southern California.

As is also true of the 2013 *MDZ* map, the 2014 *MDZ* map is visually striking because, outside of the Southwest, few significant drought hot spots occurred in forested parts of the United States. The only other sizeable hot spot in 2014 was an area of mild to moderate drought in the Northwestern United States, primarily in sections M332A–Idaho Batholith, M332B–Northern Rockies and Bitterroot Valley, M333D–Bitterroot Mountains, and M332F–Challis Volcanics. Overall, 2014 was, like 2013, a wet year for the country relative to historical data. The percentage of the area of the conterminous United States with moderate or worse drought conditions based on the Palmer Drought Severity Index peaked at 34.1 percent by the end of May, but decreased substantially, to 10.3 percent, by the end of December (National Climatic Data Center 2015c).

In fact, much of the Eastern United States had at least a mild moisture surplus in 2014 (see fig. 4.2). For example, the Southeast had four distinct areas with severe to extreme moisture surpluses (*MDZ* > 1.5), in North Carolina (primarily sections 232H–Middle Atlantic Coastal Plains and Flatwoods and 231I–Central Appalachian Piedmont), Florida (232D–Florida Coastal Lowlands-Gulf and 232K–Florida

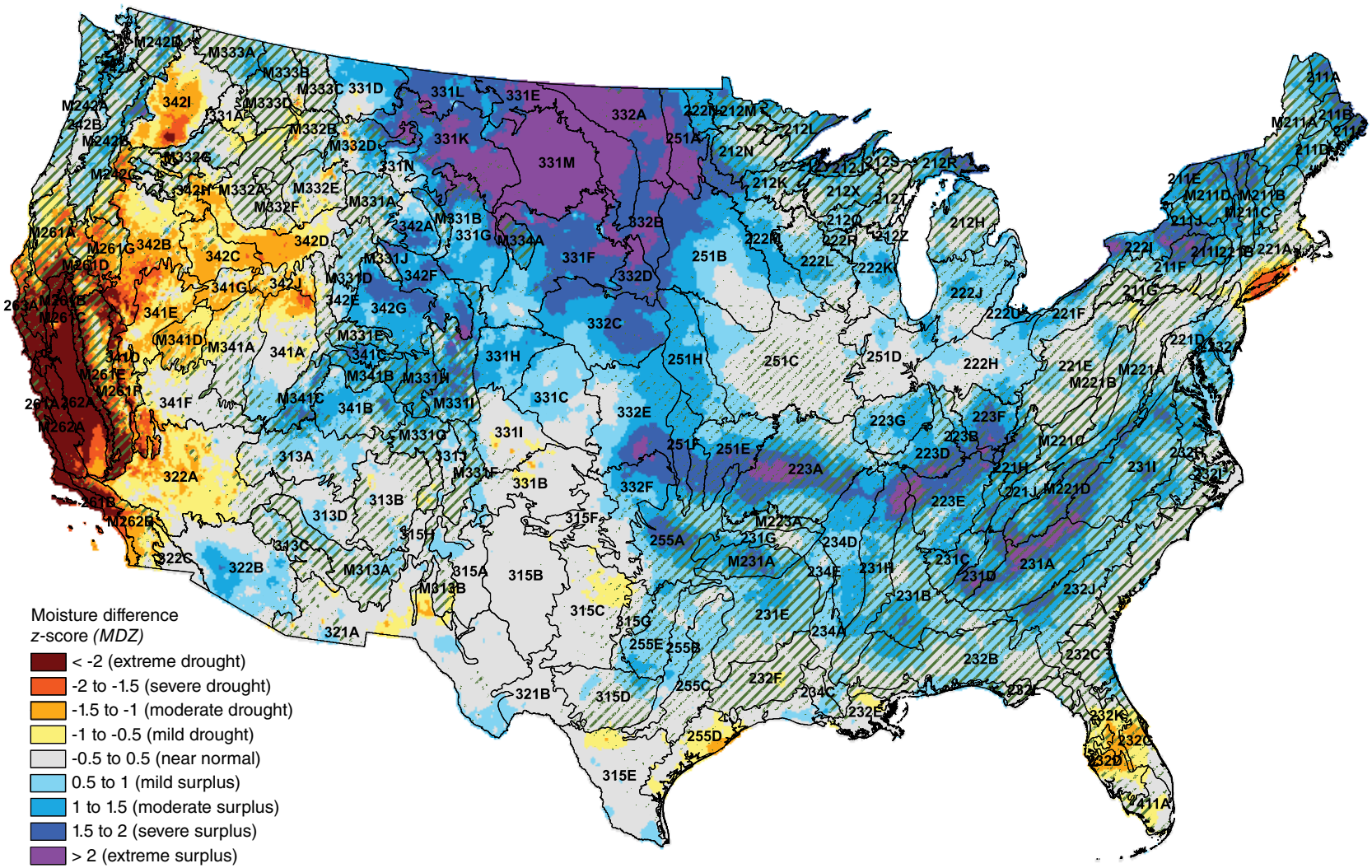

Figure 4.3—The 2013 annual (i.e., 1-year) moisture difference z-score, or MDZ, *for the conterminous United States. Ecoregion section (Cleland and others 2007) boundaries and labels are included for reference. Forest cover data (overlaid green hatching) derived from Moderate Resolution Imaging Spectroradiometer (MODIS) imagery by the U.S. Department of Agriculture, Forest Service, Remote Sensing Applications Center. (Data source: PRISM Climate Group, Oregon State University)*

Coastal Plains Central Highlands), Arkansas (231G–Arkansas Valley and M231A–Ouachita Mountains), and Tennessee (especially section 231H–Coastal Plains-Loess). Nevertheless, the most prominent areas with severe to extreme moisture surpluses during 2014 were in the Great Lakes region, including several forested sections in Ohio, Michigan, Wisconsin, and Minnesota: 212H–Northern Lower Peninsula, 212J–Southern Superior Uplands, 212K–Western Superior Uplands, 212Q–North Central Wisconsin Uplands, 212X–Northern Highlands, 212Y–Southwest Lake Superior Clay Plain, 212Z–Green Bay-Manitowac Upland, 221F–Western Glaciated Allegheny Plateau, 222L–North Central U.S. Driftless and Escarpment, and 222R–Wisconsin Central Sands. Moreover, a particularly large area of severe to extreme moisture surplus covered most of sections 251C–Central Dissected Till Plains and 251D–Central Till Plains and Grand Prairies, although neither section contains much forest. Notably, all of these areas exhibited near normal moisture conditions during 2013 (fig. 4.3). Rather, a large contiguous area of severe to extreme moisture surplus occurred further west, in the primarily nonforested Northern Great Plains region (e.g., section 331M–Missouri Plateau), while a narrow band of severe to extreme moisture surplus appeared further south (e.g., in section 223A–Ozark Highlands).

The 3-year (2012–2014; fig. 4.4) and 5-year (2010–2014; fig. 4.5) *MDZ* maps depict the recent history of moisture conditions in the conterminous United States. Perhaps most significantly, the maps clearly show that severe to extreme drought (*MDZ* < -1.5) conditions have persisted across much of the Southwestern United States for the last several years; actually, intense and widespread drought conditions have occurred in this region since the late 1990s and were also common throughout much of the 20th century (Groisman and Knight 2008, Mueller and others 2005, Woodhouse and others 2010). However, drought conditions in California and the western portion of the Southwest region appear much worse in the 3-year *MDZ* map than in the 5-year *MDZ* map, indicating that the record-setting drought conditions that have affected this region for the last few years were preceded by comparatively milder conditions in 2010 and 2011 (National Climatic Data Center 2011, 2012). A similar observation can be made for the northern portion of the Interior West region.

Elsewhere, the 5-year *MDZ* map (fig. 4.5) shows a large area of moderate to severe drought along the Gulf of Mexico coast in Texas and Louisiana, particularly in ecoregion sections 232E–Louisiana Coastal Prairies and Marshes, 232F–Coastal Plains and Flatwoods-Western

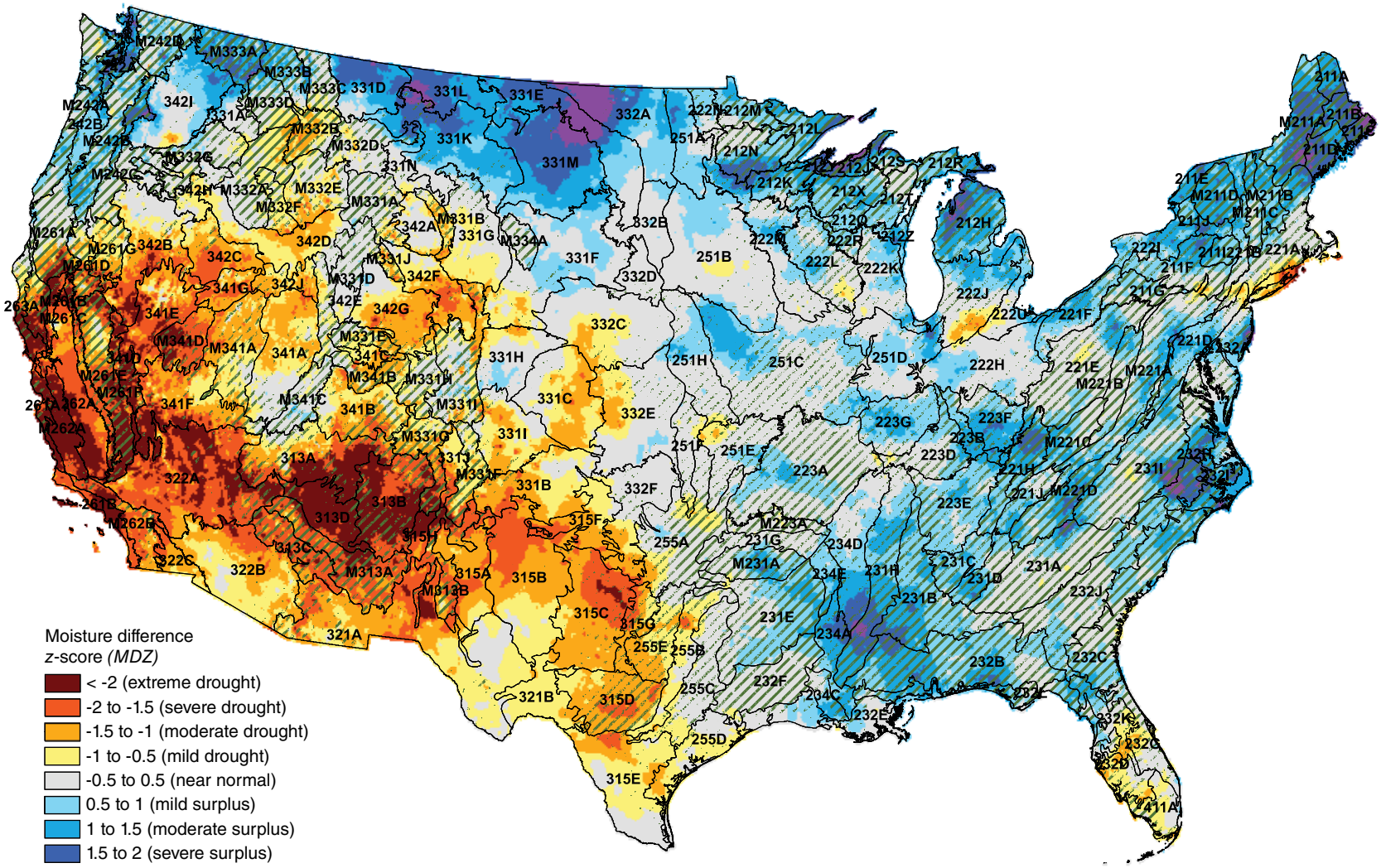

Figure 4.4—The 2012–14 (i.e., 3-year) moisture difference z*-score (*MDZ*) for the conterminous United States. Ecoregion section (Cleland and others 2007) boundaries are included for reference. Forest cover data (overlaid green hatching) derived from Moderate Resolution Imaging Spectroradiometer (MODIS) imagery by the U.S. Department of Agriculture, Forest Service, Remote Sensing Applications Center. (Data source: PRISM Climate Group, Oregon State University)*

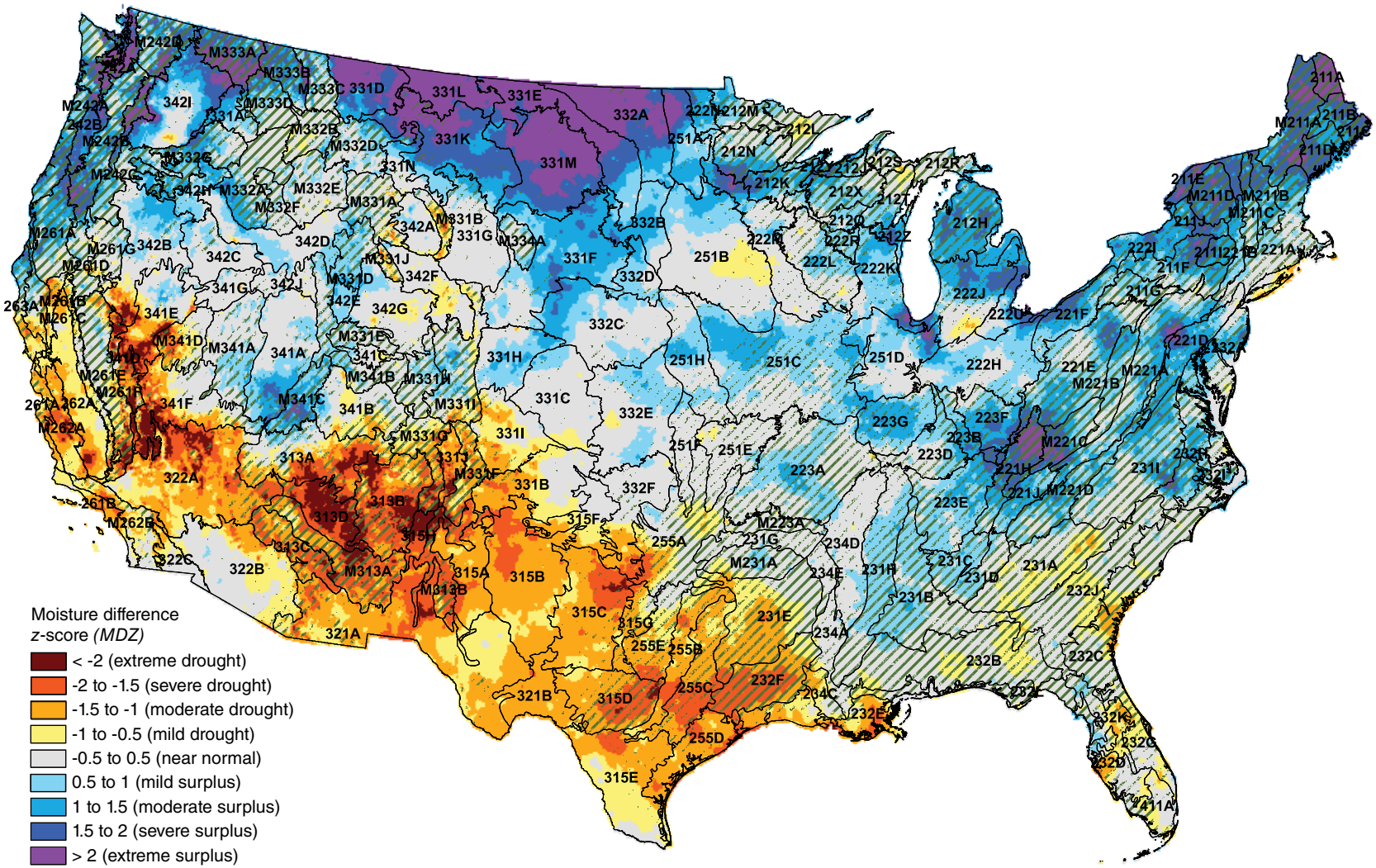

Figure 4.5—The 2010–14 (i.e., 5-year) moisture difference z*-score* (MDZ) *for the conterminous United States. Ecoregion section (Cleland and others 2007) boundaries are included for reference. Forest cover data (overlaid green hatching) derived from Moderate Resolution Imaging Spectroradiometer (MODIS) imagery by the U.S. Department of Agriculture, Forest Service, Remote Sensing Applications Center. (Data source: PRISM Climate Group, Oregon State University)*

Gulf, and 255C–Oak Woods and Prairie. By comparison, the 3-year *MDZ* map (fig. 4.4) shows little or no presence of drought conditions in these sections. Although Texas and Louisiana experienced record dryness and summer heat waves during 2010 and 2011(National Climatic Data Center 2011, 2012), the 1-year *MDZ* maps for 2013 (fig. 4.3) and 2014 (fig. 4.2) demonstrate that moisture conditions in this region have improved markedly during the last couple of years. Similarly, the 3-year and 5-year maps, as well as the 1-year map for 2013, show an area of mild to moderate drought in central Florida (sections 232D–Florida Coastal Lowlands-Gulf, 232G–Florida Coastal Lowlands-Atlantic, and 232K–Florida Coastal Plains Central Highlands) and another area of mild to severe drought in the vicinity of Long Island (in section 221A–Lower New England). However, in 2014 (see fig. 4.2) the former area displayed a moisture surplus, whereas the latter returned to near normal moisture conditions.

From a forest health perspective, the most relevant moisture surpluses are likely those that last for several years. These persistent surplus conditions are depicted in the 3-year and 5-year *MDZ* maps. For instance, the 3-year *MDZ* map (fig. 4.4) shows pockets of severe to extreme moisture surplus in various parts of the Eastern United States, including the Southeast (e.g., section 231H–Coastal Plains-Loess in Tennessee and Alabama, as well as sections 231I–Central Appalachian Piedmont and 232H–Middle Atlantic Coastal Plains and Flatwoods in North Carolina), northern New England (e.g., 211C–Fundy Coastal and Interior, 211D–Central Maine Coastal and Embayment, and M211A–White Mountains), and the Great Lakes (e.g., 212H–Northern Lower Peninsula and 212Y–Southwest Lake Superior Clay Plain). Additionally, the 3-year map shows areas of severe to extreme moisture surplus in the Pacific Northwest, primarily in sections 242A–Puget Trough, M333A–Okanogan Highland, M242C–Eastern Cascades, and M242D–Northern Cascades. The 5-year *MDZ* map (fig. 4.5) shows similar, albeit more extensive, areas of severe to extreme moisture surplus in New England and the Pacific Northwest, but there are also disparities between the maps. In particular, the moisture surplus areas in the Southeast and Great Lakes regions that are captured in the 3-year *MDZ* map do not appear in the 5-year map; instead, areas of severe to extreme surplus are shown in Kentucky (especially sections 221H–Northern Cumberland Plateau and M221C–Northern Cumberland Mountains) and Pennsylvania (sections 221D–Northern Appalachian Piedmont and M221A–Northern Ridge and Valley). This difference is explained by the high variability of moisture conditions throughout the eastern half of the country since 2010.

FUTURE EFFORTS

If the appropriate spatial data (i.e., high-resolution maps of precipitation and temperature) remain available for public use, we will continue to produce our 1-year, 3-year, and 5-year *MDZ* maps of the conterminous United States as a regular yearly component of national-scale forest health reporting. However, users should interpret and compare the *MDZ* maps presented here cautiously. Although the maps use a standardized index scale that applies regardless of the size of the time window, the window size may still merit some consideration; for instance, an extreme drought that persists over a 5-year period has substantially different forest health implications than an extreme drought over a 1-year period. Furthermore, although the 1-year, 3-year, and 5-year *MDZ* maps may together provide a comprehensive short-term overview, it may also be important to consider a particular region's longer-term moisture history when assessing the current health of its forests. For example, in geographic regions where droughts have historically occurred on a frequent (e.g., annual or nearly annual) basis, certain tree species may be better adapted to a regular lack of available moisture (McDowell and others 2008). Because of this variability in species' drought tolerance, a long period of persistent and severe drought conditions could ultimately lead to changes in regional forest composition (Mueller and others 2005); compositional changes may similarly arise from a long period of persistent moisture surplus (McEwan and others 2011). In turn, such changes are likely to affect how a region's forests respond to subsequent drought or surplus conditions. In future work, we hope to provide forest managers and other decisionmakers with better quantitative evidence regarding critical relationships between moisture extremes and significant forest health impacts such as regional-scale tree mortality (e.g., Mitchell and others 2014). We also intend to examine the role of moisture extremes as an inciting factor for other forest threats such as wildfire or pest outbreaks.

LITERATURE CITED

Adams, H.D.; Guardiola-Claramonte, M.; Barron-Gafford, G.A. [and others]. 2009. Temperature sensitivity of drought-induced tree mortality portends increased regional die-off under global-change-type drought. Proceedings of the National Academy of Sciences. 106(17): 7063–7066.

Akin, W.E. 1991. Global patterns: climate, vegetation, and soils. Norman, OK: University of Oklahoma Press. 370 p.

Allen, C.D.; Macalady, A.K.; Chenchouni, H. [and others]. 2010. A global overview of drought and heat-induced tree mortality reveals emerging climate change risks for forests. Forest Ecology and Management. 259(4): 660–684.

Alley, W.M. 1984. The Palmer Drought Severity Index: limitations and assumptions. Journal of Climate and Applied Meteorology. 23: 1100–1109.

Anderegg, L.D.L.; Anderegg, W.R.L.; Berry, J.A. 2013. Not all droughts are created equal: translating meteorological drought into woody plant mortality. Tree Physiology. 33(7): 672–683.

Archaux, F.; Wolters, V. 2006. Impact of summer drought on forest biodiversity: what do we know? Annals of Forest Science. 63: 645–652.

Clark, J.S. 1989. Effects of long-term water balances on fire regime, north-western Minnesota. Journal of Ecology. 77: 989–1004.

Cleland, D.T.; Freeouf, J. A.; Keys, J.E.; [and others]. 2007. Ecological subregions: sections and subsections for the conterminous United States. In: Sloan, A.M., tech. ed. Washington, DC: U.S. Department of Agriculture, Forest Service. Gen. Tech. Rep. WO-76D. [Map, presentation scale 1:3,500,000; colored]. Also on CD-ROM as a GIS coverage in ArcINFO format.

Clinton, B.D.; Boring, L.R.; Swank, W.T. 1993. Canopy gap characteristics and drought influences in oak forests of the Coweeta Basin. Ecology. 74(5): 1551–1558.

Daly, C.; Gibson, W.P.; Taylor, G.H. [and others]. 2002. A knowledge-based approach to the statistical mapping of climate. Climate Research. 22: 99–113.

Groisman, P.Y.; Knight, R.W. 2008. Prolonged dry episodes over the conterminous United States: new tendencies emerging during the last 40 years. Journal of Climate. 21: 1850–1862.

Grundstein, A. 2009. Evaluation of climate change over the continental United States using a moisture index. Climatic Change. 93: 103–115.

Guarín, A.; Taylor, A.H. 2005. Drought triggered tree mortality in mixed conifer forests in Yosemite National Park, California, USA. Forest Ecology and Management. 218: 229–244.

Hanson, P.J.; Weltzin, J.F. 2000. Drought disturbance from climate change: response of United States forests. The Science of the Total Environment. 262: 205–220.

Kareiva, P.M.; Kingsolver, J.G.; Huey, B.B, eds. 1993. Biotic interactions and global change. Sunderland, MA: Sinauer Associates, Inc. 559 p.

Keetch, J.J.; Byram, G.M. 1968. A drought index for forest fire control. Res. Pap. SE-38. Asheville, NC: U.S. Department of Agriculture, Forest Service, Southeastern Forest Experiment Station. 33 p.

Koch, F.H.; Coulston, J.W. 2015. Chapter 4. 1-year (2013), 3-year (2011–2013), and 5-year (2009–2013) drought maps for the conterminous United States. In: Potter, K.M.; Conkling, B.L., eds. Forest Health Monitoring: national status, trends, and analysis 2014. Gen. Tech. Rep. SRS-209. Asheville, NC: US Department of Agriculture, Forest Service, Southern Research Station: 57–71.

Koch, F.H.; Coulston, J.W.; Smith, W.D. 2012a. High-resolution mapping of drought conditions. In: Potter, K.M.; Conkling, B.L., eds. Forest Health Monitoring 2008 national technical report. Gen. Tech. Rep. SRS-158. Asheville, NC: U.S. Department of Agriculture, Forest Service, Southern Research Station: 45–62.

Koch, F.H.; Coulston, J.W.; Smith, W.D. 2012b. Mapping drought conditions using multi-year windows. In: Potter, K.M.; Conkling, B.L., eds. Forest Health Monitoring 2009 national technical report. Gen. Tech. Rep. SRS-167. Asheville, NC: U.S. Department of Agriculture, Forest Service, Southern Research Station: 163–179.

Koch, F.H.; Smith, W D.; Coulston, J.W. 2013a. Recent drought conditions in the conterminous United States. In: Potter, K.M.; Conkling, B.L., eds. Forest Health Monitoring: national status, trends, and analysis 2011. Gen. Tech. Rep. SRS-185. Asheville, NC: U.S. Department of Agriculture, Forest Service, Southern Research Station: 41–58.

Koch, F.H.; Smith, W.D.; Coulston, J.W. 2013b. An improved method for standardized mapping of drought conditions. In: Potter, K.M.; Conkling, B.L., eds. Forest Health Monitoring: national status, trends, and analysis 2010. Gen. Tech. Rep. SRS-176. Asheville, NC: U.S. Department of Agriculture, Forest Service, Southern Research Station: 67–83.

Koch, F.H.; Smith, W.D.; Coulston, J.W. 2014. Drought patterns in the conterminous United States and Hawaii. In: Potter, K.M.; Conkling, B.L., eds. Forest Health Monitoring: national status, trends, and analysis 2012. Gen. Tech. Rep. SRS-198. Asheville, NC: U.S. Department of Agriculture, Forest Service, Southern Research Station: 49–72.

Koch, F.H.; Smith, W.D.; Coulston, J.W. 2015. Drought patterns in the conterminous United States, 2012. In: Potter, K.M.; Conkling, B.L., eds. Forest Health Monitoring: national status, trends, and analysis 2013. Gen. Tech. Rep. SRS-207. Asheville, NC: US Department of Agriculture, Forest Service, Southern Research Station: 55–69.

Laurance, S.G. W.; Laurance, W.F.; Nascimento, H. E. M. [and others]. 2009. Long-term variation in Amazon forest dynamics. Journal of Vegetation Science. 20(2): 323–333.

Martínez-Vilalta, J.; Lloret, F.; Breshears, D.D. 2012. Drought-induced forest decline: causes, scope and implications. Biology Letters. 8(5): 689–691.

Mattson, W.J.; Haack, R.A. 1987. The role of drought in outbreaks of plant-eating insects. BioScience. 37(2): 110–118.

McDowell, N.; Pockman, W.T.; Allen, C.D. [and others]. 2008. Mechanisms of plant survival and mortality during drought: why do some plants survive while others succumb to drought? New Phytologist. 178: 719–739.

McEwan, R.W.; Dyer, J.M.; Pederson, N. 2011. Multiple interacting ecosystem drivers: toward an encompassing hypothesis of oak forest dynamics across eastern North America. Ecography. 34: 244–256.

McKee, T.B.; Doesken, N.J.; Kleist, J. 1993. The relationship of drought frequency and duration to time scales. In: Proceedings of the eighth conference on applied climatology. Boston, MA: American Meteorological Society: 179–184.

Millar, C.I.; Westfall, R.D.; Delany, D.L. 2007. Response of high-elevation limber pine (*Pinus flexilis*) to multiyear droughts and 20th-century warming, Sierra Nevada, California, USA. Canadian Journal of Forest Research. 37: 2508–2520.

Mitchell, P.J.; O'Grady, A.P.; Hayes, K.R.; Pinkard, E.A. 2014. Exposure of trees to drought-induced die-off is defined by a common climatic threshold across different vegetation types. Ecology and Evolution. 4(7): 1088–1101.

Monteith, J.L. 1965. Evaporation and environment. Symposia of the Society for Experimental Biology. 19: 205–234.

Mueller, R.C.; Scudder, C.M.; Porter, M.E. [and others]. 2005. Differential tree mortality in response to severe drought: evidence for long-term vegetation shifts. Journal of Ecology. 93: 1085–1093.

National Climatic Data Center. 2011. State of the climate – drought – annual report 2010. http://www.ncdc.noaa.gov/sotc/drought/201013. [Date accessed: July 28, 2015].

National Climatic Data Center. 2012. State of the climate – drought – annual report 2011. http://www.ncdc.noaa.gov/sotc/drought/201113. [Date accessed: July 28, 2015].

National Climatic Data Center. 2014. State of the climate – drought – annual report 2013. http://www.ncdc.noaa.gov/sotc/drought/201313. [Date accessed: July 19, 2015].

National Climatic Data Center. 2015a. Climatological rankings–temperature, precipitation, and drought. http://www.ncdc.noaa.gov/temp-and-precip/climatological-rankings/index.php. [Date accessed: July 28, 2015].

National Climatic Data Center. 2015b. Divisional temperature-precipitation-drought. Documentation for the nClimDiv database. ftp://ftp.ncdc.noaa.gov/pub/data/cirs/climdiv/divisional-readme.txt. [Date accessed: July 29, 2015].

National Climatic Data Center. 2015c. State of the climate – drought – annual report 2014. http://www.ncdc.noaa.gov/sotc/drought/201413. [Date accessed: July 16, 2015].

Palmer, W.C. 1965. Metereological drought. Res. Pap. No. 45. Washington, DC: U.S. Department of Commerce, Weather Bureau. 58 p.

Peng, C.; Ma, Z.; Lei, X. [and others]. 2011. A drought-induced pervasive increase in tree mortality across Canada's boreal forests. Nature Climate Change. 1(9): 467–471.

Peters, M.P.; Iverson, L.R.; Matthews, S.N. 2015. Long-term droughtiness and drought tolerance of Eastern U.S. forests over five decades. Forest Ecology and Management. 345: 56–64.

Potter, C.S.; Klooster, S.A. 1999. Dynamic global vegetation modelling for prediction of plant functional types and biogenic trace gas fluxes. Global Ecology and Biogeography. 8(6): 473–488.

PRISM Climate Group. 2015. 2.5-arcmin (4 km) gridded monthly climate data. http://www.prism.oregonstate.edu. [Date accessed: June 23, 2015].

Raffa, K.F.; Aukema, B.H.; Bentz, B.J. [and others]. 2008. Cross-scale drivers of natural disturbances prone to anthropogenic amplification: the dynamics of bark beetle eruptions. BioScience. 58(6): 501–517.

Rozas, V.; García-González, I. 2012. Too wet for oaks? Inter-tree competition and recent persistent wetness predispose oaks to rainfall-induced dieback in Atlantic rainy forest. Global and Planetary Change. 94–95: 62–71.

Rozas, V.; Sampedro, L. 2013. Soil chemical properties and dieback of *Quercus robur* in Atlantic wet forests after a weather extreme. Plant and Soil. 373(1–2): 673–685.

Schoennagel, T.; Veblen, T.T.; Romme, W.H. 2004. The interaction of fire, fuels, and climate across Rocky Mountain forests. BioScience. 54(7): 661–676.

Steinemann, A. 2003. Drought indicators and triggers: a stochastic approach to evaluation. Journal of the American Water Resources Association. 39(5): 1217–1233.

Svoboda, M.; LeComte, D.; Hayes, M. [and others]. 2002. The drought monitor. Bulletin of the American Meteorological Society. 83(8): 1181–1190.

Thornthwaite, C.W. 1948. An approach towards a rational classification of climate. Geographical Review. 38(1): 55–94.

Thornthwaite, C.W.; Mather, J.R. 1955. The water balance. Publications in Climatology. 8(1): 1–104.

Trouet, V.; Taylor, A.H.; Wahl, E.R. [and others]. 2010. Fire-climate interactions in the American West since 1400 CE. Geophysical Research Letters. 37(4): L04702.

Williams, A.P.; Allen, C.D.; Macalady, A.K. [and others]. 2013. Temperature as a potent driver of regional forest drought stress and tree mortality. Nature Climate Change. 3(3): 292–297.

Willmott, C.J.; Feddema, J.J. 1992. A more rational climatic moisture index. Professional Geographer. 44(1): 84–87.

Woodhouse, C. A.; Meko, D. M.; MacDonald, G. M. [and others]. 2010. A 1,200-year perspective of 21st century drought in southwestern North America. Proceedings of the National Academy of Sciences. 107(50): 21283–21288.

CHAPTER 5.
Tree Mortality

Mark J. Ambrose

INTRODUCTION

Tree mortality is a natural process in all forest ecosystems. However, extremely high mortality can be an indicator of forest health issues. On a regional scale, high mortality levels may indicate widespread insect or disease problems. High mortality may also occur if a large proportion of the forest in a particular region is made up of older, senescent stands.

The mission of the Forest Health Monitoring (FHM) Program is to monitor, assess, and report on the status, changes, and long-term trends in forest ecosystem health in the United States (FHM 1994). Thus, the approach to mortality presented here seeks to detect mortality patterns that might reflect subtle changes to fundamental ecosystem processes (due to such large-scale factors as air pollution, global climate change, or fire-regime change) that transcend individual tree species-pest/pathogen interactions. However, sometimes the proximate cause of mortality may be discernable. In such cases, the cause of mortality is reported, both because it is of interest in and of itself to many readers and because understanding such proximate causes of mortality might provide insight into whether the mortality is within the range of natural variation or reflects more fundamental changes to ecological processes.

DATA

Mortality is analyzed using Forest Inventory and Analysis (FIA) phase 2 (P2) data. FIA P2 data are collected across forested land throughout the United States, with approximately one plot per 6,000 acres of forest, using a rotating panel sample design (Bechtold and Patterson 2005). Field plots are divided into spatially balanced panels, with one panel being measured each year. A single cycle of measurements consists of measuring all panels. This "annualized" method of inventory was adopted, State by State, beginning in 1999. Any analysis of mortality requires data collected at a minimum of two points in time from any given plot. Therefore, mortality analysis was possible for areas where data from repeated plot measurements using consistent sampling protocols were available (i.e., where one cycle of measurements had been completed and at least one panel of the next cycle had been measured, and where there had been no changes to the protocols affecting measurement of trees or saplings). For this report, the repeated P2 data were available for all of the Central and Eastern States, and data for many States include a third cycle of measurements (i.e., a third measurement of the plots).

Once all P2 plots have been remeasured in a State, mortality estimates generally will be based on a sample intensity of approximately 1 plot:

6,000 acres of forest.[2] However, at this time not all plots have been remeasured in all the States included in this analysis. When not all plots have been remeasured, mortality estimates are based on a lower effective sample intensity. Table 5.1 shows the 37 States from which consistent, repeated P2 measurements were available, the time period spanned by the data, and the effective sample intensity. Also shown is the proportion of plots measured for a third time. The States included in this analysis, as well as the forest cover within those States, are shown in figure 5.1.

Because the data used here are collected using a rotating panel design and all available annualized data are used, the majority of data used in this mortality analysis were also used in the analysis presented in the previous FHM national report (Ambrose 2015b). Thus, it would be very unusual to see any great changes in mortality patterns from one annual report to the next. The rotating panel design may also produce a time lag of several years in detecting extraordinary mortality. Nevertheless, it is important to look at mortality patterns every year so as not to miss detecting mortality patterns that may be indicative of forest health problems as soon as they become discernable.

[2] In some States, more intensive sampling has been implemented. See table 5.1 for details.

Table 5.1— States from which repeated Forest Inventory and Analysis (FIA) phase 2 measurements were available, the time period spanned by the data, and the effective sample intensity (based on plot density and proportion of plots that had been remeasured) in the available datasets

Time period	States	Effective sample intensity	Proportion of plots measured 3 times
1999–2013	IN	1 plot: 6,000 acres	4/5
1999–2013	ME	1 plot: 6,000 acres	1.0
1999–2013	WI	1 plot: 3,000 acres[a]	4/5
1999–2014	MN	1 plot: 3,000 acres[a]	1.0
1999–2014	MO	1 plot: 6,000 acres[b]	1.0
2000–2013	MI	1 plot: 2,000 acres[c]	4/5
2000–2013	PA, VA	1 plot: 6,000 acres	1.0
2000–2014	AR	1 plot: 6,000 acres	4/5
2000–2014	IA	1 plot: 6,000 acres	1.0
2001–2013	GA, NE	1 plot: 6,000 acres	3/5
2001–2013	KS	1 plot: 6,000 acres	4/5
2001–2013	OH	1 plot: 6,000 acres	2/5
2001–2013	TX[d]	1 plot: 6,000 acres	1.0
2001–2012	TN	1 plot: 6,000 acres	2/5
2001–2013	LA	1 plot: 8,400 acres	0
2001–2014	AL	1 plot: 6,000 acres	2/7
2001–2014	IL, ND, SD	1 plot: 6,000 acres	4/5
2002-2012	KY	1 plot: 6,000 acres	0
2002–2013	FL	1 plot: 6,000 acres	0
2002–2013	NH, NY	1 plot: 6,000 acres	1/5
2002–2013	SC	1 plot: 6,000 acres	2/5
2003–2013	CT, MA, RI, VT	1 plot: 6,000 acres	1/5
2003–2014	NC	1 plot: 7,000 acres	0
2004–2013	DE, MD, NJ, WV	1 plot: 6,000 acres	0
2006–2014	MS	1 plot: 7,000 acres	0
2008–2013	OK[e]	1 plot: 7,500 acres	0

[a] In Minnesota and Wisconsin, the phase 2 inventory was done at twice the standard FIA sample intensity, approximately 1 plot per 3,000 acres.

[b] In Missouri, the phase 2 inventory was done at twice the standard FIA sample intensity, approximately 1 plot per 3,000 acres, on national forest lands and at the standard intensity of 1 plot per 6,000 acres on all other lands.

[c] In Michigan, the phase 2 inventory was done at triple the standard FIA sample intensity, approximately 1 plot per 2,000 acres.

[d] Annualized growth and mortality data were only available for eastern Texas.

[e] Annualized growth and mortality data were only available for eastern Oklahoma.

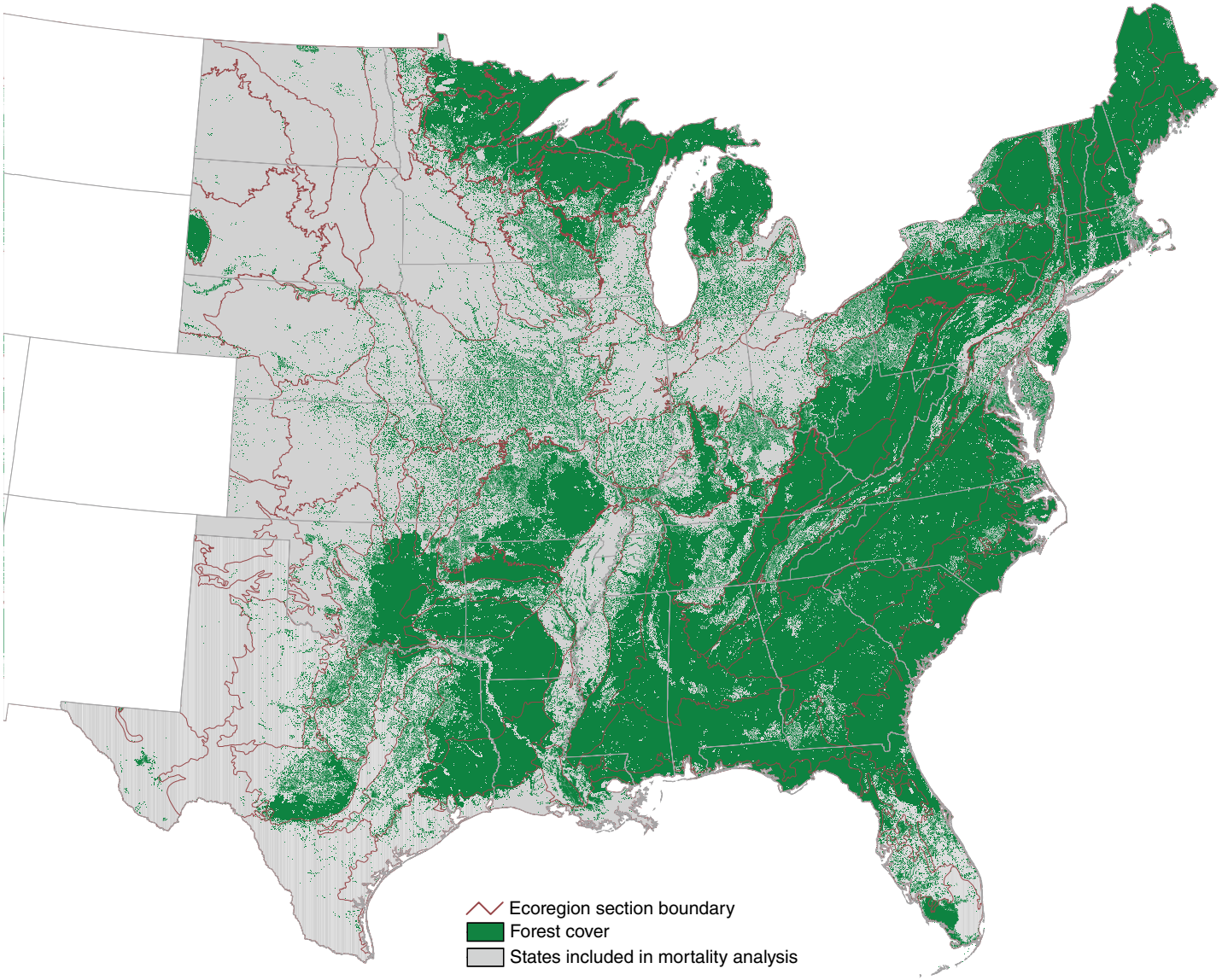

Figure 5.1—Forest cover in the States where mortality was analyzed by ecoregion section (Cleland and others 2007). Forest cover was derived from Moderate Resolution Imaging Spectroradiometer (MODIS) satellite imagery (USDA Forest Service 2008).

METHODS

The methods used in this analysis were developed for earlier FHM national reports (2001–2004), using FHM and FIA phase 3 (P3) data. FIA P2 tree (≥ 5 inches diameter at breast height, or d.b.h.) and sapling (1 inch ≤ d.b.h. < 5 inches) data were used to estimate average annual tree mortality in terms of tons of aboveground biomass per acre. The data were obtained from the public FIA Database version 6.0 (USDA Forest Service 2014). The biomass represented by each tree was calculated by FIA and provided in the FIA Database (USDA Forest Service 2015). To compare mortality rates across forest types and climate zones, the ratio of annual mortality to gross growth (MRATIO) is used as a standardized mortality indicator (Coulston and others 2005b). Gross growth rate and mortality rate, in terms of tons of biomass per acre, were independently calculated for each of 98 ecoregion sections (Cleland and others 2007, McNab and others 2007) covering the Eastern United States using a mixed modeling procedure where plot-to-plot variability is considered a random effect and time is a fixed effect. The mixed modeling approach has been shown to be particularly efficient for estimation using data where not all plots have been measured over identical time intervals (Gregoire and others 1995), which is the case for the current FIA inventory methodology. MRATIOs were then calculated from the growth and mortality rates. For details on the method, see appendix A–Supplemental Methods in Forest Health Monitoring 2001 National Technical Report (Coulston and others 2005c) and appendix A–Supplemental Methods in Forest Health Monitoring 2003 National Technical Report (Coulston and others 2005a).

In addition, the ratio of average dead tree diameter to average surviving live tree diameter (DDLD ratio) was calculated for each plot where mortality occurred. Low DDLD ratios (much less than 1) usually indicate competition-induced mortality typical of young, vigorous stands, whereas high ratios (much greater than 1) indicate mortality associated with senescence or some external factors such as insects or disease (Smith and Conkling 2005). Intermediate DDLD ratios can be hard to interpret because a variety of stand conditions can produce such DDLD values. The DDLD ratio is most useful for analyzing mortality in regions that also have high MRATIOs. High DDLD values in regions with very low MRATIOs may indicate small areas experiencing high mortality of large trees or locations where the death of a single large tree (such as a remnant pine in a young hardwood stand) has produced a deceptively high DDLD.

To further analyze tree mortality, the number of stems and the total biomass of trees that died also were calculated by species within each ecoregion. Identifying the tree species experiencing high mortality in an ecoregion is a first step in identifying what forest health issue may be affecting the forests. Although determining particular causal agents associated with all observed mortality is beyond the scope

of this report, often there are well-known insects and pathogens that are "likely suspects" once the affected tree species are identified.

Finally, a biomass weighted mean mortality age was calculated by ecoregion and species. For each species experiencing mortality in an ecoregion, the mean stand age was calculated, weighted by the dead biomass on the plot. This value gives a rough indicator of the average age of the stands in which trees died. However, the age of individual trees may differ significantly from the age assigned to a stand by FIA field crews, especially in mixed species stands. When the age of trees that die is relatively low compared with the age at which trees of a particular species usually become senescent, it suggests that some pest, pathogen, or other forest health problem may be affecting the forest.

RESULTS AND DISCUSSION

The MRATIO values are shown in figure 5.2. The MRATIO can be large if an over-mature forest is senescing and losing a cohort of older trees. If forests are not naturally senescing, a high MRATIO (> 0.6) may indicate high mortality due to some acute cause (insects or pathogens) or due to generally deteriorating forest health conditions. An MRATIO value > 1 indicates that mortality exceeds growth and live standing biomass is actually decreasing.

The highest MRATIOs occurred in ecoregion sections 331F–Western Great Plains (MRATIO = 1.73) in South Dakota and Nebraska, 332F–South-Central and Red Bed Plains (MRATIO = 1.53) in southern Kansas, and M334A–Black Hills (MRATIO = 1.32) in western South Dakota; in all three regions, mortality actually exceeded growth. Other areas of high mortality relative to growth were ecoregion sections 251F–Flint Hills (MRATIO = 0.95) in Kansas, 332D–North-Central Great Plains in South Dakota and Nebraska (MRATIO = 0.76), and 331M–Missouri Plateau (MRATIO = 0.67). Table 5.2 shows the tree species experiencing the greatest mortality in those ecoregions. Tree growth is generally slow in these ecoregion sections because of naturally dry conditions. Where the number of sample plots is small and tree growth is slow, care must be taken in interpreting mortality relative to growth.

The results of the analysis of the relative sizes of trees that died to those that lived, the DDLD ratio, are shown in table 5.3. The DDLD ratio is a plot-level indicator, so I obtained summary statistics for the ecoregions where mortality relative to growth was highest. In all cases the mean and median DDLDs were rather close to one, meaning that the trees that died were similar in size to the trees that survived. However, there were some plots with extremely high DDLD values. Interestingly, the same pattern of mean and median DDLD close to one and some high DDLD values was observed in nearly all ecoregions, regardless of the overall mortality level. With the exception of M334A–Black Hills, in all of the ecoregion sections exhibiting high mortality relative to growth, the predominant vegetation is grassland (see the forest cover in fig. 5.1). In most of them, though the ecoregions were quite large, there were

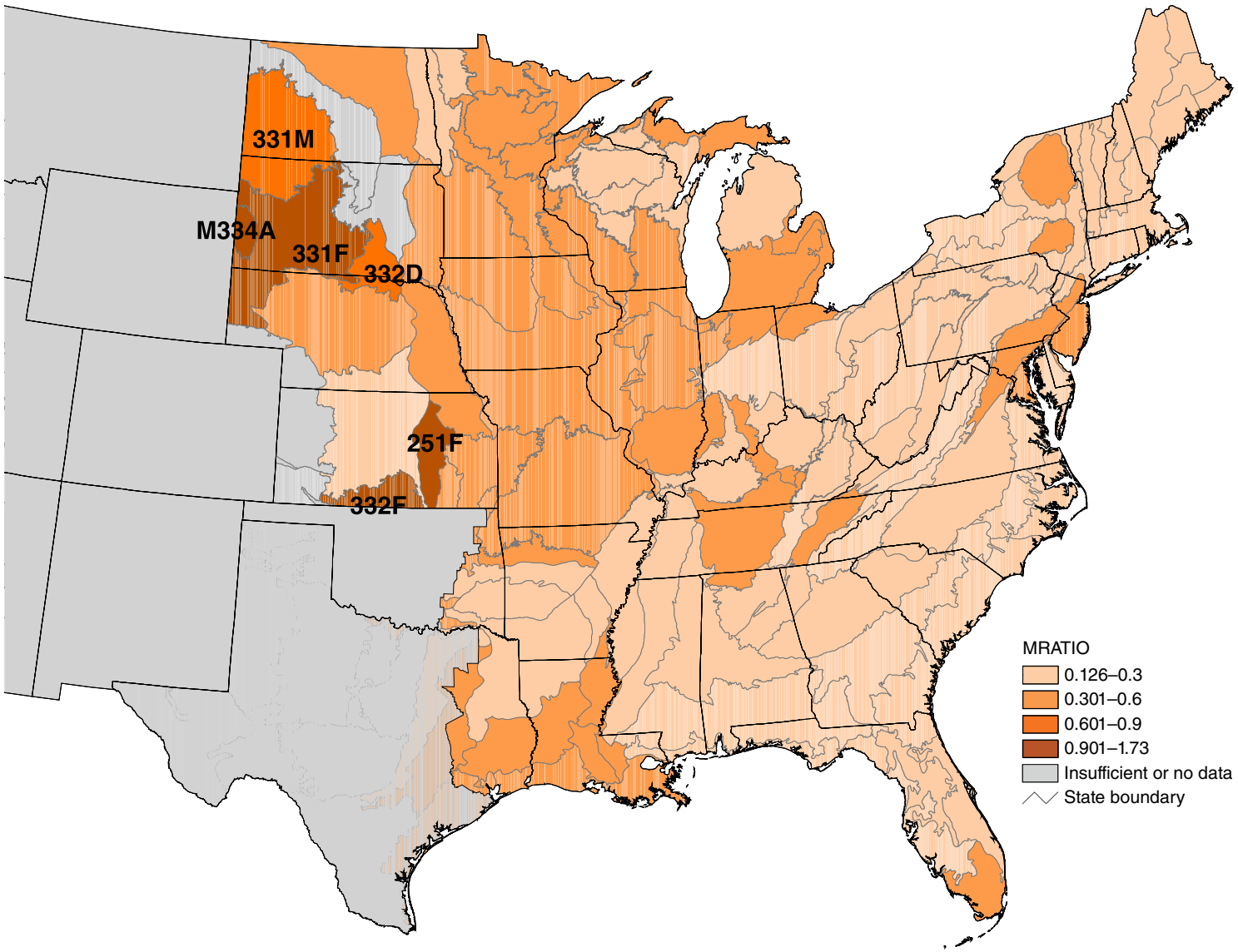

Figure 5.2—Tree mortality expressed as the ratio of annual mortality of woody biomass to gross annual growth in woody biomass (MRATIO) by ecoregion section (Cleland and others 2007). Ecoregions with high MRATIOs are identified by section number. (Data source: U.S. Department of Agriculture, Forest Service, Forest Inventory and Analysis Program)

Table 5.2—Tree species responsible for at least 5 percent of the mortality (in terms of biomass) for ecoregions where the MRATIO was 0.60 or greater

Ecoregion section	MRATIO	Tree species	Percent of total ecoregion mortality biomass	Mean age of dead trees[a]	Species percent mortality (biomass)	(stems)
251F–Flint Hills	0.95	American elm *(Ulmus americana)*	20.53	36	16.05	18.64
		Eastern redbud *(Cercis canadensis)*	15.4	58	59.16	32.59
		Green ash *(Fraxinus pennsylvanica)*	9.36	59	9.19	3.84
		White mulberry *(Morus alba)*	9.2	--	63.53	46.64
		Hackberry *(Celtis occidentalis)*	8.12	73	2.58	6.56
331F–Western Great Plains	1.73	Ponderosa pine *(Pinus ponderosa)*	61.91	51	7.97	11.14
		Green ash *(Fraxinus pennsylvanica)*	13.08	44	11.73	7.52
		Eastern cottonwood *(Populus deltoides)*	9.22	61	3.61	21.16
		Bur oak *(Quercus macrocarpa)*	5.92	61	4.82	12.84
331M–Missouri Plateau	0.67	Eastern cottonwood *(Populus deltoides)*	37.28	51	11.21	8.16
		Bur oak *(Quercus macrocarpa)*	24.81	60	7.49	6.24
		Green ash *(Fraxinus pennsylvanica)*	21.94	63	5.47	6.5
		American elm *(Ulmus americana)*	6.43	71	12.98	3.3
332D–North-Central Great Plains	0.76	American elm *(Ulmus americana)*	24.72	48	24.33	24.58
		Eastern cottonwood *(Populus deltoides)*	24.28	85	10.64	4.5
		Ponderosa pine *(Pinus ponderosa)*	15.99	44	20.37	30.72
		Green ash *(Fraxinus pennsylvanica)*	9.81	63	11.82	14.25
		Bur oak *(Quercus macrocarpa)*	9.29	64	2.06	4.2
		Eastern redcedar *(Juniperus virginiana)*	5.78	34	3.63	7.58
		Hackberry *(Celtis occidentalis)*	5.26	60	4.15	0.38
332F–South-Central and Red Bed Plains	1.53	Black willow *(Salix nigra)*	20.35	51	40.09	44
		Black locust *(Robinia pseudoacacia)*	18.56	40	22.93	39.95
		Eastern cottonwood *(Populus deltoides)*	16.36	39	6.34	7.3
		Eastern redcedar *(Juniperus virginiana)*	10.3	45	17.31	12.15
		Hackberry *(Celtis occidentalis)*	8.67	8	13.23	7.82
		Red mulberry *(Morus rubra)*	7.96	43	4.68	2.38
		American elm *(Ulmus americana)*	7.18	39	15.27	2.69
M334A–Black Hills	1.32	Ponderosa pine *(Pinus ponderosa)*	85.24	63	5.73	10.46
		Quaking aspen *(Populus tremuloides)*	5.94	72	22.15	24.84

MRATIO = ratio of annual mortality of woody biomass to gross annual growth in woody biomass.

[a] Ages are estimated from the stand age as determined by the FIA field crew. It is possible, especially in mixed-species stands, that the age of individual trees that died differed significantly from the stand age.

Table 5.3—Dead diameter–live diameter (DDLD) ratios for ecoregion sections where the MRATIO was 0.60 or greater

Ecoregion section	Mean DDLD	Maximum DDLD	Median DDLD	Minimum DDLD
251F–Flint Hills	1.04	4.77	0.79	0.25
331F–Western Great Plains	1.00	3.29	0.91	0.08
331M–Missouri Plateau	1.04	2.45	0.90	0.14
332D–North-Central Great Plains	1.12	5.38	0.91	0.15
332F–South-Central and Red Bed Plains	1.11	3.11	1.08	0.14
M334A–Black Hills	1.05	7.02	0.84	0.16

MRATIO = ratio of annual mortality of woody biomass to gross annual growth in woody biomass.

relatively few forested plots measured (67 plots in region 251F, 103 plots in region 331F, 83 plots in region 331M, 59 plots in region 332D, and 31 plots in region 332F).

In ecoregion section M334A-Black Hills, by far the largest amount of biomass that died was ponderosa pine (*Pinus ponderosa*) (table 5.2); however, this represented a relatively small proportion of the ponderosa pine in the ecoregion (about 10 percent of ponderosa pine stems and 6 percent of biomass). In the adjacent ecoregion section 331F–Western Great Plains, where the MRATIO was highest, ponderosa pine also made up the vast majority of trees that died (62 percent). Here, too, this mortality represented a relatively small proportion of the ponderosa pine (biomass and stems) in the region. The pine mortality in both ecoregions is very likely related to mountain pine beetle (*Dendroctonus ponderosae*). There has been an ongoing pine beetle outbreak in the Black Hills (South Dakota Department of Agriculture 2011, 2012, 2013, 2014), and mountain pine beetle–related mortality has been reported in western Nebraska (Nebraska Forest Service 2011, 2012) with an outbreak that began in 2009, though pine beetle-related mortality there has fallen significantly more recently (Nebraska Forest Service 2014). Drought in 2012 and 2013, affecting much of South Dakota and Nebraska (Nebraska Forest Service 2012, 2013; South Dakota Department of Agriculture 2012), may also have contributed to pine mortality, as well as that of other species, in these ecoregions.

Both ecoregions 331F and 332D have had high mortality relative to growth in recent years (Ambrose 2013, 2014, 2015a, 2015b), so the observed mortality is not a new phenomenon. Tree growth rates in these regions (especially in 331F) are quite low, so the high MRATIOs are due to a combination of low growth and high mortality. Much of the forest in these sections is riparian, and, indeed, most of the species experiencing greatest mortality (table 5.2) are

commonly found in riparian areas. The major exception was high ponderosa pine mortality in ecoregion section 331F–Western Great Plains. Ponderosa pine is not a riparian tree species, but like the riparian species, it only occurs in a relatively small area of the ecoregion, on discontinuous mountains, plateaus, canyons, and breaks in the plains (Burns and Honkala 1990).

In ecoregion section 332D–North-Central Great Plains, seven species experienced high total mortality in terms of biomass and together represent over 90 percent of the mortality in the ecoregion: American elm (*Ulmus americana*), eastern cottonwood (*Populus deltoides)*, ponderosa pine, bur oak (*Quercus macrocarpa*), green ash (*Fraxinus pennsylvanica*), hackberry (*Celtis occidentalis*), and eastern redcedar (*Juniperus virginiana*) (table 5.2). Of these, ponderosa pine and American elm suffered the largest proportional loss in terms of both biomass and number of stems and, together with eastern cottonwood, made up the largest proportion of total mortality. In the case of hackberry, the mortality in terms of biomass (4.15 percent) was much higher than the mortality in terms of number of stems (0.38 percent), which means that the trees that died were a relatively small number of very large trees. A number of different factors may be responsible for the high mortality in the ecoregion. The drought in 2012 and 2013, as well as associated winter desiccation, has been reported as severely stressing trees in much of South Dakota and Nebraska. Dutch elm disease has been responsible for elm mortality in both States (Nebraska Forest Service 2012, 2013; South Dakota Department of Agriculture 2012). Cedar bark beetle (*Phloesinus* spp.) combined with drought stress have been reported as causing mortality in juniper (redcedar) in South Dakota (South Dakota Department of Agriculture 2012, 2013). Green ash has been affected by ash/lilac borer (*Podosesia syringae*) in South Dakota (South Dakota Department of Agriculture 2012). Also, a variety of insects and diseases have been reported as affecting ponderosa pine in the South Dakota and Nebraska; their activity may have produced increased mortality in trees stressed by drought conditions.

In ecoregion 332F–South-Central and Red Bed Plains, in south-central Kansas, a wide range of species suffered high mortality, including black willow (*Salix nigra*), black locust (*Robinia pseudoacacia*), eastern cottonwood, eastern redcedar, hackberry, red mulberry (*Morus rubra*), and American elm. It is unlikely that a single pest or pathogen would produce mortality in this range of species. The most likely factor associated with this mortality is drought: 2011 through 2013 were extremely dry years in most of Kansas, with the areas of most severe drought including this ecoregion (Kansas Forest Service 2011, 2012, 2013), and drier than normal conditions persisted through 2014 (Kansas Forest Service 2014). Such severe drought could lead to tree mortality either directly or by stressing the trees so that they succumb to pests or pathogens that would normally be nonlethal.

In ecoregion 251F–Flint Hills, several species experienced high mortality: American elm, eastern redbud (*Cercis canadensis*), green ash, white mulberry (*Morus alba*), and hackberry. Most of the biomass that died was American elm, and the mortality represented 16 percent of the biomass and 19 percent of the stems of that species (table 5.2). Here also, Dutch elm disease may have been responsible for this mortality. The severe drought in Kansas, mentioned above, likely contributed to the mortality in all species.

In ecoregion 331M–Missouri Plateau, three species, eastern cottonwood, bur oak, and green ash, represented more than three-fourths of the mortality (biomass). Green ash have been affected by ash/lilac borer as well as other native ash borers, in both North and South Dakota (North Dakota Forest Service 2012, South Dakota Department of Agriculture 2012). Adverse weather conditions, including both drought and excessively wet conditions, both of which occurred during the past remeasurement cycle (Bergdahl 2013, 2014; South Dakota Department of Agriculture 2012), may have contributed to mortality by stressing trees.

This analysis shows that in most of the Eastern and Central United States, mortality has been low relative to tree growth. Mortality has been rather low in most of the areas for which data are available. The areas of highest recent mortality occurred in the mostly riparian forests of Great Plains ecoregions. A common characteristic of most of the ecoregions with high mortality is that, being very dry, they are on the margins of land suitable for forest growth. Thus, they tend to be extremely vulnerable to changes in weather patterns that might produce prolonged and/or extreme drought. Drought, combined with a variety of other biotic and/or abiotic stressors, is likely responsible for the mortality observed.

It is also important to realize that this analysis alone cannot tell the complete story regarding tree mortality. Mortality that is concentrated in highly fragmented areas or areas adjacent to human development may not be detected because areas classified as nonforest are not included in the FIA sample. Also, should a particular species be dying due to a pest or pathogen in mixed-species forests where other species are growing vigorously, this analysis is unlikely to detect it. This is especially true of species (e.g., ash) that make up a relatively small proportion of many eastern forests. To gain a more complete understanding of mortality, one should consider the results of this analysis together with other indicators of forest health, including insect and disease activity (chapter 2) and Evaluation Monitoring projects that focus on particular mortality-causing agents (chapters 7–17).

LITERATURE CITED

Ambrose, M.J. 2013. Tree mortality. In: Potter, K.M.; Conkling, B.L., eds. Forest Health Monitoring: national status, trends, and analysis 2011. Gen. Tech. Rep. SRS-185. Asheville, NC: U.S. Department of Agriculture, Forest Service, Southern Research Station: 59–68.

Ambrose, M.J. 2014. Tree mortality. In: Potter, K.M.; Conkling, B.L., eds. Forest Health Monitoring: national status, trends, and analysis 2012. Gen. Tech. Rep. SRS-198. Asheville, NC: U.S. Department of Agriculture, Forest Service, Southern Research Station: 73–83.

Ambrose, M.J. 2015a. Tree mortality. In: Potter, K.M.; Conkling, B.L., eds. Forest Health Monitoring: national status, trends, and analysis 2013. Gen. Tech. Rep. SRS-207. Asheville, NC: U.S. Department of Agriculture, Forest Service, Southern Research Station: 71–81.

Ambrose, M.J. 2015b. Tree mortality. In: Potter, K.M.; Conkling, B.L., eds. Forest Health Monitoring: national status, trends, and analysis 2014. Gen. Tech. Rep. SRS-209. Asheville, NC: U.S. Department of Agriculture, Forest Service, Southern Research Station: 73–84.

Bechtold, W.A.; Patterson, P.L., eds. 2005. The enhanced Forest Inventory and Analysis Program—national sampling design and estimation procedures. Gen. Tech. Rep. SRS-80. Asheville, NC: U.S. Department of Agriculture, Forest Service, Southern Research Station. 85 p.

Bergdahl, A.D. 2013. North Dakota forest health highlights 2012. Fargo, ND: North Dakota State University. 11 p. http://fhm.fs.fed.us/fhh/ncregion.shtml. [Date accessed: June, 15, 2015].

Bergdahl, A.D. 2014. North Dakota forest health highlights 2013. Fargo, ND: North Dakota State University. 20 p. http://fhm.fs.fed.us/fhh/ncregion.shtml. [Date accessed: June 15, 2015].

Burns, R.M.; Honkala, B.H. 1990. Silvics of North America: 1, Conifers. Agric. Handb. 654. Washington, DC: U.S. Department of Agriculture, Forest Service. 675 p.

Cleland, D.T.; Freeouf, J. A.; Keys, J.E.; [and others]. 2007. Ecological subregions: sections and subsections for the conterminous United States. In: Sloan, A.M., tech. ed. Washington, DC: U.S. Department of Agriculture, Forest Service. Gen. Tech. Rep. WO-76D. [Map, presentation scale 1:3,500,000; colored]. Also on CD-ROM as a GIS coverage in ArcINFO format.

Coulston, J.W.; Ambrose, M.J.; Riitters, K. H. [and others]. 2005a. Supplemental methods. In: Forest Health Monitoring 2003 national technical report. Gen. Tech. Rep. SRS-85. Asheville, NC: U.S. Department of Agriculture, Forest Service, Southern Research Station: 87–92.

Coulston, J.W.; Ambrose, M.J.; Stolte. K.S. [and others]. 2005b. Health and vitality. In: Conkling, B.L.; Coulston, J.W.; Ambrose, M.J., eds. Forest Health Monitoring 2001 national technical report. Gen. Tech. Rep. SRS-81. Asheville, NC: U.S. Department of Agriculture, Forest Service, Southern Research Station: 39–82.

Coulston, J.W.; Smith, W.D.; Ambrose, M.J. [and others]. 2005c. Supplemental methods. In: Conkling, B.L.; Coulston, J.W.; Ambrose, M.J., eds. Forest Health Monitoring 2001 national technical report. Gen. Tech. Rep. SRS-81. Asheville, NC: U.S. Department of Agriculture, Forest Service, Southern Research Station: 123–140.

Forest Health Monitoring (FHM). 1994. Forest Health Monitoring: a national strategic plan. Research Triangle Park, NC: U.S. Department of Agriculture, Forest Service, Forest Health Monitoring Program. 13 p.

Gregoire, T.G.; Schabenberger, O.; Barret, J.P. 1995. Linear modeling of irregularly spaced, unbalanced, longitudinal data from permanent plot measurements. Canadian Journal of Forest Research. 25: 137–156.

Kansas Forest Service. 2011. Kansas forest health highlights 2011. 4 p. http://fhm.fs.fed.us/fhh/fhh_11/KS_FHH_2011.pdf. [Date accessed: June 10, 2014].

Kansas Forest Service. 2012. Kansas forest health highlights 2012. 5 p. http://fhm.fs.fed.us/fhh/fhh_12/KS_FHH_2012.pdf. [Date accessed: June 10, 2014].

Kansas Forest Service. 2013. Kansas forest health highlights 2013. http://fhm.fs.fed.us/fhh_13/KS_FHH_2013.pdf. 6 p. [Date accessed: June 12, 2015].

Kansas Forest Service. 2014. Kansas forest health highlights 2014. 6 p. http://fhm.fs.fed.us/fhh/fhh_14/KS_FHH_2014.pdf. [Date accessed: June 12, 2015].

McNab, W.H.; Cleland, D.T.; Freeouf, J.A.; [and others], comps. 2007. Description of ecological subregions: sections of the conterminous United States [CD-ROM]. Gen. Tech. Report WO-76B. Washington, DC: U.S. Department of Agriculture, Forest Service. 80 p.

Nebraska Forest Service. 2011. Nebraska Forest Health Highlights 2011. 4 p. http://fhm.fs.fed.us/fhh/fhh_11/NE_FHH_2011.pdf. [Date accessed: June 10, 2015].

Nebraska Forest Service. 2012. Nebraska Forest Health Highlights 2012. 4 p. http://fhm.fs.fed.us/fhh/fhh_12/NE_FHH_2012.pdf. [Date accessed: June 10, 2014].

Nebraska Forest Service. 2013. Nebraska Forest Health Highlights 2013. 4 p. http://fhm.fs.fed.us/fhh/fhh_13/NE_FHH_2013.pdf. [Date accessed: June 12, 2014].

Nebraska Forest Service. 2014. Nebraska Forest Health Highlights 2014. 4 p. http://fhm.fs.fed.us/fhh/fhh_14/NE_FHH_2014.pdf. [Date accessed: June 12, 2015].

Smith, W.D.; Conkling, B.L. 2005. Analyzing forest health data. Gen. Tech. Rep. SRS-77. Asheville, NC: U.S. Department of Agriculture, Forest Service, Southern Research Station. 35 p.

South Dakota Department of Agriculture. 2011. South Dakota forest health highlights 2011. 4 p. http://fhm.fs.fed.us/fhh/fhh_11/SD_FHH_2011.pdf. [Date accessed: May 1, 2013].

South Dakota Department of Agriculture. 2012. South Dakota forest health highlights 2012. 5 p. http://fhm.fs.fed.us/fhh/fhh_12/SD_FHH_2012.pdf. [Date accessed: June 10, 2014].

South Dakota Department of Agriculture. 2013. South Dakota forest health highlights 2013. 5 p. http://fhm.fs.fed.us/fhh/fhh_13/SD_FHH_2013.pdf. [Date accessed: June 12, 2015].

South Dakota Department of Agriculture. 2014. South Dakota forest health highlights 2014. 7 p. http://fhm.fs.fed.us/fhh/fhh_14/SD_FHH_2014.pdf. [Date accessed: June 12, 2015].

U.S. Department of Agriculture (USDA) Forest Service. 2008. National forest type data development. http://fsgeodata.fs.fed.us/rastergateway/forest_type/index.php. [Date accessed: May 13, 2008].

U.S. Department of Agriculture (USDA) Forest Service. 2014. The Forest Inventory and Analysis database: database description and users manual version 6.0.1 for Phase 2. Washington, DC: U.S. Department of Agriculture, Forest Service, Forest Inventory and Analysis Program. http://fia.fs.fed.us/library/database-documentation. [Date accessed: April 17, 2015].

U.S. Department of Agriculture (USDA) Forest Service. 2015. FIA DataMart FIADB version 6.0. [Online database]. Washington: U.S. Department of Agriculture, Forest Service, Forest Inventory and Analysis Program. http://apps.fs.fed.us/fiadb-downloads/datamart.html. [Date accessed: April 27, 2015].

SECTION 2.

Analyses of Long-Term Forest Health Trends and Presentations of New Techniques

CHAPTER 6.

National Update of Forest Fragmentation Indicators, 2001—2011

Kurt H. Riitters

INTRODUCTION

This chapter summarizes temporal trends in forest fragmentation for the conterminous United States from 2001 to 2011. As distinguished from forest loss per se, forest fragmentation refers broadly to the subdivision of the remaining forest into smaller parcels, the creation of more forest edge per unit of forest area, and the increased distance between the remaining forest parcels. The processes of forest disturbance and recovery, both natural and anthropogenic, together determine the trends of forest fragmentation geographically and over time. The impacts of forest fragmentation on ecological goods and services naturally vary according to the particular circumstances of forest change, such as the natural forest condition in a given area, the particular drivers and patterns of forest change, and the specific ecological process or attribute of interest. The goal of national monitoring of forest fragmentation is to provide a consistent characterization of the status and trends of forest spatial patterns in a way that can potentially address a large number of specific concerns about a variety of ecological goods and services. For these and other reasons, the primary indicator for national monitoring is multiscale forest area density, and the primary data source is the National Land Cover Database (NLCD). The 2010 Forest Health Monitoring (FHM) national report (Potter and Conkling 2013) included a national analysis of forest fragmentation (Riitters 2013) based on the 2001 NLCD. This chapter updates the status and trends of forest fragmentation using the 2006 and 2011 NLCD.

METHODS

National Land Cover Maps

The data set included the NLCD land cover maps for the conterminous United States (CONUS) in the years 2001, 2006, and 2011 (Fry and others 2011, Homer and others 2004, Jin and others 2013, Xian and others 2009). To ensure consistency over time, the most recent NLCD editions (U.S. Geological Survey 2014a, 2014b, 2014c) of each year were used (because the 2001 and 2006 NLCD were updated when the 2011 NLCD was released). The NLCD maps identify 16 land cover classes at a spatial resolution of 0.09 ha/pixel (i.e., each pixel is 30 m by 30 m). For this analysis, the 16 NLCD land cover classes were combined into two generalized classes called forest (the NLCD deciduous, evergreen, mixed forest, and woody wetlands classes) and nonforest (all other NLCD classes). No attempt was made to identify the specific nonforest NLCD classes that were associated with the status and trends of forest fragmentation. Ocean area adjacent to land was included in the analysis but data summaries were limited to the boundaries of detailed county maps (ESRI 2005). Although this analysis did not incorporate information about NLCD classification accuracy, the overall per-pixel classification accuracy of forest versus nonforest in the NLCD is approximately 90 percent (Wickham and others 2010, 2013). The estimates of forest area and change from NLCD land cover maps differ from Forest Inventory and Analysis (FIA) forest area statistics (e.g., Oswalt and others 2014) primarily because of differences in the definition of forest (Coulston

and others 2014). For example, forest is defined as a land use by FIA whereas the NLCD defines forest as a land cover.

Fragmentation Model

National maps of forest fragmentation were derived for each of the three NLCD years by using the same techniques (Riitters and others 2002) that were used in earlier Forest Health Monitoring reports (e.g., Riitters 2013, Riitters and Coulston 2013). Those reports provide additional details and illustrations of the fragmentation model. Briefly, the fragmentation status of individual forest pixels was evaluated by measuring the forest area density (FAD) in a surrounding neighborhood and repeating that measurement for five neighborhood sizes. FAD is defined as the proportion of all pixels within a fixed-area neighborhood that are forest pixels, and the five neighborhood sizes were 4.41 ha (7 pixels by 7 pixels), 15.21 ha (13 by 13), 65.61 ha (27 by 27), 590.49 ha (81 by 81), and 5314.41 ha (243 by 243). Neighborhood size is hereafter referred to as "landscape size" and the values are rounded to three significant digits. Five neighborhood sizes were used because fragmentation naturally is scale dependent, because the effects of fragmentation may be scale dependent, and because knowledge of fragmentation as manifested at different scales is required to inform resource management as practiced at those different scales. The five selected neighborhood sizes span several orders of magnitude of measurement scale, and the smallest three sizes correspond roughly to familiar sizes in English measurement units (approximately 10 acres, 40 acres, and 160 acres). For a given year, each forest pixel was assigned a value of FAD for each landscape size by centering the neighborhoods on its location. Thus, five FAD measurements were made for each extant forest pixel for each of the three years. For a given landscape size, the forest pixels were grouped into fragmentation categories based on their FAD values (table 6.1).

In comparison to an assessment of the status of forest fragmentation at a single time, an assessment of trends of forest fragmentation over time has to account for changes in the underlying "population" of forest pixels over time (Riitters and Wickham 2012). Clearly, the loss of a forest pixel will reduce the total area of extant forest in a given fragmentation category. Similarly, the gain of a forest pixel will increase the total area in a given fragmentation category, but in this case the specific fragmentation category depends on which landscape gained the forest pixel. For example, forest area added to a forest-dominated landscape is unlikely to be classified in the rare fragmentation category. Furthermore, for a forest pixel that persists over time, its FAD values and hence fragmentation category may change according to the gains and losses of other forest pixels in its neighborhood. Thus, the patterns of forest losses and gains in relation to the extant forest pattern can have both direct and indirect effects on the fragmentation status of the extant forest area at a given time.

For data summaries, FIA regions (fig. 6.1) were selected for consistency and comparability with other Forest Service national resource assessments. For each region, the proportion

Table 6.1—The conversion of forest area density (FAD) measurements to fragmentation categories

Forest area density (FAD)	Fragmentation category[a]
FAD = 1.0	Intact
0.9 ≤ FAD < 1.0	Interior
0.6 ≤ FAD < 0.9	Dominant
0.4 ≤ FAD < 0.6	Transitional
0.1 ≤ FAD < 0.4	Patchy
0.0 < FAD < 0.1	Rare

[a]Riitters (2013).

of total forest cover in each fragmentation category was calculated for each year. This enables analysis of trends in forest fragmentation by region, but does not reflect changes in total forest area over time. To place regional results in context, a separate summary of total forest area changes over time was also compiled for each region.

For comparisons with other national assessments (USDA Forest Service 2011, 2012), a second "cumulative" model was applied to the multiscale FAD data. In the cumulative model, a given forest pixel was labeled as "intact forest" if its associated FAD equaled 1.0, as "interior forest" if FAD ≥ 0.9, and as "dominant forest" if FAD ≥ 0.6. The model is "cumulative" because a forest pixel that met the "intact" criterion also qualified as "interior" and "dominant" and one that met the "interior" criterion also qualified as "dominant." The results for the cumulative model were summarized nationally, for each of the three years, for each of five landscape sizes, by calculating the percentages of forest pixels that met the three cumulative criteria for intact, interior, and dominant forest.

RESULTS AND DISCUSSON

Net Change of Total Forest Area

In 2001, there were 2.353 million ha of forest in the conterminous United States. Total forest area decreased to 2.323 million ha in 2006 and 2.284 million ha in 2011. The total decrease from 2001 to 2011 was 69 640 ha, representing a net loss of 3.0 percent of total forest area during that period. In comparison, net regional losses from 2001 to 2011 varied from 1.0 to 5.5 percent (fig. 6.2). Most (71 percent) of the net loss of forest area was in the two southern

Figure 6.1—Forest Inventory and Analysis regions. Note: Alaska, Hawai'i, and Puerto Rico were not included in this study.

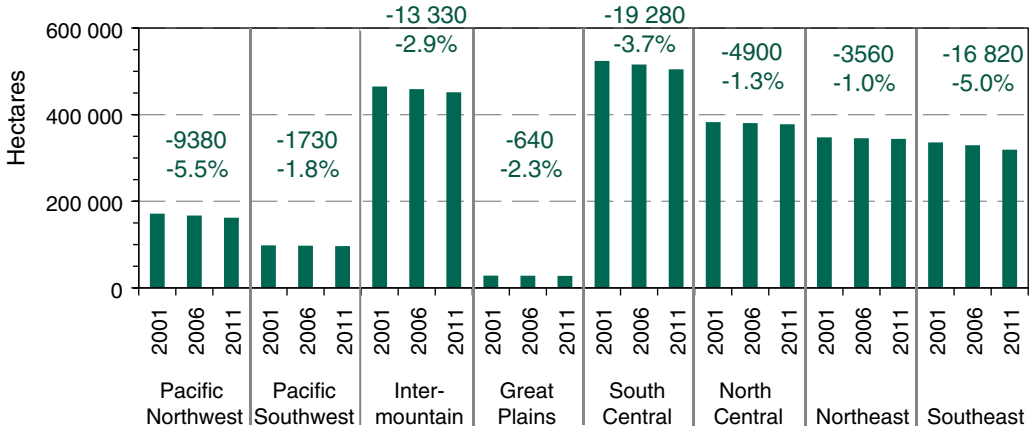

Figure 6.2—Total forest cover in 2001, 2006, and 2011, by FIA region. The net change from 2001 to 2011 is indicated for each region in hectares (top number) and percent (bottom number).

regions (36 100 ha) and the Intermountain region (13 330 ha). The largest percentage net losses were in the Pacific Northwest and Southeast regions, and the lowest percentage net losses were in the two northern regions.

Changes in Forest Fragmentation

The percentages of total forest area in each of the six fragmentation categories, nationally and by region, are shown in figure 6.3 for three of the five landscape sizes. In the following discussion, the six fragmentation categories are interpreted as a gradient of fragmentation from low fragmentation (intact category) to high fragmentation (rare category). The results for the Great Plains region are quite different from other regions because that region contains much less forest cover overall, because many of the native forest types in that region are naturally fragmented, and because a relatively larger proportion of total forest cover in that region occurs as urban tree cover.

The general trends of fragmentation category area in relation to landscape size were described in a previous FHM national report (Riitters 2013). Briefly, because forest cover tends to be more spatially correlated at a local scale than regional scale, it is easier to achieve a high FAD threshold in smaller landscapes than in larger landscapes. As a result, larger landscapes have more fragmentation than do smaller landscapes. For example, with increasing landscape size there is an increase in the total of the rare

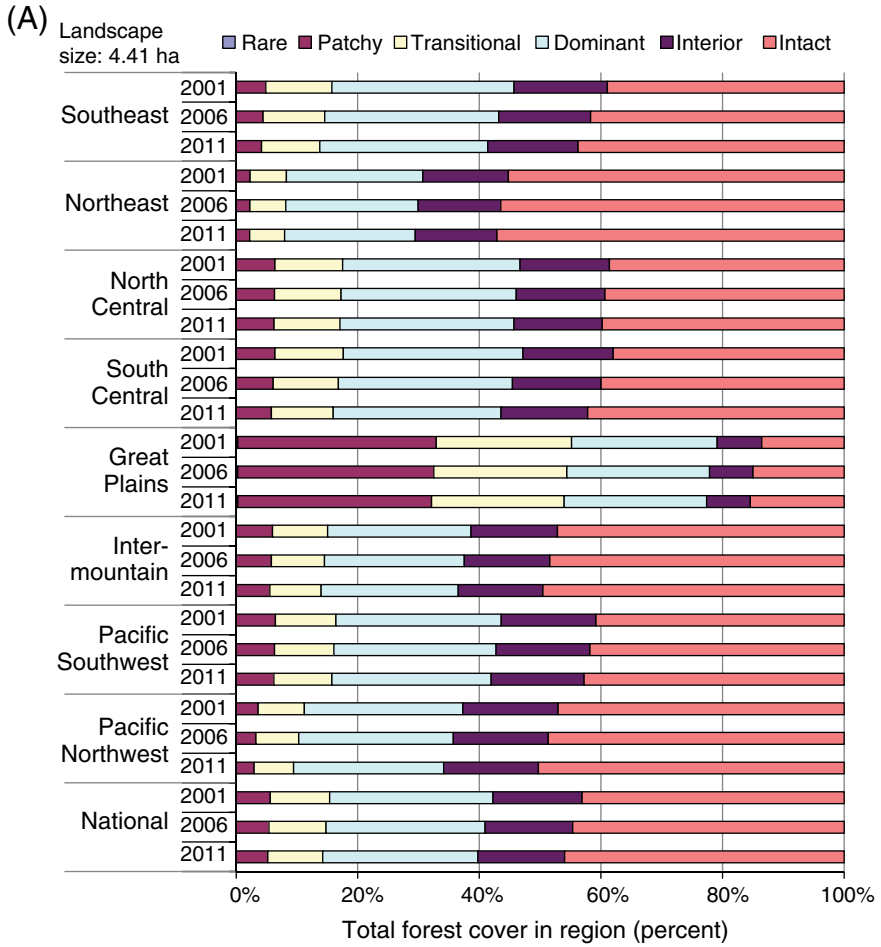

Figure 6.3—The percentage of total forest area in each of six fragmentation categories, for three landscape sizes, nationally and by region. (A) 4.41-ha landscape size; (B) 65.6-ha landscape size; (C) 590-ha landscape size.
(continued on next page)

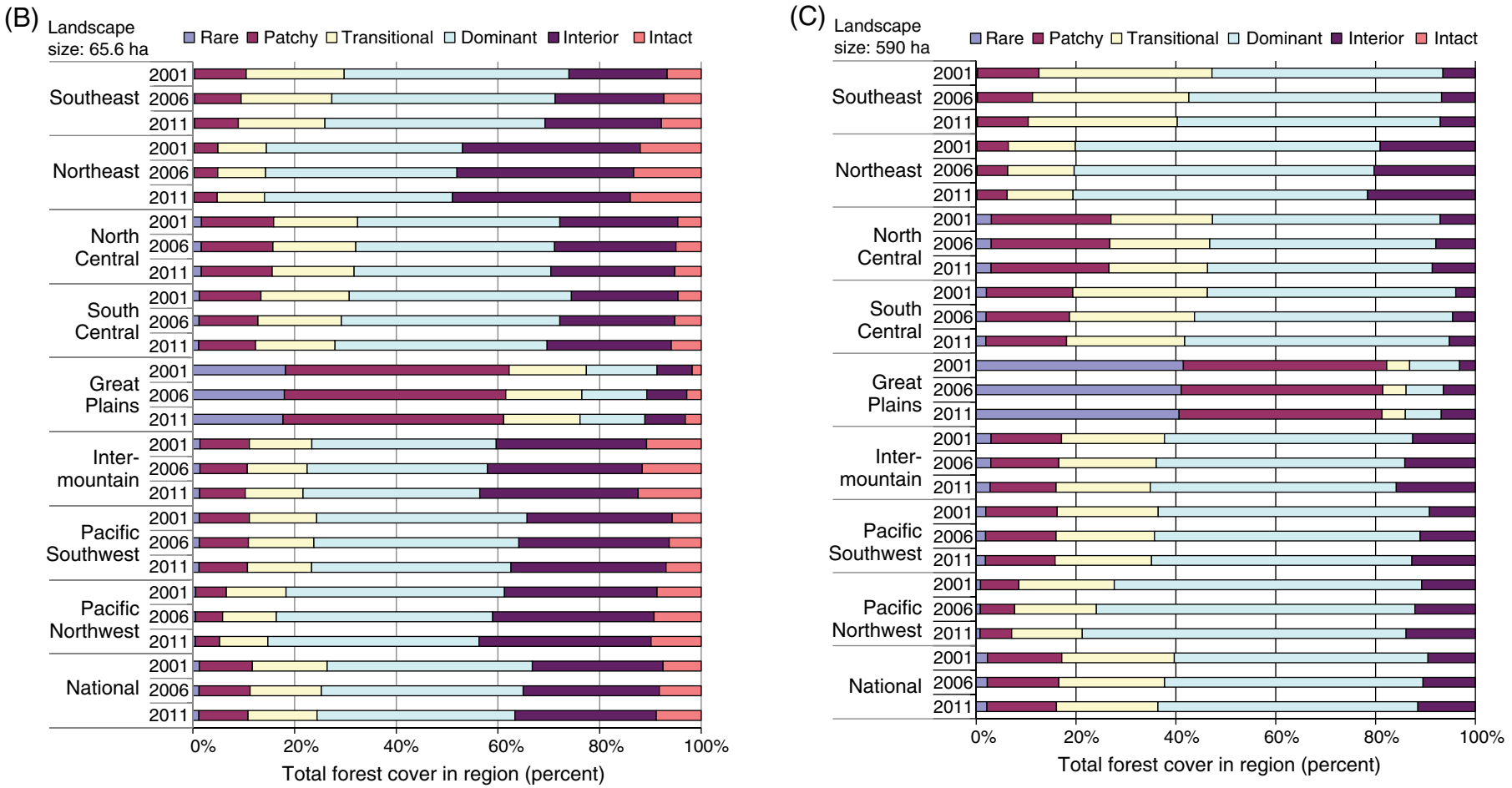

Figure 6.3 (continued)—The percentage of total forest area in each of six fragmentation categories, for three landscape sizes, nationally and by region. (B) 65.6-ha landscape size; (C) 590-ha landscape size.

plus patchy categories and a decrease in the intact plus interior categories. At the same time, however, the total of the transitional plus dominant categories increases much more than the rare plus patchy categories with increasing landscape size because forest cover still continues to dominate large landscapes even if it is more fragmented.

The temporal results indicate a net decrease in the percentage of relatively unfragmented forest cover (interior plus intact categories) in all regions and during both time periods (2001 to 2006 and 2006 to 2011). That decrease was translated to net increases in the percentage of relatively fragmented forest cover (rare plus patchy categories) in most, but not all, regions and time periods. To simplify the temporal trend information and clarify regional comparisons of fragmentation, the net changes in the area within each fragmentation category for a landscape size of 65.6 ha were expressed as annual percent change[3] from 2001 to 2011, by region (fig. 6.4). This presentation format clarifies that all regions exhibited a net loss of interior and intact forest, and that all regions except the Great Plains region exhibited a net gain of rare, patchy, and transitional forest. The Eastern United States had more

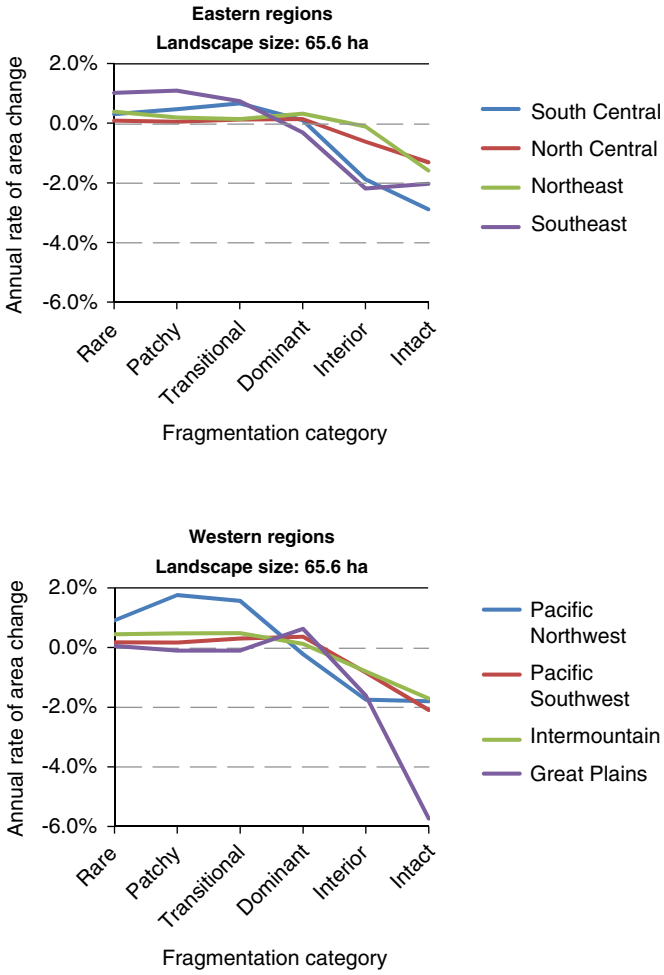

Figure 6.4—Annualized percentage of change in the area in each of six fragmentation categories, by region, from 2001 to 2011.

[3] $annual\ percent\ change = 100 * \left(\left(\frac{area\ in\ 2011}{area\ in\ 2001} \right)^{\frac{1}{10}} - 1 \right)$

fragmentation in the two southern regions than in the two northern regions. In the West, the Pacific Northwest tended to have higher fragmentation rates than the Pacific Southwest and Intermountain regions. (The percentage change results for the Great Plains region are not really comparable to the other results because of the small amount of intact area in that region in 2001.)

The national geography of forest cover change and fragmentation is further illustrated by a county-level comparison of the net percentage changes in total forest area (fig. 6.5A) and interior plus intact forest area (fig. 6.5B) from 2001 to 2011. To prepare fig. 6.5A, the total area of forest cover in each county was calculated using the 2001 and 2011 NLCD forest maps, and the difference was expressed as percentage change from the base year 2001. To prepare fig. 6.5B, the total area of intact plus interior forest in a 65.6-ha landscape was calculated for 2001 and 2011, and the difference was expressed as a percentage change from the base year of 2001. The inset map identifies forest-dominated counties containing more than 50 percent of forest cover. To interpret the maps, note that the same legend applies to both maps, and that darker blue colors indicate larger percentage losses. Most of the forest-dominated counties exhibited a net loss of total forest cover, and the rate of loss of interior plus intact forest exceeded the rate of loss of total forest cover. This result is consistent with and extends to 2011 the results for the 2001 to 2006 time period reported by Riitters and Wickham (2012). From 2001 to 2011, there was a widespread shift of the extant forest to a more fragmented condition, including places with relatively small changes in total forest cover.

The "cumulative" fragmentation model highlights changes in landscapes with lower levels of fragmentation. From 2001 to 2011, there was an increase in fragmentation of the extant forest across all landscape sizes for all three cumulative fragmentation categories (fig. 6.6). Since forested places tend to be clustered in proximity to one another, forest is usually the dominant land cover in these areas. Thus, for landscapes up to 5310 ha, at least 60 percent of forest land is in forest-dominated landscapes (fig 6.6; "Dominant forest"). However, since blocks of forest land are usually fragmented by inclusions of nonforest land, the percentage of forest land that is relatively unfragmented decreases rapidly as landscape size increases from 4.41 ha to 5310 ha (fig. 6.6; "Interior forest"). Fragmentation is so extensive that only 8 percent of forest land occurs in 65.6 ha landscapes that are completely forested (fig. 6.6; "Intact forest").

(A) Total forest cover area

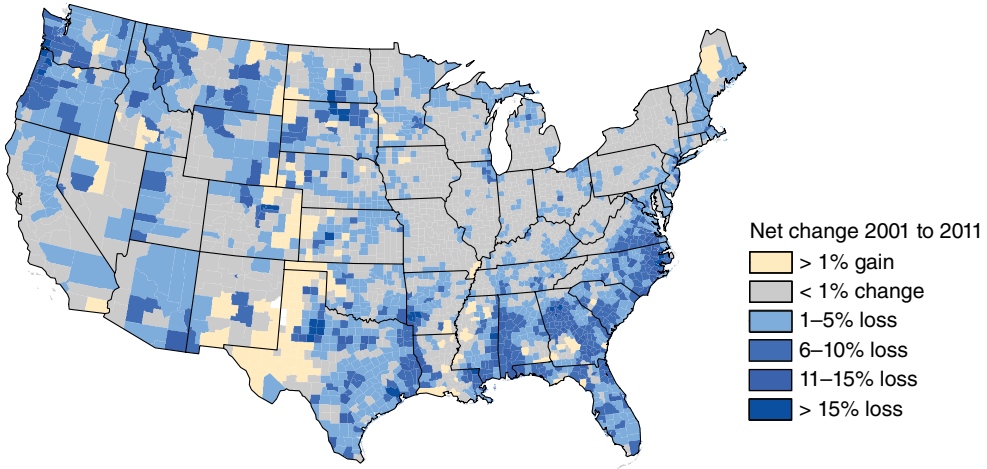

(B) Intact plus interior forest cover area

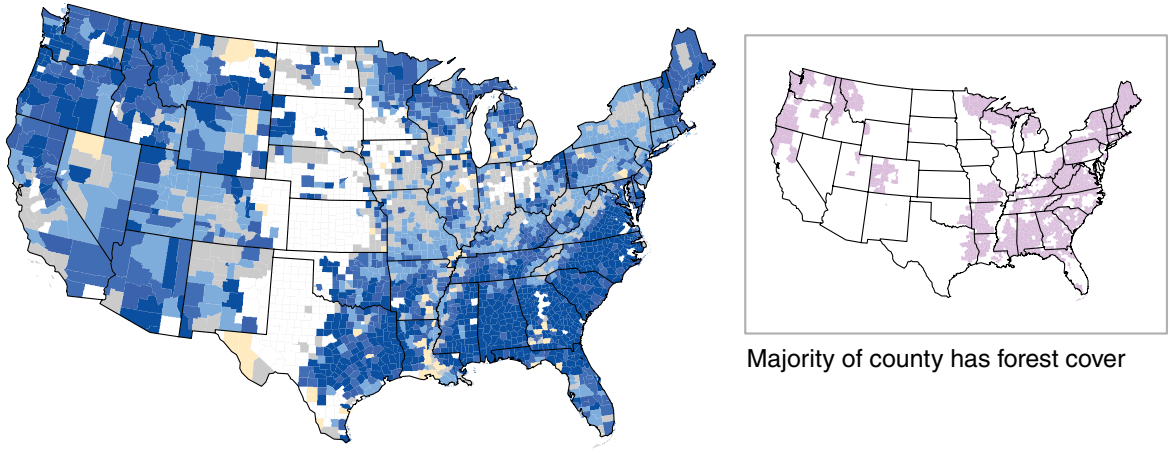

Figure 6.5—(A) The net change in total forest cover in a county from 2001 to 2011, expressed as a percentage of the total forest area in 2001. (B) The net change in intact plus interior forest cover in a county from 2001 to 2011, when analyzed at 65.6-ha scale, expressed as a percentage of the total intact plus interior forest cover in 2001. Counties without color are the 3 counties that had no forest cover in 2001 and the 498 counties that had no intact plus interior forest cover in 2001. The inset map identifies counties where more than 50 percent of total area had forest cover in 2001.

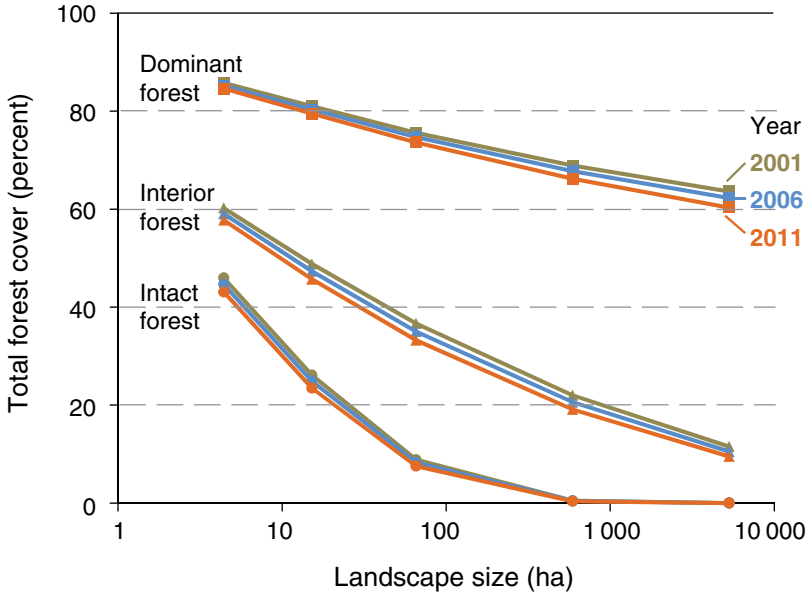

Figure 6.6—National summary of forest cover fragmentation using the cumulative classification model (see text for explanation). The chart shows the percentage of forest cover in the conterminous United States that is considered intact (completely forested landscape), interior (greater than 90 percent forested), or dominant (greater than 60 percent forested) and how those proportions change with increasing landscape size. In the cumulative model, intact is a subset of interior, which is a subset of dominant, which is a subset of total forest cover area. Green, blue, and orange symbols indicate conditions in 2001, 2006, and 2011, respectively.

SUMMARY

Analysis of national land cover maps for the years 2001, 2006, and 2011 showed that decreases in total forest cover underestimated forest fragmentation for several criteria used to define fragmentation and across several orders of magnitude of measurement scale. Although forest tends to be the dominant land cover type where forest occurs, fragmentation is pervasive and increasing over time, even in regions exhibiting relatively small changes in total forest cover area. In addition to regional differences in the change of total forest cover, there is important regional variation in the area and rate of change of relatively unfragmented forest. It is important to continue monitoring the status and trends of forest fragmentation in a consistent way nationally, and the next update to this analysis will be conducted upon the release of the 2016 national land cover map.

LITERATURE CITED

Coulston, J.W.; Reams, G.A.; Wear, D.N.; Brewer, C.K. 2014. An analysis of forest land use, forest land cover and change at policy-relevant scales. Forestry. 87: 267–276.

ESRI. 2005. ESRI data & maps 2005 [DVD]. Redlands, CA: Environmental Systems Research Institute.

Fry, J.; Xian, G.; Jin, S. [and others]. 2011. Completion of the 2006 National Land Cover Database for the conterminous United States. Photogrammetric Engineering & Remote Sensing. 108: 858–859.

Homer, C.; Huang, C.; Yang, L. [and others]. 2004. Development of a 2001 National Land Cover Database for the United States. Photogrammetric Engineering & Remote Sensing. 70: 829–840.

Jin, S.; Yang, L.; Danielson, P. [and others]. 2013. A comprehensive change detection method for updating the National Land Cover Database to circa 2011. Remote Sensing of Environment. 132: 159–175.

Oswalt, S.N.; Smith, W.B.; Miles, P.D.; Pugh, S.A. 2014. Forest resources of the United States, 2012: a technical document supporting the update of the 2010 RPA Assessment. General Technical Report WO-91. Washington, DC: U.S. Department of Agriculture, Forest Service. 218 p.

Potter, K.M.; Conkling, B.L. 2013. Forest Health Monitoring: national status, trends, and analysis 2010. General Technical Report SRS-176. Asheville, NC: U.S. Department of Agriculture, Forest Service, Southern Research Station. 162 p.

Riitters, K. 2013. Fragmentation of forest, grassland, and shrubland. In: Potter, K.M.; Conkling, B.L., eds. Forest Health Monitoring: national status, trends, and analysis 2010. General Technical Report SRS-176. Asheville, NC: U.S. Department of Agriculture, Forest Service, Southern Research Station: 53–65.

Riitters, K.H.; Coulston, J.W. 2013. Fragmentation of Eastern United States forest types. In: Potter, K.M.; Conkling, B.L., eds. Forest Health Monitoring: national status, trends, and analysis 2011. General Technical Report SRS-185. Asheville, NC: U.S. Department of Agriculture, Forest Service, Southern Research Station: 71–78.

Riitters, K.H.; Wickham, J.D.; O'Neill, R.V. [and others]. 2002. Fragmentation of continental United States forests. Ecosystems. 5: 815–822.

Riitters, K.; Wickham, J. 2012. Decline of forest interior conditions in the conterminous United States. Scientific Reports. 2: 653. DOI: 10.1038/srep00653. [Published online: September 13, 2012].

U.S. Department of Agriculture (USDA) Forest Service. 2011. National report on sustainable forests, 2010. FS-979. Washington, DC: U.S Department of Agriculture, Forest Service, Washington Office. 214 p.

U.S. Department of Agriculture (USDA) Forest Service. 2012. Future of America's Forest and Rangelands: Forest Service 2010 Resources Planning Act Assessment. General Technical Report WO-87. Washington, DC: U.S. Department of Agriculture, Forest Service. 198 p.

U.S. Geological Survey. 2014a. National Land Cover Database 2001 land cover. 2011 Ed. Sioux Falls, SD: U.S. Geological Survey. [Date accessed: April 25, 2014].

U.S. Geological Survey. 2014b. National Land Cover Database 2006 land cover. 2011 Ed. Sioux Falls, SD: U.S. Geological Survey. [Date accessed: April 25, 2014].

U.S. Geological Survey. 2014c. National Land Cover Database 2011 land cover. 2011 Ed. Sioux Falls, SD: U.S. Geological Survey. [Date accessed: April 25, 2014].

Wickham, J.D.; Stehman, S.V.; Fry, J.A. [and others]. 2010. Thematic accuracy of the NLCD 2001 land cover for the conterminous United States. Remote Sensing of Environment. 114: 1286–1296.

Wickham, J.D.; Stehman, S.V.; Gass, L. [and others]. 2013. Accuracy assessment of NLCD 2006 land cover and impervious surface. Remote Sensing of Environment. 130: 294–304.

Xian, G.; Homer, C.; Fry, J. 2009. Updating the 2001 National Land Cover Database land cover classification to 2006 by using Landsat imagery change detection methods. Remote Sensing of Environment. 113: 1133–1147.

SECTION 3.

Evaluation Monitoring Project Summaries

Each year the Forest Health Monitoring (FHM) Program funds a variety of Evaluation Monitoring (EM) projects, which are "designed to determine the extent, severity, and causes of undesirable changes in forest health identified through Detection Monitoring (DM) and other means" (FHM 2009). In addition, EM projects can produce information about forest health improvements. EM projects are submitted, reviewed, and selected in two main divisions: base EM projects and fire plan EM projects. More detailed information about how EM projects are selected, the most recent call letter, lists of EM projects awarded by year, and EM project poster presentations can be found on the FHM Web site: www.fs.fed.us/foresthealth/fhm.

Beginning in 2008, each FHM national report contains summaries of recently completed EM projects. Each summary provides an overview of the project and results, citations for products and other relevant information, and a contact for questions or further information. The summaries provide an introduction to the kinds of monitoring projects supported by FHM and include enough information for readers to pursue specific interests. Eleven project summaries are included in this report.

LITERATURE CITED

Forest Health Monitoring (FHM). 2009. Evaluation monitoring. Forest Health Monitoring Fact Sheet Series. http://www.fs.fed.us/foresthealth/fhm/. [Date accessed: June 19, 2015].

CHAPTER 7.

Distribution and Intensification of Bur Oak Blight in Iowa and the Midwest

(Project NC-EM-B-10-01)

Thomas C. Harrington
Douglas L. McNew

INTRODUCTION

A new, late-season leaf disease on bur oak (*Quercus macrocarpa*) had been observed in southern Minnesota, southwest Wisconsin, eastern Nebraska, and Iowa since the mid-1990s. Symptoms of the new disease included necrosis of the leaf tissue along the veins and death of entire leaves, usually starting in late July (Pokorny and Harrington 2011). Branches in the lower crown were generally the most severely affected, and severity of the disease tended to increase year to year in individual trees. Distinctive fruiting bodies (conidiomata) of a fungus were found along the veins of affected leaves, and the fungus was tentatively identified as *Tubakia dryina*. However, the cause of the disease had not been established before this project, and the incidence of the disease appeared to be increasing.

When investigations began in 2008, it became apparent that there are a number of *Tubakia* species on bur oak and other oak species in Iowa. A fungus that matched the description of *T. dryina* was found on white oak (*Q. alba*) but rarely on bur oak, and the *Tubakia* sp. associated with the new disease appeared to be distinct. The new disease was named bur oak blight (BOB). The spotty nature of BOB initially suggested that pathogen was invasive and had not fully expanded its potential range. Alternatively, an increase in early-season rain events (climate change) over the past two decades could explain the apparent elevated incidence and severity of the disease (Harrington 2011). To help resolve these questions and characterize the diversity of *Tubakia* spp. on oaks in the Upper Midwest, the following objectives were developed: (1) determine the distribution of BOB and follow within-tree intensification and spread to new trees in Story County, Iowa; (2) determine the geographic distribution of bur oak blight in Iowa and the Midwest; (3) collect specimens and isolates of *Tubakia* spp. from diseased *Quercus* spp. and other hosts across the Eastern United States; (4) delineate species of *Tubakia* using morphology and DNA sequences and determine their host and geographic ranges; and (5) provide a review of *Tubakia* spp. with descriptions of new and old species.

METHODS

An informal survey of the *Tubakia* spp. on oaks and distribution of BOB in Iowa and the Midwest was conducted through examination of specimens in herbaria and collections of symptomatic oak leaves provided by numerous collaborators in Iowa and other States. We and our cooperators sampled extensively in late summer and early fall in 2009 through 2014 to determine the distribution of BOB in Iowa, Minnesota, and surrounding States. For all samples, we examined leaves for necrosis and presence of fruiting bodies; if *Tubakia* fruiting bodies were present, we conducted isolations and confirmed the species identification using polymerase chain reaction (PCR) and ribosomal DNA (rDNA) sequencing. Morphological features and further DNA sequence comparisons using other genes were used to help delineate putative species of *Tubakia*.

We conducted detailed epidemiological studies in a grove of 39 mature bur oak on a bottomland site at Brookside Park in Ames, IA, from 2009 through 2012. We monitored the progress of symptoms and isolated healthy twigs and leaves from affected ones. For disease ratings, the top and bottom half of the tree crown were separately evaluated for the crown area with symptomatic branches: 0 = no symptoms, 1 = less than 1/3 of the area with symptomatic branches, 2 = less than 2/3 of the area symptomatic, and 3 = 2/3 or more of the branches symptomatic. The disease rating for the whole tree was the sum of the lower and upper crown ratings, resulting in a scale ranging from 0 to 6.

We also determined September disease ratings and amount of overwintering inoculum on all trees in seven mature bur oak groves (four upland and three bottomland sites) in and around Ames.

RESULTS AND DISCUSSION

We sequenced the rDNA of more than 250 isolates of *Tubakia* spp. from oak trees in Iowa and adjacent States and identified six species of *Tubakia* (table 7.1). Each of the species was

Table 7.1—Putative *Tubakia* spp., common hosts, States, and leaf symptoms caused by six species of *Tubakia* identified on bur oak and other oak species

Tubakia sp.	Hosts	States	Leaf symptoms
Tubakia iowensis	*Q. macrocarpa,* rarely *Q. bicolor*	Illinois, Iowa, Kansas, Minnesota, Missouri, Nebraska, South Dakota, Wisconsin	Vein necrosis, petiole necrosis, small necrotic spots
Tubakia dryina	*Q. alba, Q. macrocarpa*	Illinois, Iowa, Missouri, Wisconsin	Leaf spots
Tubakia sp. A	*Q. macrocarpa*	Illinois, Iowa, Missouri, New Jersey, Wisconsin	Leaf spots, vein necrosis
Tubakia sp. B	*Q. macrocarpa, Q. muehlenbergii, Q. stellata, rarely Q. alba, Q. bicolor*	Arkansas, Iowa, Kansas, Minnesota, Missouri, Wisconsin	Leaf spots, vein necrosis
Tubakia sp. C	*Q. ellipsoidalis, Q. imbricaria, Q. rubra*	Iowa, Minnesota, Wisconsin	Discrete circular leaf spots, vein necrosis
Tubakia sp. D	*Q. imbricaria, Q. laurifolia, Q. macrocarpa, Q. marilandica, Q. nigra, Q. palustris, Q. rubra, Q. velutina, Q virginiana;* rarely *Q. alba, Q. muehlenbergii, Q. stellata*	Arkansas, Florida, Illinois, Iowa, Kansas, Louisiana, Maryland, Minnesota, Missouri, New Hampshire, New Jersey, Ohio, Oklahoma, Wisconsin	Irregular leaf spots, vein necrosis

isolated at least once from surface-sterilized, healthy leaves, showing that they were all endophytes in oak, but they were also isolated from necrotic leaf tissue, necrotic twigs, or acorns. All six species were isolated at least once from bur oak, but only one was associated with the extensive late-season leaf mortality that is characteristic of BOB.

The European *T. dryina* was the least common fungus in the region. A second uncommon fungus, *Tubakia* sp. A, appears to be the species originally described as *Actinopelte americana*, which was mostly isolated from healthy twigs and leaves of bur oak at our Brookside Park study site. Two undescribed species were leaf pathogens on members of the red oak (*Q. rubra)* group; one of these was occasionally found on *Q. rubra* trees with severe symptoms of veinal leaf necrosis, and the second species was less common and caused discrete, circular leaf spots as well as veinal necrosis. The causal agent of bur oak blight was described as *T. iowensis*, and a closely related species was tentatively named *Tubakia* sp. B (Harrington and others 2012). The latter appeared to have a broader host range on members of the white oak group and was more often associated with leaf spots than veinal necrosis. Besides bur oak, *T. iowensis* was found rarely on swamp white oak (*Q. bicolor*).

Bur oak blight was found to be a very host-specific disease, and the survey work at Brookside Park showed that it has a unique disease cycle. *T. iowensis* forms two types of asexual fruiting bodies (Harrington and others 2012). The most common type of fruiting body forms on necrotic leaf veins during the summer and serves as secondary inoculum during wet summers. But the most important type of fruiting body develops on petioles of leaves that remain attached to the twig through the winter months and mature the next spring.

Extensive sampling of naturally infected trees and greenhouse inoculation studies (West 2015) confirmed that the overwintering inoculum (from crustose fruiting bodies on petioles) leads to infection of emerging shoots during spring rains, latent infections without symptoms, and petiole necrosis 2 months later (Harrington and McNew, in press). The necrosis of the petiole prevents leaf abscission, and the fruiting bodies develop slowly on the dead petiole tissue for release of spores the next spring. Unusually wet springs for the last 20 years and buildup of overwintering inoculum in individual trees may be why the disease recently became conspicuous (Harrington 2013). Eradicative fungicide (propiconazole) injections of mature, blighted bur oak trees in early June reduced the number of dead leaves hanging on twigs through the winter and reduced disease severity for up to 3 years in a majority of trees in a study in Ames (Harrington 2012).

Bur oak blight was found to be most severe on mature trees on upland, former savanna sites, where the fire tolerant *Q. macrocarpa* var. *oliviformis* is well adapted (Deitschmann 1965, Great Plains Flora Association 1986). We identified *T. iowensis* throughout the geographic

range of this small-acorn variety of bur oak (fig. 7.1). The disease was found in almost every Iowa county, though only low incidence of disease was found in the southeast corner of the State, and BOB was less common at some locations in the Loess Hills (western Iowa) and the denser forests of eastern Iowa than elsewhere. The disease also was very widespread in Minnesota, where, like in Iowa, *Q. macrocarpa* var. *oliviformis* is common.

The disease also was found on upland bur oak in States bordering Iowa and Minnesota (fig. 7.1). It was found in eastern South Dakota but not in North Dakota, where *Q. macrocarpa* var. *depressa* occurs on well-drained soils. Bur oak blight was not found on the large-acorned *Q. macrocarpa* var. *macrocarpa*, which is a bottomland variety common in the eastern and southern ranges of bur oak (Deitschmann 1965). In central Iowa, planted bur oak with small acorns may show severe BOB symptoms, but planted bur oak trees with larger acorns did not. *Tubakia iowenis* appears to be very specific to the upland variety of bur oak, and we suspect that there was little selection pressure for disease resistance in this variety when the climate was drier.

In seven permanent plots of mature, natural groves around Ames, IA, disease severity was found to be generally increasing from 2009 through 2014. The trend for more disease over the years is associated with consistently wet springs, a change in Iowa climate (Takle 2011) that appears to lead to buildup of the disease

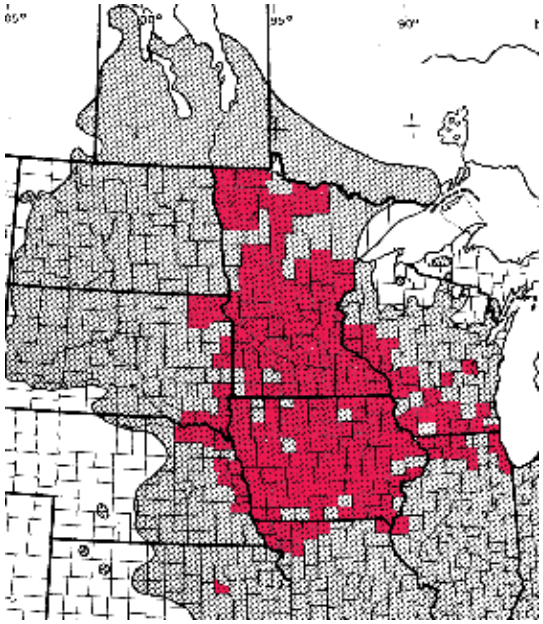

Figure 7.1—The northwestern distribution of Quercus macrocarpa *(gray) and the counties where* Tubakia iowensis *and bur oak blight were confirmed (red).*

in individual trees. The disease severity was higher on the four upland sites than on the three bottomland sites (fig. 7.2). All trees on these sites had relatively small acorns and appeared to be *Q. macrocarpa* var. *oliviformis*, but there may have been more introgression of *Q. macrocarpa* var. *macrocarpa* into the bottomland sites than on the upland sites.

Severe BOB occurs in remnant savanna stands, and the bur oak ecotype adapted to thin, upland soils appears to be particularly vulnerable. However, even on upland sites, there

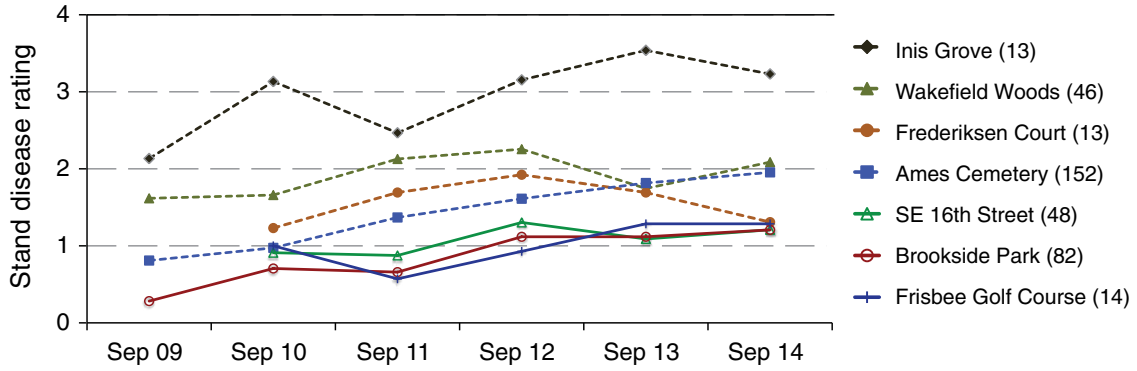

Figure 7.2—Average disease severity ratings for bur oak blight in four upland groves (dashed lines) and three bottomland groves (solid lines) of Quercus macrocarpa *in and around Ames, IA, from September 2009 through September 2014. Ratings for each tree range from 0 (no symptoms) to 6 (symptomatic branches throughout crown). Average is for all trees in the grove, with the number of trees in each grove indicated in parentheses.*

appears to be a wide variation in susceptibility within a stand, with severely affected trees next to healthy trees. In preliminary studies (West 2015), seedlings from acorns on trees with bur oak blight were not more susceptible to *T. iowensis* in inoculation trials than were seedlings from acorns on nearby healthy bur oak trees. The apparent resistance of some trees may be related to timing of bud break and inoculum release during warm spring rains.

CONCLUSIONS

Although six species of *Tubakia* were found on oaks in Iowa and elsewhere, only the newly described species, *T. iowensis*, causes bur oak blight. *T. iowensis* was found to be very host specific and widespread throughout the assumed geographic range of *Q. macrocarpa* var. *oliviformis*, a fire-tolerant variety adapted to upland savannah forests. Genetic variation in the pathogen and apparent variation in susceptibility in the host suggest that *T. iowensis* is native and not invasive. Nonetheless, disease severity was found to be generally increasing in natural groves. The most important phases in the BOB disease cycle include infection of developing shoots, a long latent phase, late season necrosis of petioles, failure of abscission, and development of primary (spring) inoculum on the petioles of leaves that remain attached to the tree. Consecutive springs of high rainfall during bud break and shoot expansion are believed to increase severity of disease in individual trees. An increase in spring rainfall during the last two decades may explain the sudden recognition of BOB, and the apparent shift in climate in this region raises concerns about the future health of bur oak in the region.

ACKNOWLEDGMENTS

Numerous individuals contributed oak samples that were critical to this study. We gratefully acknowledge this assistance, and we particularly would like to thank Jill Pokorny of the U.S. Forest Service in St. Paul, MN, who coordinated collection of most of the Minnesota material.

CONTACT INFORMATION

Thomas C. Harrington: tcharrin@iastate.edu.

LITERATURE CITED

Deitschmann, G.H. 1965. Bur oak (*Quercus macrocarpa* Michx.). In: Fowells, H.A., comp. Agric. Handb. 271. Silvics of forest trees of the United States. Washington, DC: U.S. Department of Agriculture: 563–568.

Great Plains Flora Association. 1986. Flora of the Great Plains. Lawrence, KS: University Press of Kansas. 1392 p.

Harrington, T.C. 2011. It looks like bur oak blight (BOB) really isn't that new. ISU/DNR Woodland Owners Newsletter No. 74. https://www.extension.iastate.edu/forestry/newsletters/woodland_owners/pdf/January%20 2011.pdf. [Date accessed: June 11, 2015].

Harrington, T.C. 2012. Update on bur oak blight (BOB) and a potential fungicide treatment. Iowa State University Extension, Horticulture & Home Pest News. http://www.ipm.iastate.edu/ipm/hortnews/2012/9-12/buroakblight.html. [Date accessed: June 11, 2015].

Harrington, T.C. 2013. Exotic pathogens or shifts in climate? Laurel wilt and bur oak blight. In: Forest Health Technology Enterprise Team, eds. Publication FHTET 13-01. Proceedings, 24th USDA Interagency Research Forum on Invasive Species. Fort Collins, CO: U.S. Department of Agriculture, Forest Service: 39–41.

Harrington, T.C.; McNew, D.M. [In press]. Bur oak blight. In: Bergdahl, A., ed. Diseases of the trees of the Great Plains. Gen. Tech. Rep. U.S. Department of Agriculture, Forest Service.

Harrington, T.C.; McNew, D.M.; Yun, H.Y. 2012. Bur oak blight, a new disease on *Quercus macrocarp*a caused by *Tubakia iowensis* sp. nov. Mycologia. 104: 79–92.

Pokorny, J.D.; Harrington, T.C. 2011. Bur oak blight. USDA Forest Service Pest Alert NA-PR-02-11. Newtown Square, PA: U.S. Department of Agriculture, Forest Service, Northeastern Area State and Private Forestry. 2 p.

Takle, E.S. 2011. Climate changes in Iowa. In: Iowa Climate Change Impacts Committee, eds. Climate change impacts on Iowa, 2010. Des Moines, IA: Iowa Press: 8–13.

West, A.M. 2015. Ecological specialization of *Tubakia iowensis*, and searching for variation in resistance to bur oak blight. Ames, IA: Iowa State University. 70 p. M.S. thesis.

CHAPTER 8.

Determining the Extent of the Invasive Nonnative *Ailanthus* Tree Using Helicopter Mapping within Appalachian Ohio Oak Forests

(Project NE-EM-F-11-01)

Joanne Rebbeck
Cheryl Coon
Aaron Kloss

INTRODUCTION

Concern is growing about future sustainability of oaks in the oak-hickory forests of the Eastern United States. Oaks serve as keystone species in forests by providing a community structure and an environment that maintains critical processes. Their hard mast is vital to wildlife; the wood is important for the forest products industry; and they are tolerant of environmental conditions such as drought often associated with future climate scenarios. Ohio's forests are currently at a crossroads. Historical fire regimes have been interrupted. The dominant oak systems are declining and gradually being replaced by more shade-tolerant and fire-sensitive trees (Hutchinson and others 2012). Forest health is being impacted by nonnative invasive plant and insect species. Without an ecosystem approach to restoration, forest composition will continue to shift away from oak-hickory, invasive species will occupy more of the landscape, biological diversity will continue to be lost, and forests will lose their resiliency and ability to respond to climate change (Johnson and others 2009).

Ailanthus altissima, an aggressive invasive tree, can invade and expand dramatically when forests are disturbed (Albright and others 2010). It invades disturbed habitat via abundant wind-dispersed seed and can persist and expand by clonal growth. The Wayne National Forest (WNF) identified sustaining oak forests as a primary objective in its Forest Management Plan. Oak forests of the Appalachians require fire disturbance to restore and maintain their ecological function; however, *Ailanthus* is present in many mixed oak forest landscapes. *Ailanthus* competes directly with oaks and represents a barrier to the reintroduction of fire since it may benefit from the disturbance. The U.S. Department of Agriculture (USDA) Forest Service, Northern Research Station (NRS); the Ohio Division of Forestry (ODOF); and the WNF initiated a project to aerially map the invasive tree, *Ailanthus*, in southern Ohio (Rebbeck 2012, Rebbeck and others 2014). Because invasive species do not recognize property boundaries, mapping across all ownerships within the proclamation boundaries of the WNF was initiated in 2011. *Ailanthus* is dioecious, with up to 350,000 seeds produced per tree annually (Kowarik and Saümel 2007). Because its

seeds persist into winter months when there is no interfering leaf cover, the ideal time to conduct aerial surveys is early to middle winter (fig. 8.1). The technique used was based on aerial *Ailanthus* mapping the ODOF initiated in 2008 in partnership with the NRS on Ohio State forests. Seed-bearing *Ailanthus* were mapped utilizing a Digital Aerial Sketchmapping System (DASM) run on a laptop computer with a touch screen display and stylus; the system allows the manual recording of digitally sketched and georeferenced features onto a base map. DASM technology, developed by the USDA Forest Health Technology Enterprise Team and Remote Sensing Applications Center, is commonly used to conduct annual forest health surveys from fixed wing aircraft in many U.S. States (Schrader-Patton 2003).

The primary objective of the project was to identify and map seed-producing *Ailanthus* trees across large forested landscapes in southeast Ohio. These data would then be used to prioritize invasive control treatments in conjunction with oak restoration treatments such as prescribed fire and overstory thinning. Additional impact would be achieved by sharing these georeferenced maps of *Ailanthus* infestations with groups such as the ODOF and Natural Resources Conservation Service, who work with private landowners to control invasive plants.

Figure 8.1—Aerial view of seed-bearing Ailanthus *trees in February 2011 on the Marietta Unit of the Wayne National Forest. Three representative seed clusters are identified with red arrows. (photo by Thomas Shuman, Ohio Department of Natural Resources)*

METHODS

Survey Areas

The Athens, Marietta, and Ironton Units of the WNF are located within the Unglaciated Allegheny Plateau where topography is highly dissected, consisting of sharp ridges, steep slopes, and narrow valleys. The forest spans portions of 12 southeastern Ohio counties. The WNF Proclamation Boundary covers 833,990 acres. However, 71 percent of the land within these boundaries is privately owned. It is a diverse landscape but is primarily represented by mixed oak-hickory forests. These units have a long history of past disturbance including clearcutting for farming, livestock grazing, and charcoal production as well as mineral, gas, oil, and coal extraction, which began in the early 1800s. Current disturbances include prescribed burning, timber harvesting, recreation trails, and oil/gas extraction.

Aerial Survey Methods

A Bell 206 B3 JetRanger helicopter owned and operated by the Ohio Department of Natural Resources (ODNR) Division of Wildlife was used for the aerial sketchmapping surveys. Just prior to each surveying session, sketchmappers reviewed mapping protocols, use of digital sketching software and hardware, and aerial photographs of seed-bearing *Ailanthus* trees. One sketchmapper sat in the co-pilot's seat and one in the rear on the opposite side of the aircraft. Each recorded the position of seed-bearing female *Ailanthus* on a tablet laptop computer that utilized a Holux M-241 GPS logger. Laptops were equipped with stylus-touchable screens, and loaded with GeoLink Powermap software (Michael Baker Jr., Inc., Jackson, MS). Reference base maps included U.S. Geological Survey 7.5-minute quadrangle maps (digital ortho quads [DOQs]) at a 1:24,000 scale and the survey boundaries. Laptops were linked to a Bluetooth-enabled EMTAC GPS receiver and an onboard Garmin™ 496 GPS unit. Survey altitudes were 373–600 feet above ground level at a speed of 5–80 miles per hour, depending on environmental conditions, forest density, and structure. Survey lines were spaced approximately 1,000 feet apart in a general north-south orientation. Both single and multipoints of individual seed-bearing *Ailanthus* trees were collected when one to several trees were spotted. If multipoints were not feasible (e.g., large areas with dense clusters of seed-bearing trees), a polygon was recorded instead, and the estimated percentage of cover of *Ailanthus* within the polygon was assigned a cover class of ≤25 percent, 26–50 percent, 51–75 percent, or 76–100 percent cover (Rebbeck

and others 2015). At the beginning, midpoint, and end of each flight, both sketchmappers collected data on the same trees and prominent landscape features (large building structures, road intersections) to assess mapping accuracy. ESRI ArcGIS® (Version 10, Redlands, CA) software was utilized for postprocessing of data. Coordinates were downloaded to handheld GPS units (Garmin™ GPSmap 76CSx, Olathe, KS) so that mapping accuracy could be assessed on the ground. The handheld units included 2.0 GB microSD storage cards with a GPS accuracy of < 33 feet and a differential global positioning system (DGPS) accuracy of 10–16 feet. Ground-truthing was conducted several weeks after aerial surveys on a subset of the mapped *Ailanthus* (Rebbeck and others 2015).

RESULTS

Between 2011 and 2013, approximately 163,256 acres were sketchmapped in a total of 45 flight hours (3,600 acres per hour) (table 8.1). On the Marietta Unit, more than 1,300 *Ailanthus* infested areas were mapped, representing a total of 6,388 acres (8 percent of the surveyed land) (fig. 8.2). However, because only polygon data were collected during the 2011 Marietta survey flights, the actual number of female *Ailanthus* trees is unknown. On the Ironton Unit, only 65.2 acres (0.08 percent of the surveyed 83,522 acres) were mapped as infested with *Ailanthus*. The vast difference between infested acres on the Marietta and Ironton Units created uncertainty as to whether the Ironton Unit truly had such low levels, or whether the late

Table 8.1—Summary of *Ailanthus* aerial surveys conducted on the Wayne National Forest between 2011 and 2013

Survey unit	Survey year-month	Number of days/hours of mapping	Total area surveyed	Mapped infested area	Number of mapped female *Ailanthus*	Female tree d.b.h.		Number of mapped polygons	Size of mapped polygons	
						Range	Mean		Range	Mean
			acres	*acres*		--------- *inches* ----------			-------- *acres* ---------	
Athens	2013-January	2/10	87,307	41	259	3.6–20.5	8.2 (± 7.2)	23	0.3–7.8	1.8 (± 1.88)
Ironton	2011-February	2/12	83,522	65	18	—	—	20	0.3–10.2	3.6 (± 3.28)
	2013-January	2/10	112,832	4	39	—	—	3	0.9–1.6	1.3 (± 0.47)
Marietta	2011-January, February	6/18	79,734	6,388	N/A	3.5–10.2	6.9 (± 2.2)	1,356	0. 1–71.6	4.7 (± 7.16)

— = Trees were not measured at the Ironton survey unit.

d.b.h. = diameter at breast height.

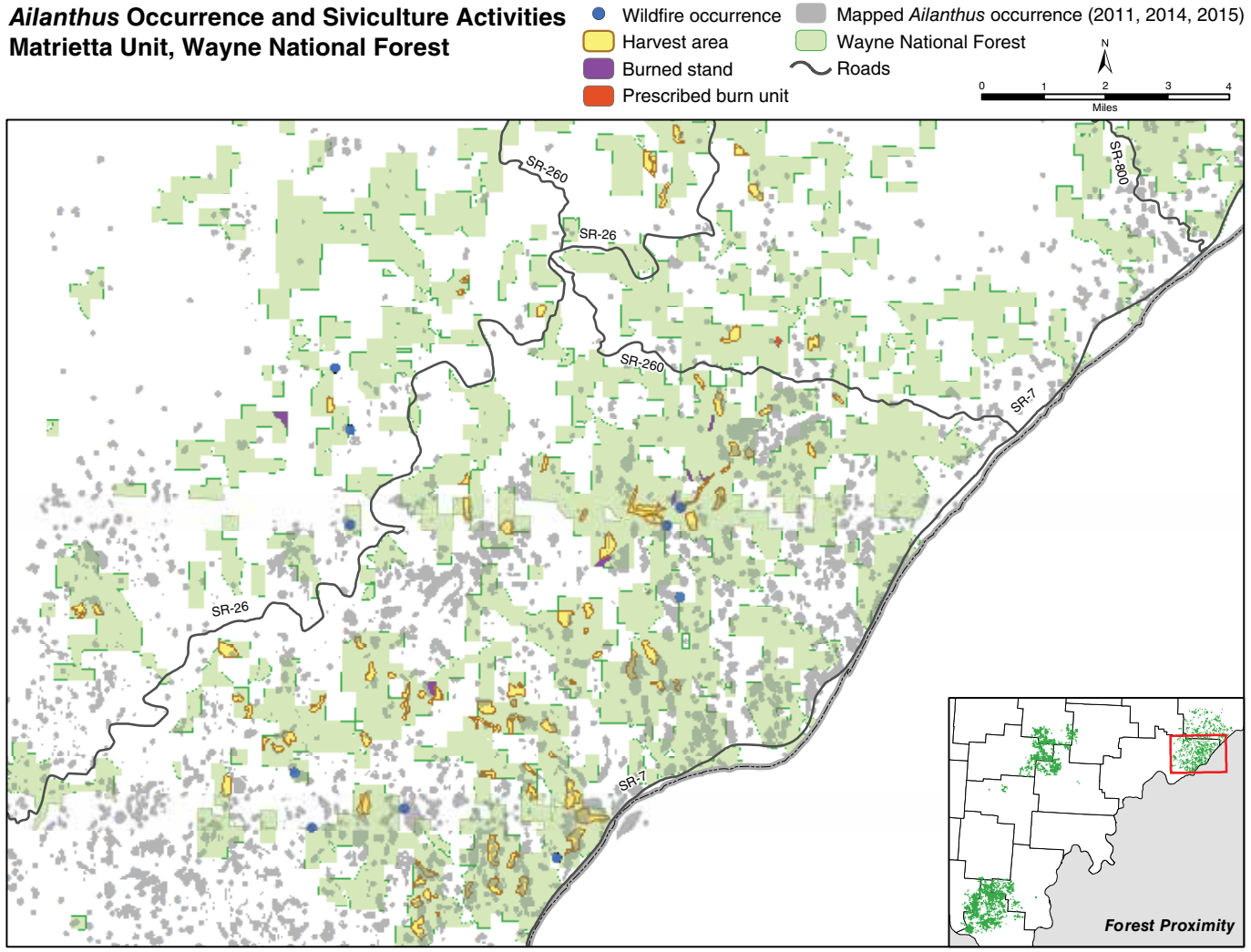

Figure 8.2—Map of the Marietta Unit of the Wayne National Forest. Note the high density of private inholdings and the high density of Ailanthus*-infested areas shown as brown polygons mapped in early 2011.*

(March) aerial surveys failed to detect areas of infestation because the seed clusters had dropped. To determine this, the entire Ironton Unit (112,832 acres) was surveyed in January 2013. The mapped data confirmed that, indeed, few seed-bearing females were present on that landscape. Within the Athens Unit survey area, 259 female seed-bearing *Ailanthus* female trees and 23 polygons were mapped. Of the 23 polygons, 6 had a cover of ≤ 25 percent, 8 had 26–50 percent cover, 3 had *Ailanthus* cover of 51–75 percent recorded, and 3 had no assigned *Ailanthus* cover attribute. Ground-truthing surveys were conducted in summer 2013 covering approximately 4,400 acres and 50 miles of roads. Within the ground-truthed area, 62 of the 70 aerially mapped females were relocated. The relocation distance of the ground-mapped female *Ailanthus* trees ranged from 3 to 492 feet. During ground surveys, male (non-seed bearing) trees were identified as individuals or in clumps (8 percent of total ground mapped), but most were mixed with females (33 percent of total ground-mapped *Ailanthus*) (Rebbeck and others 2015).

These aerial mapping data were used to prioritize *Ailanthus* control treatments in conjunction with oak restoration treatments. Since 2011, the National Wild Turkey Federation (NWTF) has partnered with the Wayne National Forest to maintain open land wildlife habitat by controlling *Ailanthus* within the WNF. Maintenance of these open habitats within oak-hickory forests benefits many regionally important wildlife species. Between 2011 and 2014, approximately 835 acres were treated with herbicides for *Ailanthus* control. In 2015, 747 acres are planned to be treated utilizing stem injection herbicide treatments (fig. 8.3).

DISCUSSION

This project demonstrated that helicopter digital sketchmapping technology can be used to economically and efficiently map *Ailanthus* in forested landscapes during the dormant season and utilize data to prioritize and develop control treatment plans. We estimated survey costs at $0.40 per acre, based on a commercial rate of $960 per hour for helicopter rental, pilot's time, and two sketchmappers for an average 8-hour day. Although rates for fixed-wing aircraft hourly costs are considerably lower, fixed wing does not provide the required lower speed, maneuverability, and visibility needed. Traveling at speeds of 55–80 miles per hour in a helicopter compared with those of about 130 miles per hour in a fixed-wing aircraft improves the likelihood that infestations will be accurately located, sketched, and assigned correct attribute features. Estimates of coverage ranged from

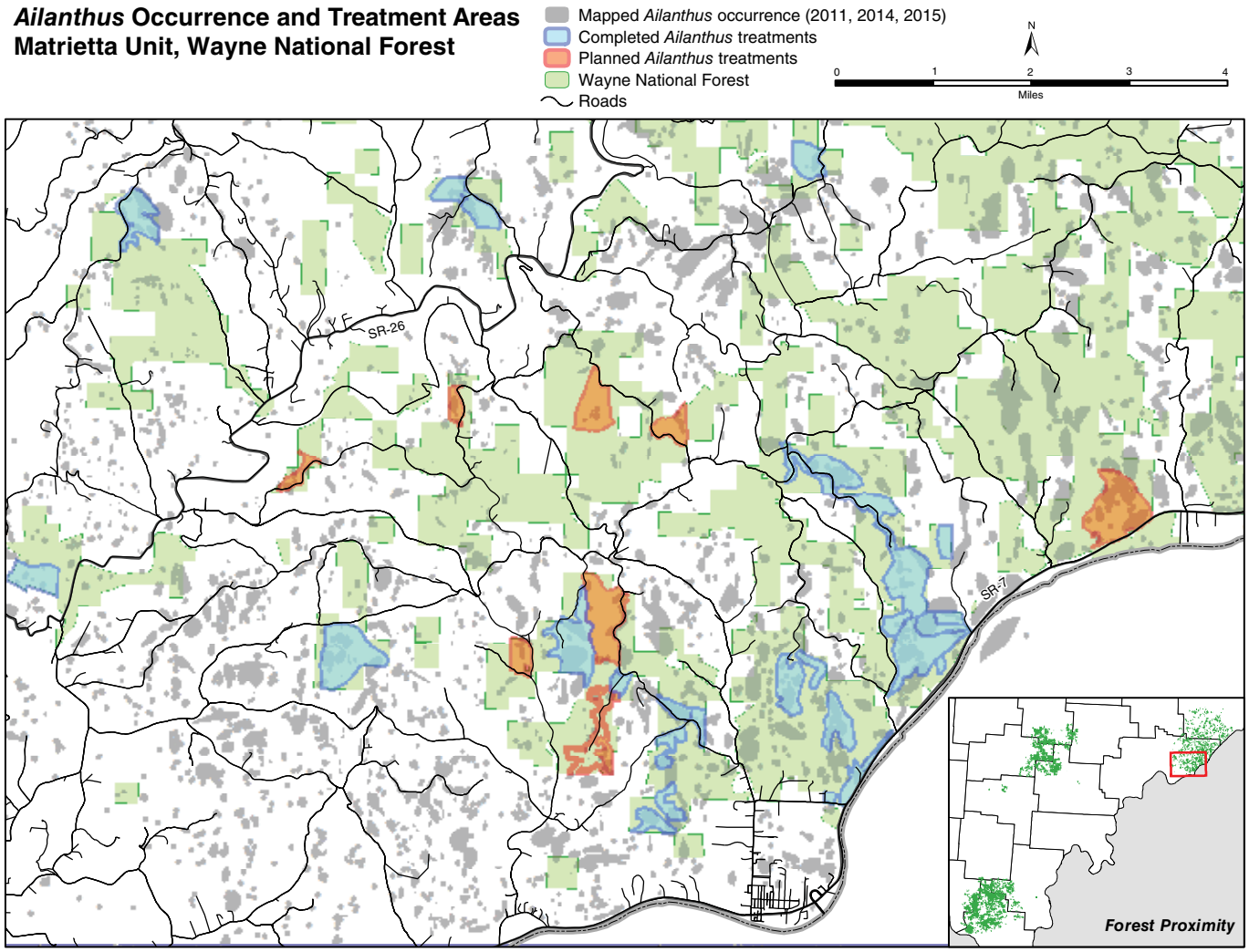

Figure 8.3—Distribution of Ailanthus *populations from aerial surveys and herbicide treatment areas on the Marietta Unit of the Wayne National Forest between 2011 and 2015.*

2,000 to 7,000 acres per hour, depending on the level of *Ailanthus* infestation and flight altitude. If more *Ailanthus* was present, then more time per acre was required for mapping. For example, the rate of mapping for the lightly infested WNF Ironton Unit was 6,960 acres per hour compared with 2,215 acres per hour for the heavily infested Marietta Unit. Another advantage of this mapping tool is quick access to the data. Very little post-flight processing is needed to generate georeferenced maps and/or downloadable point data onto GIS devices. It should be noted that downloading polygon data onto handheld units requires more storage capacity compared to waypoint data. The greatest limitation of this technology is the accuracy of the sketchmapping. This is a highly subjective skill that combines both art and science. Standardization of methods is critical and sketchmapper performance improves with experience. During all flights, sketchmappers should periodically record known land features such as road intersections, bridges, or prominent structures as spatial accuracy checks. Implementation of the aerial survey standards and quality assurance and quality control guidelines, developed by the U.S. Forest Service Forest Health Technology Enterprise Team, are available at http://www.fs.fed.us/foresthealth/technology/ads_standards.shtml.

This same approach could also be used to aerially map another invasive nonnative woody species, princess tree (*Paulownia tomentosa*). Sketchmappers were able to distinguish and map its prominent seed clusters, which were clearly visible and distinctive from *Ailanthus* during leaf-off surveys. Early indications show great promise for detection of this problematic nonnative as well. Unfortunately, not all invasive species can be mapped at the same time because of differences in their phenology. For successful mapping, timing of surveys must be linked to a prominent and distinctive feature of the target species. In the case of *Ailanthus* and *Paulownia*, winter leaf-off surveys are the most appropriate time.

CONCLUSIONS

This technology provides forest managers with readily available and affordable, landscape-level data of seed-producing *Ailanthus* populations. Since the mapping focuses on identifying seed-bearing trees, it underrepresents the magnitude of infestations. Maps from aerial data allowed managers to develop and implement control plans to treat *Ailanthus* on over 1,600 acres on the Marietta Unit of the WNF. Proactive control of invasive plants in advance of silvicultural treatments such as timber harvest or prescribed

fire provides a huge advantage for managers to minimize the impacts and spread of invasive woody species such as *Ailanthus*.

ACKNOWLEDGMENTS

The authors thank Joe Barber, Buster Keaton, Tom Shuman, Danzil Walker, Courtney Streithorst, and ODNR Divisions of Forestry and Wildlife for assistance in the aerial mapping. We greatly appreciate the support of Timothy Fox for assistance in the field. We thank Aurora Roemmich and Nicole Stump, U.S. Forest Service Wayne National Forest, for their support and cooperation. The authors appreciate the support and cooperation from Robert Boyles, Dan Balser, Michael Bowden, Greg Guess, and Chad Sanders of the Ohio Department of Natural Resources, Division of Forestry. We thank Qinfeng Guo, Manfred Mielke, and Rob Trickel for their helpful review comments.

CONTACT INFORMATION

Joanne Rebbeck: jrebbeck@fs.fed.us.

LITERATURE CITED

Albright, T.P.; Chen, H.; Chen, L.J.; Guo, Q. 2010. The ecological niche and reciprocal prediction of the disjunct distribution of an invasive species: the example of *Ailanthus altissima*. Biological Invasions. 12: 2413–2427.

Hutchinson, T.F.; Yaussy, D.A., Long, R.P. [and others]. 2012. Long-term (13-year) effects of repeated prescribed fires on stand structure and tree regeneration in mixed-oak forests. Forest Ecology and Management. 286: 87–100.

Johnson, P.S.; Shifley, S.R.; Rogers, R. 2009. The ecology and silviculture of oaks. 2d ed. Cambridge, MA: CAB International. 580 p.

Kowarik, I.; Saümel I. 2007. Biological flora of Central Europe: *Ailanthus altissima* (Mill.) Swingle. Perspectives in Plant Ecology, Evolution and Systematics. 8: 207–237.

Rebbeck, J. 2012. Fire management and woody invasive plants in oak ecosystems. In: Dey, D.C.; Stambaugh, M.C.; Clark, S.L.; Schweitzer, C.J., eds. Proceedings, 4th fire in eastern oak forests conference; 2011 May 17–19; Springfield, MO. Gen. Tech. Rep. NRS-P-102. Newtown Square, PA: U.S. Department of Agriculture, Forest Service, Northern Research Station: 142–155.

Rebbeck, J.; Hutchinson, T.; Iverson, L. [and others]. 2014. *Ailanthus* and prescribed fire, is it a volatile combination? In: Waldrop, T.A., ed. Proceedings of the wildland fire in the Appalachians: discussions among managers and scientists conference; 2013 October 8–10; Roanoke, VA. Gen. Tech. Rep. SRS-199. Asheville, NC: U.S. Department of Agriculture, Forest Service, Southern Research Station: 48–51.

Rebbeck, J.; Kloss, A.; Bowden, M. [and others]. 2015. Aerial detection of seed-bearing female *Ailanthus altissima*: a cost-effective method to map an invasive tree in forested landscapes. Forest Science. 61: 1068–1078.

Schrader-Patton, C. 2003. Digital aerial sketchmapping. RSAC-1202-RPT2. Fort Collins, CO: U.S. Department of Agriculture, Forest Service, Forest Health Technology Enterprise Team and Remote Sensing Applications Center. 17 p.

CHAPTER 9.

Current Health Status of American Beech and Distribution of Beech Bark Disease in Wisconsin

(Project NC-EM-B-11-01)

Holly A. Petrillo

INTRODUCTION

Beech bark disease (BBD) is an exotic insect and disease complex that results from the interaction of the exotic beech scale insect, *Cryptococcus fagisuga* Lind., and at least two species of fungi in the genus *Neonectria* (Ehrlich 1934, Lohman and Watson 1943, Spaulding and others 1936). Impacted forests suffer high mortality of American beech (*Fagus grandifolia*), in some cases within a few years of first detection. American beech is an important component of many forests in Wisconsin, in particular along Lake Michigan where tourism is economically important, and in parts of the Menominee Reservation. BBD was first identified in Wisconsin in Door County in 2009, and the extent and severity of the disease in Wisconsin's forests are currently being evaluated. BBD was first identified in Michigan in 2000 and has spread throughout the range of beech in Michigan, with 100 percent mortality in the most significant areas of infestation. Approximately 18 million American beech (sapling sized and larger) are currently found in Wisconsin, and beech volume is estimated at 37 million cubic feet (USDA Forest Service 2015). Four million acres of forest that contain beech, primarily mixed with maple and birch, are growing on the eastern side of the State. Besides being an important timber species, beech nuts are highly valued by wildlife. Beech may be the only nut producer in some parts of its range.

BBD has caused heavy mortality of American beech throughout its range in Michigan and in the Northeastern United States (Hane 2003, Latty and others 2003, McGee 2000, Petrillo and others 2005, Runkle 1990, Twery and Patterson 1984, Witter and others 2005). Based on the significant beech resource present in Wisconsin, managers expect similar mortality in the future. Because BBD has not been present throughout the range of beech in Wisconsin for very long, results from this research can help managers determine how at risk their stand(s) may be and decrease the overall impact of BBD before mortality occurs.

PROJECT OBJECTIVES

1. Establish a long-term monitoring system of Type 1 (extensive—less detailed, greater number of plots) and Type 2 plots (intensive—more detailed, subset of extensive plots) based on the Beech Bark Disease Monitoring and Impact Analysis System in Wisconsin beech forests over a 3-year period.

2. Collect baseline data showing the current conditions of the beech resource and northern hardwood stands containing beech.

3. Develop GIS maps that delineate the occurrence of beech scale and beech bark disease presence and severity in Wisconsin.

4. Identify areas at high risk, develop a risk model, and prioritize research needs for BBD in Wisconsin.

METHODS

This project initiated the development of the Wisconsin Beech Bark Disease Monitoring and Impact Analysis System (WI-BBDMIAS), in response to the identification of the beech scale and American beech mortality in 2009 in Door County. The WI-BBDMIAS is modeled after a very similar monitoring system in Michigan, which comprises more than 200 monitoring plots throughout the State. The WI-BBDMIAS includes two plot types: Type 1 (extensive—less detailed, greater number of plots) and Type 2 (intensive—more detailed, subset of extensive plots).

Type 1 plots consist of 30 prism points, 2 chains 40 m apart from each other, along transects, typically 5 by 6 or 3 by 10 points depending on the layout of the stand. A 20BAF prism is used to calculate basal area of all species, live and dead, at each prism point. The nearest American beech tree to each prism point is then sampled, for a total of 30 beech measured in each stand. For each beech tree sampled, the following variables are measured: diameter at breast height (d.b.h.), live crown ratio, crown density, crown dieback, foliage transparency, crown light exposure, tree vigor/condition, crown class/position, up to three tree damages, and the percentage of beech scale coverage. Beech scale coverage is estimated using a transparency frame 12.5 cm by 28 cm, placed 1.5 m above the ground on the north, south, east, and west sides of the tree. Other studies have found beech scale infestations to be higher on the protected north and east sides of the tree, especially in the early stages of infestation (Houston 1994). U.S. Forest Service Forest Inventory and Analysis protocols are used for all forest health metrics (USDA Forest Service 2015).

The number of plots located in each county is based on the amount of beech present in the county, the amount of publicly owned land in that county, and distance from current infestation. American beech is limited to the eastern part of Wisconsin, and plots were prioritized in areas where public visibility was greatest (along Lake Michigan, Door County, and State parks and recreation areas) and on the Menominee Reservation where American beech is an important part of the forest resource.

Areas at most risk for mortality from BBD were determined using the following criteria: (1) the average percentage of beech basal area present, and (2) the average percentage of beech scale present in each stand. These two factors were used to determine which stands had a low to high risk of mortality from BBD based on the current data.

RESULTS AND DISCUSSION

Seventy-nine extensive plots were established in 11 counties, covering the range of American beech in Wisconsin (fig. 9.1). Twenty-one intensive plots were also established, most of them concentrated in Door County and the Menominee Reservation where we were particularly concerned about overall forest health, not just of the beech resource, due to the severity of the disease currently in Door County and the importance of the forest resource to the Menominee Tribe. Currently, nine Wisconsin counties have positive beech scale identification: Dodge, Door, Forest, Manitowoc, Marinette, Menominee, Oconto, Ozaukee, and Sheboygan.

Presence of beech scale was recorded in 43 (54 percent) of the 79 extensive plots (table 9.1). Although the beech scale has been found throughout most of the range of American beech in Wisconsin, scale population levels are very low in most areas, except for Door County. On average, for trees with beech scale present, only 1.1 percent of the tree is covered with scale. In stands with beech scale present, an average of 24 percent of the beech trees have scale present on the boles.

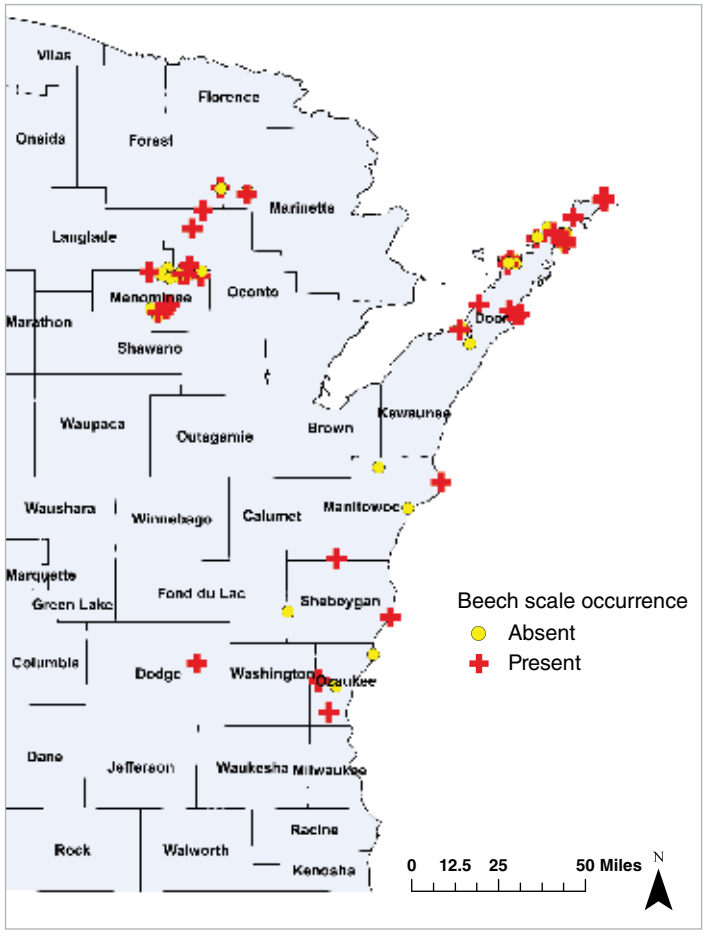

Figure 9.1—Beech scale presence (red crosses) and absence (yellow circles) in monitoring plots established for the Wisconsin Beech Bark Disease Monitoring and Impact Analysis System (as of 2014).

Table 9.1—Number of extensive plots established and number and percentage with positive beech scale identification in Wisconsin counties, 2011–13

County	Total number of plots	Number of plots with scale	Percentage of plots with scale
Dodge	1	1	100
Door	30	20	67
Fond du Lac	1	0	0
Forest	3	1	33
Langlade	1	0	0
Manitowoc	4	2	50
Marinette	5	1	20
Menominee	22	8	36
Oconto	5	5	100
Ozaukee	6	4	67
Sheboygan	1	1	100

Based on the current distribution and severity of beech scale in Wisconsin, the areas of highest risk for mortality due to BBD are in the northern part of Door County, where the forests are dominated with American beech and there is currently an established beech scale population (fig. 9.2). Mortality from BBD has already occurred throughout Door County, and beech scale populations tend to decrease in stands with extensive mortality in what are called "aftermath" forests because of a lack of host material (Cale and others 2015, Houston 1994). Therefore, the risk map only categorizes stands that currently have high levels of beech scale and are at high risk of mortality in the future. Areas of moderate risk include southern Door County and locations on and adjacent to

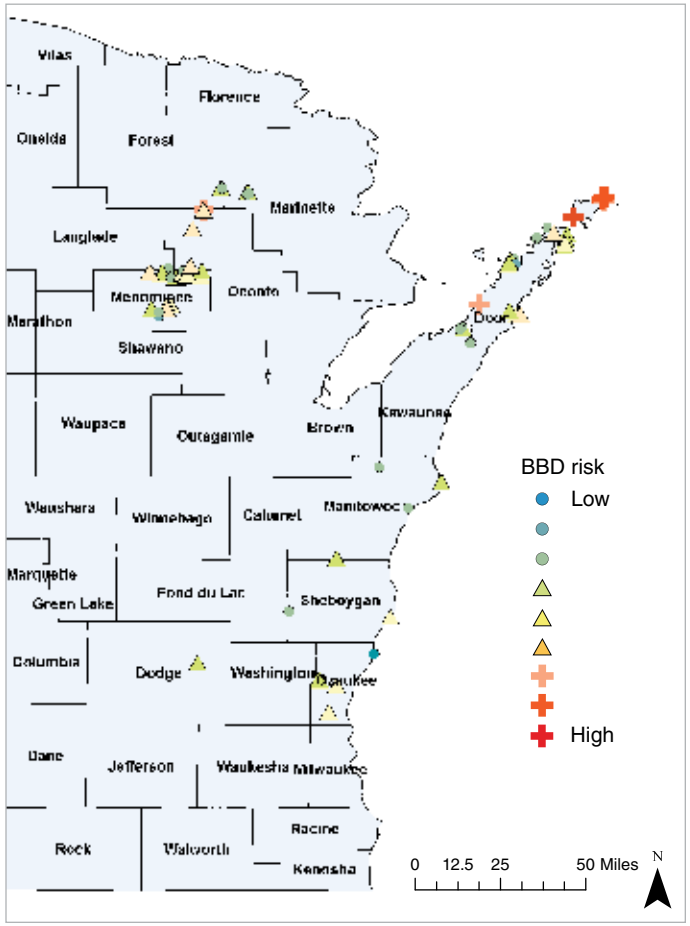

Figure 9.2—Risk map showing low to high risk of mortality from beech bark disease (BBD) in monitoring plots. The risk model for BBD was developed using the following criteria: (1) the average percent beech basal area (BA) present and (2) the average percent beech scale present in each stand. Plots with the highest risk are depicted with a cross symbol, dark red being the highest risk. Triangles represent plots with moderate risk; light orange is high-moderate risk and green is a low-moderate risk. Circles represent plots with low risk; green is moderate-low and blue is the lowest risk.

the Menominee Reservation, where beech is a significant part of the stand but scale populations are still relatively low.

Wieferich and others (2011) found that beech scale populations in Michigan can move 1.2–5.5 miles (3.3–14.3 km) per year. Rate of spread and dispersal of beech scale is highly influenced by the density of American beech within a stand and the direction of the prevailing winds (Griffin and others 2003, Houston 1994). Once in a stand, many factors may influence BBD severity, including presence of genetically resistant beech, nitrogen concentrations in bark tissue, density of hemlock (*Tsuga canadensis*), and local climate conditions (Houston and Valentine 1988, Latty and others 2003, Twery and Patterson 1984, Wargo 1988).

Very little data are available to predict how quickly mortality may occur once beech scale is found in a stand. Based on the Wisconsin risk map, the areas with highest risk are likely to experience mortality within the next 1–3 years, with the moderate risk areas of Door County likely to experience mortality shortly after that, possibly within 5–7 years. It could take decades for mortality to occur in the areas with low risk, based on the current very low beech scale populations and low densities of beech in some of the stands. Menominee Tribal Enterprises is actively reducing American beech basal area throughout the Tribal lands, and it is taking special precautions to leave trees likely to have resistance to BBD. Therefore, even though many stands within Menominee County currently are showing a moderate risk of mortality from beech bark disease, those stands may never see aftermath forest conditions if the beech basal area is reduced enough and resistant trees are remaining. The infancy of BBD in Wisconsin may allow us to contribute to the small amount of knowledge regarding how rapidly mortality may occur once it enters a stand. Future research on BBD in Wisconsin should use the data gathered in this study as a baseline from which to determine mortality rates, so land managers may have a better idea of how long BBD may be present in a stand before mortality occurs.

CONCLUSIONS

Management guidelines for BBD in Wisconsin have recently been developed by the Wisconsin Department of Natural Resources. Management recommendations are based on the percentage of beech basal area in the stand. Land managers can use the risk map to determine at what level of risk their stand(s) may be, based both on beech basal area and also where beech scale is most prevalent. Monitoring plots established as part of the WI-BBDMIAS should continue to be visited to help determine not only where the beech scale is present and its density levels, but also its rate of spread to help managers determine how quickly beech scale may move into new areas or throughout a stand and how quickly mortality may occur.

CONTACT INFORMATION

Holly A Petrillo: hpetrill@uwsp.edu.

LITERATURE CITED

Cale, J.A.; Teale, S.A.; Johnston, M.T. [and others]. 2015. New ecological and physiological dimensions of beech bark disease development in aftermath forests. Forest Ecology and Management. 336: 99–108.

Ehrlich, J. 1934. The beech bark disease: A *Nectria* disease of *Fagus*, following *Cryptococcus fagi* (Baer). Canadian Journal of Forest Research. 10: 595–691.

Griffin, J.M.; Lovett, G.M.; Arthur, M.A.; Weathers, K.C. 2003. The distribution and severity of beech bark disease in the Catskill Mountains, N.Y. Canadian Journal of Forest Research. 33: 1754–1760.

Hane, E.N. 2003. Indirect effects of beech bark disease on sugar maple seedling survival. Canadian Journal of Forest Research. 33: 806–813.

Houston, D.R. 1994. Major new tree disease epidemics: beech bark disease. Annual Review of Phytopathology. 32: 75–87.

Houston, D.R.; Valentine, H.T. 1988. Beech bark disease: the temporal pattern of cankering in aftermath forests in Maine. Canadian Journal of Forest Research. 18: 38–42.

Latty, E.F.; Canham, C.D.; Marks, P.L. 2003. Beech bark disease in northern hardwood forests: the importance of nitrogen dynamics and forest history for disease severity. Canadian Journal of Forest Research. 33: 257–268.

Lohman, M.; Watson, A.J. 1943. Identity and host relations of *Nectria* species associated with diseases of hardwoods in the Eastern States. Lloydia. 6: 77–108.

McGee, G.G. 2000. The contribution of beech bark disease-induced mortality to coarse woody debris loads in northern hardwood stands of Adirondack Park, New York, U.S.A. Canadian Journal of Forest Research. 30: 1453–1462.

Petrillo, H.A.; Witter, J.A.; Thompson, E.M. 2005. Michigan Beech Bark Disease Monitoring and Impact Analysis System. In: Evans, C.E.; Lucas, J.A.; Twery, M.J., eds. 2005. Beech bark disease: proceedings of the beech bark disease symposium, Saranac Lake, NY, June 16–18, 2004. Gen. Tech. Rep. NE-331. Newtown Square, PA: U.S. Department of Agriculture, Forest Service, Northeastern Research Station: 48–51.

Runkle, J.R. 1990. Eight years of change in an old *Tsuga canadensis* woods affected by beech bark disease. Bulletin of the Torrey Botanical Club. 117: 409–419.

Spaulding, P.; Grant, T.J.; Ayres, T.T. 1936. Investigations of *Nectria* diseases in hardwoods of New England. Journal of Forestry. 34: 169–179.

Twery, M.J.; Patterson, W.A., III. 1984. Variations in beech bark disease and its effects on species composition and structure of northern hardwood stands in central New England. Canadian Journal of Forest Research. 14: 565–574.

U.S. Department of Agriculture (USDA) Forest Service. 2015. Forest inventory data online (FIDO). http://apps.fs.fed.us/fia/fido/index.html. [Date accessed: March 24, 2015].

Wargo, P.M. 1988. Amino nitrogen and phenolic constituents of bark of American beech, *Fagus grandifolia*, and infestation by beech scale, *Cryptococcus fagisuga*. European Journal of Forest Pathology. 18: 279–290.

Wieferich, D.J.; McCullough, D.G.; Hayes, D.B.; Schwalm, N.J. 2011. Distribution of American beech (*Fagus grandifolia*) and beech scale (*Cryptococcus fagisuga* Lind.) in Michigan from 2005 to 2009. Northern Journal of Applied Forestry. 28(4): 173–179.

Witter, J.A.; Stoyenoff, J.L.; Petrillo, H.A. [and others]. 2005. Effects of beech bark disease on trees and ecosystems. In: Evans, C.E.; Lucas, J.A.; Twery, M.J., eds. 2005. Beech bark disease: proceedings of the beech bark disease symposium, Saranac Lake, NY, June 16–18, 2004. Gen. Tech. Rep. NE-331. Newtown Square, PA: U.S. Department of Agriculture, Forest Service, Northeastern Research Station: 2–15.

CHAPTER 10.

Investigation of Rapid White Oak *(Quercus alba)* Mortality within the Ozark Plateau and Adjacent Forest-Prairie Transition Ecoregion

(Project NC-EM-B-13-01)

Sharon E. Reed
James T. English
Rose Marie Muzika

INTRODUCTION

Between 2011 and 2014, foresters and landowners in Missouri reported abnormally high levels of white oak (*Quercus alba*) mortality, with large numbers of white oak trees dying abruptly after leaf-out or during late summer. Entire tree crowns rapidly wilted and dead leaves remained attached to branches. Foresters reported that mortality occurred mostly on lower slopes and in the bottoms of upland drainages. This new syndrome was named rapid white oak mortality (RWOM). Reports of RWOM peaked in 2012, but reports of new mortality are still being received. A number of regional events, including a late spring freeze in 2007, record amounts of precipitation in 2008 and 2009, a jumping oak gall outbreak in 2010, and a severe drought in 2012 may have played a role in the mortality event. The Iowa Department of Natural Resources also received reports of white oak mortality between 2011 and 2014. A one-year study was conducted during 2014 to describe the geographic distribution and the characteristics of RWOM. The first study objective was to develop a database that documented the occurrence of white oak mortality within Arkansas, Missouri, and Iowa and associated site characteristics. The second study objective was to characterize insect pests and fungal pathogens associated with declining white oak at two Ozark study locations in Missouri, with particular emphasis on *Phytophthora cinnamomi*. As part of objective two, the physical distribution of mortality within stands was documented along with associated site characteristics.

METHODS

Geographic Distribution (Objective 1)

A one-page survey with 24 questions was created and distributed to foresters in Arkansas, Iowa, and Missouri. Foresters walked a 0.2-ha area within an affected site and reported location, site characteristics, and types of trees dead or dying. A separate survey with 12 questions was created and distributed to landowners. Landowners reported on location of dying oaks; if the dead and dying trees were in the white or red oak groups; and general information about site, including topography, slope position, and relative size of the affected area. Foresters and landowners filled out forms between June and October 2014.

Characterization of Two Study Sites (Objective 2)

Sunklands Conservation Area (SCA) in the southern Missouri Ozarks and Harmon Springs campground in the northern half of the Mark Twain National Forest (MTNF) were selected to characterize insects and pathogens associated with white oak mortality. White oak species made up 33 and 45 percent of the oak-hickory forest at SCA, and MTNF, respectively. Ephemeral streams were present at both locations.

ArcMap® 10.1 was used to randomly generate geographic coordinates for potential plots. Forty-one plots were established within a three-stand area in SCA, and 39 plots were established in a three-stand area in MTNF. Sampling was only

performed in sections of stands without signs of active management. Crown vigor of white oak trees was estimated on a scale of 1 to 6 and averaged for each plot (McConnell and Balci 2014). Site characteristics, including elevation, aspect, slope steepness, and slope position were recorded. The percentage of rock content was measured for high and low vigor plots. General information about soils was downloaded from the U.S. Department of Agriculture (USDA) Natural Resources Conservation Service Web soil survey. The numbers of live and dead tree stems with a diameter breast height (d.b.h.) of 5 cm or greater were counted for each white oak species, the red oak group, and all other genera. Crown positions of all dead stems and their estimated d.b.h. were noted.

Characterization of Insect and Fungal Pathogens (Objective 2)

Soils were sampled around three living white oak trees in each high and low vigor plot. Four soil samples were taken at the base of each white oak tree and were combined. Each soil sample was flooded and baited with *Quercus robur* leaves (McConnell and Balci 2014). After 48, 96, and 144 hours, infected leaf tissues were embedded in PARPNH medium. Resulting oomycete colonies were purified and grouped into morphotypes. Representative isolates of each morphotype were identified by DNA sequencing of the internal transcribed spacer (ITS) region, the mitochondrial cox2 locus, or both.

To sample for Armillaria fungi, the root collar of one severely declining or dead *Q. alba* tree in each high and low vigor plot was inspected for signs of Armillaria infection. Pieces of symptomatic tree tissues were embedded in water agar with streptomycin, and resulting colonies later transferred to lactic acid-amended malt agar. Morphological characteristics were used to identify colonies as Armillaria. DNA sequencing of the ITS region and restriction fragment length polymorphisms (RFLPs) were used to differentiate among three species known to occur in Missouri, *Armillaria mellea*, *A. tabescens*, and *A. gallica* (Baucom 2005, Harrington and Wingfield 1995).

All declining white oak trees in high and low vigor plots were examined for signs of Hypoxylon canker, including stroma occurring on branches or the main stem.

To collect insects associated with declining white oak trees, 2 main stem logs (30 cm length) and 4 branch logs were removed from each of 13 white oak trees at SCA that had a crown vigor rating of 4 or 5. Logs were also removed from five trees at MTNF with vigor ratings of 4 or 5 or that were recently dead. Most branch material from MTNF was dried out at the time of felling, so logs were removed from the stem at approximately 2, 5, and 7 m from the ground. Each main stem log was placed individually in emergence buckets. Branch logs from the same tree were placed together in one emergence bucket. Cerambycid, scolytid, and buprestid insects were collected over a 9-month period.

RESULTS

Reported Distribution (Objective 1)

White oak mortality was reported at 63 locations in Missouri and 2 locations in Iowa. The majority of forester reports were from the southeast and adjacent quadrants of Missouri (fig. 10.1). Mortality was also reported twice in southeastern Iowa and once in southwestern and northeastern Missouri. More than three-quarters of foresters reported white oak mortality on lower slopes and a quarter reported mortality on upper slopes. White oak mortality occurred on slopes with inclines between 0 and 60 percent; however, most reported mortality occurred on inclines of 20 percent or less. Mortality was reported similarly on slopes of all aspect.

Landowner surveys were received, including six, seven, and eight from Arkansas, Iowa, and Missouri, respectively. All Arkansas landowners reported trees in the white oak group dead or dying on upper slopes, and a third of landowners reported mortality on lower slopes as well. Almost half of Iowa landowners reported trees in the white oak group dead or dying on upper slopes, and nearly half of landowners reported mortality on lower slopes. Half of Missouri landowners (fig. 10.1) reported trees in the white oak group dead or dying on upper slopes and half reported mortality on lower slopes.

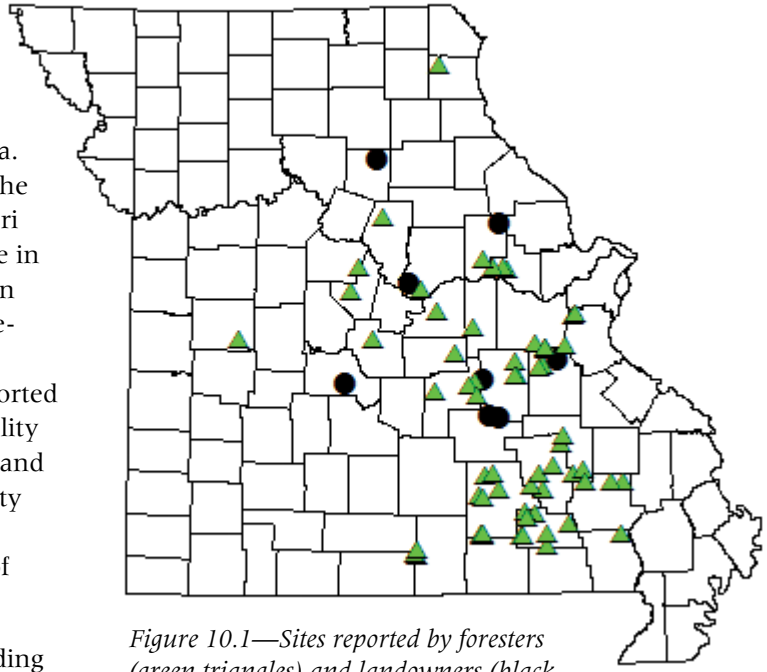

Figure 10.1—Sites reported by foresters (green triangles) and landowners (black circles) with rapid white oak mortality between 2011 and 2014.

Characterization of Study Sites (Objective 2)

Plots were established at the bottom of the hill and on the hillsides at MTNF and SCA. Nine plots were classified as high and 17 plots classified as low vigor at MTNF, whereas 17 plots were classified as high and 17 plots classified as low vigor at SCA. Low vigor plots were disproportionately associated with lower slope positions and the drainage bottom at both sites (fig. 10.2). Accordingly, high vigor plots tended to be at higher elevations at MTNF (316 ± 3 versus 309 ± 3 m) and SCA (309 ± 6 versus 264 ± 2 m) and on steeper slopes than low vigor plots at MTNF (21 ± 1.6 versus 10 ± 1.5 percent) and SCA (31 ± 1 versus 15 ± 3 percent). No aspect appeared to be associated with low vigor plots. Soils in low vigor plots were mostly gravelly silt loams or were occasionally loams or sandy loams. Soils ranged from well drained to somewhat excessively well drained.

Overall white oak mortality was 22 percent and 21 percent within the study areas at MTNF and SCA, respectively. Mortality was greatest in drainages at the bottom of the slope where more than half of all white oaks were dead (table 10.1). At both sites, mortality on lower slopes and in drainages mostly occurred among dominant, co-dominant, and suppressed crown classes while on upper slopes, mortality mostly occurred within the suppressed crown class (table 10.2). All crown classes were affected, with most of the mortality in each crown class occurring on the lower slope and in the drainage at both sites.

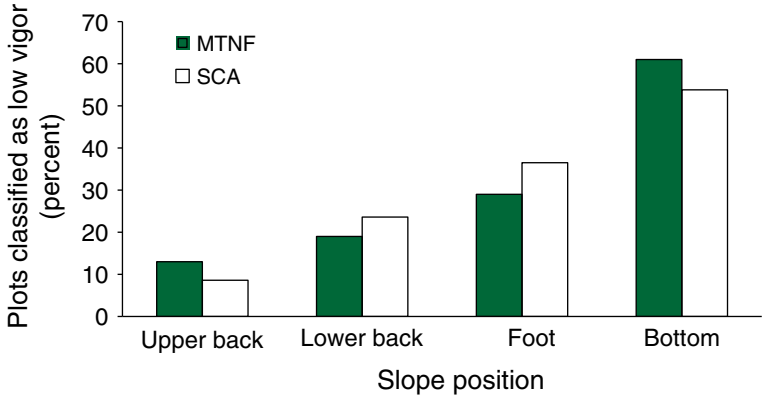

Figure 10.2—Percentages of plots rated as low vigor at each slope position for two locations in the Missouri Ozarks during 2014. MTNF = Mark Twain National Forest; SCA = Sunklands Conservation Area.

Eight oomycete species were detected in soils taken from the bases of white oak trees. *Phytophthora cinnamomi*, *Phytopythium vexans*, *Pythium* sp. I-845, and *Pythium* sp. UZ12 were detected at both MTNF and SCA. *Phytophthora cactorum*, *Phytophthora pini*, and *Phytophthora* sp. 1 were detected only at SCA, whereas *Phytophthora europaea* and *Pythium sensicosum* were detected only at MTNF.

Table 10.1—Percentage of mortality of white oak trees at different slope positions for two locations in the Missouri Ozarks during 2014

Slope position	MTNF		SCA	
	No. live and dead	Mortality	No. live and dead	Mortality
	stems / ha	*%*	*stems / ha*	*%*
Bottom	141	61	108	54
Lower half	558	24	425	30
Upper half	448	10	301	10

MTNF = Mark Twain National Forest; SCA = Sunklands Conservation Area.

Table 10.2—Relative contribution of each crown class to mortality at each slope position at Harmon Springs within Mark Twain National Forest (MTNF) and Sunklands Conservation Area (SCA) during 2014

Location and slope position	Number of dead *Q. alba*	*Q. alba* trees in each crown class		
		Dominant / codominant	Intermediate	Suppressed
	stems/ha	*percent*		
MTNF				
Bottom	86	38	20	42
Lower half	133	21	19	62
Upper half	34	14	9	76
SCA				
Bottom	58	36	14	50
Lower half	128	24	24	52
Upper half	31	7	7	86

Phytophthora cinnamomi was the most frequently detected oomycete, with detections in 12 plots at MTNF and in 7 plots at SCA. *P. cinnamomi* was detected more frequently on lower slopes and in drainages than on upper slopes and the summit at MTNF. *P. cinnamomi* was detected more frequently on upper slopes than on lower slopes at SCA.

Armillaria was isolated from roots of dead or severely declining white oak trees in 12 MTNF and 16 SCA plots. *Armillaria mellea*, *Armillaria gallica*, and *Armillaria tabescens* were isolated from high and low vigor plots at both locations. *A. gallica* was isolated more frequently from low vigor plots than *A. mellea*. *A. tabescens* was isolated infrequently.

Stroma of Hypoxylon canker occurred only on dead trees in plots at MTNF and SCA.

Three species of cerambycids and three species of scolytids were emerged from white oak logs. The scolytid *Xyleborinus gracilis* was the only insect species emerged from logs taken from MTNF and SCA. Other scolytids, *Monarthrum fasciatum* and *Monarthrum mali*, as well as cerambycid species, *Graphiusurus fasciatus*, *Neoclytus mucronatus*, and *Xylotrechus colonus*, were unique to logs taken from MTNF.

DISCUSSION

White oak mortality was largely associated with lower slope positions and bottoms of slopes in this survey of Ozark Plateau forests. This distribution of mortality was especially obvious for trees in the dominant and co-dominant crown class. As expected, *Armillaria mellea* and a *Biscogniauxia* sp. were commonly associated with declining and dead white oaks. *Phytophthora cinnamomi* was also frequently associated with declining white oaks, as was reported in a previous survey of declining red and white oaks within Missouri (Schwingle and others 2007). However, additional species of *Phytophthora*, including *P. cactorum* and *P. pini*, were also associated with declining trees in this survey. In many natural and agricultural ecosystems, *Phytophthora* causes root diseases in areas of high soil moisture that favor production and release of infective zoospores. Consequently, the occurrence of *Phytophthora* species in bottomland and lower slope locations was not surprising. Less frequent detection of *Phytophthora* around trees at higher slope positions may be associated with the occurrence of intermittent soil saturation and water flow patterns and bears further investigation.

The boring beetle, *Xyleborinus gracilis*, was commonly recovered from declining and recently dead white oak trees in this survey. This finding was unexpected. *Xyleborinus gracilis* is native to the Southeastern United States, but it was not detected in Missouri until 2008 and is infrequently collected in aerial trap surveys (Reed and Muzika 2010). Ambrosia beetles native to the Eastern United States mostly attack severely stressed, moribund, or dead trees and their associated fungi are not pathogenic. Nonetheless, the timing of *X. gracilis* beetle attack in relation to host condition and the types of fungi associated with these beetles should be explored.

The widespread occurrence of white oak mortality on bottomland and lower sites contrasts sharply with the decline of red oak species that occurs predominantly on ridge tops and upper slopes. That decline is attributed to the combined effects of advanced tree age, high stem density, and drought, conditions not commonly noted in the present white oak survey (Fan and others 2012). The opportunistic pathogens, *Armillaria* spp. and *Biscogniauxia* spp., reported in the white oak survey are also commonly associated with red oak decline

(Bruhn and others 2000, Stephen and others 2001). However, the frequent detection of *Phytophthora* species was unique to white oak.

CONCLUSION

Further analyses are needed to understand the interactions among weather events and site and biotic factors that determine the distribution of white oak mortality and the likelihood of occurrence on specific sites. Such data could be incorporated into risk models for locations within the Ozark Plateau and Forest Prairie–Transition area to improve management outcomes.

CONTACT INFORMATION

Sharon Reed: reedsh@missouri.edu.

LITERATURE CITED

Baucom, D. 2005. *Armillaria* species in the Missouri Ozark Forests. Columbia, MO: University of Missouri–Columbia. 79 p. M.S. thesis.

Bruhn, J.N.; Wetteroff, J.J., Jr.; Mihail, J.D. [and others]. 2000. Distribution of *Armillaria* species in upland Ozark Mountain forests with respect to site, overstory species composition, and oak decline. European Journal of Forest Pathology. 30: 43–60.

Fan, Z.; Fan, X.; Crosby, M.K. [and others]. 2012. Spatio-temporal trends of oak decline and mortality under periodic regional drought in the Ozark highlands of Arkansas and Missouri. Forests. 3: 614–631.

Harrington, T.C.; Wingfield, B.D. 1995. A PCR-based identification method for species of *Armillaria*. Mycologia. 87: 280–288.

McConnell, M.E.; Balci, Y. 2014. *Phytophthora cinnamomi* as a contributor to white oak decline in mid-Atlantic United States forests. Plant Disease. 98: 319–327.

Reed, S.E.; Muzika, R.M. 2010. The influence of forest stand and site characteristics on the composition of exotic dominated ambrosia beetle communities (Coleoptera: Curculionidae: Scolytinae). Environmental Entomology. 39: 1482–1491.

Schwingle, B.W.; Juzwik, J.; Eggers, J.; Moltzan, B. 2007. *Phytophthora* species in soils associated with declining and non-declining oak in Missouri forests. Plant Disease. 91: 633.

Stephen, F.M.; Salisbury, V.B.; Oliveria, F.L. 2001. Red oak borer, *Enaphalodes rufulus* (Coleoptera: Cerambycidae), in the Ozark Mountains of Arkansas, U.S.A.: an unexpected and remarkable forest disturbance. Integrated Pest Management Reviews. 6: 247–252.

CHAPTER 11.

The Influence of Mountain Pine Beetle Outbreaks on Carbon Productivity and Storage in Central U.S. Rockies Lodgepole Pine Forests

(Project INT-EM-B-10-03)

E. Matthew Hansen
Michael C. Amacher
Helga Van Miegroet
James N. Long
Michael G. Ryan

INTRODUCTION

Recent widespread and severe bark beetle outbreaks in western North America have resulted in larger carbon (C) pools in beetle-killed trees than in fire-killed trees (Hicke and others 2013). Mortality from these outbreaks modifies forest structure, changes the course of forest development, and affects nutrient and carbon cycling at multiple scales of time and space (Edburg and others 2012, Hansen 2014, Hicke and others 2012). Knowledge of post-outbreak C productivity (the rate of stand-level C accumulation from live plants) and storage (the amount of C biomass held in stands at a point in time) will aid prediction of regional forest C balance (i.e., the net rate of C accumulation or loss from the ecosystem) (Kashian and others 2013). More information is needed to understand the possible contributions of post-outbreak stands to atmospheric carbon dioxide (CO_2) content. For example, Kurz and others (2008) suggest that the recent outbreaks in western Canada were large enough to increase global atmospheric CO_2, whereas eddy covariance data suggest that post-outbreak stands are near C neutral (Brown and others 2012, Moore and others 2013).

Cycles of birth, growth, death, and renewal occur at all ecological scales, including entire ecosystems (Holling 1992). In lodgepole pine (*Pinus contorta*) systems, stand-replacing wildfires may occur at intervals up to 300 years or more (Arno 1980). A disturbance-adapted species, lodgepole pine rapidly recolonizes burned landscapes, typically forming pure, even-aged stands (Lotan and others 1985) that become increasingly susceptible to mountain pine beetle (*Dendroctonus ponderosae*) outbreaks as trees grow into diameters favored by beetles, usually after stand ages of 80 years (Amman and others 1977). Recurring outbreaks are possible thereafter every 20–50 years (Alfaro and others 2004, Cole and Amman 1980). These outbreaks are partial disturbances that kill varying amounts of overstory pines and generally leave nonpines (e.g., fir and spruce) and understory pines undamaged (Hansen 2014).

These beetle-caused changes in stand structure and subsequent stand development modify C productivity (i.e., the rate of C accumulation in live plants) for decades after infestation. Although the death of each beetle-killed tree immediately results in reduced stand-level productivity, surviving trees accelerate growth because of reduced competition for resources. Moreover, seedlings are commonly recruited into beetle-caused canopy gaps (Hansen 2014). Thus, productivity can recover to pre-outbreak levels, with recovery times ranging from 5 to 56 years (Edburg and others 2011, Kashian and others 2013, Pfeifer and others 2010, Romme and others 1986). Meanwhile, C productivity in uninfested even-aged stands typically reaches maximum rates within a few decades after stand establishment then slowly diminishes over the life of the stand (Ryan and others 1997). In lodgepole pine stands, this peak occurs at age 24–60 years and declines to 16–48 percent of peak values by age 200–350 years (Kashian and others 2013, Pearson and others

1987, Ryan and Waring 1992). It is therefore possible that frequent partial disturbances, such as from beetle outbreaks, might stimulate C productivity by returning stand development to conditions similar to earlier, more productive stages (Kimmins 1987).

The impact of outbreaks on C storage is confounded by rate changes in pool inputs (i.e., C productivity) and outputs (i.e., C release via decomposition). As outlined above, input rates initially decline but productivity will recover to levels at or, possibly, above pre-outbreak rates. Output rates will vary by substrate type (e.g., fallen needles will decompose within a few years whereas infested boles will persist for decades) and beetle-caused changes in stand structure will modify microclimates, affecting process rates. All of these rate changes vary with time, and long-term patterns (e.g., > 100 years) must be considered to fully understand the influence of outbreaks.

Our objectives were to measure and model the effects of mountain pine beetle outbreaks on C productivity and storage in lodgepole pine type of the central U.S. Rockies. Various aspects of this subject have been examined by previous investigators (Edburg and others 2011, Kashian and other 2013, Pfeifer and others 2010, Romme and others 1986). We present the most comprehensive analysis to date, combining empirical and simulated data to examine short- and long-term C responses among undisturbed and infested lodgepole pine stands. We installed plots in undisturbed and infested stands, with a range of time since infestation (3–80 years), to quantify C storage, C productivity, and decomposition of litter and fine woody debris. We augmented these observations with growth and yield model simulations of C storage and productivity under developmental trajectories with and without mountain pine beetle infestation.

METHODS

After consultation with U.S. Forest Service entomologists, we identified potential field sites in lodgepole pine type with and without evidence of previous mountain pine beetle infestation in three landscapes of the central U.S. Rockies (fig. 11.1). These stands were dominated by lodgepole pine, including the understory for most stands, although some stands also had varying amounts of subalpine fir, Engelmann spruce, Douglas-fir, and/or whitebark pine. Each landscape included an uninfested, mature class of plots with stand ages 118–145 years old. Additional disturbance history classes were: (1) uninfested old-growth (> 200 years old); (2) stands with an outbreak c. 1984; (3) stands with an outbreak c. 1974; (4) stands with an outbreak c. 1930; and (5) stands with an initial outbreak c. 1930 and subsequent outbreak c. 1999–2006 (note that not all classes were available at each of the three landscapes; see Hansen and others 2015). To minimize environmental differences, plot locations were randomly selected within each landscape and disturbance history class using restrictions on elevation, aspect, and slope (e.g., 300-m elevation "window"). Thirty-six plots were installed during 2008–2009 and monitored

Figure 11.1—Plot locations (circles) at three landscapes with undisturbed and mountain pine beetle-infested lodgepole pine stands. Infested stands represented a range of time since disturbance. The green polygons represent lodgepole pine distribution.

for at least 3 years. Sampling methods were based on U.S. Department of Agriculture, Forest Service, Forest Inventory and Analysis phase 3 protocols (USDA Forest Service 2008). These include measurements of over- and understory trees, downed woody material, vegetation, and soils (fig. 11.2). Some protocols were modified to meet the needs of our study, and additional measurements were included to estimate litterfall and decomposition rates. Carbon pool sizes were calculated by multiplying biomass, estimated from allometric equations (Lambert and others 2005), by component-specific

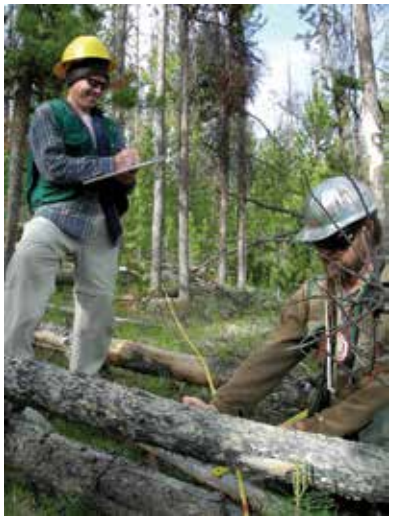

Figure 11.2—A survey crew sampling downed woody materials in a lodgepole pine stand infested by mountain pine beetles about 10 years earlier, Sawtooth National Forest, Idaho. (photo by Matt Hansen, U.S. Department of Agriculture Forest Service)

C concentrations (e.g., foliage, bark, stemwood) derived by analyzing off-plot tree tissue samples. All plots were remeasured 3 years after the original surveys and plot-level C productivity was estimated as the difference in total C storage (adjusted to an annual basis) plus litterfall C. Forest floor decomposition rates were estimated by dividing the C mass by the annual litterfall C flux. We also measured 1-year mass loss of litterbags and tongue depressors, the latter a proxy for fine woody debris. Net ecosystem C balance (i.e., the net rate of C accumulation or loss from live and dead biomass) was calculated by subtracting estimated decomposition rates of snags, downed woody materials, and forest floor from estimates of C productivity (see Hansen and others 2015 for full details).

We used the Forest Vegetation Simulator (FVS) (Dixon 2002) to augment our field data and simulated development with and without mountain pine beetle disturbance. These simulations allowed us to examine complete chronosequences of C productivity and storage, rather than discrete post-outbreak intervals dictated by availability of suitable plots. Moreover, pre-outbreak stand conditions were held constant with the simulations, thus overcoming confounding influences due to environment and initial stand structure. Note that the empirical and simulated data were not intended as validation for each other; rather, each method has inherent advantages and disadvantages and using both methods enhances the data from which to infer beetle-caused impact to C cycling. Input data sources were our field data as well as "bare-ground" conditions, the latter initiated with median values of postfire seedling density as well as snag, downed woody material, and forest floor biomasses measured from recently burned stands. FVS has > 20 regionally specific variants; we used the Tetons and Utah variants. One-hundred-year simulations were created based on the field data (i.e., mature stands) and 200-year simulations with the bare-ground data (i.e., newly established stands). For simulations with mountain pine beetle disturbance, we used the FVS-Mountain Pine Beetle extension and manually scheduled infestations every 40 years beginning at stand age 100 years. To demonstrate the influence of infestation severity, we ran bare-ground simulations using the default mortality algorithms as well as simulations with reduced mortality rates. The simulations included regeneration at each 10-year time step with a pulse of lodgepole regeneration one time step after any infestation; this mimics post-outbreak recruitment observed in the field (Hansen 2014). Using the same allometric equations used to estimate biomass for our field data, we calculated aboveground C in the trees with additional compartments (e.g., nontree vegetation, snags, forest floor, and roots) estimated using the Fire and Fuels Extension of FVS. Carbon productivity was calculated by dividing the time step C accumulation in trees by the number of years in the time step (see Hansen and others 2015 for details of FVS keywords and settings used). We derived net ecosystem C balance by comparing total C storage at each 10-year time step; increasing

total C storage was considered to indicate positive net C balance (i.e., C sink), whereas decreasing total C storage was considered to indicate negative C balance (i.e., C source).

We used generalized linear mixed models to detect differences among the disturbance history classes for the field and simulated data. Additional analyses were conducted using combined disturbance history classes (e.g., uninfested mature and old-growth compared to all infested disturbance history classes). In a preliminary analysis, we tested for differences among the three landscapes by comparing C productivity and storage among the uninfested mature class plots. Because no significant differences were found, we analyzed all data from the three landscapes in single models using "landscape" as a random variable (see Hansen and others 2015 for full details).

RESULTS AND DISCUSSION

Total system C storage was not significantly different among most disturbance history classes using the field data; the only significant difference was between old-growth plots and plots infested a second time c. 2002 (fig. 11.3). Combined infested classes, however, had about 19 percent less total C than combined undisturbed classes. The outbreaks redistributed C from the live overstory compartment to the snags/downed woody material compartment. Time since outbreak diminished these differences; the oldest post-outbreak class plots (infested c. 1930) were not significantly different from the undisturbed class plots for any

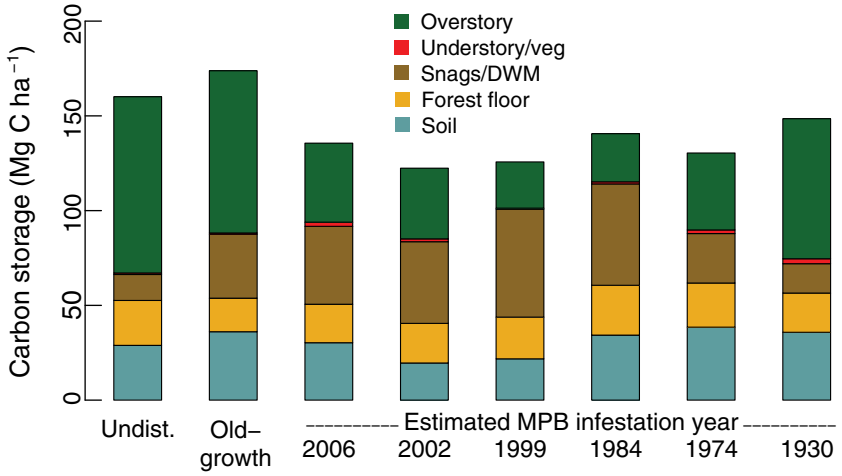

Figure 11.3—Mean carbon storage by compartment among disturbance history classes. Total system carbon (C) storage was significantly different only between old-growth plots and plots infested a second time c. 2002. Combined infested-class plots, however, had significantly less (about 19 percent) total C than combined undisturbed and old-growth plots. Carbon storage by compartment was significantly different among the disturbance history classes. Most notably, infestations transferred C from live overstory to dead compartments although the plots infested c. 1930 were not significantly different than the undisturbed plots for any compartment (see Hansen and others 2015 for full details). Note: DWM = downed woody material; MPB = mountain pine beetle.

compartment. Results from the FVS-simulated data were generally similar. For simulations based on the field data, trajectories with repeated beetle disturbance averaged 1–30 percent less total C storage than did undisturbed trajectories. For simulations based on the bare-ground data, trajectories with repeated beetle disturbance had 7–34 percent less average total C storage than did undisturbed trajectories, depending on outbreak severity and FVS variant (fig.11.4). In summary, C storage is reduced by mountain pine beetle outbreaks, but levels remain robust because C is transferred from live to dead compartments, and decomposition is drawn out over many decades (fig. 11.3). These results support Pfeifer and others' (2010) conclusion that lodgepole pine C storage is resilient to mountain pine beetle disturbance.

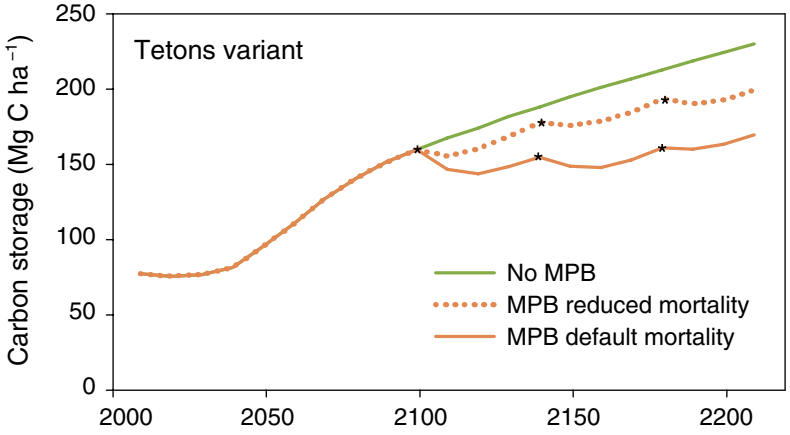

Figure 11.4—FVS-simulated total system carbon storage through time, with and without repeated mountain pine beetle outbreaks using bare-ground data and the Tetons variant. The asterisks indicate outbreak events. Results using the Utah variant were comparable (Hansen and others 2015). Note: MPB = mountain pine beetle.

Carbon productivity results using the field data were similar to the C storage results in that undisturbed and infested class plots were not significantly different (with one pairwise exception; fig. 11.5, top panel), whereas *combined* infested class plots had about 19 percent less C productivity than combined undisturbed class plots. From the field data-based FVS simulations, Utah variant, 100-year averaged C productivity results indicated no significant differences between trajectories with and without repeated mountain pine beetle (MPB) outbreaks. Results using the Tetons variant were variable depending on whether the stand had been previously infested. Among undisturbed stands, trajectories without MPB infestation had greater 100-year averaged C productivity than did trajectories with repeated mountain pine beetle outbreaks, whereas the opposite was the case for stands with previous infestation (Hansen and others 2015). Temporal patterns of post-outbreak C productivity can be seen in results from simulations using bare-ground simulations, Tetons variant (fig. 11.6). Using the default beetle-caused mortality algorithm, C productivity was decreased after an outbreak but generally rebounded to values at or above that of the undisturbed trajectory within 20–30 years. Moreover, the reduced severity

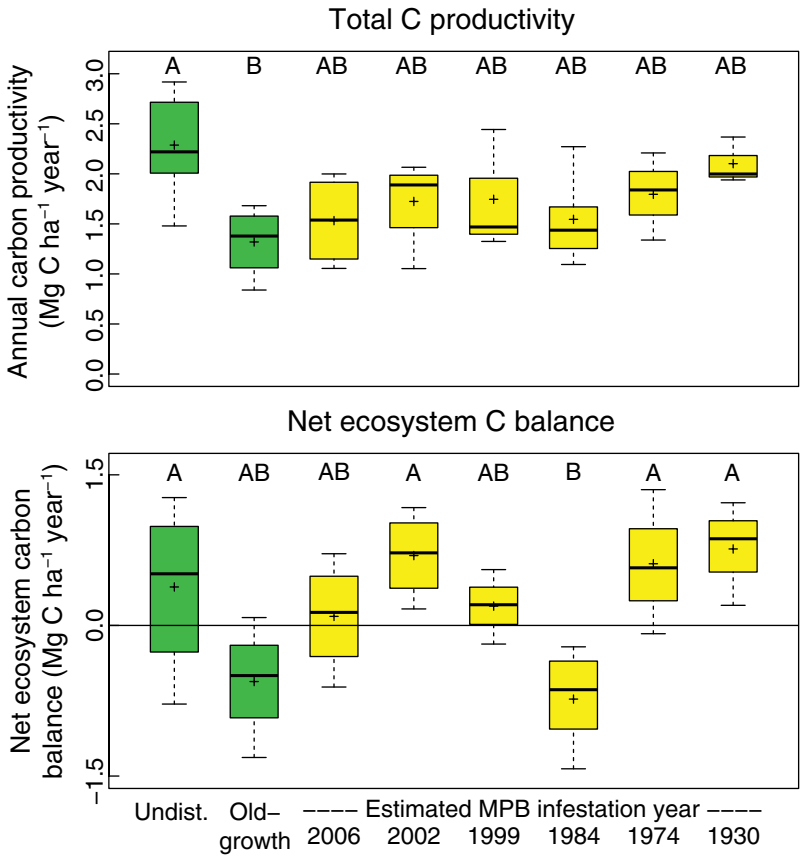

Figure 11.5—Boxplots of total carbon (C) productivity (top panel) and net ecosystem C balance (bottom panel) among disturbance history classes (empirical data). Green boxes indicate disturbance history classes without evidence of beetle infestation and yellow boxes indicate infested classes. Solid lines are the medians, plusses are the means, boxes represent the 25th and 75th percentiles, and whiskers are 1.5 times the interquartile range. Disturbance history classes with the same letter within each panel were not significantly different using multiple range tests (α = 0.10). Note: MPB = mountain pine beetle.

simulation showed heightened C productivity, relative to the undisturbed trajectory, for each 10-year time step after the first outbreak. In this case, C productivity of the surviving trees is predicted to accelerate such that 10-year production more than compensates for the partial loss of canopy trees. Bare-ground results using the Utah variant (not shown; see Hansen and others 2015) were comparatively moderate in that 200-year averaged C productivity of the default and reduced severity trajectories was only about 3 percent higher than that of the undisturbed trajectory.

We expected to observe changes in forest floor dynamics because of increased litterfall from infested trees followed by reduced litterfall thereafter from the reduced surviving canopy. Instead, we found almost no differences in forest floor pool sizes (fig. 11.3), litterfall, or forest floor decomposition rates among the disturbance history classes in the field (Hansen and others 2015). Multiple factors suggest that beetle-caused changes in forest floor inputs and outputs will be ephemeral and difficult to detect: (a) annual litterfall may include up to 20 percent of total needle volume even without beetle-caused mortality; (b) many trees survive outbreaks, and the timing of infestation of trees within a stand occurs over several years rather than a single year; (c) timing of needle fall from infested trees is likewise a distribution rather than a discrete event; (d) pine needles are a relatively high quality substrate for decomposition and 50 percent of

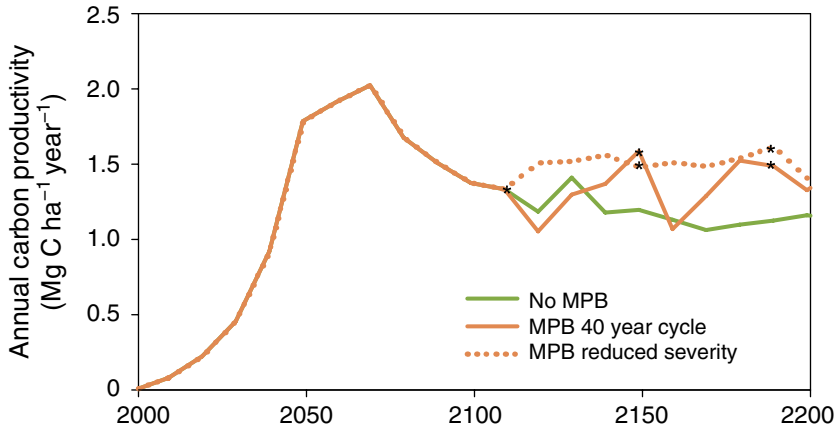

Figure 11.6—FVS-simulated C productivity through time, with and without repeated mountain pine beetle outbreaks using bare-ground data and the Tetons variant. The asterisks indicate outbreak events. Results using the Utah variant differed in that post-outbreak productivity was relatively reduced (Hansen and others 2015). Note: MPB = mountain pine beetle.

fresh litter mass can be lost in as little as 2 years. Nevertheless, it is reasonable to expect that outbreaks likely cause at least some increase in litterfall during the early post-outbreak years with a concomitant (albeit short-lived) increase in forest floor pool size. Thereafter, the decrease in litterfall may be offset by the warmer, drier post-outbreak environment, which slows decomposition and results in stable forest floor pool size as the overstory recovers along with litterfall rates.

Field data–derived estimates of net ecosystem C balance found that, with one exception, the infested disturbance history classes were near C neutral to net C sinks with mean values not significantly different from those of undisturbed plots (fig. 11.5, bottom panel). FVS simulations based on the field data similarly showed that stands generally remained net C sinks despite repeated beetle outbreaks (Hansen and others 2015). An exception for this was found with previously uninfested stands that became net C sources for 10–30 years depending on stand age and infestation severity. Simulations based on the bare-ground data likewise showed that recently infested stands became net C sources for 10–20 years before switching to net C sinks (downward and upward trends of infested trajectories in fig. 11.4). A key reason infested stands remain relatively C neutral is because most C in lodgepole pine systems is held in tree boles. Beetle-killed snags can remain standing for 10 years or more with very little decomposition. Even after falling, snags may remain elevated off the ground (fig. 11.2), and even fallen boles in direct contact with the soil can take multiple decades to decompose (Hansen 2014). The temporary loss of live lodgepole from beetle infestation (i.e., reduced C input rates) is more important to net C balance than the increase in dead substrates (i.e., decomposition potential or output rates) (Kashian and others 2013, Moore and others 2013). Thus, the potential for beetle outbreaks to temporarily switch stands from net C sinks to net C sources is dependent on factors such as stand age, infestation severity, and disturbance history. Also, because of increasing diversity of stand ages, species composition, and size classes with increasing spatial scales, stand-level effects will be muted at the landscape scale.

CONCLUSIONS

Mountain pine beetle outbreaks significantly modify C productivity and storage in central U.S. Rockies lodgepole pine ecosystems by redistributing C from live (sinks) to dead pools (sources). Impacted stands recover to, if not above, pre-outbreak rates within a few decades (fig. 11.6). Moreover, decreases in total C storage range from 1–34 percent, according to our simulation results, and total C storage among post-outbreak stands is considerable (figs. 11.3 and 11.4). This is because decomposition of killed trees (i.e., C output rate) proceeds relatively slowly whereas C productivity recovery to pre-outbreak rates (i.e., input rate) occurs more quickly. Ecosystem creation and destruction is inevitable (Holling 1992) and mountain pine beetle is one agent of reorganization in that cycle. Lodgepole pine systems rely on disturbance (Lotan and others 1985) and are resilient to impacts from mountain pine beetle with respect to C storage and productivity.

CONTACT INFORMATION

Matt Hansen: matthansen@fs.fed.us.

LITERATURE CITED

Alfaro R.I.; Campbell, R.; Vera, P. [and others]. 2004. Dendroecological reconstruction of mountain pine beetle outbreaks in the Chilcotin Plateau of British Columbia. In: Shore, T.L.; Brooks, J.E.; Stone J.E., eds. Information Report BC-X-399. Challenges and solutions: proceedings of the mountain pine beetle symposium. Victoria, BC: Natural Resources Canada, Canadian Forest Service, Pacific Forestry Centre,: 245–246.

Amman, G.D.; McGregor, M.D.; Cahill, D.B.; Klein, W.H. 1977. Guidelines for reducing losses of lodgepole pine to the mountain pine beetle in unmanaged stands in the Rocky Mountains. Gen. Tech. Rep. INT-36. Ogden, UT: U.S. Department of Agriculture, Forest Service, Intermountain Research Station. 28 p.

Arno, S.F. 1980. Forest fire history in the northern Rockies. Journal of Forestry. 78(8): 460–465.

Brown, M.G.; Black, T.A.; Nesic, Z. [and others]. 2012. The carbon balance of two lodgepole pine stands recovering from mountain pine beetle attack in British Columbia. Agricultural and Forest Meteorology. 153: 82–93.

Cole, W.E.; Amman, G.D. 1980. Mountain pine beetle dynamics in lodgepole pine forests—part I: course of an infestation. Gen. Tech. Rep. INT-89. Ogden, UT: U.S. Department of Agriculture, Forest Service, Intermountain Research Station. 56 p.

Dixon, G.E. 2002. Essential FVS: a user's guide to the Forest Vegetation Simulator. http://www.fs.fed.us/rm/pubs/rmrs_gtr292/2002_dixon.pdf. [Date accessed: January 6, 2015].

Edburg, S.L.; Hicke, J.A.; Brooks, P.D. [and others]. 2012. Cascading impacts of bark beetle-caused tree mortality on coupled biogeophysical and biogeochemical processes. Frontiers in Ecology and Environment. 10: 416–424.

Edburg, S.L.; Hicke, J.A.; Lawrence, D.M.; Thornton, P.E. 2011. Simulating coupled carbon and nitrogen dynamics following mountain pine beetle outbreaks in the Western United States. Journal of Geophysical Research. 116. doi:10.1029/2011JG001786. [Published online: December 23, 2011].

Hansen, E.M. 2014. Forest development and carbon dynamics following mountain pine beetle outbreaks. Forest Science. 60(3): 476–488.

Hansen, E.M.; Amacher, M.C.; Van Miegroet, H. [and others]. 2015. Carbon dynamics in central U.S. Rockies lodgepole pine type after mountain pine beetle outbreak. Forest Science. 61(4): 665–679.

Hicke, J.A.; Allen, C.D.; Desai, A. [and others]. 2012. Effects of biotic disturbances on forest carbon cycling in the United States and Canada. Global Change and Biology. 18: 7–34.

Hicke, J.A.; Meddens, A.J.H.; Allen, C.D.; Kolden, C.A. 2013. Carbon stocks of trees killed by bark beetles and wildfire in the Western United States. Environmental Research Letters. 8: 035032.

Holling, C.S. 1992. Cross-scale morphology, geometry and dynamics of ecosystems. Ecological Monographs. 62: 447–502.

Kashian, D.M.; Romme, W.H.; Tinker, D.B. [and others]. 2013. Post-fire changes in forest carbon storage over a 300-year chronosequence of *Pinus contorta*-dominated forests. Ecological Monographs. 83: 49–66.

Kimmins, J.P. 1987. Forest ecology. New York: Macmillan Publishing Company. 531 p.

Kurz, W.A.; Dymond, C.C.; Stinson, G. [and others]. 2008. Mountain pine beetle and forest carbon feedback to climate change. Nature 452: 987–990.

Lambert, M.C.; Ung, C.H.; Raulier, F. 2005. Canadian national tree aboveground biomass equations. Canadian Journal of Forest Research. 35: 1996–2018.

Lotan, J.E.; Brown, J.K.; Neuenschwander, L.F. 1985. Role of fire in lodgepole pine forests. In: Baumgartner, D.M.; Krebill, R.G.; Arnott, J.T.; Weetman, G.F., eds. Proceedings of the symposium lodgepole pine: the species and its management. Pullman, WA: Washington State University Cooperative Extension: 133–152.

Moore, D.J.P.; Trahan, N.A.; Wilkes, P. [and others]. 2013. Persistent reduced ecosystem respiration after insect disturbance in high elevation forests. Ecological Letters. 16: 731–737.

Pearson, J.A.; Knight, D.H.; Fahey, T.J. 1987. Biomass and nutrient accumulation during stand development in Wyoming lodgepole pine forests. Ecology. 68: 1966–1973.

Pfeifer, E.M.; Hicke, J.A.; Meddens, A.J.H. 2010. Observations and modeling of aboveground tree carbon stocks and fluxes following a bark beetle outbreak in the Western United States. Global Change Biology. 17: 339–350.

Romme W.H.; Knight, D.H.; Yavitt; J.B. 1986. Mountain pine beetle outbreaks in the Rocky Mountains: regulators of primary productivity? American Naturalist. 127: 484–494.

Ryan, M.G.; Binkley, D.; Fownes, J.H. 1997. Age-related decline in forest productivity: patterns and process. Advances in Ecological Research. 27: 213–262.

Ryan, M.G.; Waring, R.H. 1992. Maintenance respiration and stand development in a subalpine lodgepole forest. Ecology. 73: 2100–2108.

U.S. Department of Agriculture (USDA) Forest Service. 2008. Interior West Forest Inventory and Analysis: field procedures, version 3.02. http://www.fs.fed.us/rm/ogden/data-collection/pdf/p2_manual_08.pdf. [Date accessed: March 2, 2015].

CHAPTER 12.

Forest Fuels and Predicted Fire Behavior in the First 5 Years after a Bark Beetle Outbreak With and Without Timber Harvest

(Project INT-EM-F-11-04)

Carolyn Sieg
Kurt Allen
Chad Hoffman
Joel McMillin

INTRODUCTION

Unprecedented levels of tree mortality from native bark beetle species have occurred in a variety of forest types in Western United States and Canada in recent decades in response to beetle-favorable forest and climatic conditions (Bentz 2009, Meddens and others 2012). Previous studies suggest that bark beetle outbreaks alter stand structural attributes and fuel profiles, and thus affect the fire environment and potential fire hazard (Jenkins and others 2008, 2014). A number of factors influence post-outbreak fire hazard, including the time since mortality, the proportion of trees killed, and the spatial pattern of dead trees (Hicke and others 2012; Hoffman and others 2012a, 2015; Linn and others 2013; Simard and others 2011). There is also a concern that accumulation of heavy woody fuels as dead trees fall to the ground can lead to large surface fuel loads that are higher than the recommended amounts for fireline construction, fire intensity, and sustaining ecosystem services such as soil protection and wildlife habitat (Brown and others 2003). In some forest types, post-outbreak logging (salvage) of dead trees has been used to recuperate the value of the trees and to potentially reduce fire hazard and enhance forest recovery (Collins and others 2011, 2012). Recent studies have explored post-outbreak stand structure, surface fuels, snag retention rates, and predicted fire behavior in ponderosa pine *(Pinus ponderosa)* forests (Chambers and Mast 2014, Hansen and others 2015, Hoffman and others 2012b), but the effects of post-outbreak timber harvest are largely unstudied in this drier forest type.

Forest Health Protection (FHP) national Insect and Disease Detection Survey (IDS) documented 416,000 acres of ponderosa pine forest impacted by mountain pine beetle (*Dendroctonus ponderosae*) in the Black Hills National Forest (NF) between 1996 and 2012 (Harris 2013). The objectives of this project were to quantify changes in stand structure, fuel loading, and predicted fire behavior during the first 5 years following high levels of bark beetle-caused mortality in stands with and without post-mortality timber harvest that removed the dead trees.

METHODS

We established 47 plots in 2007 in beetle-infested ponderosa pine stands on the Black Hills NF and sampled them in 2009 and 2012. Fifteen 0.05-acre plots were left untreated ("mortality-only") and 32 plots were timber-harvested ("mortality/TH"). In mortality/TH plots, trees killed by bark beetles were removed by whole-tree harvesting in the winter 2007/2008, and nonmerchantable portions of harvested trees were removed offsite. At the time the plots were established, infested trees still had green foliage.

We quantified stand structure attributes by measuring the diameter at breast height (d.b.h., measured at 4.5 feet height) for trees > 2 inches d.b.h. and the height of the lowest live branch of each tree, and recorded whether the tree was alive or dead. We measured stump diameters for recently cut trees in mortality/TH treatments. We calculated basal area and tree density and estimated canopy base height (CBH) as the average of the lowest live branch heights for

each plot. We reconstructed pre-outbreak basal area and tree density by including trees killed by the bark beetles into totals. For logged stands, we converted stump diameters into d.b.h. measures based on locally derived algorithms from 130 trees we measured on the study site.

We tallied surface fuels along two 50-foot planar transects centered on each plot center by time-lag size diameter classes following Brown's (1974) protocols. Size diameter classes included: 1-hour (< 0.25 inches), 10-hour (0.25–1 inch), 100-hour (1.1–3 inches) and 1000-hour (> 3 inches). We tallied 1- and 10-hour fuel classes along the distal 6 feet of each transect end, 100-hour fuels along the distal 12 feet per transect end, and 1000-hour fuels along the entire length of each transect. We classified 1000-hour fuels as either sound or rotten. Woody fuel loading by size classes on each plot was calculated using Brown's (1974) algorithms. Total coarse woody debris (CWD; material > 3 inches diameter) was the sum of sound and rotten 1000-hour fuels; total woody fuel load was the sum of loadings in all size classes.

We analyzed changes in overstory and surface fuels response variables through time using generalized linear mixed models (PROC GLIMMIX; SAS Institute 2014) with log-link functions and unstructured covariance specifications for the residuals, with plot as the random effect, repeated measure subject. We used dead tree density as a covariate to control for differing levels of tree mortality and compared means using Tukey's multiple range tests (Holm 1979).

We used the Crown Fire Initiation and Spread (CFIS) model (Cruz and others 2004) to predict the probability of crown fire initiation across a range of wind speeds. CFIS predicts crown fire probability (both passive and active) based on 10-m open wind speed, CBH, fine dead fuel moisture content, and surface fuel consumption. In addition to probability of crown fire initiation, CFIS also classifies fires as either "surface" or "crown fire" and differentiates crown fires as either "passive," which burn the crowns of individual trees or small groups of trees (also called "torching"), or "active," which burn continuously through the fuels complex (Scott and Reinhardt 2001). We estimated canopy bulk density (CBD) using equations from Cruz and Alexander (2003); CBD affects the estimation of fire type in CFIS. Dead fuel moisture contents were set at 6 percent for all simulations.

RESULTS AND DISCUSSION

Pre-outbreak, stands were 100 percent ponderosa pine, averaged 9.8–11.6 inches d.b.h., and were 55 feet tall with an average CBH of 30 feet. Mortality-only stands had higher basal areas ($p < 0.001$; fig. 12.1A) and tree densities ($p < 0.001$) before the outbreak than mortality/TH stands. The decline in tree density and basal area by 2 years post-outbreak was significant ($p < 0.001$) in both stand types. By 5 years post-outbreak, tree density was reduced a total of 70–79 percent and basal area was 78–85 percent lower than pre-outbreak levels due to bark beetle-induced tree mortality. In addition to reducing tree density and basal area, by 5 years post-outbreak, mortality of mostly larger trees

resulted in stands of significantly ($p < 0.01$) smaller diameter trees (7.8–9 inches d.b.h.) in both stand types and significantly ($p < 0.001$) lower CBH in mortality/TH stands.

The bark beetle outbreak also resulted in large numbers of snags, especially on mortality-only stands. By 5 years post-outbreak, mortality-only stands averaged 240 snags per acre and mortality/TH stands averaged 31 snags per acre. The loss of much of the overstory from the bark beetle outbreak also stimulated prolific tree regeneration. By 5 years post-outbreak, seedling densities averaged 1,636 seedlings per acre on mortality-only stands and 1819 seedlings per acre on mortality/TH plots. The majority of the seedlings established post-outbreak.

Bark beetle-caused tree mortality resulted in little change in woody surface fuels by 2 years post-outbreak, but a dramatic increase by 5 years post-outbreak. Two years post-outbreak, total woody surface fuel loading did not differ significantly ($p = 0.42$) between mortality-only (6.7 tons per acre) and mortality/TH stands (8.1 tons per acre) (fig. 12.1B), and CWD averaged 4.5 tons per acre on mortality-only stands and 4.3 tons per acre on mortality/TH stands ($p = 0.88$). Five years post-outbreak, however, total woody surface fuel load was higher ($p < 0.001$) on mortality-only stands (30.7 tons per acre) than on mortality/TH stands (8.1 tons per acre). The same pattern was observed for CWD fuel loading, as mortality-only stands had more ($p < 0.001$) fuels in this class (24.5 tons per acre) than mortality/TH stands (5.5 tons per acre).

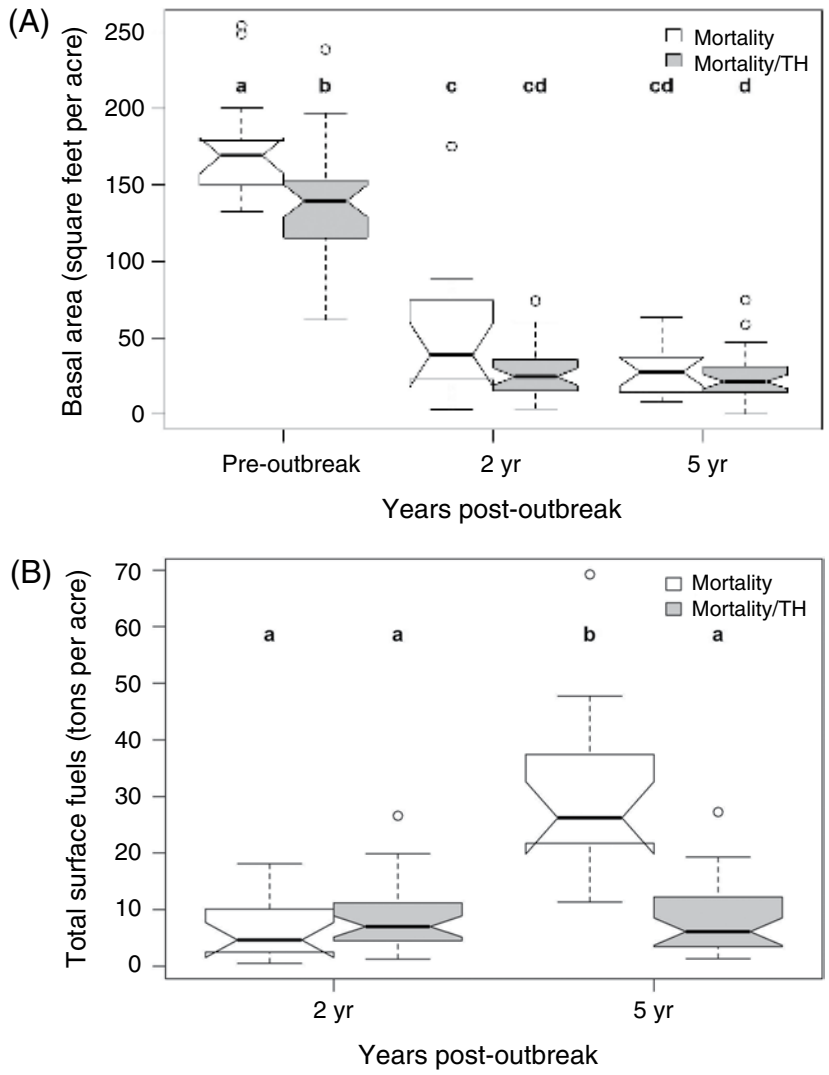

Figure 12.1— (A) Average basal area pre-outbreak and 2 and 5 years post-outbreak, and (B) average total surface load 2 and 5 years post-outbreak on mortality-only and mortality/timber-harvested. Significantly different (α =0.05) means are indicated with different letters. Note: TH = timber-harvested.

Stand structural changes and surface fuel accumulations resulting from the bark beetle-induced tree mortality led to changes in predicted crown fire potential through time. At wind speeds < 10 miles per hour, surface fires were predicted for pre-outbreak stands; above 10 miles per hour, active crown fires were predicted (table 12.1). At 2 years post-outbreak, the pattern of surface fires switching to active crown fires at wind speeds above 10 miles per hour was maintained in mortality-only stands due to higher tree densities and CBD.

In contrast, in mortality/TH stands, crown fires occurring above 10-mile-per-hour winds were predicted to be passive. Due to the lower CBH in mortality/TH stands, however, the probability of crown fire occurrence was predicted to be higher at 2 years post-outbreak than in mortality-only stands (fig. 12.2). At 5 years post-outbreak, due to higher surface fuel accumulation in mortality-only stands, surface fires were predicted to transition to passive crown fires at lower wind speeds and become active crown fires at wind speeds above 17 miles per hour (table 12.1),

Table 12.1—Major fire type by wind speed for pre-outbreak and 2 and 5 years post-outbreak, on mortality-only and mortality/timber-harvested (TH) stands

	Wind speed			
	< 5	6–9	10–17	> 17
	miles per hour			
Pre-outbreak	S	S	A	A
2 year mortality-only	S	S	A	A
2 year mortality/TH	S	S	P	P
5 year mortality-only	S	P	P	A
5 year mortality/TH	S	S	P	P

S = surface fire; A = active crown fire; P = passive crown fire.

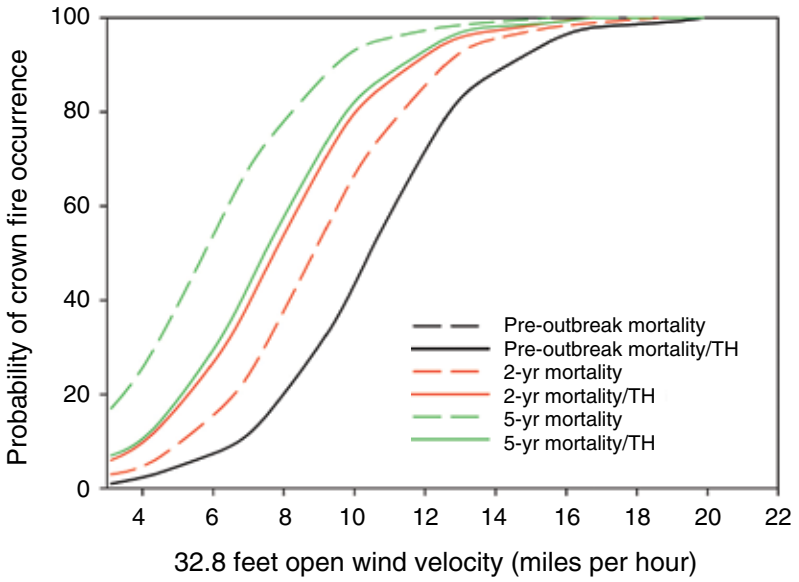

Figure 12.2—Probability of crown fire occurrence by wind speed for pre-outbreak, and 2 and 5 years post-outbreak for mortality-only and mortality/timber-harvested stands. Pre-outbreak mortality-only and mortality/timber-harvested stands have the same crown fire probability, and thus these lines appear as a single line. Note: TH = timber-harvested.

and the probability of crown fire occurrence was higher in mortality-only stands than in mortality/TH stands (fig. 12.2).

DISCUSSION

This study documented dramatic changes in forest structure, surface fuels, and predicted fire behavior within 5 years following a mountain pine beetle outbreak in Black Hills ponderosa pine forests. In addition to time since outbreak, initial tree densities and level of mortality influenced post-outbreak attributes. Within 2 years post-outbreak, tree density and basal area were reduced 60–80 percent. Residual post-outbreak trees had smaller diameters and lower crown base heights due to the mortality of the larger trees, which left shorter trees with crowns closer to the ground. By 5 years post-outbreak, the basal area of all stands was below the threshold of 120 square feet per acre for high susceptibility to mountain pine beetle infestations (Schmid and others 1994).

Snagfall proceeded quickly, resulting in a shift from most plots having CWD loadings below recommended levels 2 years post-outbreak to most of the mortality-only stands having loadings above recommended levels by 5 years post-outbreak. Two years post-outbreak, total CWD loadings in mortality-only and mortality/TH stands were below (65–66 percent of the stands) or within (33–34 percent of the stands) recommended levels for dry coniferous forests (5–20 tons per acre; Brown and others 2003); no stands had loadings above recommended levels. Five years post-outbreak, none of the mortality-only stands had woody fuel loadings below recommended levels; 53 percent of the stands had levels within and 47 percent of the stands had levels above recommended levels. In contrast, at 5 years post-outbreak, CWD fuel loadings in mortality/TH stands were mostly (59 percent) below or within (38 percent) recommended levels; only one stand (3 percent) had CWD loadings above recommended levels. In a previous study in Arizona, 20 percent of the stands killed by both ips and *Dendroctonus* beetles had CWD loadings above recommended levels 5 years post-outbreak (Hoffman and others 2012b). We attributed the greater proportion of plots with higher CWD loadings at 5 years in our study compared to those in the Southwest study to higher pre-outbreak tree densities in the Black Hills. Mortality stands in Arizona averaged 162 ponderosa pine trees per acre compared to an average range of between 178 and 327 trees per acre in the Black Hills. The generally low level of woody surface material on the mortality/TH stands was a reflection of the harvesting techniques used. Trees were whole-tree harvested when the needles were still green and limbed at landings adjacent to the stands. Thus logging prevented the buildup of woody surface fuels following the bark beetle outbreak, similar to model projections following whole-tree harvest of dead trees in other forest types (Donato and others 2013).

The combination of lower CBD and CBH plus higher woody fuel loadings has several implications for predicted crown fire potential following bark beetle-induced tree mortality in

Black Hills ponderosa pine stands. Lower CBH is predicted to allow surface fires to transition into the crowns more readily. Heavy woody surface fuel loadings by 5 years post-outbreak in mortality-only stands were predicted to provide an additional avenue for fires to transition into crowns. With time, as downed wood becomes rotten and more ignitable and herbaceous fine fuels increase, high severity surface fires are likely to occur and result in additional tree mortality and severe soil heating (Brown and others 2003, Hyde and others 2012). Prescribed burning under moderate weather conditions and high 1000-hour fuel moistures has the potential to reduce woody surface fuel loading with fewer detrimental consequences (Stevens-Rumann and others 2012).

Post-outbreak timber harvest of dead trees in the mortality/TH stands prevented the type of surface fuel buildup that occurs without timber harvest following bark beetle-induced tree mortality, thus resulting in a lower crown fire potential, and crown fires were predicted to be mostly passive. However, on both mortality-only and on mortality/TH stands, high tree seedling densities will eventually increase crown fire risk if allowed to grow. Prescribed burning can be an effective tool in reducing seedling numbers, but as seedlings mature they become less resistant to fire mortality (Battaglia and others 2009). Prescribed burning could be useful in suppressing pine regeneration and preventing the development of hyper-dense stands in the future and it could easily be accomplished in stands where dead trees have been removed by timber harvest.

ACKNOWLEDGMENTS

Funding was provided by Forest Health Monitoring Evaluation Monitoring grant INT-EM-F-11-04. Chris Hoffman, Chris Looney, Emma Gustke, Al Dymerski, Brittany Deranleau, John Wilson, James Wilson, Tania Begaye, Addie Hite, Katherine Gibble, and Danna Muise helped with field work and data entry. Scott Baggett developed statistical models and Benjamin Bird drafted figure 12.1; Jeri Lyn Harris and Matt Hansen provided comments on an earlier draft.

CONTACT INFORMATION

Carolyn Sieg: csieg@fs.fed.us.

LITERATURE CITED

Battaglia, M.; Smith, F.W.; Shepperd, W.D. 2009. Predicting mortality of ponderosa pine regeneration after prescribed fire in the Black Hills, South Dakota, USA. International Journal of Wildland Fire. 18: 176–190.

Bentz, B.J., ed. 2009. Bark beetle outbreaks in western North America: causes and consequences. Logan, UT: Utah State University. 42 p.

Brown, J.K. 1974. Handbook for inventorying downed woody material. Gen. Tech. Rep. INT-16. Ogden, UT: U.S. Department of Agriculture, Forest Service, Intermountain Forest and Range Experiment Station. 24 p.

Brown, J.K.; Reinhardt, E.D.; Kramer, K.A. 2003. Coarse woody debris: managing benefits and fire hazard in the recovering forest. Gen. Tech. Rep. RMRS-105. Fort Collins, CO: U.S. Department of Agriculture, Forest Service Rocky Mountain Research Station. 16 p.

Chambers, C.L.; Mast, J.N. 2014. Snag dynamics and cavity excavation after bark beetle outbreaks in southwestern ponderosa pine forests. Forest Science. 60: 713–723.

Collins, B.J.; Rhoades, C.C.; Battaglia, M.A.; Hubbard, R.M.; 2012. The effects of bark beetle outbreaks on forest development, fuel loads and potential fire behavior in salvage logged and untreated lodgepole pine forests. Forest Ecology and Management. 284: 260–268.

Collins, B.J.; Rhoades, C.C.; Hubbard, R.M.; Battaglia, M.A. 2011. Tree regeneration and future stand development after infestation and harvesting in Colorado lodgepole pine. Forest Ecology and Management. 261: 2168–2175.

Cruz, M.G.; Alexander M.E.; Wakimoto, R.H. 2003. Assessing canopy fuel stratum characteristics in crown fire prone fuel types of western North America. International Journal of Wildland Fire. 12: 39–50.

Cruz, M.G.; Alexander M.E.; Wakimoto, R.H. 2004. Modeling the likelihood of crown fire occurrence in conifer forest stands. Forest Science. 50: 640–658.

Donato, D.C.; Simard, M.; Romme, W.H. [and others]. 2013. Evaluating post-outbreak management effects on future fuel profiles and stand structure in bark beetle-impacted forests of Greater Yellowstone. Forest Ecology and Management. 303: 160–174.

Hansen, E.M.; Johnson, M.C.; Bentz B.J. [and others]. 2015. Fuel loads and simulated fire behavior in "old stage" beetle-infested ponderosa pine of the Colorado Plateau. Forest Science. 61(4): 644–664.

Harris, J.L., comp.; R2 staff Forest Health specialists. 2013. Forest health conditions, 2012, Rocky Mountain Region (R2). State & Private Forestry & Tribal Relations, Forest Health Protection, R2-13-RO-31. Golden, CO: U.S. Department of Agriculture, Forest Service. 68 p.

Hicke, J.A.; Johnson, M.C.; Hayes, J.L.; Preisler, H. K. 2012. Effects of bark beetle-caused tree mortality on wildfire. Forest Ecology and Management. 217: 81–90.

Hoffman, C.M.; Morgan, P.; Mell, W. [and others]. 2012a. Numerical simulation of crown fire hazard immediately after bark beetle-caused mortality in lodgepole pine forests. Forest Science 58(2): 178–188.

Hoffman, C.M.; Sieg, C.H.; McMillin, J.D.; Fulé, P.M. 2012b. Fuel loadings five years after a bark beetle outbreak in southwestern USA ponderosa pine forests. International Journal of Wildland Fire. 21:306–312.

Hoffman, C.M.; Parsons, R.; Linn, R. [and others]. 2015. Modeling interactions of beetle attacks and fire behavior over time in lodgepole pine stands using FIRETEC. Agriculture and Forest Meteorology. 204: 79–93.

Holm, S. 1979. A simple sequentially rejective multiple test procedure. Scandinavian Journal of Statistics. 6: 65–70.

Hyde, J.C.; Smith, A.M.S.; Ottmar, R.D. 2012. Properties affecting the consumption of sound and rotten coarse woody debris in northern Idaho: a preliminary investigation using laboratory fires. International Journal of Wildland Fire. 21: 596–608.

Jenkins, M.J.; Hebertson, E.; Page, W.; Jorgensen, C.A. 2008. Bark beetles, fuels, fires and implications for forest management in the Intermountain West. Forest Ecology and Management. 254: 16–34.

Jenkins, M.J.; Runyon, J.B.; Fettig, C.J. [and others]. 2014. Interactions among the mountain pine beetle, fires, and fuels. Forest Science. 60: 489–501.

Linn, R.R.; Sieg, C.H.; Hoffman, C.M. [and others]. 2013. Modeling wind fields and fire propagation following bark beetle outbreaks in spatially-heterogeneous pinyon-juniper woodland fuel complexes. Agriculture and Forest Meteorology. 173: 139–153.

Meddens, A.J.H.; Hicke, J.A.; Ferguson, C.A. 2012. Spatiotemporal patterns of observed bark beetle-caused tree mortality in British Columbia and the Western United States. Ecological Applications. 22(7): 1876–1891.

SAS Institute. 2014. SAS/STAT® 13.2 User's Guide The GLIMMIX Procedure. Cary, NC: SAS Institute.

Schmid, J.M.; Mata, S.A.; Obedzinski, R.A. 1994. Hazard rating ponderosa pine stands for mountain pine beetles in the Black Hills. Res. Note RM-529. Fort Collins, CO: U.S. Department of Agriculture, Forest Service, Rocky Mountain Forest and Range Experiment Station. 4 p.

Scott, J.H.; Reinhardt, E.D. 2001. Assessing crown fire potential by linking models of surface and crown fire behavior. Res. Pap. RMRS- 29. Fort Collins, CO: U.S. Department of Agriculture, Forest Service, Rocky Mountain Research Station. 66 p.

Simard, M.; Romme, W.H.; Griffin, J.M.; Turner, M.G. 2011. Do mountain pine beetle outbreaks change the probability of active crown fire in lodgepole pine forests? Ecological Monographs. 81: 3–24.

Stevens-Rumann, C.S.; Sieg, C.H.; Hunter, M.E. 2012. Ten years after wildfires: how does varying tree mortality impact fire hazard and forest resiliency? Forest Ecology and Management. 267: 199–208.

CHAPTER 13.

Implement Interagency Whitebark Pine Monitoring for the Greater Yellowstone Ecosystem

(Project INT-EM-F-12-01)

Kristen L. Legg
Erin Shanahan
Nancy Bockino
Kelly McCloskey
Steve Munson
Darren Blackford

INTRODUCTION

Whitebark pine (*Pinus albicaulis*) occurs on over 2 million acres in the Greater Yellowstone Ecosystem (GYE). As a keystone and foundation species, whitebark pine influences ecosystem functions such as biodiversity, vegetation structure, and hydrology. It has declined throughout its range in the Northern Rockies due to the combined effects of mountain pine beetle (*Dendroctonus ponderosae*), white pine blister rust (*Cronartium ribicola*), altered fire regimes, and climate change.

Recognizing the need to cohesively manage whitebark pine across the GYE, the Greater Yellowstone Coordinating Committee's Whitebark Pine Subcommittee (GYCC WBPSC) developed the Greater Yellowstone Whitebark Pine Strategy (GYCC WBPSC 2011), which identified monitoring, research, protection, and restoration as management objectives to conserve whitebark pine. Since 2004, the National Park Service Greater Yellowstone Network (GRYN) has implemented an interagency whitebark pine long-term monitoring program across the GYE. Since changes in fire regimes may detrimentally impact the whitebark pine resource, the GYCC WBPSC initiated a research project in 2009 to study whitebark pine regeneration in paired burned versus unburned sites where historic wildfires occurred (pre-1994).

The primary project objective was to evaluate how whitebark pine responds to wildland fire in the GYE in order to develop short- and long-term whitebark pine management strategies. This 3-year Evaluation Monitoring project resulted in the completion of the following two activities:

(1) Conducted a third visit to 176 long-term monitoring plots established in 2004–2007 to:
- Estimate the proportion of whitebark pine (> 1.4 m high) infected with white pine blister rust;
- Estimate survival of individual whitebark pine (> 1.4 m high) associated with several disturbance agents (i.e., fire, mountain pine beetle, and white pine blister rust);
- Assess whitebark pine regeneration within established plots.

(2) Revisited 6 of 10 wildland fire areas, each with 8 burned/unburned paired plots established in 2009 to:
- Determine the abundance and distribution of whitebark pine regeneration;
- Document site and stand characteristics;
- Document presence and severity of disturbance agents, including white pine blister rust and mountain pine beetle.

METHODS

Both activities described above resulted in the collection of site characteristics associated with each plot such as slope, elevation, and aspect; tree characteristics such as diameter at breast height (d.b.h.), tree status (live or dead), and presence of disturbance agents (such as

white pine blister rust, mountain pine beetle, and fire); seed reproduction (presence of cones, conelets, or cone scars); and existing whitebark pine regeneration (trees ≤ 1.4 m tall). Whenever possible, spatial burn severity data were used, although this was more difficult to do for fires that occurred before 1985.

Long-Term Monitoring Program

Details of the sampling design and field methodology are described in the Greater Yellowstone Whitebark Pine Long-term Monitoring Protocol (GYWBPMWG 2011). The basic approach is a two-stage cluster design. Stands of whitebark pine are the primary units and 10-m by 50-m monitoring plots are the secondary units. From 2004 to 2007, 176 permanent plots were established in 150 whitebark pine stands across the GYE (fig. 13.1). Within each transect, all whitebark pine trees >1.4 m tall were tagged in order to evaluate changes in blister rust infection and monitor survival rates over time. Each monitoring plot was visited once every four years and all 176 were revisited at least twice by the end of 2014.

Burned/Unburned Plot Surveys

Detailed descriptions of the methods used to establish paired plots for this survey can be found in the Whitebark Pine Monitoring for the Greater Yellowstone Ecosystem: Regeneration Study 2009–2014 summary (Bockino 2015). In 2009, baseline data were collected on 8 paired burned/unburned plots in each of 10 wildfire areas (fig. 13.2). The burned/unburned plots from six of the wildfire areas were revisited

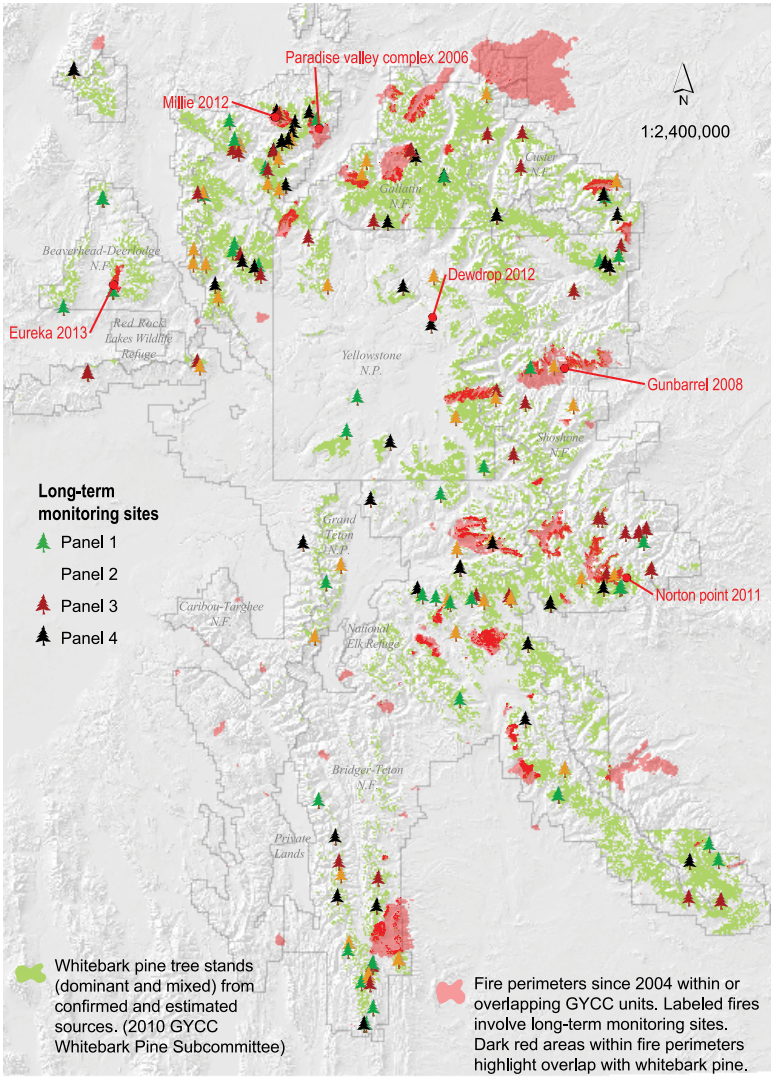

Figure 13.1—Map of the distribution of long-term monitoring plots across the Greater Yellowstone Ecosystem with current whitebark pine distribution and wildland fire perimeters that have occurred since 2004. Note: GYCC = Greater Yellowstone Coordinating Committee.

once from 2012 to 2014 (Ann's, Hidden Lake, Mountain Ash Creek, Coyote, Corral Creek, and Hellroaring wildfires); all burned before 1994. Two subplots were sampled at all sampling points:

(1) A variable-radius plot was installed to sample overstory (variable-radius "overstory" plots were sampled using a slope-corrected Speigel relaskop to estimate overstory tree composition and basal area. Depending on stand density and in order to achieve a sample of 10–15 trees per plot, the basal area factor used was 10, 20, or 40. All conifers and aspen > 1.37 m tall were included in this sample.); and

(2) A fixed-radius plot was installed to sample regeneration of whitebark pine ≤10 cm d.b.h.

Within each wildfire area the burn severity for each plot was classified as: complete burn (all overstory tree mortality), partial burn (evidence of fire, some overstory tree survival), and unburned (no evidence of wildfire).

RESULTS AND DISCUSSION

Long-Term Monitoring Program

From 2012 to 2014, all 176 monitoring plots were visited. We estimate that between 20 to 30 percent of the whitebark pine trees > 1.4 m tall are infected with white pine blister rust in the GYE, and since 2004 approximately 27 percent have died. Within the monitoring program's tagged tree population, most of the mortality was observed in trees > 10 cm d.b.h. These findings were associated with the recent mountain pine

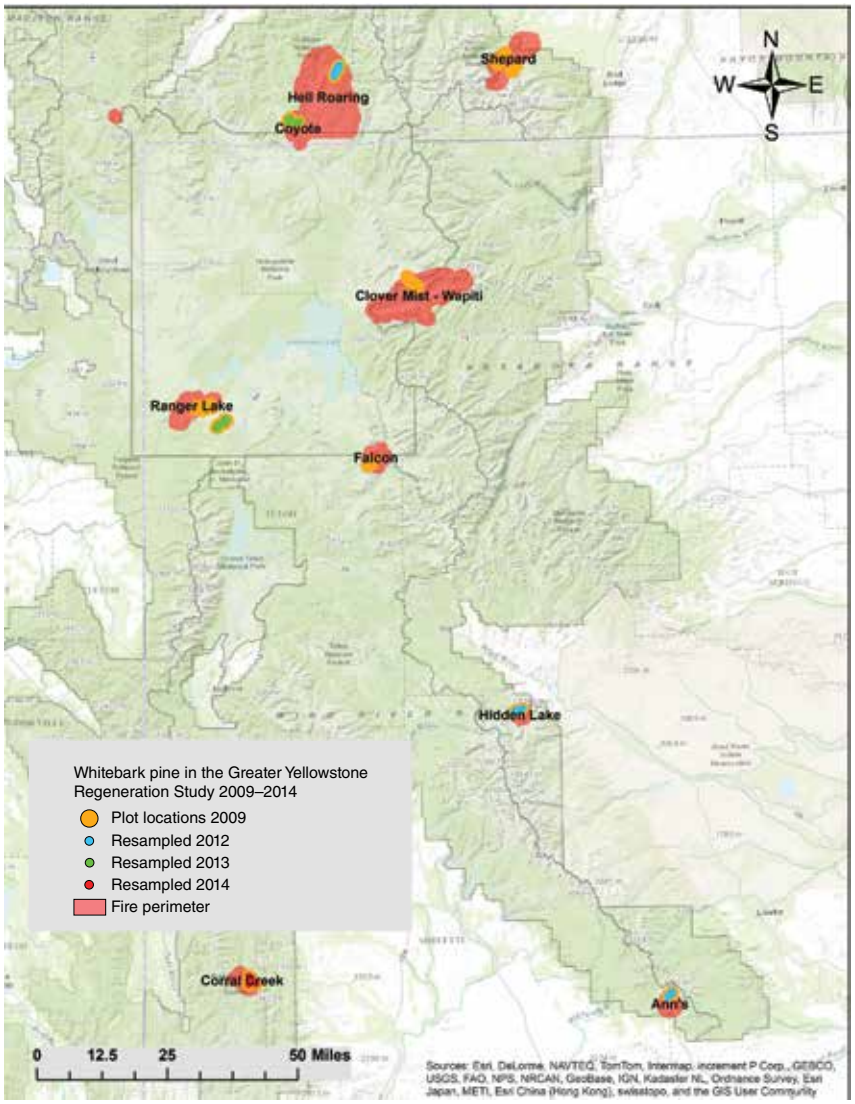

Figure 13.2—Paired burned/unburned study site locations. In 2009, baseline data were collected from 16 plots at each of 10 study sites. From 2012 to 2014, six study sites were revisited (Ann's, Hidden Lake, Mountain Ash Creek, Coyote, Corral Creek, and Hellroaring) (Source: Bockino 2015). Note: GYCC = Greater Yellowstone Coordinating Committee.

beetle outbreak and are similar to results produced from other studies (MacFarlane and others 2013). An average density of 53 understory whitebark pine trees (≤ 1.4 m tall) per plot or 500 m^2 were documented on the long-term monitoring plots (GYWBPMWG 2014, Shanahan and others 2014). Since transect establishment in 2004, wildland fire has affected 16 of the 176 transects (fig. 13.1). Of the 14 burned monitoring plots surveyed (2 of the 16 burned after our most recent site visits in 2013 and 2014), we recorded 50 percent to 90 percent of exposed ground or thick herbaceous cover depending on the time interval since the wildfire occurred. A summary of the results of these surveys for each monitoring plot is available upon request. Whitebark pine has regenerated on four plots that experienced various burn intensities (low: some trees left live to high: complete burn). One severely burned plot (214-1) in the 2007 Wicked Creek Fire Complex, Gallatin National Forest, had whitebark pine regeneration within and adjacent to the plot during the 2014 survey.

By 2014, approximately 1,440 tagged trees had died since initiation of the monitoring program (2004–2007). Figure 13.3 shows the

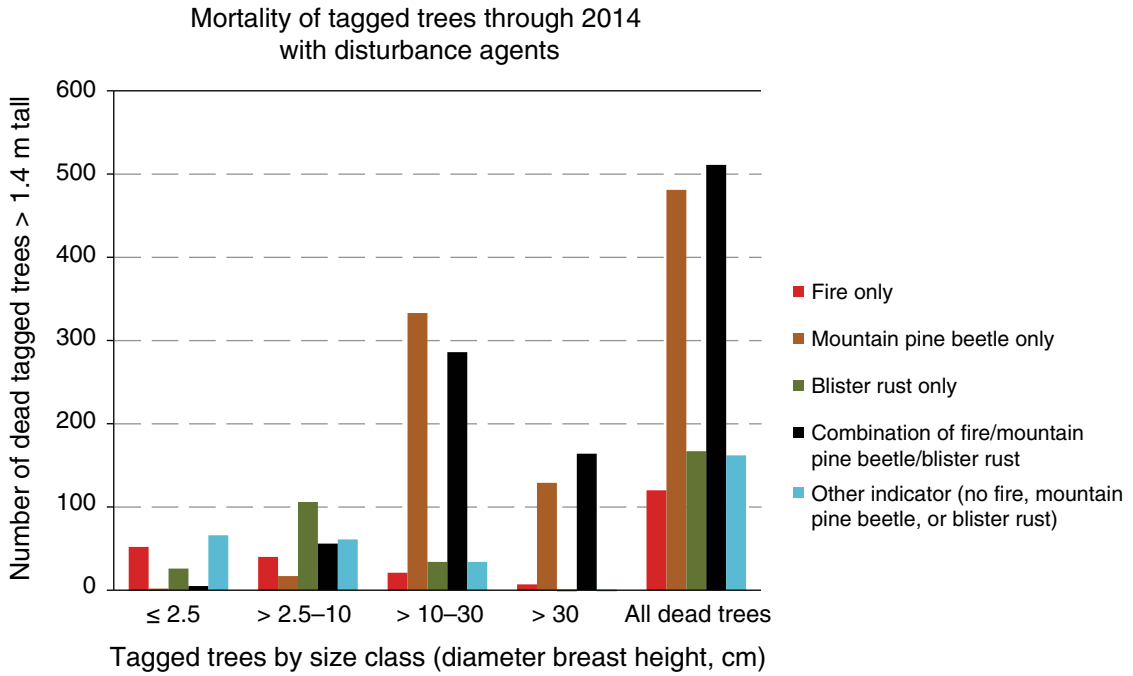

Figure 13.3—Tagged tree mortality since transect establishment through 2014 and disturbance agent. Evidence associated with fire, mountain pine beetle, white pine blister rust, a combination of the three, or other were recorded for each dead tagged tree by diameter breast height size class (≤ 2.5 cm, > 2.5–10 cm, > 10–30 cm, and > 30 cm). Two hundred and forty-eight dead tagged trees had evidence of fire damage.

distribution of whitebark pine mortality by disturbance agent (fire, mountain pine beetle, white pine blister rust, a combination of the three, or other) in four d.b.h. size classes. We recorded a total of 248 dead, tagged trees with evidence (scorched to completely burned) of recent wildfire damage and of those 170 were burned in the 2012 Millie Fire on the Gallatin National Forest. All reports related to this effort may be found at http://science.nature.nps.gov/im/units/gryn/monitor/whitebark_pine.cfm (accessed April 14, 2015).

Burned/Unburned Plot Surveys

Preliminary results for the eight paired burned/unburned plots from each of the six wildland fire areas are described in detail in a summary report (Bockino 2015). A preliminary evaluation of these data indicates that there are several long-term successional trajectories for whitebark pine post-fire disturbances. Figure 13.4 depicts this trajectory for the wildfire sites measured in 2009 and again in 2012. The abundance of whitebark pine regeneration by size class, burned or unburned, and length of time since burn varied among the study sites. These data on regeneration dynamics—establishment, survivorship, growth, and disturbance interactions—will be analyzed in the near future.

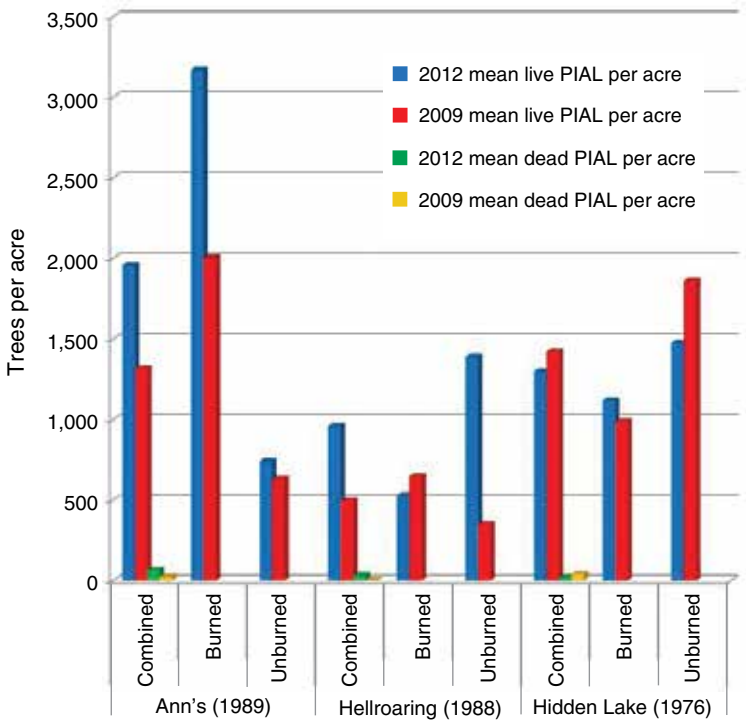

Figure 13.4—An example of comparing data from three wildfire study areas read in 2009 and again in 2012 with summary of live and dead whitebark pine (Pinus albicaulis—*PIAL) per acre. Combined are the mean of the burned and unburned data. This is for trees of all sizes. (Source: Bockino 2015)*

CONCLUSIONS

Evaluation Monitoring program funds provided the necessary resources to enable data collection for short (< 10 years) and long-term (decades) evaluation of the status of whitebark pine after wildfire events in the GYE. Ongoing surveys of these sites will determine whitebark pine response in burned areas and provide an evaluation of the effects of previous, current, and future disturbance agents (i.e., disease, insects, and climate change). Further analysis will include the addition of other parameters such as water balance (the integration of temperature, precipitation, and a site's physical characteristic), competition from other species, and distance to mature whitebark pine (potential seed source) that may affect successful whitebark pine regeneration and survival within post-fire event sites. This information will be useful to resource managers responsible for whitebark pine conservation and to the Greater Yellowstone Coordinating Committee Whitebark Pine Subcommittee as they adapt the whitebark pine strategy.

ACKNOWLEDGMENTS

We would like to thank all the field crew staff responsible for plot installation and data collection. We also would like to thank Gregg DeNitto, USDA Forest Service, and Roy Renkin, National Park Service, for thoughtful review of this report. This project was supported by the USDA Forest Service Forest Health Monitoring Program, and the National Park Service's Greater Yellowstone Network and Grand Teton National Park.

CONTACT INFORMATION

Kristin Legg: kristin_legg@nps.gov.

LITERATURE CITED

Bockino, N.K. 2015. Whitebark pine monitoring for the Greater Yellowstone Ecosystem: regeneration study 2009–2014 summary [unpublished report]. 44 p. Available from Greater Yellowstone Network, 2327 University Way, Suite 2, Bozeman, MT 59715.

Greater Yellowstone Coordinating Committee Whitebark Pine Subcommittee (GYCC WBPSC). 2011. Whitebark pine strategy for the Greater Yellowstone Area. Bozeman, MT: Greater Yellowstone Coordinating Committee. 45 p. http://www.fedgycc.org/wp-content/uploads/2015/06/WBPStrategyFINAL5.31.11.pdf. [Date accessed: February 28, 2015].

Greater Yellowstone Whitebark Pine Monitoring Working Group (GYWBPMWG). 2011. Interagency whitebark pine monitoring protocol for the Greater Yellowstone Ecosystem, version 1.1. 141 p. Bozeman, MT: Greater Yellowstone Coordinating Committee. http://science.nature.nps.gov/im/units/gryn/monitor/whitebark_pine.cfm. [Date accessed: February 28, 2015].

Greater Yellowstone Whitebark Pine Monitoring Working Group (GYWBPMWG). 2014. Summary of preliminary step-trend analysis from the Interagency Whitebark Pine Long-term Monitoring Program—2004–2013: prepared for the interagency grizzly bear study team. Natural Resource Data Series NPS/GRYN/NRDS–2014/600. Fort Collins, CO: National Park Service. http://science.nature.nps.gov/im/units/gryn/monitor/whitebark_pine.cfm. [Date accessed: February 28, 2015].

MacFarlane, W.W.; Logan, J.A.; Kern, W.R. 2013. An innovative aerial assessment of Greater Yellowstone Ecosystem mountain pine beetle-caused whitebark pine mortality. Ecological Applications. 23: 421–437.

Shanahan, E.; Irvine, K.M.; Roberts, D. [and others]. 2014. Status of whitebark pine in the Greater Yellowstone Ecosystem: a step-trend analysis comparing 2004–2007 to 2008–2011. Natural Resource Technical Report NPS/GRYN/NRTR–2014/917. Fort Collins, CO: National Park Service. http://science.nature.nps.gov/im/units/gryn/monitor/whitebark_pine.cfm. [Date accessed: February 28, 2015].

CHAPTER 14.

Impact of Bark Beetle Infestation on Fuel Loads and Fire Behavior in "Old-Stage" Southwestern Ponderosa Pine

(Project INT-EM-F-12-02)

E. Matthew Hansen
Morris C. Johnson
Barbara J. Bentz
James C. Vandygriff
A. Steven Munson

INTRODUCTION

Bark beetle (Coleoptera: Curculionidae, sf. Scolytinae) infestations modify fuels and, consequently, modeled fire behavior in conifer ecosystems of the Western United States (Hicke and others 2012, Jenkins and others 2014). Changes in fuels will vary with space and time since infestation, and impacts on fire behavior will be correspondingly complex (Simard and others 2011). Multiple studies have focused on quantifying fuels and modeled or observed fire behavior in currently infested (known as "red-stage" because killed trees still retain fading yellow-red needles) and recently infested (known as "gray-stage" because all needles have fallen, revealing the tree boles and branches) pine stands, particularly in lodgepole pine type (*Pinus contorta*). Less research has been conducted in "old-stage" stands (wherein beetle-killed trees have mostly fallen, the fallen needles have mostly decomposed, and advance regeneration forms ladder fuels), especially for relatively arid types such as ponderosa pine (*Pinus ponderosa*) (Hicke and others 2012).

Since 1995, we have monitored permanent plots in ponderosa pine type on the Colorado Plateau that experienced a bark beetle outbreak c. 1992–1996. Infested trees were killed by a suite of bark beetles including mountain pine beetle (*Dendroctonus ponderosae*), round-headed pine beetle (*D. adjunctus*), western pine beetle (*D. brevicomis*), larger Mexican pine beetle (*D. approximatus*), red turpentine beetle (*D. valens*), and pine engraver beetles (*Ips pini, I. knausi*). Data from these plots were originally used to analyze factors that influence the transition from endemic to epidemic beetle population phases and to parameterize a stand-level, bark beetle risk rating model (Chojnacky and others 2000). We remeasured these plots in 2012 and added planar intercept sampling to characterize surface fuels as a function of infestation severity. Fuel load data were used in a fire simulation model, the Fire and Fuels Extension of the Forest Vegetation Simulator (FFE-FVS) (Dixon 2002, Rebain 2010). Our objectives were to quantify the effects of infestation severity on fuels and modeled fire behavior in old-stage ponderosa pine (i.e., 15–20 years after infestation).

METHODS

Forty-five ponderosa pine-dominated sites with varying degrees of bark beetle-caused host mortality were identified during 1995–1996 in southern Utah, northern Arizona, and southwestern Colorado. At each site, we installed two parallel transects, each with 10 contiguous 405-m^2 circular plots. For each tree ≥ 7.6 cm diameter at breast height (d.b.h.), we measured species d.b.h., crown ratio, and Keen tree class (Keen 1943). A subset of trees was measured for age, total height, and crown base height. Year of attack was estimated for all bark beetle-infested stems, and beetle species were identified by egg gallery patterns and sizes (Chojnacky and others 2000). Trees < 7.6 cm d.b.h. were measured with a 13.5-m^2 plot centered on the overstory plot. Pre-outbreak stand conditions were estimated by recoding recently killed trees as live. We remeasured

these plots in 2012 and added planar intercept sampling to quantify surface fuel loads based on Fire Effects Monitoring and Inventory System (FIREMON) protocols (Lutes and others 2006) (fig. 14.1). This was done to 321 of the original 900 plots, randomly selected from 3 strata defined by beetle-infested basal area (BA) (0, 0.01–0.37, or > 0.37 m^2 $plot^{-1}$); these classes were chosen based on the distribution of killed BA among the plots. Planar intercept data were entered into FIREMON software to summarize surface fuel loads. These outputs, along with the over- and understory tree data, were used to create input files for FFE-FVS (Utah variant).

FVS is a growth and yield model (our simulations did not include tree growth) and FFE adds fuel dynamics and potential fire behavior. As with all U.S. operational fire models, FFE-FVS calculates surface fire behavior using the equations of Rothermel (1972) and Albini (1976), which consider factors such as slope, fuel loads, and environmental conditions. Based on Scott and Reinhardt's (2001) rules and using surface and aerial fuels, FFE-FVS output includes torching index (the 6.1 m wind speed predicted to initiate a crown fire) and crowning index (the 6.1 m wind speed predicted to sustain an active crown fire). Note that lower values of these indices indicate increased crown fire hazard. Predictions of fire type are based on an algorithm comparing the user-defined wind speed with the torching and crowning indices. There are four possible fire types: surface (crowns do not burn), passive (individual trees or groups of trees torch), conditional-crown (surface fire from an adjacent stand will continue as a surface fire or crown fire from an adjacent stand will continue as a crown fire), and active crown (fire moves through tree crowns, burning all crowns and killing all trees). For each plot, we modeled fire behavior with custom fuel models that represent the observed fuel loads and dynamic, FFE-selected fuel models that have

Figure 14.1—Measuring surface fuels with planar intercept sampling, Kaibab National Forest, Arizona, 2012. The fallen ponderosa pine snags were killed by Dendroctonus *bark beetles c. 1992–1996. (photo by Barbara J. Bentz, U.S. Department of Agriculture, Forest Service)*

been previously defined and calibrated. (Note: we only report results from custom models herein; results from dynamically selected models are comparable and are reported in Hansen and others 2015.) "Extreme" weather conditions, used to model fire type, were calculated from a centrally located fire weather station and represent the 90th percentile temperature and wind conditions and the 10th percentile fuel moisture conditions.

Statistical analyses were conducted using generalized linear mixed models (fuel loads and fire behavior parameters) and multinomial logistic regression models (categorical fire types) (see Hansen and others 2015 for full details including parameter value estimates). Explanatory variables were infested tree density (i.e., trees per ha) and BA from the c. 1992–1996 outbreak, and we report the best fitting for each response variable. Tested covariates included infestation severity (infested tree density or BA per ha) from intervals other than 1992–1996, elevation, slope, aspect, pre-outbreak stand conditions, and time since last fire. To produce figures 14.2–14.5, we used median dataset values of significant covariates. Changing the covariate values modifies the scale, but not the character, of the relationships between the response and explanatory values.

RESULTS AND DISCUSSION

Dendroctonus bark beetles generally infest larger diameter trees, leaving a residual live stand of smaller trees (Hansen 2014). These changes were reflected in our data, which showed significantly reduced live total BA, ponderosa pine BA, canopy cover, and ponderosa pine diameter as a function of infestation severity (infested tree density or BA; data not shown, but see Hansen and others 2015). The density of live trees ≥ 7.6 cm d.b.h. increased as a function of infestation severity. Presumably, advance regeneration measured in the original surveys grew into that size class by 2012, more than replacing the density of infested trees. Likewise, seedling density was positively related to infestation severity, suggesting successful recruitment into beetle-caused canopy gaps. Regarding fuels that support crown fires, the increase in ladder fuels (reflected by reduced canopy base heights) is countered by the beetle-caused decrease in canopy bulk density (fig. 14.2).

Similarly, fuel component loading showed different trends with increasing infestation severity. Litter depth and loads decreased with increasing infestation severity (fig. 14.3) (note that litter is a primary carrier of fire among many fuel models; Scott and Burgan 2005). This is because of the reduced live foliar biomass after bark beetle infestation, with commensurate reductions in litterfall. Moreover, sufficient time had lapsed since infestation that the pulse of fallen needles from killed trees had mostly decomposed. In contrast, fuel loads of woody materials increased as a function of infestation severity, especially among the largest diameter material (1000-hour fuels; i.e., ≥ 7.6 cm diameter) (fig. 14.3). This reflects snagfall of beetle-killed trees.

A fuels-relevant feature of bark beetle outbreaks is the degree of spatiotemporal variation in infestation. In red-stage stands, there might be 5 or more years' difference in timing of attack among killed trees. Thus, an infested red-stage stand will contain a mix of trees: uninfested, currently infested with green needles, recently infested with fading needles, and previously infested with fallen needles. Although this temporal variability is less important in old-stage stands, the role of spatial variability continues. That is, there is considerable variation in infestation severity among stands in an infested forest or landscape,

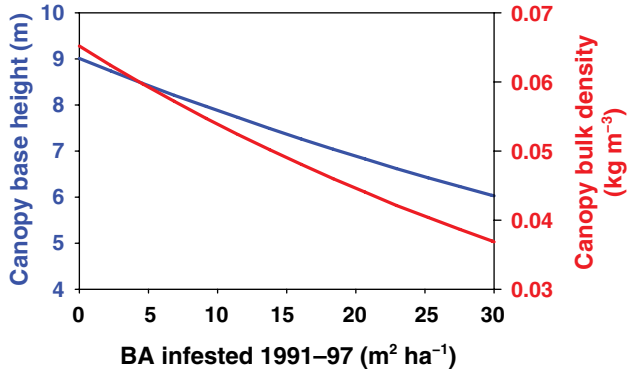

Figure 14.2—Canopy base height and canopy bulk density as a function of bark beetle infestation severity during an outbreak 15–20 years before measurements. Note: BA = basal area.

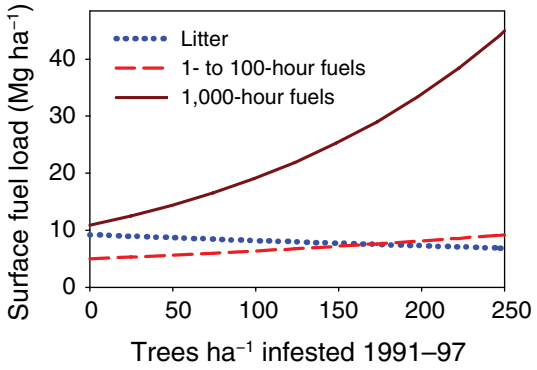

Figure 14.3—Surface fuels as a function of infestation severity 15–20 years after a bark beetle outbreak.

with few stands experiencing complete overstory mortality (Hansen 2014). This variation occurred even at the substand scale among our plots. For example, one of our sites averaged 133 infested pines per ha, but the plots within the site varied from 25 to 790 infested pines per ha.

From the FFE-FVS simulations, torching index was negatively related to infestation severity from the c. 1992–1996 outbreak (i.e., torching is more likely with increasing beetle severity; fig. 14.4). This result is related to the decreased canopy base heights resulting from post-outbreak seedling recruitment and release of advance regeneration. Conversely, crowning index was predicted to increase as a function of infestation severity (i.e., crown fire behavior is less likely with increasing beetle severity; fig. 14.4). This outcome is related to the reduced canopy bulk density after the beetle-caused deaths of the largest overstory trees. Moreover, the resulting canopy gaps decrease continuity in canopy fuels. Surface fire rate of spread was predicted to increase as a function of infestation severity (results not shown). Modeling by Page and Jenkins (2007) in lodgepole pine indicated that this behavior is mostly related to increased within-canopy wind speeds due to the loss of canopy sheltering; drying of surface fuels minimally affected rate of spread, and surface fuel loads had no effect.

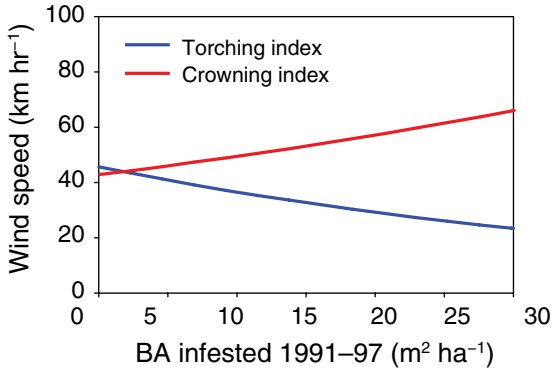

Figure 14.4—Torching and crowning indices (the 6.1 m wind speeds predicted to initiate and sustain a crown fire, respectively) as a function of infestation severity 15–20 years after a bark beetle outbreak. Lower values of these indices indicate higher crown fire hazard. Note: BA = basal area.

The net result of these beetle-related changes in fire behavior is captured by predictions of fire type as a function of infestation severity (fig. 14.5). Under the "extreme" fire weather conditions used in the simulations, surface fires are most probable in uninfested stands, whereas increasing infestation severity results in heightened probability of passive fires. The simulations predict that the probability of conditional or active crown fire in these old-stage ponderosa pine stands is low, under the simulated weather conditions, regardless of bark beetle infestation. Conceivably, active crown fires observed elsewhere in southwestern ponderosa pine have been affected by even higher wind speeds and lower fuel moistures.

These simulated fire behavior results should be interpreted cautiously. All operational fire models, including FFE-FVS, are limited by the underlying assumptions of the Rothermel (1972) and Van Wagner (1977) models. These assumptions are questionable even under ideal conditions (Cruz and Alexander 2010), and application of these models is further compromised when applied to spatially variable stands, such as from bark beetle infestation. Moreover, previous modeling applications in beetle-infested lodgepole pine have produced variable results, especially for red-stage stands where assumptions vary widely regarding the amounts and moisture levels of foliage on beetle-killed trees. Finally, 1,000-hour fuels are the fuel class most conspicuously affected in old-stage stands (fig. 14.3) and these fuels are not considered in the Rothermel and Van Wagner models. Although attempts to include these fuels in simulations of old-stage lodgepole pine resulted in predictions of greatly increased combustion energy (Page and Jenkins 2007, Schoennagel and others 2012), it is uncertain to what extent 1,000-hour fuels affect rate of spread or probability of active crown fire (Hansen and others 2015). Although flawed, operational models are the only practical

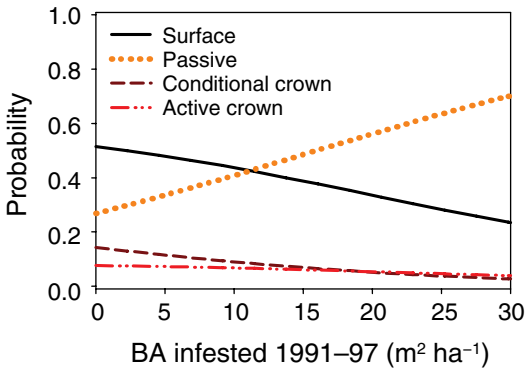

Figure 14.5—Fire type probabilities as a function of infestation severity 15–20 years after a bark beetle outbreak. These results were simulated using extreme weather conditions (i.e., 90th percentile temperature and wind speed and 10th percentile fuel moistures from a centrally located fire weather station). Note: BA = basal area.

method for assessing changes in fire behavior as a function of modifications to fuel profiles, even for research purposes. Researchers and managers are aware of model limitations and use the simulations to inform fuelbed changes on fire behavior. We advise the reader to consider relative, rather than absolute, differences in fire behavior as a function of infestation severity.

CONCLUSIONS

Stand structure and fuelbed conditions in old-stage ponderosa pine stands of the Colorado Plateau were modified by bark beetle infestation similar to previous descriptions for ponderosa and lodgepole pine (Hansen 2014, Hicke and others 2012, Hoffman and others 2012, Jenkins and others 2014). For example, quadratic mean diameter, BA, canopy bulk density, and canopy base heights were reduced following the loss of large-diameter host trees. Litter, a primary carrier of fire in many fuel models, was reduced in old-stage stands because of decreased litterfall and decomposition of fallen needles from killed trees. In contrast, woody fuels of all size classes increased after infestation, especially among the largest sizes.

These beetle-caused changes in ponderosa pine fuel profiles modified simulated fire behavior similar to previous descriptions for old-stage lodgepole pine (Hicke and others 2012, Page and Jenkins 2007, Simard and others 2011). The hazard of torching behavior increased in conjunction with lowered canopy base heights, but the hazard of active crown fire decreased in conjunction with reduced canopy fuels. Thus, increasing infestation severity resulted in heightened probability of passive fire (torching of individual crowns or groups of crowns) concomitant with reduced probability of surface fire. These results are partially supported by modeling, using the NEXUS model, in gray-stage ponderosa pine stands of Arizona (Hoffman and others 2012). In that case, decreased canopy fuels similarly increased predicted crowning indices. Unlike our study, however, canopy base heights were also increased in infested stands, resulting in increased torching indices. This difference reflects the insufficient stand developmental time, in the case of Hoffman and others, for recruitment of new seedlings and release of advance regeneration.

Our simulations indicated that active crown fires are not probable, using the extreme weather conditions simulated, in these stands regardless of infestation severity. It is possible that even more extreme weather conditions would shift this outcome, but we see no evidence that bark beetle history will affect the probability of active or conditional-crown fires given current stand conditions (fig. 14.5). Moreover, spatial variability in beetle-caused tree mortality will result in diminished beetle-driven effects on fire behavior at increasing spatial scales.

CONTACT INFORMATION

Matt Hansen: matthansen@fs.fed.us.

LITERATURE CITED

Albini, F.A. 1976. Estimating wildfire behavior and effects. Gen. Tech. Rep. INT-GTR-30. Ogden, UT: U.S. Department of Agriculture, Forest Service, Intermountain Research Station. 92 p.

Chojnacky, D.C.; Bentz, B.J.; Logan, J.A. 2000. Mountain pine beetle attack in ponderosa pine: comparing methods for rating susceptibility. Rep. RMRS-RP-26. Fort Collins, CO: U.S. Department of Agriculture, Forest Service, Rocky Mountain Research Station. 10 p.

Cruz, M.G.; Alexander, M.E. 2010. Assessing crown fire potential in coniferous forests of western North America: a critique of current approaches and recent simulation studies. International Journal of Wildland Fire. 19: 377–398.

Dixon, G.E. 2002. Essential FVS: A user's guide to the Forest Vegetation Simulator. 248 p. www.fs.fed.us/rm/pubs/rmrs_gtr292/2002_dixon.pdf. [Date accessed: January 6 2015].

Hansen, E.M. 2014. Forest development and carbon dynamics following mountain pine beetle outbreaks. Forest Science. 60(3): 476–488.

Hansen, E.M.; Johnson, M.C.; Bentz, B.J. [and others]. 2015. Fuel loads and simulated fire behavior in "old-stage" beetle-infested ponderosa pine of the Colorado Plateau. Forest Science. 61(4): 644–664.

Hicke, J.A.; Johnson, M.C.; Hayes, J.L.; Preisler, H.K. 2012. Effects of bark beetle-caused tree mortality on wildfire. Forest Ecology and Management. 271: 81–90.

Hoffman, C.M.; McMillin, J.D.; Sieg, C.H.; Fulé, P.Z. 2012. Influence of bark beetle-caused mortality on fuel loadings and crown fire hazard in southwestern ponderosa pine stands. In: Potter, K.M.; Conkling, B.L., eds. Gen. Tech. Rep. SRS-167. Forest Health Monitoring: 2009 national technical report. Asheville, NC: U.S. Department of Agriculture, Forest Service, Southern Research Station: 241–246.

Jenkins, M.J.; Runyon, J.B.; Fettig, C.J. [and others]. 2014. Interactions among the mountain pine beetle, fires, and fuels. Forest Science. 60(3): 489–501.

Keen, F.P. 1943. Ponderosa pine tree classes redefined. Journal of Forestry. 41(4): 249–253.

Lutes, D.C.; Keane, R.E.; Caratti, J.F. [and others]. 2006. FIREMON: The fire effects monitoring and inventory system [CD-ROM]. Gen. Tech. Rep. RMRS-GTR-164-CD. Fort Collins, CO: U.S. Department of Agriculture, Forest Service, Rocky Mountain Research Station. 1 CD.

Page, W.G.; Jenkins, M.J. 2007. Predicted fire behavior in selected mountain pine beetle infested lodgepole pine. Forest Science. 53: 662–674.

Rebain, S.A., comp. 2010. The fire and fuels extension to the forest vegetation simulator: updated model documentation. USDA For. Serv. Int. Rep. 409 p. Revised 2013. www.fs.fed.us/fmsc/ftp/fvs/docs/gtr/FFEguide.pdf. [Date accessed: April 17, 2014].

Rothermel, R.C. 1972. A mathematical model for predicting fire spread in wildland fuels. Res. Pap. INT-RP-115. Ogden, UT: U.S. Department of Agriculture, Forest Service, Intermountain Research Station. 40 p.

Schoennagel, T.; Veblen, T.T.; Negrón, J.F.; Smith, J.M. 2012. Effects of mountain pine beetle on fuels and expected fire behavior in lodgepole pine forests, Colorado, USA. PloS One. 7(1): e30002. doi:10.1371/journal.pone.0030002. [Published online: January 17, 2012].

Scott, J.H.; Burgan, R.E. 2005. Standard fire behavior fuel models: a comprehensive set for use with Rothermel's surface fire spread model. Gen. Tech. Rep. RMRS-GTR-153. Fort Collins, CO: U.S. Department of Agriculture, Forest Service, Rocky Mountain Research Station. 72 p.

Scott, J.; Reinhardt, E.D. 2001. Assessing crown fire potential by linking models of surface and crown fire behavior. Res. Paper RMRS-RP-29. Fort Collins, CO: U.S. Department of Agriculture, Forest Service, Rocky Mountain Research Station. 59 p.

Simard, M.; Romme, W.H.; Griffin, J.M.; Turner, M.G. 2011. Do mountain pine beetle outbreaks change the probability of active crown fire in lodgepole pine forests? Ecological Monographs. 81: 3–24.

Van Wagner, C.E. 1977. Conditions for the start and spread of crown fire. Canadian Journal of Forest Research. 7: 23–34.

CHAPTER 15.

Monitoring Mountain Pine Beetle Life Cycle Timing and Phloem Temperatures at Multiple Elevations and Latitudes in California

(Project WC-EM-09-02)

Barbara Bentz
James Vandygriff
Camille Jensen
Tom Coleman
Patricia Maloney
Sheri Smith
Amanda Grady
Greta Schen-Langenheim

INTRODUCTION

The mountain pine beetle (MPB) (*Dendroctonus ponderosae* Hopkins, Coleoptera: Curculionidae, Scolytinae), a native of western North America, mainly infests and reproduces in live trees within the genus *Pinus,* and successful offspring production often results in the death of the host tree. The range of MPB is expansive, spanning from Baja California Norte, Mexico, to northern British Columbia (BC) and western Alberta, Canada, yet suitable pine hosts extend beyond the current northern and southern geographical extent (Bentz and others 2010, Safranyik and others 2010). Mountain pine beetle has been at outbreak levels across parts of western North America over the past 2 decades. Ongoing changes in climatic conditions are hypothesized to be driving a northward expansion of MPB in northern BC and Alberta, Canada (Safranyik and others 2010) and contributing to sustained population outbreaks in high elevation forests where persistent activity was previously constrained by cold temperatures (Amman 1973). Increasing minimum temperatures increase brood survival (Régnière and Bentz 2007, Weed and others 2015), and at high elevations increasing summer temperatures allow some individuals to shift from one generation every two years to one generation every year (Bentz and others 2014). It is clear that in addition to susceptible stand conditions and drought (Chapman and others 2012), warmer temperatures are influencing MPB.

Mountain pine beetle life cycle timing has historically been reported as univoltine (i.e., one generation per year) at low elevations with a mix of univoltine and semivoltine (i.e., one generation every 2 years) at high elevations (Amman 1973, Reid 1962). The capacity for MPB to complete two generations in a single year (i.e., bivoltinism) is unclear. Bivoltinism was reported to have occurred in California and Oregon (Evenden and others 1943, Furniss and Carolin 1977) and speculated to occur with warming temperatures at 3000 m in Colorado (Mitton and Ferrenberg 2012). Bentz and Powell (2014), however, suggest that bivoltinism across the current range of MPB is constrained by a lack of sufficient thermal energy and evolved developmental thresholds that ensure overwintering success.

Little information is available on MPB life cycle timing in California. To predict future MPB response to changing climatic conditions, baseline information is needed. Our objectives were (1) to develop a baseline database of MPB life cycle timing and associated phloem temperatures in several host trees at multiple elevations and latitudes across California (CA) and (2) using the field-collected data, to evaluate a current MPB phenology model in areas other than where model parameters were derived. This information will provide a reference for evaluating potential future population response to changing climate and help identify areas with high probability of climate-induced shifts in population success and where management

interventions may be most effective. Here, we provide a brief description of our methods and highlight results from the project. A more complete description of data collected and results can be found in Bentz and others (2014).

METHODS

Mountain pine beetle adults emerge from trees and fly to attack new live trees where mating and oviposition occur, and new brood will develop within the phloem throughout the next 1 to 2 years. The timing of emergence and flight is dependent on temperature and typically occurs in the summer months. For our study, we define a brood to be a group of individuals that develop from eggs laid by parents that attacked trees in the same season. The length of time for brood to develop and emerge from a tree is considered a generation. We classified brood that emerged from a tree the summer following parent attacks as univoltine and the brood that required 2 years to complete a generation as semivoltine. To be considered a bivoltine brood, two complete generations must occur within 1 year.

Data from six sites were included in this study (fig. 15.1). At each site, data were collected for a period of 1 to 3 years, including two MPB generations and associated phloem and air temperatures (table 15.1). Prior to MPB flight, three to five live trees were selected at each site

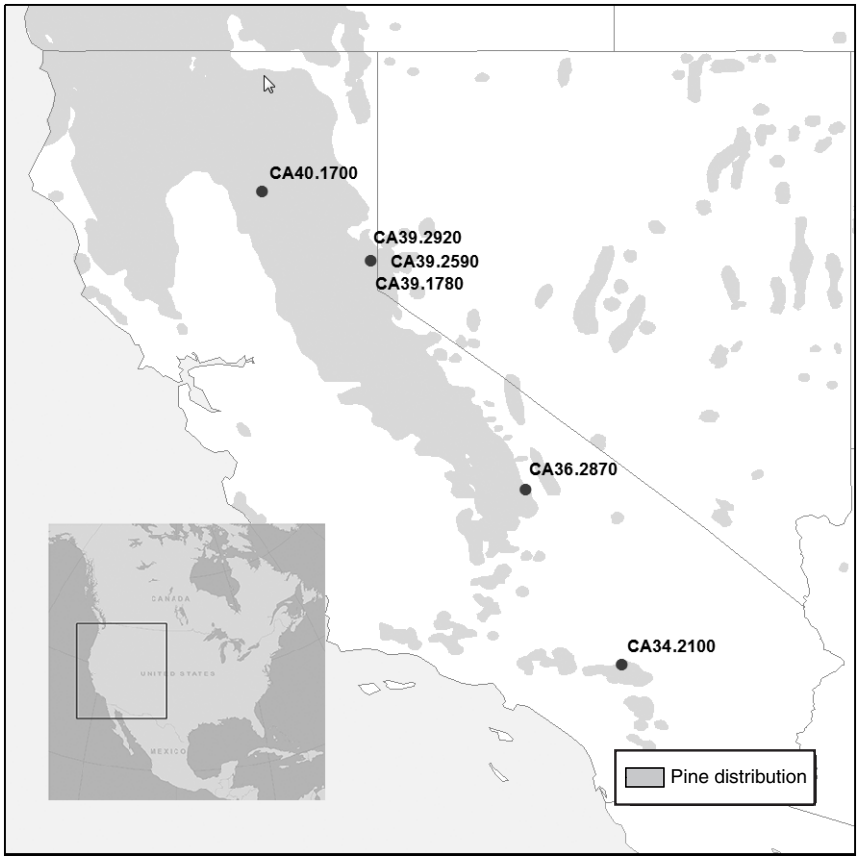

Figure 15.1—Map of study sites in the Western United States. Also shown is the distribution (Little 1971) of major pine host species for mountain pine beetle (i.e., Pinus albicaulis, P. contorta, P. flexilis, P. lambertiana, P. monticola, *and* P. ponderosa*). Three sites were installed along an elevational gradient at CA39, shown here as a single point. See table 15.1 for site information.*

Table 15.1—Study site location in California, years the site was sampled, mountain pine beetle population phase, and *Pinus* host tree species

Forest	Site name	Years	Population phase	DBH (mean ± SD)	Latitude	Longitude	Elevation	Host tree species
							m	
Lassen	CA40.1700-09	2009–10	Endemic	50.55 ± 6.4	40.2238	-121.4331	1700	*P. lambertiana*
Lassen	CA40.1700-10	2010–11	Endemic	39.37 ± 8.6	40.2103	-121.4341	1700	*P. lambertiana*
Tahoe	CA39.1780-09	2009–10	Endemic	33.27 ± 5.3	39.3926	-120.1841	1780	*P. contorta*
Tahoe	CA39.1780-10	2010–11	Endemic	33.78 ± 6.1	39.3922	-120.1863	1780	*P. contorta*
Lake Tahoe Basin Management Unit	CA39.2590-09	2009–11	Endemic	46.74 ± 8.1	39.2984	-119.9330	2590	*P. monticola* *P. contorta*
Lake Tahoe Basin Management Unit	CA39.2590-10	2010–12	Endemic	44.96 ± 4.6	39.2998	-119.9310	2590	*P. monticola* *P. contorta*
Lake Tahoe Basin Management Unit	CA39.2920-09	2009–12	Endemic	33.53 ± 2.8	39.3218	-119.9390	2920	*P. albicaulis*
Lake Tahoe Basin Management Unit	CA39.2920-10	2010–12	Endemic	39.12 ± 3.1	39.3217	-119.9386	2920	*P. albicaulis* *P. contorta*
Inyo	CA36.2870-09	2009–10	Endemic	43.43 ± 18.5	36.4693	-118.1252	2870	*P. flexilis*
Inyo	CA36.2870-10	2010–11	Endemic	47.24 ± 19.6	36.4695	-118.1253	2870	*P. flexilis*
San Bernardino	CA34.2100-09	2009–10	Endemic	50.89, 46.2	34.2653	-116.9089	2100	*P. monophylla*
San Bernardino	CA34.2100-10	2010–11	Endemic	33.27	34.2635	-116.9087	2100	*P. monophylla*

Note: site names are a combination of the State abbreviation, approximate latitude, elevation (m), and parent attack year and are arranged by latitude with the most northerly sites at the top. Also shown is the mean (± SD) d.b.h. (diameter at breast height) of trees sampled at each site.

based on tree size (> 20.2 cm diameter at breast height, or d.b.h.). To ensure MPB attacks, an aggregation lure [(S) *trans*-verbenol and racemic *exo*-brevicomin, Synergy Semiochemicals Corp., Burnaby, BC, Canada] was placed on each live tree when MPB flight activity was observed in the area (based on pheromone traps and emergence cages in the vicinity). Aggregation lures were removed once attacks were initiated on each tree to allow the natural attack process to continue. Beetle attacks were monitored twice weekly on the entire circumference of each tree bole from 0.305 m to 1.524 m above ground until attacks ceased. Attacks were not monitored at the CA36.2870 site. After the entire circumference of each tree bole was successfully mass attacked, based on the total number of attacks, emergence cages were installed at 1.4 m above the ground on the north and south bole aspects. A centrifuge tube attached to the bottom of the enclosure collected all beetles emerging from under the bark within each cage. Adult MPB emergence into cages was monitored twice weekly at each site. The date of median attack and median emergence among all trees at a site was calculated.

We used the field collected data to evaluate a mechanistic MPB phenology model. The model was originally parameterized using lab-derived data on lifestage-specific development times at a range of constant temperatures (Bentz and others 1991, Powell and Bentz 2014, Régnière and others 2012). Populations from central Idaho and northern Utah were used in model parameterization. The model predicts lifestage-specific development timing, including adult emergence, given hourly temperatures and an input distribution of attacks. To evaluate how well the model predicts adult emergence in CA, we initiated model runs with the observed number of attacks on a single tree. Observed hourly phloem temperatures from that same tree, on the north and south bole aspects, were used to drive the model. Predicted emergence of adults was then graphically compared to field-observed emergence.

RESULTS

Life cycle timing and air temperature varied among sites and among years at the same site (figs. 15.2 and 15.3). A strictly univoltine life cycle was observed both years at two sites (CA40.1700, CA39.1780). At CA36.2870, we were unable to monitor attacks, although the emergence timing suggested univoltinism. At the highest elevation sites (CA39.2920, CA39.2590), we observed a mixture of univoltine and semivoltine brood (often within the same tree). At the warmest site, CA34.2100-09, some brood adults emerged from a single tree (T2) the fall following attacks earlier that summer (faster than univoltine). Median attacks on a second tree (T5) at that site coincided with emergence from T2, and peak brood adult emergence from this tree was on July 24, 2010. To be classified as bivoltine, brood from attacks made in the fall 2009 would need to have completed development and emerged

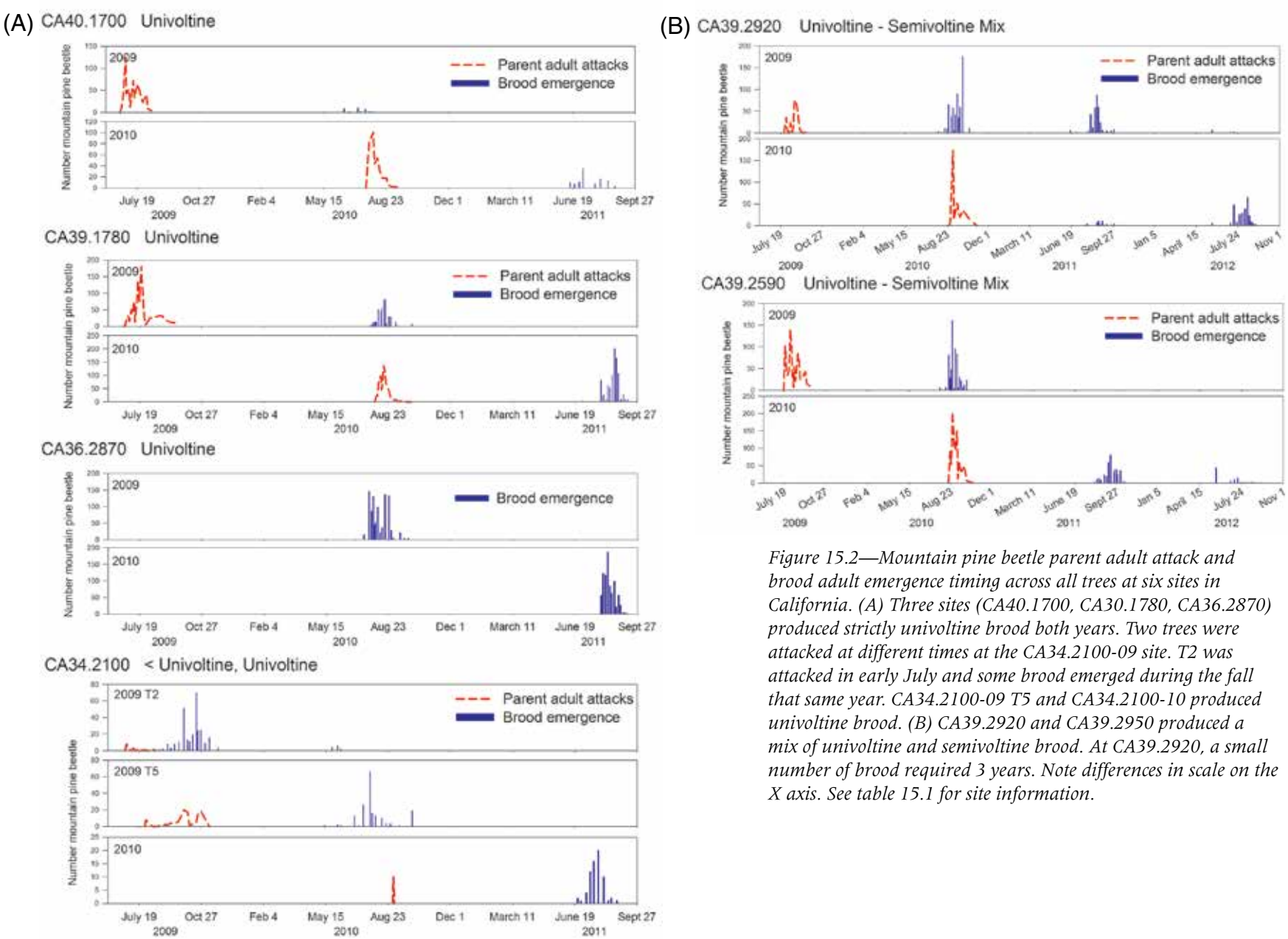

Figure 15.2—Mountain pine beetle parent adult attack and brood adult emergence timing across all trees at six sites in California. (A) Three sites (CA40.1700, CA30.1780, CA36.2870) produced strictly univoltine brood both years. Two trees were attacked at different times at the CA34.2100-09 site. T2 was attacked in early July and some brood emerged during the fall that same year. CA34.2100-09 T5 and CA34.2100-10 produced univoltine brood. (B) CA39.2920 and CA39.2950 produced a mix of univoltine and semivoltine brood. At CA39.2920, a small number of brood required 3 years. Note differences in scale on the X axis. See table 15.1 for site information.

by June 2010 (i.e., two complete generations in a single year). This did not happen. The next generation at CA34.2100 was initiated from attacks that occurred in July and August 2010, and brood from these attacks emerged in July 2011, a strictly univoltine life cycle. Therefore, the CA34.2100 site produced three generations in 2 years, a fractional voltinism faster than strict univoltinism, but not bivoltinism (fig. 15.2). The opposite extreme was the highest elevation site, CA39.2920, where 1.1 percent of offspring from attacks in 2009 emerged in 2012, a life cycle that required 3 years to complete (fig. 15.2).

With the exception of the summer generation at the most southern site and the mostly semivoltine generation at the highest elevation site, generation time (number of days between median attack and median emergence) across sites and years was between 300 and 400 days (fig. 15.4, table 15.2). The thermal energy required to complete a generation, however, varied between 86 and 447 degree days (DD) >15 °C (table 15.2). The site with the shortest generation time (110 days) accumulated the greatest thermal heat during the generation (484 DD), and the site with the longest generation time (695 days) accumulated the smallest thermal heat over the generation (74.6 DD) (fig. 15.4).

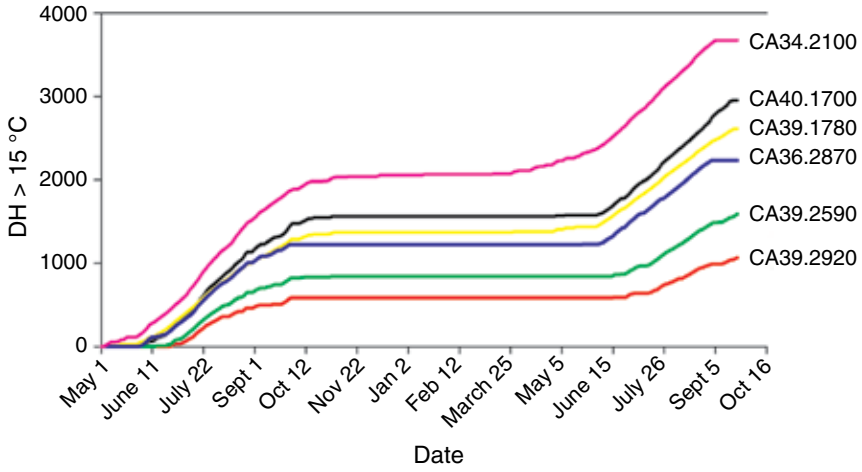

Figure 15.3—Cumulative degree hours (DH) > 15 °C (based on air temperature) accumulated between May 1 and September 30 the year following 2009 attacks at each site. See table 15.1 for site information.

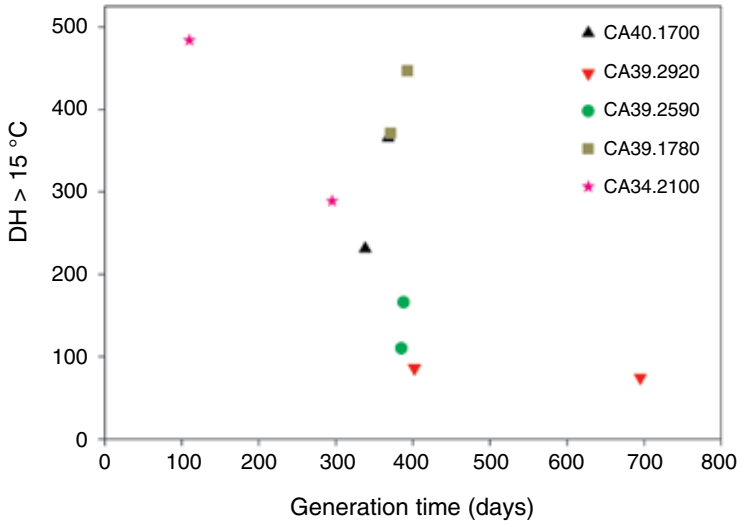

Figure 15.4—Generation time (number of days between median attack and median emergence) of mountain pine beetle at five California sites and the degree days (DD) > 15 °C required to complete a generation at each site. Generation time and air temperature were monitored for two beetle generations at each site. See table 15.1 for site information.

Table 15.2—Proportion brood that emerged in 1 year (univoltine) and the associated total number of brood adults sampled from cages at each site (N)

Site	Proportion univoltine (N)	Generation time	DD >15 °C	Average air temp.	Average July–Aug. max. air temp.	Average Dec.–Jan. min. air temp.
		days		----------*°C*----------		
CA40.1700-09	100 (32)	368	365.95	5.9	25.2	-3.9
CA40.1700-10	100 (101)	338	231.37	6.2	24.0	-2.8
CA39.2920-09[a]	64.2[b] (944)	402	86.27	1.3	16.8	-8.4
CA39.2920-10[a]	13.8 (319)	695	74.59	1.2	16.3	-7.1
CA39.2590-09	100 (616)	388	166.20	3.3	21.3	-6.6
CA39.2590-10[a]	71.5 (884)	385	110.16	2.4	19.1	-6.2
CA39.1780-09	100 (454)	393	447.00	5.0	25.8	-8.7
CA39.1780-09	100 (863)	371	371.32	4.5	26.2	-8.1
CA36.2870-09	100 (968)	–	–	4.4	20.6	-7.5
CA36.2870-10	100 (839)	–	–	4.6	20.5	-5.7
CA34.2100-09 T2	4.0[c] (170)	110	484.16	8.8	27.0	-3.8
CA34.2100-09 T5	100 (176)	295	288.75	8.8	27.0	-3.8
CA34.2100-10	100 (69)	–	–	8.1	25.7	-3.7

– = timing of the attacks on the trees was not recorded, so generation time and DD were therefore not quantifiable.

[a] Remainder of brood emerged > 1 year following attacks.

[b] 1.1 percent emerged in 3 years.

[c] Remainder of brood emerged < 1 year following attacks.

Note: Sites are arranged with the most northerly at the top (see table 15.1 for site information). Generation time (days) is the number of days between median attack and median emergence at each site, information available for a portion of the sites. DD >15 °C is the accumulated degree days warmer than 15 °C between median attack and median emergence. Average annual temperature, average daily maximum air temperature in July and August, and average daily minimum air temperature in December and January were calculated using sensors located at each site.

Median predicted univoltine MPB emergence at the CA39.1780-09 site was within a few days of observed emergence (fig. 15.5A). Similar results were observed for emergence of univoltine beetles at the CA39.2920-09, although predicted median emergence timing of semivoltine beetles the following year at the same site was 20–30 days slower than observed (fig. 15.5B and 15.5C). Model-predicted MPB emergence timing was substantially faster than observed in a tree at the warmest and most southern site (CA34.2100-09 T2) that produced a generation of beetles between June and November of the same year (fig. 15.5D).

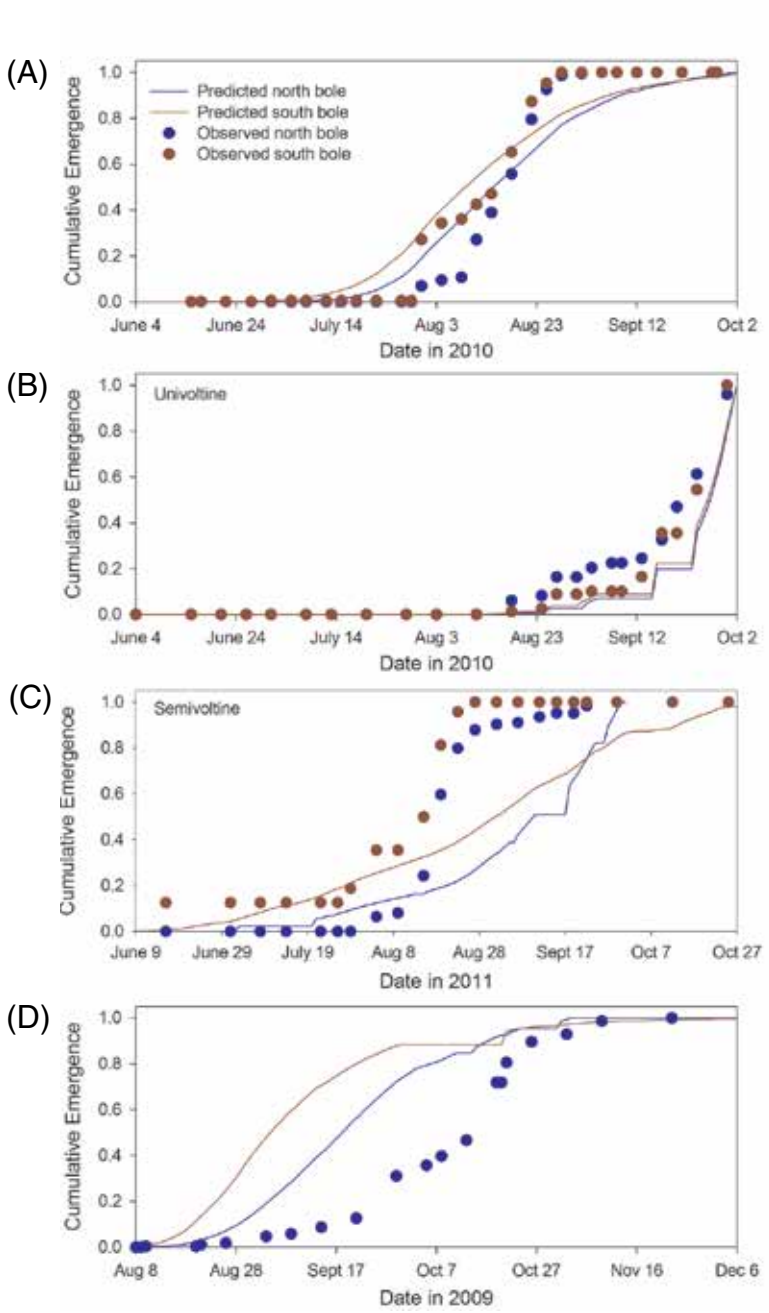

Figure 15.5—Model-predicted and observed mountain pine beetle emergence from the north and south bole aspect of a single tree at three sites: (A) CA39.1780-09, (B) CA39.2920-09 univoltine, (C) CA39.2920-09 semivoltine, and (D) CA34.2100-09 T2. Emergence predictions were generated from a MPB phenology model using hourly phloem temperatures measured in the field for each beetle generation.

DISCUSSION

Our results show that MPB lifecycle timing in California is univoltine at warmer sites and a mix of univoltine and semivoltine at cooler sites, similar to findings in other parts of the range of MPB (Amman 1973, Bentz and others 2014, Reid 1962). The DD >15 °C required to complete a generation varied considerably. The cooler the site, the fewer thermal units were needed for completion of a generation regardless of the number of days (figs. 15.3 and 15.4). In fact, the site with the shortest generation time accumulated more than six times the thermal heat of the site with the longest generation time. Despite this, we did not observe bivoltinism at the warmest site, which was also at the most southern location. Although a generation was completed in a single summer (i.e., between June and October) at the most southern site, the thermal energy and timing of that energy were not sufficient to complete a second generation across winter (i.e., between October and June). Adult emergence the second summer did not occur until July, potentially shifting the population to a univoltine lifecycle the next year (i.e., July to July).

One explanation for this pattern is the different thermal thresholds and rates of development among lifestages that serve to maintain seasonality. A high threshold for pupation (15–17 °C) has evolved in MPB to enable adult emergence synchrony and to reduce the likelihood that cold-sensitive lifestages (i.e., eggs and pupae) will be present during winter (Logan and Bentz 1999, Régnière and others 2012). These thresholds also play an important role in univoltinism, a trait important to population success. Results from this project suggest that the evolved adaptations that promote univoltinism and emergence synchrony allow populations in cool environments to efficiently use available thermal energy and provide flexibility to shift from semivoltine to univoltine cycles in warm years. In contrast, at the warmest sites excess thermal units beyond what is needed by specific lifestages are acquired and the use of thermal energy is therefore less efficient. The adaptations have served to maintain univoltinism at both warm and cold sites but may also constrain a shift to bivoltinism (Bentz and Powell 2014). The amount and seasonality of thermal energy required to surpass this constraint is currently unclear.

The MPB phenology model can provide predictions of thermal regimes under various future climate conditions that will be advantageous for MPB population success based on predicted emergence timing (Bentz and others 2010). When combined with a demographic model (Powell and Bentz 2009, 2014), population growth under multiple future climate conditions can also be predicted. Because of genetic differences in MPB temperature response across the Western United States (Bentz and others 2011), however, it is unclear where the model, which was parameterized using populations from central Idaho and northern Utah, can be used. Field collected data from this project were ideal for evaluating the model at sites in California. We initiated the MPB phenology with observed tree attack

information in one year, used observed hourly phloem temperature measurements to drive the model, and then compared model predictions of adult emergence 1 and 2 years later with observed emergence from field plots. Model predictions of median MPB adult emergence 1 year later were within a few days of observed emergence at univoltine sites in central and northern CA. Although the model accurately predicted that semivoltine brood emergence would occur, predicted timing was slightly less accurate than for univoltine brood. A majority of brood emerging the second year of attack could have overwintered as a brood adult (Bentz and others 2014), and the model did not adequately capture emergence timing of these overwintered adults. Model predictions of the timing of brood emergence from a tree in southern California, where a generation was completed in a single summer, were earlier than what was observed in the field. This result, however, was anticipated. In common garden laboratory experiments, MPB from southern populations required significantly more days to complete a generation at a constant temperature compared to a population from a northern population reared at the same constant temperature, implying genetic differences among populations along a latitudinal cline (Bentz and others 2011). Our results suggest the MPB phenology model best predicts temperature-dependent traits of MPB in central and northern California, compared to southern California.

CONCLUSIONS

MPB lifecycle timing in CA is univoltine at warmer sites and a mix of univoltine and semivoltine at cooler sites. Due to nonlinearities in thermal thresholds among lifestages, degree days did not adequately explain MPB lifecycle timing. Instead, a mechanistic model that inherently includes these nonlinearities provides an enhanced tool for predicting MPB phenology and ultimately population success. Based on preliminary runs using field-collected temperature and lifecycle timing data, the current MPB phenology model can be used to predict thermal regimes advantageous for MPB from central to northern California. New laboratory data and model parameters that describe MPB response to temperature in southern populations are needed. Warming temperatures are influencing range expansion in Canada into habitats previously too cool for MPB. A model parameterized for southern populations would provide a tool for evaluating thermal regimes with a high probability of climate-induced shifts in population success and potential MPB range expansion into habitats in the Southwest United States and Mexico that are currently too warm.

CONTACT INFORMATION

Barbara Bentz: bbentz@fs.fed.us.

LITERATURE CITED

Amman, G.D. 1973. Population changes of the mountain pine beetle in relation to elevation. Environmental Entomology. 2(4): 541–547.

Bentz B.J.; Bracewell, R.B.; Mock, K.E.; Pfrender, M.E. 2011. Genetic architecture and phenotypic plasticity of thermally-regulated traits in an eruptive species, *Dendroctonus ponderosae*. Evolutionary Ecology. 25(6): 1269–1288.

Bentz B.J.; Logan, J.A.; Amman, G.D. 1991. Temperature-dependent development of the mountain pine beetle (Coleoptera, Scolytidae) and simulation of its phenology. Canadian Entomologist. 123(5): 1083–1094.

Bentz, B.J.; Powell, J.A. 2014. Mountain pine beetle seasonal timing and constraints to bivoltinism: a comment on Mitton and Ferrenberg (2012). American Naturalist. 184(6): 787–796.

Bentz, B.J.; Régnière, J.; Fettig, C.J. [and others]. 2010. Climate change and bark beetles of the Western US and Canada: Direct and indirect effects. BioScience. 60: 602–613.

Bentz, B.J.; Vandygriff, J.C.; Jensen, C. [and others]. 2014. Mountain pine beetle voltinism and life history characteristics across latitudinal and elevational gradients in the Western United States. Forest Science. 60(3): 434–449.

Chapman, T.B.; Veblen, T.T.; Schoennagel, T. 2012. Spatiotemporal patterns of mountain pine beetle activity in the southern Rocky Mountains. Ecology. 93: 2175–2185.

Evenden, J.C.; Bedard, W.D.; Struble, G.R. 1943. The mountain pine beetle, an important enemy of western pines. Circular 664. Washington, DC: U.S. Department of Agriculture. 25 p.

Furniss, R.L.; Carolin, V.M. 1977. Western forest insects. Misc. Publ. 1339. Washington, DC: U.S. Department of Agriculture, Forest Service. 654 p.

Little, E. L. 1971. Atlas of United States trees. Volume 1. Conifers and Important Hardwoods. Misc. Publ. 1146. Washington, DC: U.S. Department of Agriculture. 9 p., 200 maps.

Logan, J.A.; Bentz, B.J. 1999. Model analysis of mountain pine beetle (Coleoptera: Scolytidae) seasonality. Environmental Entomology. 28: 924–934.

Mitton, J.B.; Ferrenberg, S.M. 2012. Mountain pine beetle develops an unprecedented summer generation in response to climate warming. American Naturalist. 179: E163–E171.

Powell, J.A.; Bentz, B.J. 2009. Connecting phenological predictions with population growth rates for mountain pine beetle, an outbreak insect. Landscape Ecology. 24: 657–672.

Powell, J.A.; Bentz, B.J. 2014. Phenology and density-dependent dispersal predict patterns of mountain pine beetle (*Dendroctonus ponderosae*) impact. Ecological Modelling. 273: 173–185.

Régnière, J.; Bentz, B. 2007. Modeling cold tolerance in the mountain pine beetle, *Dendroctonus ponderosae*. Journal of Insect Physiology. 53: 559–572.

Régnière, J.; Powell, J.; Bentz, B.; Nealis, V. 2012. Effects of temperature on development, survival and reproduction of insects: experimental design, data analysis and modeling. Journal of Insect Physiology. 58: 634–647.

Reid, R. 1962. Biology of the mountain pine beetle, *Dendroctonus monticolae* Hopkins, in the east Kootenay region of British Columbia I. life cycle, brood development, and flight periods. Canadian Entomologist. 94: 531–538.

Safranyik, L.; Carroll, A.; Régnière, J. [and others]. 2010. Potential for range expansion of mountain pine beetle into the boreal forest of North America. Canadian Entomologist. 142: 415–442.

Weed, A.S.; Bentz, B.J.; Ayres, M.P; Holmes, T.P. 2015. Geographically variable response of *Dendroctonus ponderosae* to winter warming in the Western United States. Landscape Ecology. 30: 1075–1093.

CHAPTER 16.

Monitoring Plots to Evaluate Spread Characteristics, Stand/Site Attributes, Management, and Disturbance Relationships of Black Stain Root Disease in Douglas-fir Plantations in Northern California

(Project WC-EM-B-14-03)

Vinci D. Keeler
Peter A. Angwin
Todd J. Drake
Roger L. Siemers

INTRODUCTION

Black stain root disease, caused by the vascular wilt pathogen *Leptographium wageneri*, is widely distributed in Douglas-fir (*Pseudotsuga menziesii*) on substantial acreages throughout the forests of northern California and western Oregon. As a vascular wilt pathogen, *Leptographium wageneri* kills its hosts by growing within and plugging up the water-conductive tissues of the xylem (Hessburg and others 1995). Symptoms of the disease include the presence of individual or small groups of dead and declining trees with sparse chlorotic crowns, reduced growth, and heavy stress cone crops (fig. 16.1). Basal resinosis is another common symptom. The most common diagnostic sign of the disease is a dark brown to purple-black stain in the sapwood of infected roots and lower stems (fig. 16.2).

Although black stain root disease is the most prevalent forest disease of Douglas-fir in northern California (Dale 1995, USDA Forest Service 1994), data on the spread and intensification of the disease are currently lacking. The disease is a management concern not only in commercial second-growth plantations and forests but also on lands that have been designated as late successional reserves (LSRs) under the President's Northwest Forest Plan. Douglas-fir plantations on the Happy Camp Ranger District of the Klamath National Forest provide a representation of the disease situation in many areas of the region. In a 1993 black stain root disease detection survey performed throughout the district, 156 of 1,151 surveyed stands were found to contain infection centers. In 1996, 30 of these stands were randomly selected for intensive survey through the installation of transects and permanent monitoring plots. The transects and plots were remeasured in 2000–2001. In 2012, plans were initiated to commercially thin several of the stands. Because this provides an excellent opportunity to track and compare the distribution and impacts of black stain root disease in thinned and unthinned stands, a new project was initiated to collect

Figure 16.1—Dead and dying Douglas-fir with black stain root disease. (photo by Pete Angwin, U.S. Department of Agriculture, Forest Service)

Figure 16.2—Dark sapwood stain associated with black root disease. (photo by Pete Angwin, U.S. Department of Agriculture, Forest Service)

pre-treatment baseline data to track and compare these impacts. Objectives of the study were to (1) continue the establishment and remeasurement of transects and permanent plots to track black stain root disease incidence and impacts on the Happy Camp Ranger District of the Klamath National Forest, and (2) provide pre-thinning baseline data for a comparison of how management and site disturbance affects the incidence and impacts of black stain root disease in Douglas-fir plantations in northern California.

METHODS

In 2013 and 2014, transects and monitoring plots in the 30 previously surveyed stands were remeasured and remonumented. Three of these stands are due to be thinned. Thinning will be done to a 30- to 35-foot spacing with a feller-buncher and rubber-tired skidder, leaving approximately 60 trees per acre. Remonumenting was done by taking GPS readings of all transect end points, infection centers, and plots, from which GIS maps were constructed. In 2014, a new paired plot survey was initiated to enable a more detailed analysis of the influence of this practice on the spread rate of the disease. For this paired plot survey, new, larger plots were established in pairs in 14 stands that are due to be thinned. Because only three of the previously surveyed stands are due to be thinned, paired plots were established in 11 additional new stands that will be thinned. These stands were identified as infested in the 1993 black stain root disease detection survey but had not been surveyed further. Because the stands lacked transects and smaller monitoring plots, however, installation of these was initiated in 2014 so that none of the thinned stands would lack the full complement of monitoring plots. Fires on the Klamath National Forest interrupted the installation of these plots, leaving four stands to be completed. This portion of the project will be completed in 2015.

The installation of plots in 11 new stands expands the monitoring network to 41 stands, 14 of which will be thinned and 27 of which will not. Locations of the stands are shown in figure 16.3. The data taken in the current pre-thin survey provide a baseline for

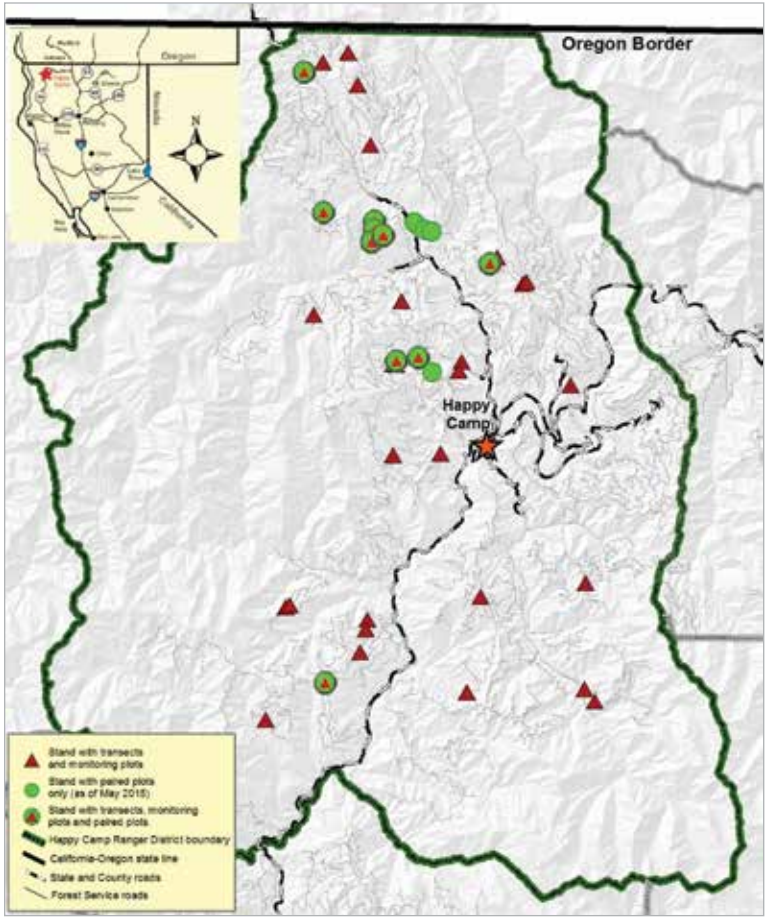

Figure 16.3—Location of black stain root disease monitoring plots on the Happy Camp Ranger District, Klamath National Forest.

the tracking of growth and disease impacts between measurement periods and between thinned and unthinned stands. Post-treatment evaluations will occur shortly after the thinning is completed, with periodic remeasurements every 5–10 years. The layout of transects, monitoring plots, and paired plots within a stand is illustrated in figure 16.4, and the surveys were run as follows:

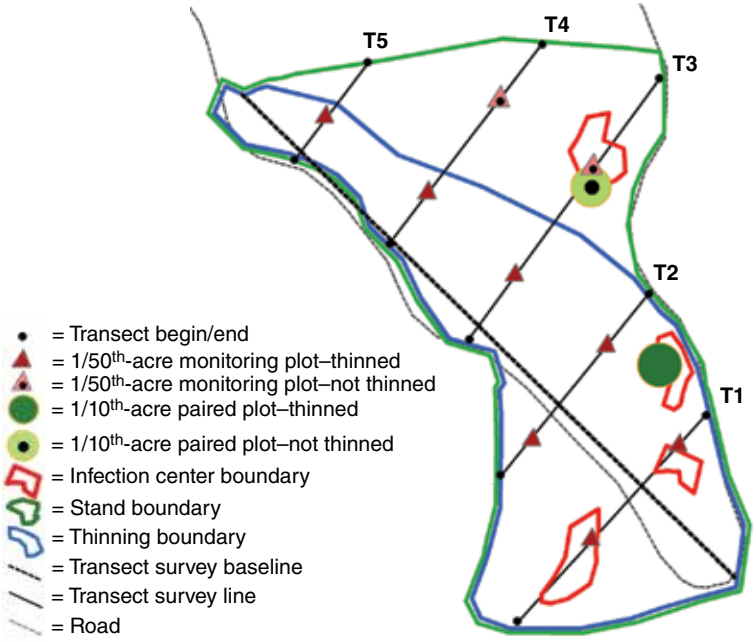

Figure 16.4—Layout of thinning treatment, transects, monitoring plots, and paired plots in a forest stand on the Happy Camp Ranger District, Klamath National Forest.

Transect Surveys

Parallel transect lines were run three chains (198 feet) apart, perpendicular to a baseline located along the longest axis of the stand. Whenever a black stain root disease center was encountered, GPS readings of its location were taken and its length and width were estimated. Perimeters of larger, more irregularly shaped infections were mapped with a GPS for more accurate size estimates. Infection center boundaries were defined by the inner faces of the first healthy-appearing host trees along the margin.

Monitoring Plot Survey

Along each transect, 1/50th-acre circular plots were established in three-chain intervals. In each plot, the number of conifer trees larger than 1 foot in height of each species was counted and recorded, as well as the height, diameter at breast height (d.b.h.), crown condition class, and the number of black stain root disease-infected Douglas-fir. Similar counts were made of standing and downed Douglas-fir. Basal area of the live trees was also measured at each plot center with a Basal Area Factor (BAF)-15 prism.

Paired Plot Survey

Twenty-three sets of 1/10th-acre paired plots were established in the 14 stands that will be thinned. In several stands, more than one plot pair was installed. Each plot pair had similar age and structure and was placed over the advancing edge of an active infection center, allowing the movement of the disease front to be tracked. When the thinning treatment is implemented, portions of these 14 stands will be excluded from thinning so that each plot pair will consist of one thinned and one unthinned plot. Data collected were similar to those on the monitoring plots, with the addition of basal area measurements of all live Douglas-fir, all live and standing dead Douglas-fir, all live trees of all species, and all live and standing dead trees of all species.

Data Analysis

Data analysis is ongoing, comparing both plot and transect survey data taken between measurements. Thinned and unthinned comparisons will compare treated and untreated units and pre- and post-thin measurements. In particular, the paired plots will enable a paired t-test analysis of statistical significance of differences in black stain root disease-caused mortality rates between thinned and unthinned plots and between measurements.

RESULTS

As expected, black stain root disease was found only in Douglas-fir. The disease was present in closely spaced conifers as well as in more open-grown trees. In general, symptoms in individual infected trees became worse between 2000–2001 and 2013–2014. Trees with thinning crowns became chlorotic, chlorotic trees died and became snags, and many snags became downed logs. Most infection centers increased in size between the measurements. However, some small infection centers showed no signs of further expansion, even to immediately adjacent healthy Douglas-fir. Even though infection centers appeared to be expanding, most were still

fairly small. In the current survey, 80 percent of the infection centers were less than 1/10th acre in size, 9 percent were between 1/10th and 1/4th acre, and 11 percent were larger than 1/4th acre. Though not directly measured, we estimated that active infection center edges expanded at a rate of roughly 1 foot per year.

DISCUSSION AND CONCLUSIONS

As stated above, the installation of plots in 11 new stands expands the black stain root disease monitoring network to 41 stands, 14 of which will be thinned, and 27 of which will not. The stands are representative of conditions in young second-growth Douglas-fir in northern California and beyond. Most of the stands in this study were originally old growth that was clear-cut in the 1960s, 1970s, and 1980s. Most were logged with ground-based equipment, though some on steeper ground were cable logged. *L. wageneri* was likely present at low endemic levels in the living trees in the old growth stands. Disturbance, as well as altered stand composition and environment most likely resulted in increased disease intensity and distribution in the second-growth stands. Although exact cause-and-effect relationships are often difficult to identify, field observations indicated positive correlations between the disease and the percentage of Douglas-fir in the stands, clay soils, gentler slopes, and past logging with ground-based equipment. Although black stain root disease caused the death of many individual Douglas-fir trees, expansion of infection centers was relatively slow, allowing the uninfested portions of the stands to grow as fast, large, and healthy as permitted by site quality. However, transport of the pathogen by insect vectors can easily cause more rapid disease spread, and any factors that favor the vectors can increase this spread. Data from these plots will continue to identify which environmental variables and management practices affect the spread and intensification of the pathogen and to what degree. Establishment and measurement of plots prior to commercial thinning has provided a baseline for the tracking of forest growth and disease impacts in treated and untreated stands. In addition, the paired plots will clarify the relationships between thinning and disease spread and intensification. The data will also be used for the validation and calibration of root disease models for the range of stand conditions in Region 5.

CONTACT INFORMATION

Pete Angwin: pangwin@fs.fed.us, or Todd Drake: tjdrake@fs.fed.us.

LITERATURE CITED

Dale, J. W., tech. coord. 1995. California forest health in 1994 and 1995. Rep #R5-FPM-PR-002. San Francisco, CA: U.S. Department of Agriculture, Forest Service, Pacific Southwest Region. 63 p.

Hessburg, P.F.; Goheen, D.J.; Bega, R.V. 1995. Black stain root disease of conifers. Forest Insect & Disease Leaflet 145. Washington, DC: U.S. Department of Agriculture, Forest Service. 9 p.

U.S. Department of Agriculture (USDA) Forest Service. 1994. California forest health past and present. Rep #R5-FPM-PR-001. San Francisco, CA: U.S. Department of Agriculture, Forest Service, Pacific Southwest Region. 70 p.

CHAPTER 17.

Forest Health Monitoring in Southern California: High-temporal Monitoring Using Advanced Image Analysis Techniques

(Project WC-EM-F-11-01)

Carlos Ramirez
Shengli Huang
Kama Kennedy
Jeffrey Mallory

INTRODUCTION

Developing an adaptive management strategy to aid in the restoration of ecosystem function and health requires timely monitoring information. Although plot-based data provide critical detailed information on the status of the ecosystem, they are costly, time consuming to acquire, and do not provide wall-to-wall spatial coverage. The lack of spatial coverage can underestimate certain forest dynamics that exhibit clustered spatial patterns on the landscape. Additionally, the temporal resolution is generally low, especially relative to the frequency of earth observation systems. For this project, we accessed the ability of the Forest Inventory and Analysis (FIA) plot data coupled with 30-m imagery from the Landsat5 archive to provide timely indicators of ecosystem status. Annual assessments can be provided by combining ground-plot data with large-scale imagery. It should be noted that an initial exploratory assessment of the FIA plots was conducted to assess forest mortality since we had two measurements between 2000 and 2010. Only 3 of 195 plots showed a measurable amount of mortality, making it impossible to determine forest trends from the plot data alone.

The area of interest encompasses multiple National Forests (NFs) including San Bernardino, Cleveland, and the eastern portion of the Angeles National Forests and adjacent areas. A Mediterranean climate typifies the area's climate regime, with cool moist winters and hot dry summers. This bioregion frequently experiences prolonged drought conditions, frequent wildfires, and substantial areas of tree mortality due to a variety of biotic and nonbiotic factors. These processes produce a highly dynamic ecosystem that requires frequent temporal monitoring.

Existing automated classification methods have been deemed ineffective because of the lack of automation and low efficiency over a large area (Chen and others 2015). For this study, an automated land cover mapping algorithm called the Automatic UpdaTe On Land Cover Database (AutoLCD[1]) was developed to assess changes in land cover in the South Coast bioregion of California that experienced drought and high incidences of bark-beetle mortality from 2003 to 2005 (Walker and others 2006). Since many monitoring objectives quantify annual changes (Hansen and Loveland 2012), this algorithm

[1] Huang, S.; Ramirez, C.; Kennedy, K. [and others]. In preparation. AutoLCD: a potential tool to automatically update large-area land cover database from times series satellite data. Remote Sensing of Environment.

was developed to assess land cover changes across the project area in annual time steps. The automated nature of AutoLCD allowed for quick and efficient analysis of land cover changes to monitor the biophysical characteristics such as biomass, carbon storage, and leaf area index.

METHODS

The AutoLCD algorithm uses existing land cover baseline and disturbance information to select candidate training pixels to update land cover in each time step. As an example, if we have multiple years of Landsat data but we are interested in information on land cover changes for a particular year, the tool compares the Landsat data with the baseline land cover data and with other Landsat years to detect changed and unchanged areas. The land cover class for an unchanged area is inherited from the baseline classification for the year being assessed. However, pixels that have experienced disturbance are reclassified by identifying their "similar" pixels within the unchanged area of the baseline classification and then using the majority as a pixel's classification value (fig. 17.1). This process is repeated for every pixel in the changed area. This basic premise

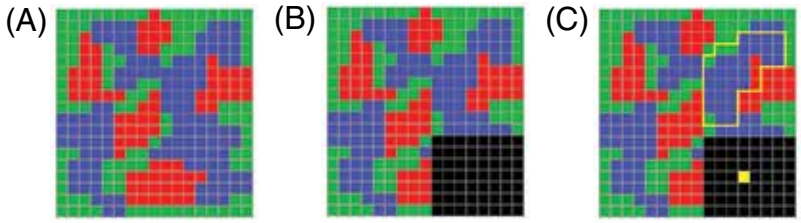

Figure 17.1—Basic concept of AutoLCD algorithm: (A) a baseline classification where red, green, and blue indicate different land cover values; (B) black areas indicate changed areas; the classification for unchanged areas are inherited from the baseline classification; (C) for one pixel within the change area (yellow pixel), its "similar" surrogates are enclosed by the yellow polygon. The majority of these "similar" pixels, which are blue in this case, are deemed as the land cover value for the yellow pixel.

that the majority classification relies on is a measure of similarity (Huang and others 2013) using several metrics derived from Landsat (e.g., reflectance, normalized difference vegetative index [NDVI], etc.), as well as physiographic and topographic variables (e.g., national forest boundaries, elevation zones, ecoregions, aspect). Expert rules (e.g., pixel categorized as "barren land" when NDVI is less than 0.02) were also incorporated into the AutoLCD processing chain. More detailed explanation of AutoLCD can be found in Huang and others (see footnote 1). For

this project, the 2009 baseline classification has 10 land cover types determined from two known sources: (1) land cover classes in the national forests generated from Landsat data, and (2) land cover classes outside of national forests from the National Land Cover Database (Jin and others 2013).

We selected an annual times series of optimal Landsat images for the years 2002 to 2010. The images were selected near the yearly anniversary of a baseline set of images in order to minimize climatic and phenologic influences. The images used in the classification process are composed of surface-reflectance data from the Landsat Ecosystem Disturbance Adaptive Processing System (LEDAPS) and derivative spectral indices [i.e., NDVI, normalized burn ratio (NBR)] (Masek and others 2006). We used AutoLCD to classify each year's Landsat data for all scenes spanning the project area.

After annual discrete land covers were produced with AutoLCD, we used a three pixel minimum patch size (2700 m^2) in eight directions and applied landscape metrics to five land cover classes: shrubland, conifer-hardwood mix, hardwood, conifer, and dry grass. These five land cover classes have experienced moderate and high severity fires since 2002. Subsequently, FRAGSTATS (McGarigal and others 2012) was used to quantify the spatial structure of the AutoLCD time series in terms of land cover composition and configuration within the landscape. To achieve this, various landscape metrics were selected: (1) total class area (CA), (2) number of patches (NP), (3) largest patch index (LPI), (4) average patch area (AREA_MN), (5) total area (TA), (6) total edge (TE), (7) interspersion and juxtaposition index (IJI), (8) Shannon's diversity index (SHDI), (9) Shannon's evenness index (SHEI), (10) contagion (CONTAG), (11) percentage of landscape (PLAND), (12) edge density (ED), and (13) patch density (PD). Using similar metrics, Linh and others (2012) suggested that certain changes to the spatial configuration of land cover types reduce ecological resilience at the landscape level.

RESULTS AND DISCUSSION

A detailed portion of an annual land cover map produced for the entire study area using the AutoLCD algorithm is shown in figure 17.2 (A-D). To evaluate the classification accuracy, 240 points were randomly selected for visual interpretation from National Agriculture Imagery Program (NAIP) imagery (USDA 2005) and compared with the 2005 AutoLCD classification results. The comparison showed an overall classification accuracy of 79 percent and an overall kappa coefficient of 0.76. Although we did not assess additional years, based on trends examined in the land cover time series, we expect a similar level of accuracy for each time step.

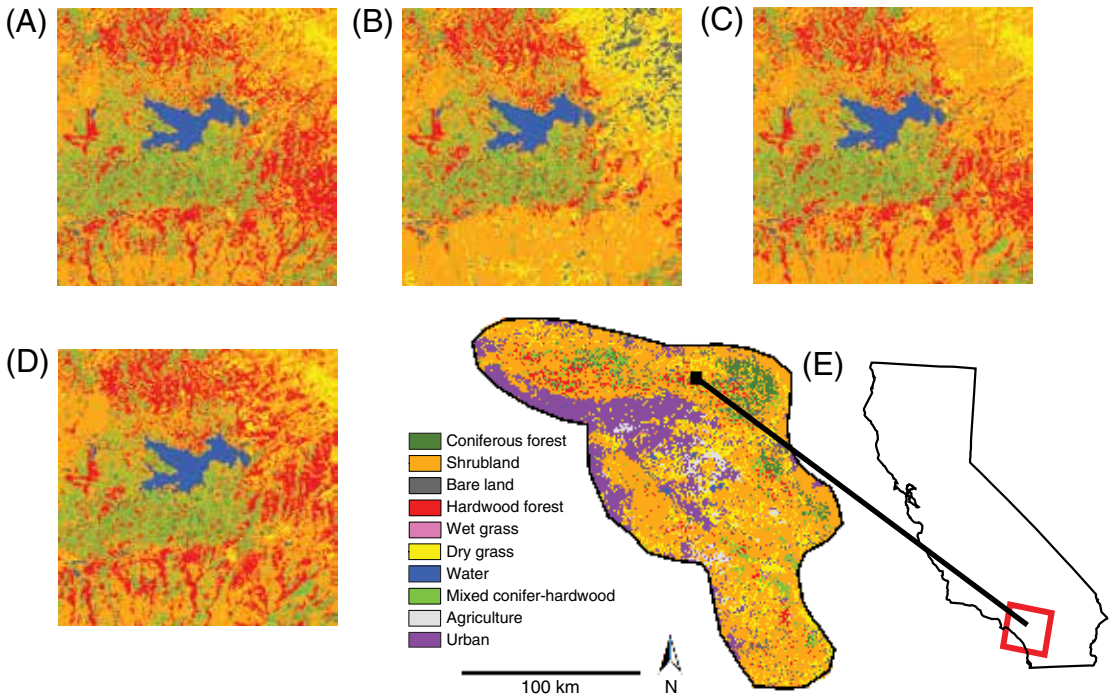

Figure 17.2—Land cover classes updated with the AutoLCD algorithm are shown for a small section (9 km x 9 km) of the entire study area for the years (A) 2003, (B) 2005, (C) 2007, and (D) 2010. The last panel (E) shows the general location in southern California and the magnified area as indicated by the black square.

Figure 17.3 illustrates the successional changes that occurred after moderate and high intensity fires moved through the project area. In 2003, approximately 303 515 ha (California Department of Forestry and Fire Protection 2003) burned, which contributed to the decline of tree and shrub cover and an increase of senesced grass in 2004. The 2006 Sawtooth Complex fire burned approximately 250 901 ha in San Bernardino County, which was dominated by shrub cover and is reflected in the downward trend in shrubland (fig. 17.3). In 2007, large fires (i.e., Zaca, Moonlight, and Angora) once again resulted in large changes in land cover. The area predominately affected was once chaparral-dominated communities, as seen in the continued decline of shrubland in year 2008. In 2009, the Station Fire consumed approximately 64 750 ha of the Angeles NF and reduced hardwood cover by 79 percent, reduced areas of conifer-hardwood mix by 13 percent, and reduced conifer cover by 8 percent. Despite these local decreases, shrubland areas across the entire study area continued to increase from 2002 to 2010.

Forest health is threatened when biotic and/or abiotic factors are severely disrupted and resiliency is compromised. Walker and others (2004) define ecological resilience as "the capacity of a system to absorb disturbance and reorganize while undergoing change so

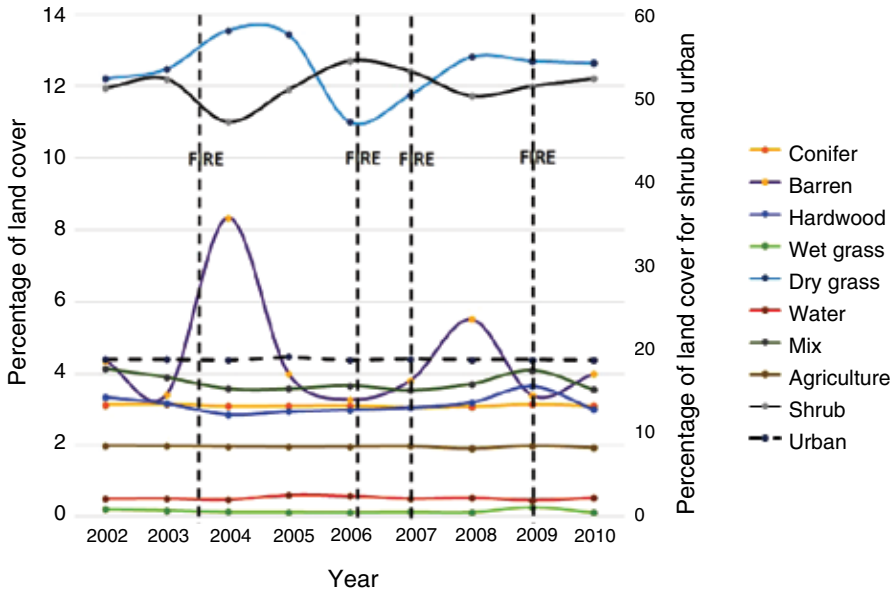

Figure 17.3—Land cover over time across all ownerships.

as to still retain essentially the same function, structure, identity, and feedbacks." Fire is one of the most influential processes that has changed the vegetation dynamics in the study area. The changes to the edge structure and land cover composition on the landscape influence the adjacent communities (Harper and others 2005). Successional trends following large moderate to high severity fires in southern California have been well documented (Franklin and others 2006, Franklin 2007, Goforth and Minnich 2008, Keeley 1998, Keeley and others 2004). Typical post-fire vegetation dynamics following major disturbances include a high intensity flush of herbaceous plants the first two years with their decline in the third year (Franklin 2007). Sprouting of heat resistant buds in shrubs and hardwoods along with sprouting of fire dependent obligate seeders from stored seed banks buried in the soil continue to expand cover and dominate the landscape in years after. Conifer and the conifer portion of the conifer-hardwood mix land covers are the least successful in recovery as seedling replacement and regeneration can be practically nonexistent, and in some high severity fires conifer can be completely extirpated from the landscape (Franklin 2007, Goforth and Minnich 2008). Pre-fire and post-fire heterogeneity, vegetation dynamics, life history traits, and successional trends show up as changing vegetation patterns (change) in the landscape. The gradients of change are quantifiable using landscape metrics. Spatial landscape metrics were computed for the 2002 and 2010 land cover classifications and are displayed in table 17.1.

Table 17.1—Spatial landscape metrics for selected classes, 2002 and 2010

Year	TYPE	CA	PLAND	NP	PD	LPI	TE	ED	AREA_MN
		ha	*%*	*number*	*number/ha*	*%*	*m*	*(m/ha)*	*ha*
2002	Conifer	68 940.99	3.1351	16,096	0.732	1.346	24 726 930	11.2446	4.2831
2002	Shrubland	1 126 861	51.2441	43,344	1.9711	39.4732	169 369 890	77.021	25.9981
2002	Hardwood	73 551.78	3.3448	32,641	1.4844	0.2817	34 188 900	15.5474	2.253
2002	Grassland	268 620.7	12.2155	62,396	2.8375	0.3856	94 526 490	42.986	4.3051
2002	Mix	90 955.62	4.1362	29,933	1.3612	0.1329	37 763 640	17.173	3.0386
2010	Conifer	68 195.61	3.1012	13,708	0.6234	1.4193	23 380 260	10.6322	4.9749
2010	Shrubland	1 151 373	52.3588	42,473	1.9315	40.5777	161 026 920	73.2271	27.1084
2010	Hardwood	65 951.1	2.9991	30,615	1.3922	0.2059	30 308 640	13.7829	2.1542
2010	Grassland	278 266.6	12.6542	63,562	2.8905	1.4723	92 987 850	42.2863	4.3779
2010	Mix	78 028.74	3.5484	28,301	1.287	0.1241	33 911 070	15.4211	2.7571

CA = total class area; PLAND = percentage of landscape; NP = number of patches; PD = patch density; LPI = largest patch index; TE = total edge; ED = edge density; AREA_MN = average patch area.

The conifer habitat exhibited a class area (CA) loss of 745 ha, a reduction in the number of patches (NP) by 2,388, but an increase in mean patch area (AREA_MN) of 0.7 ha. Conversely, the conifer-hardwood mix class exhibited a loss of 12 926 ha and a decrease in the number of patches by 1,632 with most loss due to conifers and not hardwood. The hardwood component of the mix typically resprouts whereas the conifer component has poor regeneration success as seen in the high severity Cedar Fire of 2003 (Franklin and others 2006, Goforth and Minnich 2008). The poor regeneration in conifer equates to a shift in vegetation dynamics and development of new ecotones that favor vegetation species with fire-adapted abilities to fulfill the niche once occupied by the conifer component. Not only will there be a shift in species composition but also a shift in structural attributes, particularly the percentage of cover and height. Where there is not a species compositional shift, a structural ecotone may be manifested on the landscape. Changes in species and structural attributes will lead to greater exposure to abiotic factors such as direct sunlight, temperature, and wind. The physical structure of vegetation within this time period has changed. Resiliency is apparent to some degree in hardwoods but not yet with conifer regeneration to a pre-fire ecosystem functional condition. As noted above, forest health issues are still apparent in this time period. The analysis for the hardwood land cover class shows a class area loss of 7601 ha, number of patches decreasing by 2,026, and patch area mean decreasing by 0.1 ha. In the earlier to middle part of the study, the hardwoods gradually increased with a portion of the loss due to the 2009 Station Fire on the Angeles NF. Since many of these hardwood species resprout, we expect that ecosystem resiliency will increase.

The shrubland experienced an increase in area by 24 512 ha, a decrease in patch number by 871, and an increase in the mean patch area by 1.1 ha. This combination of metrics suggests shrubland occurs as larger parcels that have decreased in number with an overall increase in shrubland occupancy. Shrubland appears to be resilient in this area as it recovers quickly from moderate to high severity fires due to its resprouting and obligate seeding capacities.

Dry grassland experienced an increase in total area by 9646 ha, an increase in the number of patches by 1,166, and an increase in the mean patch area of nearly 0.1 ha. Grasses respond very quickly under moderate to high fire conditions within the first 2 years and occupy a greater proportion of the fire landscape than does woody vegetation (fig. 17.3).

Analysis at the landscape level exhibited a decrease in the total number of patches across all class types to 5895 ha while the mean area patch increased by 0.22 ha (table 17.2). Shannon's diversity index (SHDI) is the amount of patch per class (McGarigal and others 2012) and Shannon's evenness index (SHEI) is expressed as the observed level of diversity divided by the maximum possible diversity for a given patch richness (McGarigal and others 2012). These indices decreased from 2002 to 2010, indicating that the patches of land cover types slightly declined in heterogeneity and evenness. Furthermore, the interspersion and juxtaposition index (IJI) decreased from about 64 percent to 61 percent, indicating a trend toward land cover types becoming less dispersed across the landscape.

Discrete land cover changes within specific categories produced with AutoLCD enable us to better understand ecosystem changes quickly and in an automated manner. In addition, monitoring the progression of trends of biophysical characteristics such as biomass, carbon storage, and leaf area index is also important. There are three basic steps to integrate the data:

1. Because the cycle of FIA single plot measurements spans 10 years and the plots undergo changes, a subset of the full complement of FIA plots is automatically selected for each individual year and the measurement (e.g., biomass increment) is accordingly adjusted for annual increase or decrease.

2. Since the number of FIA plots sampled in an individual year may be limited, the pixels that are "extremely similar" to the FIA plots (in terms of remote sensing metrics and abiotic factors such as elevation, precipitation, temperature, aspect, soil type, and drainage) are identified and the sampled FIA attributes are assigned to these pixels. The original FIA plots and these newly identified pixels are categorized as "expanded plots."

3. A comparable "similar" process as discussed above is used to identify the closely related pixels as a group. After identifying which "expanded plots" fall within this group, the weighted mean of field-derived parameters such as biomass is assigned to these pixels. The basic idea of this algorithm is comparable

Table 17.2—Landscape level metrics, 2002 and 2010

Year	TA	NP	LPI	AREA_MN	CONTAG	IJI	SHDI	SHEI
	ha	*number*	*%*	*ha*	*%*	*%*		
2002	2 199 008	243,249	39.4732	9.04	53.33	64.3	1.52	0.66
2010	2 199 008	237,354	40.5777	9.26	56.38	61.09	1.49	0.62

TA = total area; NP = number of patches; LPI = largest patch index; AREA_MN = average patch area; CONTAG = contagion; IJI = interspersion and juxtaposition index; SHDI = Shannon's diversity index; SHEI = Shannon's evenness index.

to the K-Nearest Neighbors-(K-NN) method (McRoberts and others 2007, McRoberts and Tomppo 2007).

Further explanation of the biomass estimation process and results may be found in an upcoming paper by Huang and others.[2]

CONCLUSIONS

There is a pressing need to develop robust, efficient, and accurate automated approaches for cost-effective monitoring of land cover changes at moderate spatial resolution scales. AutoLCD provides such a mechanism to automatically update regional, and potentially global, land cover changes from Landsat or Landsat-like imagery. The AutoLCD algorithm provides a mechanism for rapidly assessing the state of the ecosystem as a function of trends in land cover change. An additional strength of AutoLCD is that it can be easily adapted to work with other passive optical imagery, such as WorldView2/3, AVIRIS, and other sensors.

Major fires in southern California have contributed to the shaping of the landscape and ecosystem. The transition between successional stages influences the patch number, patch shape, mean patch size, and spatial pattern on the landscape for land cover classes. Over time, hardwoods, conifer-hardwood mix, and conifers in particular have been strongly influenced by these interactions. At the landscape level, evidence of fragmentation exists over the study period and the capacity for ecological resilience is in question. Structurally dependent species will experience habitat and continuity loss as their ecosystems become further stressed under issues such as climate change. However, we expect hardwood forests and woodlands to recover to an unknown extent. AutoLCD can be used to provide frequent temporal monitoring of land cover to better assess forest health, ecosystem resiliency, and/or fragmentation of landscapes.

[2] Huang, S.; Ramirez, C.; Kennedy, K.; Mallory, J. In preparation. Integrating field measurements and remote sensing for ecosystem biophysics parameterization across spatial and temporal domains. Forest Ecology and Management.

CONTACT INFORMATION

Carlos Ramirez: carlosramirez@fs.fed.us.

LITERATURE CITED

California Department of Forestry and Fire Protection. 2003. 2003 fire siege. http://www.fire.ca.gov/fire_protection/fire_protection_2003_siege.php. [Date accessed: May 1, 2015].

Chen, Jun; Chen, Jin; Liao, A. [and others]. 2015. Global land cover mapping at 30 m resolution: a pixel-object-knowledge-based operational approach. ISPRS Journal of Photogrammetry and Remote Sensing. 103: 7–27.

Franklin, J. 2007. Vegetation dynamics and exotic plant invasion following high severity crown fire in a southern California conifer forest. Plant Ecology. 207: 281–295.

Franklin, J; Spears-Lebrun, L.A.; Deutschman, D.H.; Marsden, K. 2006. Impact of a high-intensity fire on mixed evergreen and mixed conifer forests in the Peninsular Ranges of southern California, USA. Forest Ecology and Management. 235: 18–29.

Goforth, B.R.; Minnich, R.A. 2008. Densification, stand replacement wildfire, and extirpation of mixed conifer forest in Cuyamaca Rancho State Park, southern California. Forest Ecology and Management. 256: 36–45.

Hansen, M.C.; Loveland, T.R. 2012. A review of large area monitoring of land cover change using Landsat data. Remote Sensing of Environment. 122: 66–74.

Harper, K. A.; Macdonald, S. E.; Burton, P. J. [and others]. 2005. Edge influence on forest structure and composition in fragmented landscapes. Conservation Biology. 19(3): 768–782.

Huang, S.; Jin, S.; Dahal, D. [and others]. 2013. Reconstructing satellite images to quantify spatially explicit land surface change caused by fires and succession: a demonstration in the Yukon River Basin of interior Alaska. ISPRS Journal of Photogrammetry and Remote Sensing. 79: 94–105.

Jin, S.; Yang, L.; Danielson, P. [and others]. 2013. A comprehensive change detection method for updating the National Land Cover Database to circa 2011. Remote Sensing of Environment. 132: 159–175.

Keeley, J.E. 1998. Postfire recovery and management: the October 1993 large fire episode in California. In: Moreno, J.M., ed. Large forest fires. Leiden, The Netherlands: Backhuys Publishers: 69–90.

Keeley, J.E.; Fotheringham, C.J.; Moritz, M.A. 2004. Lessons from the 2003 wildfires in southern California. Journal of Forestry. 102: 26–31.

Linh, N.H.K.; Erasmi, S.; Kappas, M., 2012. Quantifying land use/cover change and landscape fragmentation in Danang City, Vietnam: 1970–2009. International Archives of the Photogrammetry, Remote Sensing and Spatial Information Sciences. 39: 501–506.

Masek, J. G.; Vermote, E. F.; Saleous, N. E. [and others]. 2006. A Landsat surface reflectance dataset for North America, 1990–2000. IEEE Geoscience and Remote Sensing Letters. 3(1): 68–72.

McGarigal, K.; Cushman, S.A.; Ene, E. 2012. FRAGSTATS v4: spatial pattern analysis program for categorical and continuous maps [computer software program]. Amherst, MA: University of Massachusetts, Amherst. http://www.umass.edu/landeco/research/fragstats/fragstats.html. [Date accessed: January 12, 2016].

McRoberts, R.E.; Tomppo, E.O. 2007. Remote sensing support for national forest inventories. Remote Sensing of Environment. 110: 412–419.

McRoberts, R.E.; Tomppo, E.O.; Finley, A.O.; Heikkinen, J. 2007. Estimating areal means and variances of forest attributes using the K-Nearest Neighbors technique and satellite imagery. Remote Sensing of Environment. 111: 466–480.

U.S. Department of Agriculture (USDA). 2005. Indiana NAIP 2005 Imagery. Salt Lake City, UT: Farm Service Agency Aerial Photography Field Office.

Walker, B.; Holling, C.S.; Carpenter, S.R.; Kinzig, A. 2004. Resilience, adaptability and transformability in social–ecological systems. Ecology and Society 9(2): 5. http://www.ecologyandsociety.org/vol9/iss2/art5. [Date accessed: January 12, 2016].

Walker, R.; Rosenberg, M.; Warbington, R. [and others]. 2006. Inventory of tree mortality in southern California mountains (2001–2004) due to bark beetle impacts. http://frap.cdf.ca.gov/projects/mast/reports.php. [Date accessed: June 1, 2015].

ACKNOWLEDGMENTS

This research presented in this report was supported in part through the project "Forest Health Monitoring, Assessment, and Analysis" of Cost Share Agreement 14-CS-11330110-042 (June 10, 2014 through June 30, 2016) and the project "Forest Health Monitoring, Assessment, and Analysis" of Cost Share Agreement 15-CS-11330110-067 (July 8, 2015 through November 30, 2016) between North Carolina State University (this institution is an equal opportunity provider) and the U.S. Department of Agriculture, Forest Service, Southern Research Station, Asheville, NC. This research was supported by funds provided by the U.S. Department of Agriculture, Forest Service, Southern Research Station, Asheville, NC.

The editors and authors of this report thank the following for their reviews and constructive comments: Kevin Bigsby, John Coulston, Gregg DeNitto, Andrea Diss-Torrance, Chris Fettig, Qinfeng Guo, Tom Hall, Matt Hansen, Jeri Lyn Harris, Zachary Heath, Shuang Li, Jinxun Liu, Duncan Lutes, Joel McMillin, Roger Magarey, Sparkle Malone, Manfred Mielke, Jose Negron, Donald Owen, Jill Pokorny, Roy Renkin, David Shaw, Stephanie Snyder, Glen Stanosz, Brytten Steed, Patricia Terletzky-Gese, Rob Trickel, Denys Yemshanov, and Stan Zarnoch.

AUTHOR INFORMATION

Sections 1 and 2, Forest Health Monitoring Research

Mark J. Ambrose, Research Assistant, North Carolina State University, Department of Forestry and Environmental Resources, Raleigh, NC 27695.

John W. Coulston, Supervisory Research Forester, U.S. Department of Agriculture, Forest Service, Southern Research Station, Knoxville, TN 37919.

Frank H. Koch, Research Ecologist, U.S. Department of Agriculture, Forest Service, Southern Research Station, Eastern Forest Environmental Threat Assessment Center, Research Triangle Park, NC 27709.

Jeanine L. Paschke, Geographic Information Systems Analyst, Cherokee Nation Technologies, Fort Collins, CO 80526.

Kevin M. Potter, Research Associate Professor, North Carolina State University, Department of Forestry and Environmental Resources, Raleigh, NC 27695.

Kurt H. Riitters, Research Ecologist, U.S. Department of Agriculture, Forest Service, Southern Research Station, Research Triangle Park, North Carolina 27709.

Section 3, Evaluation Monitoring Project Summaries

Kurt Allen, Entomologist, U.S. Department of Agriculture, Forest Service Region 2 Forest Health Management, Rapid City, SD 57701.

Michael C. Amacher, Research Soil Scientist, U.S. Department of Agriculture, Forest Service, Rocky Mountain Research Station, Logan, UT 84321.

Peter A. Angwin, Plant Pathologist, U.S. Department of Agriculture, Forest Service, Forest Health Protection, Northern California Shared Service Area Office, Redding, CA, 96002.

Barbara J. Bentz, Research Entomologist, U.S. Department of Agriculture, Forest Service, Rocky Mountain Research Station, Logan, UT 84321.

Darren Blackford, Intermountain Region Entomologist, Forest Health Protection, Ogden, UT 84401.

Nancy Bockino, Vegetation Specialist, Grand Teton National Park, Moose, WY 83012.

Tom Coleman, Entomologist, U.S. Department of Agriculture, Forest Service, Forest Health Protection, San Bernardino, CA 92408.

Cheryl Coon, Forest Botanist, U.S. Department of Agriculture, Forest Service, Hoosier National Forest, Bedford, IN 47421.

Todd J. Drake, Forester, Happy Camp Ranger District, Klamath National Forest, Happy Camp, CA 96039.

James T. English, Professor, University of Missouri Plant Sciences Division, Columbia, MO 65211.

Amanda Grady, Entomologist, U.S. Department of Agriculture, Forest Service, Forest Health Protection, Flagstaff, AZ 86001.

E. Matthew Hansen, Entomologist, U.S. Department of Agriculture, Forest Service, Rocky Mountain Research Station, Logan, UT 84321.

Thomas C. Harrington, Professor, Iowa State University, Department of Plant Pathology and Microbiology, Ames, IA 50011.

Chad Hoffman, Assistant Professor, Colorado State University, Fort Collins, CO 80521.

Shengli Huang, Senior Remote Sensing Analyst, U.S. Department of Agriculture, Forest Service, Southwest Region, McClellan, CA 95652.

Camille Jensen, Research Associate, University of California, Davis, CA 95616.

Morris C. Johnson, Research Fire Ecologist, U.S. Department of Agriculture, Forest Service, Pacific Northwest Research Station, Seattle, WA 98103.

Vinci D. Keeler, Deputy District Ranger, Shasta Lake Ranger District, Shasta-Trinity National Forest, Shasta Lake, CA 96003.

Kama Kennedy, Inventory Forester, U.S. Department of Agriculture, Forest Service, Southwest Region, McClellan, CA 95652.

Author Information, cont.

Aaron Kloss, Natural Resources Administrator 1, Ohio Department of Natural Resources, Ohio Division of Forestry, Columbus, OH 43229.

Kristin L. Legg, Program Manager, National Park Service, Greater Yellowstone Network, Bozeman, MT 59715.

James N. Long, Professor, Department of Wildland Resources, Utah State University, Logan, UT 84322.

Jeffrey Mallory, Vegetation Mapping Specialist, U.S. Department of Agriculture, Forest Service, Southwest Region, McClellan, CA 95652.

Patricia Maloney, Research Associate, University of California, Plant Pathology, Davis, CA 95616.

Kelly McCloskey, Vegetation Ecologist, Grand Teton National Park, Moose, WY 83012.

Joel McMillin, Entomologist, U.S. Department of Agriculture, Forest Service Region 4, Forest Health Protection, Boise, ID 83709.

Douglas L. McNew, Iowa State University, Department of Plant Pathology and Microbiology, Ames, IA 50014.

A. Steven Munson, Intermountain Region Group Leader/Entomologist, U.S. Department of Agriculture, Forest Service, Forest Health Protection, Ogden, UT 84403.

Rose Marie Muzika, Professor, University of Missouri, Forestry Department, Columbia MO 65211.

Holly A. Petrillo, Associate Professor, University of Wisconsin-Stevens Point, College of Natural Resources, Stevens Point, WI 54481.

Carlos Ramirez, Vegetation Mapping and Inventory Lead, U.S. Department of Agriculture, Forest Service, Southwest Region, McClellan, CA 95652.

Joanne Rebbeck, Research Plant Physiologist, U.S. Department of Agriculture, Forest Service, Northern Research Station, Delaware, OH 43015.

Sharon E. Reed, Research Scientist, University of Missouri, Plant Sciences Division, Columbia MO 65211.

Michael G. Ryan, Senior Research Scientist, Colorado State University, Natural Resources Ecology Laboratory, Fort Collins, CO 80523.

Greta Schen-Langenheim, Research Associate, U.S. Department of Agriculture, Forest Service, Rocky Mountain Research Station, Logan, UT 84321.

Erin Shanahan, Field Ecologist, National Park Service, Greater Yellowstone Network, Bozeman, MT 59715.

Carolyn Sieg, Research Ecologist, U.S. Department of Agriculture, Forest Service, Rocky Mountain Research Station, Flagstaff, AZ 86001.

Roger L. Siemers, Forest Culturist, Klamath National Forest, Yreka, CA 96097.

Sheri Smith, Regional Entomologist, U.S. Department of Agriculture, Forest Service, Forest Health Protection, Susanville, CA 96130.

Helga Van Miegroet, Professor, Utah State University, Department of Wildland Resources, Logan, UT 84322.

James C. Vandygriff, Entomologist, U.S. Department of Agriculture, Forest Service, Rocky Mountain Research Station, Logan, UT 84321.

Potter, Kevin M.; Conkling, Barbara L., eds. 2016. Forest health monitoring: national status, trends, and analysis 2015. Gen. Tech. Rep. SRS-213. Asheville, NC: U.S. Department of Agriculture, Forest Service, Southern Research Station. 199 p.

The annual national report of the Forest Health Monitoring (FHM) Program of the Forest Service, U.S. Department of Agriculture, presents forest health status and trends from a national or multi-State regional perspective using a variety of sources, introduces new techniques for analyzing forest health data, and summarizes results of recently completed Evaluation Monitoring projects funded through the FHM national program. In this 15th edition in a series of annual reports, survey data are used to identify geographic patterns of insect and disease activity. Satellite data are employed to detect geographic patterns of forest fire occurrence. Recent drought and moisture surplus conditions are compared across the conterminous United States. Data collected by the Forest Inventory and Analysis Program are employed to detect regional differences in tree mortality. National Land Cover Database land cover maps are used to summarize temporal trends in forest fragmentation for the conterminous United States from 2001 to 2011. Eleven recently completed Evaluation Monitoring projects are summarized, addressing forest health concerns at smaller scales.

Keywords—Change detection, drought, fire, forest health, forest insects and disease, fragmentation, tree mortality.

Scan this code to submit your feedback, or go to www.srs.fs.usda.gov/pubeval

A copy of this report is available for download at www.srs.fs.usda.gov/pubs/.

Please direct inquiries about the availability of hard copies to pubrequest@fs.fed.us.
Number of copies is limited to two per person.